POTENTIAL CANCER CHEMOPREVENTIVE PROPERTIES OF RESVERATROL METABOLITES

Thesis submitted for the degree of

Doctor of Philosophy

at the University of Leicester

by

Ketan R. Patel, BSc.

Department of Cancer Studies and Molecular Medicine

University of Leicester

June 2011

ABSTRACT

Potential cancer chemopreventive properties of resveratrol metabolites

Ketan R. Patel

Resveratrol (*trans*-3,5,4′-trihydroxystilbene), a naturally occurring polyphenol present in grapes and red wine has undergone investigation as a potential cancer chemopreventive agent. Resveratrol is rapidly and extensively metabolised to its major phase II metabolites, including resveratrol sulfates and glucuronides. It is not yet known whether resveratrol metabolites contribute to the beneficial effects attributed to resveratrol, or whether resveratrol regeneration can occur from the metabolites.

Resveratrol and metabolite pharmacokinetics were investigated in the plasma of healthy human volunteers receiving 0.5, 1.0, 2.5 and 5.0 g resveratrol daily. Concentrations were also quantified in malignant and non-malignant colon tissue removed from colorectal cancer patients, who received 0.5 or 1.0 g resveratrol daily. A mixture of resveratrol monosulfates and individual monoglucuronide isomers were synthesised. Resveratrol monosulfates were administered to mice to determine their pharmacokinetics. The effects of the metabolites on proliferation in HCA-7, HT-29 and HCEC colon cell lines were assessed.

In healthy volunteers, resveratrol metabolites were shown to be the major species recovered from plasma. Average volunteer plasma AUC_{last} for resveratrol-4′-*O*-glucuronide and resveratrol-3-*O*-sulfate were approximately 36- and 81-fold greater respectively than for resveratrol, following 0.5 g resveratrol dosing. In colon tissues from cancer patients resveratrol generally predominated, with resveratrol sulfate glucuronide being the most prominent metabolite. In mice administered monosulfates, resveratrol formation was found to occur, with measurable concentrations in plasma, mucosa, liver, lung and pancreas. The conversion of resveratrol sulfates to resveratrol was also observed in cells *in vitro*. Uptake of the metabolites and intracellular resveratrol correlated with effects on proliferation. Whilst resveratrol monoglucuronides had a limited inhibitory effect on cell proliferation, monosulfates caused a more pronounced reduction, with the greatest effect in HT-29 followed by HCA-7 cells, and little or no effect in HCEC cells. Further investigations will improve our understanding of the role of resveratrol metabolites in chemoprevention.

ACKNOWLEDGEMENTS

I would firstly like to thank Professor Andy Gescher and Professor Will Steward for setting up this PhD project and giving me the opportunity to undertake the research. I am extremely grateful for this and for all of the support over the years. I want to express my appreciation to Dr Karen Brown, who has been a great supervisor and a big help throughout. Thank you also to Dr Robert Britton, who helped with the metabolite synthesis and to everyone who has been involved with the resveratrol studies, including Dr Victoria Brown, Dr David Boocock and all of our overseas colleagues and collaborators. These clinical trials would not have been possible without the hard work of many individuals, and of course the participation of the volunteers and cancer patients, to whom I am very grateful.

I would like to express my gratitude to all of the members of the Cancer Studies and Molecular Medicine group, past and present, and to everyone who has helped me along the way. In particular, I wish to thank Dr Tim Marczylo, Dr Darren Cooke, Mr Ankur Karmokar, Dr Stewart Sale, Mrs Stephanie Euden, Dr Hong Cai, Dr Lynne Howells, Dr Christoph Boes, Miss Isobel Fong and Mr Shaban Saad.

Last, but not least, a special thanks to my mother and to my siblings Kalpesh, Shila, and Bhakti. I would like to dedicate this thesis to my family and to my late father who have all helped to get me here.

LIST OF CONTENTS

INDEX OF FIGURES

CHAPTER 1

CHAPTER 2

CHAPTER 3

CHAPTER 4

CHAPTER 5

INDEX OF TABLES

CHAPTER 1

CHAPTER 2

CHAPTER 3

CHAPTER 4

CHAPTER 5

LIST OF ABBREVIATIONS

^{1}H-NMR	Proton nuclear magnetic resonance
5-FU	5-fluorouracil
AMPK	5′-AMP-activated protein kinase
ANOVA	Analysis of variance
AOM	Azoxymethane
APC	Adenomatous polyposis coli gene
ATP	Adenosine triphosphate
AU	Absorbance units
AUC	Area under the concentration-time curve
AUC_{inf}	Area under the concentration-time curve from time zero extrapolated to infinity
AUC_{last}	Area under the concentration-time profile from time zero to the last quantifiable concentration
BCRP	Breast cancer resistance protein
BLQ	Below the limit of quantitation
BMI	Body mass index
BSA	Bovine serum albumin
cAMP	Cyclic AMP
CDKs	Cyclin-dependent kinases
C_{max}	Maximum concentration
COX-1	Cyclooxygenase-1
CV	Coefficient of variation
CYP	Cytochrome P450
DMBA	7,12-dimethylbenz[α]anthracene
DMH	1,2-dimethylhydrazine
DMSO	Dimethyl sulfoxide
DNA	Deoxyribonucleic acid
DPPH	Diphenyl-p-picrylhydrazyl

EGCG	Epigallocatechin-3-gallate
FAP	Familial adenomatous polyposis
FDA	Food and Drug Administration
GI	Gastrointestinal
GST-π	Glutathione S-transferase
HCl	Hydrochloric acid
HepG2	Human hepatoblastoma cells
HIV-1	Human immunodeficiency virus
HPA	Health Protection Agency
HPLC-UV	High performance liquid chromatography-UV
IC_{50}	Half maximal inhibitory concentration
IG	Intragastric
IGF-1	Insulin-like growth factor 1
IGFBP-3	IGF-binding proteins
IP	Intraperitoneal
IS	Internal standard
IV	Intravenous
i-κB	Inhibitory kappa B
LC3	Microtubule-associated protein 1 light chain 3
LC-MS/MS	Liquid chromatography-tandem mass spectrometry
LDL	Low-density lipoprotein
LOD	Limit of detection
LOQ	Limit of quantitation
m/z	Mass to charge ratio
M_1dG	Malondialdehyde-DNA
MeOH	Methanol
Min	Multiple intestinal neoplasia
MRM	Multiple reaction monitoring
mRNA	Messenger RNA
MRP	Multidrug resistance protein

NADPH	Nicotinamide adenine dinucleotide phosphate
NF-κB	Nuclear factor kappa B
Nox1	NADPH oxidase 1
NSAID	Non-steroidal anti-inflammatory drug
OATP	Organic anion-transporting polypeptide
PBMC	Peripheral blood mononuclear cell
PBS	Phosphate buffered saline
PD	Pharmacodynamic
PGE_2	Prostaglandin synthase
PI	Propidium iodide
PK	Pharmacokinetic
QR1	Quinone reductase 1
RM	Resection margin
RNA	Ribonucleic acid
ROS	Reactive oxygen species
RPM	Revolutions per minute
RSD	Relative standard deviation
RT-PCR	Reverse transcriptase-polymerase chain reaction
SD	Standard deviation
SRM	Single reaction monitoring
Std	Standard
SULT	Sulfotransferase
TIC	Total ion current
T_{last}	Time of last observed concentration
TLC	Thin layer chromatography
T_{max}	Time of maximum peak concentration
TNM	Tumour/nodes/metastases
TPA	12-O-tetradecanoylphorbol-13-acetate
UGT	Uridine diphosphate glucuronosyltransferase
UV	Ultraviolet

LIST OF PUBLICATONS

Patel K., Scott E., Brown V., Gescher A., Steward W. and Brown K. Clinical trials of resveratrol. *Annals of the New York Academy of Sciences*, 2011. **1215** (1): 161-9.

Patel K., Brown V., Jones D., Britton R., Hemingway D., Miller A., West K., Booth T., Perloff M., Crowell J., Brenner D., Steward W., Gescher A. and Brown K. Clinical Pharmacology of Resveratrol and Its Metabolites in Colorectal Cancer Patients. *Cancer Research*, 2010. **70** (19): 7392-9.

Brown V., Patel K., Viskaduraki M., Crowell J., Perloff M., Booth T., Vasilinin G., Sen A., Schinas A., Piccirilli G., Brown K., Steward W., Gescher A. and Brenner D. Repeat Dose Study of the Cancer Chemopreventive Agent Resveratrol in Healthy Volunteers: Safety, Pharmacokinetics and Effect on the Insulin-like Growth Factor Axis. *Cancer Research*, 2010. **70** (22): 9003-11.

Boocock, D., Faust, G., Patel, K., Schinas, J., Brown, V., Ducharme, M., Booth, T., Crowell, J., Perloff, M., Gescher, A., Steward, W. and Brenner, D. Phase I Dose Escalation Pharmacokinetic Study in Healthy Volunteers of Resveratrol, a Potential Cancer Chemopreventive Agent. *Cancer Epidemiology Biomarkers & Prevention*, 2007. **16** (6): 1246-52.

Boocock, D., Patel, K., Faust, G., Normolle, D., Marczylo, T., Crowell, J., Brenner, D., Booth, T., Gescher A. and Steward, W. Quantitation of trans-resveratrol and detection of its metabolites in human plasma and urine by high performance liquid chromatography. *Journal of Chromatography B*, 2007. **848** (2): 182-7.

LIST OF CONFERENCE ABSTRACTS

Patel, K., Britton, R., Brown, V., Gescher, A., Steward, W. and Brown, K.

Potential contribution of resveratrol sulfate metabolites to the cancer chemopreventive activity of resveratrol. Poster presentation. The National Cancer Research Institute (NCRI) Meeting Abstracts, Liverpool, UK, November 2010.

Patel K., Brown V., Britton R., Sale S., Cai H., Gescher A., Steward W. and Brown K. Investigating the potential chemopreventive activity of resveratrol sulfate metabolites. Poster presentation. The NCRI Meeting Abstracts, Birmingham, UK, September 2008.

Patel, K., Boocock, D., Brown V., Normolle D., Marczylo T., Crowell J., Brenner D., Booth T., Brown K., Britton R., Steward W., Gescher A and Brown K.

Role of metabolites in the bioactivity of resveratrol. Poster presentation. British Association of Cancer Research (BACR) Special Conference 'Diet & Cancer: Susceptibility, Prevention & Therapy'. University of Nottingham, UK, June 2007.

Patel, K., Boocock, D., Brown V., Normolle D., Marczylo T., Crowell J., Brenner D., Booth T., Brown K., Britton R., Steward W. and Gescher A.

Pharmacokinetics of single dose resveratrol in healthy volunteers in relation to formation of sulfate and glucuronide metabolites. Poster presentation. Cancer Research-UK Midlands Researchers' Meeting Abstracts, Birmingham, UK, May 2007.

CHAPTER ONE: INTRODUCTION

1.1 Cancer and epidemiology

Cancer can be defined as any abnormal and uncontrolled cell growth that can spread locally through invasion or via the bloodstream and lymphatic system to other parts of the body by metastasis. It is a complex disease which varies in age of onset, cell type, rate of growth, state of cellular differentiation, invasiveness, metastatic potential, response to treatment, and prognosis [1]. Cancer incidence is on the rise and currently an estimated ten million new cases are diagnosed annually worldwide and this number is expected to increase to 15 million new cases in the year 2020 [2]. The change in UK cancer incidence over a 33-year period, between 1975 and 2008 is illustrated in Figure 1.1.

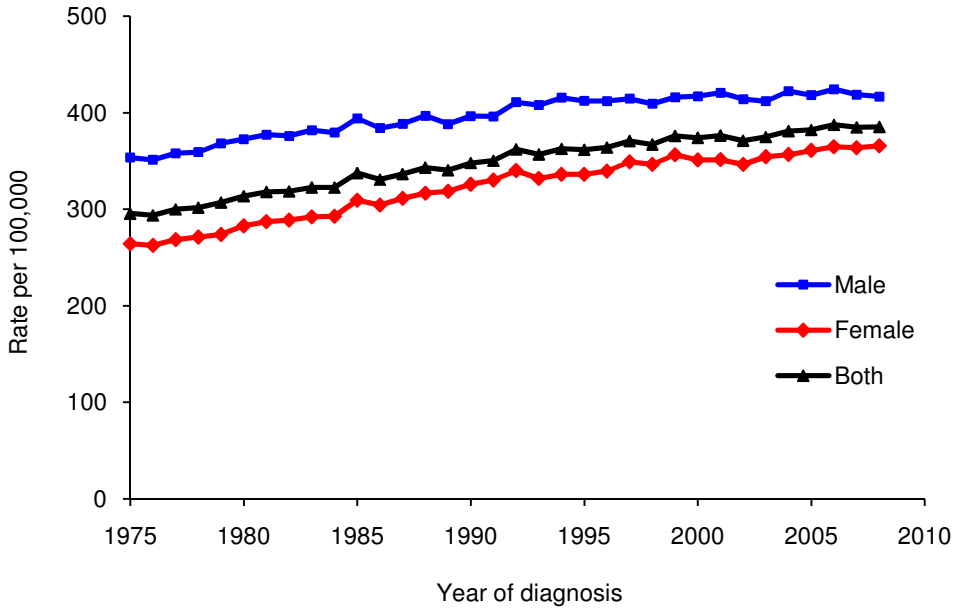

Figure 1.1 The incidence rates for cancers in the UK
The European age-standardised incidence rates for all cancers in the UK between 1975 and 2008. Data taken from http://info.cancerresearchuk.org/

There are many different forms of cancer which can affect numerous tissues and organs of the body. However, lung, breast, colorectal, stomach and liver cancer are among the five most

common cancers in the world in terms of new cases being diagnosed [2]. Although there are similarities in the patterns of incidence around the world, there are geographical differences with certain cancers being more prevalent than others. Liver cancer, for example, is significantly more common in developing countries as compared to developed countries and the converse is true of prostate cancer [3]. Furthermore, studies of migrants have shown changes in risk associated with migration, with rates becoming similar to those found in the local population. Higher rates of breast cancer are observed after migration from European countries of relatively low risk, such as Italy and Poland, to Australia where rates are higher [2]. Similarly, male Jews born in Europe or the United States, have a higher risk of developing colon cancer than those born in Asia or Africa [4]. Although genetic factors have some role to play, these differences can mainly be accounted for by variations in environmental factors and lifestyle, which are important influences in determining the onset of cancer. Some estimates suggest that 80 - 90% of cancers are potentially preventable through reducing environmental and lifestyle risk factors [5]. Poor diet [6], smoking [7] and excessive alcohol consumption [8] have all been associated with an increase in the incidence of cancer. Other factors linked to the development of cancer include infection with hepatitis B and C viruses, excessive exposure to sunlight, ionising radiation and environmental chemicals.

The high prevalence and increasing incidence of cancer, combined with the rise in life expectancy, and changes in environment and lifestyle, highlight the importance of tackling this disease, through both prevention and treatment.

1.1.1 Carcinogenesis

Carcinogenesis refers to the process by which cancers are generated through a multistep mechanism, and involves the transformation of a normal cell into a cancer cell. The sequence of events which take place during the course of carcinogenesis can be separated into three distinct phases; initiation, promotion and progression [9], [10]. The initial critical event is a mutation in the deoxyribonucleic acid (DNA) sequence, which can be brought about by man-

made or natural chemicals, radiation, physical agents and viruses, or as a result of errors in DNA replication and repair. Initiation is a rapid and irreversible process involving a chain of extracellular and intracellular events. These include the initial uptake or exposure to chemical or physical carcinogens and their transport to organs and tissues where detoxification or metabolic activation can occur, followed by the induction of DNA damage [11]. Examples of chemical carcinogens include tobacco smoke, diesel exhaust and certain pesticides. Some of the most common forms of physical carcinogens are radiation, and fibrous particles including asbestos. Chemical carcinogens can be broadly classified as genotoxic or nongenotoxic. Unlike genotoxic chemicals, nongenotoxic agents (for example steroid hormones, infectious agents such as the hepatitis B virus and chemical irritants) have carcinogenic effects without interacting directly with the DNA, and they are thought to exert their effects by increasing cell proliferation [12].

The promotion phase of carcinogenesis, which is a much longer stage, involves the proliferation and expansion of initiated cells as a result of altered gene expression [13]. Finally, during the progression phase there is a continued expansion of cells containing multiple mutations. The last stage is an extension of promotion, and leads to the growth and formation of tumours due to additional genetic alterations. Both promotion and progression phases are prolonged and the cycle of events may take many years.

The stages of carcinogenesis were deduced primarily from studies in animal models and also from epidermal cell culture experiments [14]. These early experiments involved chemical induction of tumours by use of known skin carcinogens in mice, and exposure of mouse epidermal cells to carcinogens *in vitro*. The initiation phase was found to require a single application of 7,12-dimethylbenz[α]anthracene (DMBA) to mouse skin, whereas repeated applications of 12-O-tetradecanoylphorbol-13-acetate (TPA) resulted in tumour promotion [15]. A simplified diagram outlining the various stages of carcinogenesis is given in Figure 1.2.

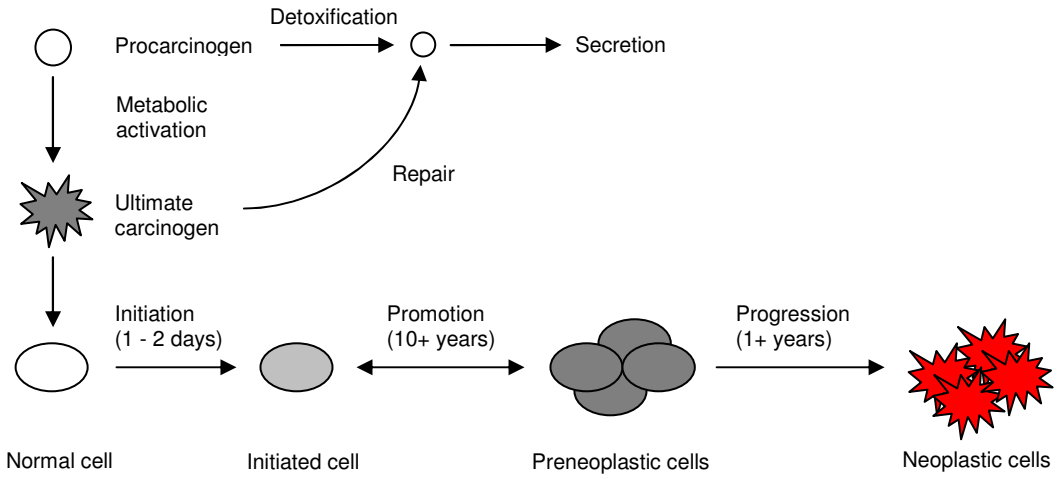

Figure 1.2 Representation of the multi-stage process of carcinogenesis
Carcinogenesis is initiated as a result of DNA damage induction and generation of fixed mutations. Most carcinogens require metabolic activation *in vivo*, which can result in the formation of initiated cells. Initiated cells can undergo tumour promotion into preneoplastic cells following exposure to promoting agents, which progress to neoplastic cells.

1.1.2 Colorectal cancer

Colorectal cancer, also often referred to as colon cancer or bowel cancer, affects the lower part of the digestive system – the large bowel and the rectum. Colorectal cancers are thought to arise from irregular growths in the colon, called adenomatous polyps. These pre-malignant lesions, which are often benign, are the result of molecular and cellular alterations [16]. Some of these changes include alterations in oncogenes, loss of tumour suppressor genes, and abnormalities in genes that are involved in DNA repair [17].

Worldwide, colorectal cancer affects over a million people every year. It ranks third in frequency of incidence, and death due to this cancer affects similar numbers of men and women [2]. The incidence of this disease varies significantly between developing and developed countries, with rates increasing with industrialisation and urbanisation [18]. Experimental and epidemiological data indicate the importance of components of the Western diet in modulation of this disease, which may account for these differences. For example, a high intake of red meat is related to

an elevated risk of colorectal cancer, whereas a diet rich in fibre or vegetables may be protective [19]. A link between alcohol intake and colon cancer has also been demonstrated; in men and women with an alcohol intake of 30 g/day or greater (≥ 2 drinks/day), there was a modest relative elevation in colon cancer, mainly at the highest levels of alcohol intake [20]. In addition, smoking [21] and lack of physical activity [22] have been shown to be other associated risk factors. It is possible that an improvement in diet may reduce the likelihood of developing colon cancer, for example olive oil consumption and colorectal cancer incidence has been investigated, and after allowing for other dietary factors, olive oil was found to be negatively associated with the disease [23]. However, further studies are required to evaluate how components of the diet may affect this disease.

Another important determining factor is age; increasing incidence is observed with age, with the disease becoming more prevalent after the age of forty, and rising steeply until the age of eighty [24]. Figure 1.3 shows how colon cancer occurrence changes with age in the UK population.

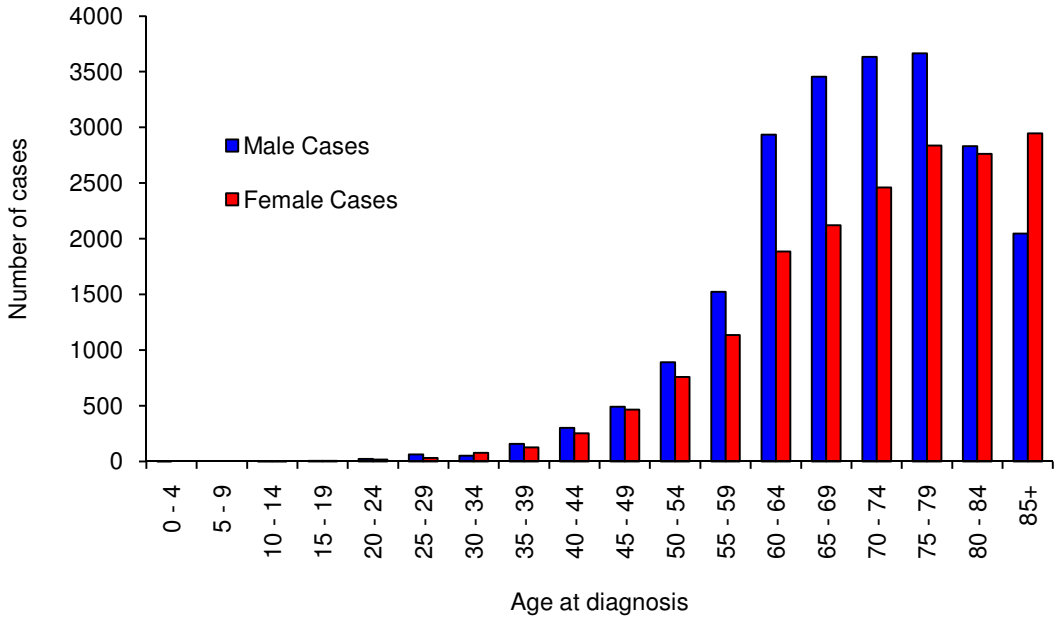

Figure 1.3 The occurrence of colon cancer in relation to age
Occurrence rates of colon cancer measured in the UK in 2008. Data taken from http://info.cancerresearchuk.org/

Stronger risk factors for developing this form of cancer include inflammatory bowel disease and the genetic disorder, familial adenomatous polyposis (FAP). FAP is an autosomal dominant inherited disease with variable phenotypic expression. FAP has been linked to germline mutations of the adenomatous polyposis coli (*APC*) gene that encodes a protein with important functions in the regulation of cell growth [25]. Sufferers have almost 100% risk of developing this cancer [26]; however, the risk is reduced significantly when patients enter a screening-treatment program [27]. The majority of young patients diagnosed with FAP undergo early colectomy [28].

1.1.3 Treatment of colorectal cancer

Colorectal cancer may take many years to develop and early detection and treatment are extremely important as advanced stages have poorer prognosis [29]. However, many of the symptoms of colorectal cancer are non-specific, such as a change in bowel habit, general abdominal discomfort, weight loss and tiredness, and therefore, concerted efforts at early screening programmes are crucial [30].

The staging of colorectal cancer is essential when considering treatment options particularly in the non-metastatic setting. Dukes' cancer staging is based upon how far the cancer has penetrated into the lining of the colon [31]. A more recent and common staging system is the tumour/nodes/metastases (TNM) system, which takes into account whether the cancer involves lymph nodes and has spread to other organs. When caught in the early stages, average survival figures are good, but unfortunately many patients present when the disease is metastatic and the purpose of treatment is to improve survival whilst maintaining a good quality of life.

When the cancer is localised, the aim of treatment is to try and cure the patient with a complete removal of tumour/cancerous growth. Surgical resection of the primary tumour (along with the nearby lymph nodes) remains the main chance of cure when the cancer is limited to the bowel

[32]. Following the complete removal of a cancer by surgery, cancer cells can still remain in the body and continue growing, causing relapse, and therefore chemotherapy is often also used. Chemotherapy can be used in the neoadjuvant (prior to surgery) or adjuvant (post surgery) setting, or as the primary therapy (palliative). Clinical trials have convincingly demonstrated that postoperative adjuvant chemotherapy is of benefit to all patients with node-positive disease [33].

Some of the key chemotherapeutic drugs used to treat colorectal cancer patients include 5-fluorouracil (5-FU), capecitabine, irinotecan and oxaliplatin plus 5-FU in combination [34]. The majority of chemotherapeutic drugs can be divided into alkylating agents, antimetabolites, anthracyclines, plant alkaloids and topoisomerase inhibitors. All of these drugs affect cell division or DNA synthesis in some way. The benefits that chemotherapeutic drugs may confer include an improvement in the quality of life and/or an increase in life expectancy. However, the common side effects associated with these medicines include mouth ulcers, diarrhoea, and lowered resistance to infection [35]. Specially targeted delivery vehicles aim to increase effective levels of chemotherapy for tumour cells compared to normal cells for an increased tumour kill and/or reduced toxicity. Most colorectal cancers should be preventable through increased surveillance, improved lifestyle, and perhaps the use of dietary chemopreventive agents. Reducing the risk and preventing the onset of cancer would clearly be an ideal solution.

1.2 Cancer chemoprevention

Chemoprevention can be defined as the use of agents to inhibit, or delay the development of cancer either by blocking the DNA damage that initiates carcinogenesis, and/or by arresting or reversing the progression of premalignant cells in which such damage has already occurred [36].

Chemopreventive agents can be synthetic or naturally derived, and may form part of existing diets. Determination of the lack of toxicity of chemopreventive agents is extremely important, as long term administration of agents should be possible with few or no adverse effects. This

makes naturally derived compounds particularly attractive for research in this field. Some examples of chemoprevention trials with synthetic and natural agents, in relation to colorectal cancer are discussed in more detail here.

1.2.1 Synthetic and naturally-derived agents evaluated for the chemoprevention of colon cancer

1.2.1.1 Aspirin

The group of drugs that has generated the most interest in the context of colorectal cancer prevention are the non-steroidal anti-inflammatory drugs (NSAIDs), which inhibit cyclooxygenase (COX) enzymes. COX-2, also called prostaglandin H_2 synthase, is an enzyme which catalyses the first stage in the oxidation of arachidonic acid to prostaglandin H_2, a precursor for the prostaglandins (e.g. PGE_2), which can stimulate tumour cell growth [37]. COX-2 is involved with tumour promotion during colorectal cancer progression, and is often overexpressed in human cancer tissue including colorectal neoplasms [38]. To assess the role of COX-2 in tumourigenesis, the effects of COX-2 gene knockouts have been tested in *Apc*$^{\Delta 716}$ mice, a model of human familial adenomatous polyposis. Knockout mice had a dramatically reduced number and size of intestinal polyps compared to mice with both genes [39]. Therefore, inhibition of the COX-2 enzyme can be used as a target for colorectal cancer prevention and therapy.

Population based studies have provided evidence to suggest that NSAIDs such as aspirin can lead to a reduction in the relative risk of developing colorectal cancer [40]. In a large US cohort of male health professionals aged between 40 - 75, the relationship between aspirin and other NSAID use and the risk of colorectal adenomas, and cancer incidence was examined [41]. Regular users of aspirin (≥ 2 times per week) were shown to have a lower risk for total and advanced colorectal cancer (after adjusting for variables such as age and history of polyps). This association was even stronger in respondents who used aspirin consistently. A reduction

in cancer death rates of the oesophagus, stomach, colon, and rectum, following more frequent aspirin use has also been reported [42]. For each of these cancers, mortality rates were approximately 40% lower among those who used aspirin 16 times/month or more for at least a period of one year, compared to those who did not take aspirin.

Despite the benefits of aspirin, use of this drug for cancer prevention in healthy individuals has been limited by its gastrointestinal (GI) and renal toxicity. NSAIDs have reported to be associated with a two- to four-fold increase in GI complications including ulcers and bleeding, and their use accounts for thousands of hospitalisations and deaths each year [43].

1.2.1.2 Celecoxib

Another synthetic NSAID that has undergone clinical testing is celecoxib. Unlike aspirin, celecoxib is a selective COX-2 inhibitor. The effect of celecoxib on colorectal polyps in 77 patients with FAP was recorded in a double-blind, placebo-controlled trial in which patients received either 100 or 400 mg of celecoxib twice daily and underwent endoscopy at the beginning and end of the study [44]. The response to treatment was expressed as percentage change from the baseline number and size of polyps. After six months, patients who received 400 mg of celecoxib twice daily had a 23.5% reduction in the mean number of colorectal polyps, compared to the placebo group. A smaller, but still significant reduction compared to the placebo group was observed in the patients receiving 100 mg of celecoxib twice daily (6.5%) [44]. A separate six-month study, which examined the effect of a 400 mg twice daily dose, also found a significant reduction in duodenal polyposis following repeated celecoxib use [45].

While these studies demonstrate the efficacy of celecoxib in reducing polyp recurrence, there is also evidence to suggest cardiovascular risk associated with celecoxib usage. Celecoxib at 200 or 400 mg taken twice daily or 400 mg daily elevated blood pressure and increased myocardial infarction, stroke and heart failure by almost double [46]. The mechanism by which celecoxib may increase these effects is not fully understood and warrants further investigation.

1.2.1.3 Curcumin

The phenolic compound curcumin, which is an active constituent of turmeric and is derived from the dried roots of the plant *Curcuma longa*, has been investigated as a potential chemopreventive agent, (as reviewed recently by Shureiqi and Baron [47]). This has involved studies in preclinical mouse models of intestinal tumourigenesis as well as a number of human clinical trials. The effects of a curcumin diet on azoxymethane-induced colon carcinogenesis were investigated in male F344 rats. Rats fed on a supplemented diet containing 2000 ppm of curcumin had a lower incidence of colon adenocarcinomas and smaller tumour volumes (reduced by > 57%) compared to those fed on a controlled diet [48]. Similarly, a separate study which used the multiple intestinal neoplasia (Min) mouse as a model of FAP in humans, showed that 0.2% and 0.5% curcumin in the diet reduced colon adenoma multiplicity by 39% and 40% respectively [49].

The safety of curcumin has been assessed in a number of human clinical trials [50], [51]. In the first of these trials, single oral doses administered to healthy volunteers ranged from 0.5 - 12 g per day and these were found to be safe, with minimal toxicity [50]. On a dose escalation study in 25 cancer patients, these same doses were taken for a period of three months. Curcumin was not toxic at doses of up to 8 g per day. The bulky 12 g daily doses were unacceptable to patients [51]. Histological improvements were seen in seven patients, whereas two patients developed malignancy despite treatment. In an independent study, where patients with advanced colorectal malignancy were given curcumin (36 - 180 mg) daily for up to four months, five out of fifteen had stable disease at four months of follow-up evaluation [52]. The inhibition of the growth of pre-cancerous and cancerous cells, without affecting healthy cells is the ultimate aim of cancer chemoprevention, particularly with agents which may need to be administered in the long-term in healthy individuals [53]. Overall, the results of the above trials supported a biological effect of curcumin in the chemoprevention of cancer. However, no placebo groups were used in any of these trials, making it difficult to draw definite conclusions, and further trials with curcumin are required.

1.3 Overview of molecular pathways potentially relevant to chemopreventive agents

1.3.1 Cell cycle progression

Several pathways and processes are involved in the events which lead to cell division. This series of ordered and tightly-regulated processes is called the cell cycle, and can be characterised by different stages through which cells pass [54]. The somatic cell cycle is divided into four distinct phases, as shown by Figure 1.4.

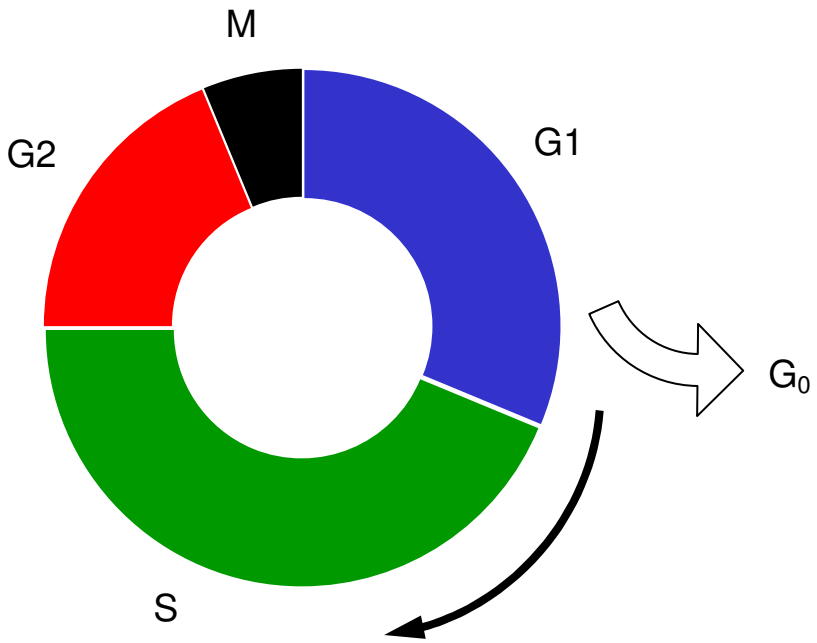

Figure 1.4 Stages of the normal eukaryotic cell cycle

The four stages of the cell cycle, characterised by G1, S, G2 and M phases. In G1 and G2 (gap) phases cells grow in size in preparation for division. During the S (synthesis) phase, DNA is replicated, and in the M (mitosis) phase, cell division occurs, giving rise to daughter cells. Cells can enter a quiescent state, termed G_0. The solid arrow indicates the direction of the cycle and the size of the coloured segments indicates the relative amount of time cells normally spend in each stage of the cycle.

During the first and second phases (S and M phases respectively), cells undergo basic events in cell division such as generation of a single and faithful copy of its genetic material (synthesis or S phase), and partitioning of all of the cellular components between two identical daughter cells (mitosis or M phase). These processes of DNA synthesis and mitosis are separated by 'gap' periods (G_1 and G_2), during which RNA and proteins are synthesised and there is a rearrangement of cells in preparation for the successful completion of the S and M phases respectively [55]. Once cells have stopped cycling after division, due to alterations in the mitogenic signalling, they enter a state of quiescence (G_0).

In tumour cells, the duration of the cell cycle is the same length or longer than that of the normal cell cycle. However, in tumour cells there are a higher proportion of cells that are in active cell division (compared to quiescent cells in G_0 phase). The uncontrolled proliferation is characteristic of tumour cells. Molecular analysis of tumourous tissue has shown that cell cycle regulators are frequently mutated in human tumours, which highlights the importance of maintenance of the cell cycle in the prevention of human cancer [56]. Several proteins, such as the cyclins and the cyclin-dependent kinases (CDKs) are known to regulate the timing of events in the cell cycle. Overexpression of the G1 phase cyclin, cyclin D1, is commonly observed and associated with human malignancy in colonic tumours [57]. Numerous dietary agents, including genistein and curcumin as well as 13-*cis* retinoic acid have been shown to block the deregulated cell cycle in cancer cells *in vitro* [58].

1.3.2 Apoptosis

Apoptosis, programmed cell death or 'cell suicide', is a vital physiological process required for the elimination of damaged or abnormal cells. It can be triggered by a variety of physiological signals, resulting in a disruption and breakdown of cellular membranes and ultimately finishing with the cell corpse being engulfed by nearby phagocytic cells [59].

Defects in apoptosis allow neoplastic cells to live beyond their normal lifespan, accumulate genetic mutations, sustain growth under hypoxia and oxidative stress, and promote tumour angiogenesis. Evasion of apoptosis is recognised as one of the six essential alterations in cell cycle physiology that dictates malignant growth and is a hallmark of most, and perhaps all types of cancer [59]. Due to the complex nature of apoptosis, it is unlikely that the activation or inactivation of a single component of the cell signalling mechanism will alter the ultimate fate of the cell and lead to programmed cell death. Many growth factors and their receptors, as well as their membrane, cytoplasmic and nuclear downstream effectors have been identified as oncogenes or tumour-suppressor genes [55]. One major feature of apoptosis is the activation of the caspases. These are a family of proteases whose substrates include large protein precursors capable of destroying endonucleases; as well as proteins involved in DNA repair, ribonucleic acid (RNA) splicing, signal transduction and transcription [54].

A possible strategy for preventing cancer is the development of compounds for the promotion of apoptosis in targeted premalignant and cancer cells. Some of the agents with chemopreventive activity that have been shown to induce apoptosis through the activation of caspases, include curcumin [60], apple polyphenols [61] and silibinin [62].

1.3.3 Senescence

Cells respond to DNA damage by alterations in regulation of the cell cycle, the induction of apoptosis and senescence, all of which have been proposed to reduce the number of cancerous cells [63]. Cellular senescence is a response to nonlethal stress that results in persistent cytostasis with a distinct morphological and biochemical phenotype [64]. Senescent cells are also permanently removed from the cell cycle [65], and limit excessive aberrant proliferation, therefore, the state of senescence protects against the development of cancer [66]. The analysis of senescence markers, such as the expression of β-galactosidase allows determination of this process. β-galactosidase is expressed in several human cell lines upon senescence in culture, but not in presenescent cells [67]. One of the mechanisms by which

selenium can act as a chemopreventive agent following DNA damage, is through induction of senescence, which inhibits cancer cell proliferation [63].

1.4 Resveratrol

The phytochemical resveratrol (*trans*-3,5,4′-trihydroxystilbene; Figure 1.5) is a naturally occurring polyphenol which can be found in a number of plants including *Polygonum cuspidatum* and *Vitis vinifera* (grapevines). It is produced in response to environmental stress such as exposure to ultraviolet radiation, injury or pathogenic attack. When *V. vinifera* is infected with the *Botrytis cinerea* fungus, resveratrol is synthesised in the grape skin and has a defensive role, resulting in a significant reduction of the fungus [68]. Resveratrol is also an antioxidant [69].

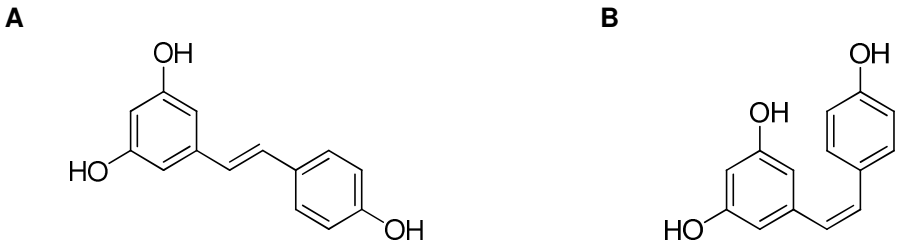

Figure 1.5 Chemical structures of resveratrol
Resveratrol exists in the *cis* and more stable *trans* isomeric form [70]. The chemical structures of *trans*-resveratrol (*trans*-3,4′,5-trihydroxystilbene) (**A**) and *cis*-resveratrol (**B**), both have a molecular weight of 228.2.

The presence of resveratrol in plants consumed by humans is limited. In Western diets, the major sources of resveratrol include red grapes (particularly the skins), wine, mulberries, peanuts and peanut products [71]. Analysis of resveratrol concentrations in wine have been shown to be consistently higher in red compared to white wine. In red wines, the amount of resveratrol may generally vary between 0.5 to 10 mg/l [72]. In contrast, with the exception of

Swiss and German wines, virtually all white wines tested in a global survey of levels in commercial wines, gave values of <0.1 mg/l [73]. This variation can be attributed to differences in the production process. Although both types of wine are produced by fermentation, red wine is fermented in the presence of the grape skins for a longer period (maceration), which allows more time for the resveratrol to be absorbed into the wine. Maceration of the resveratrol-containing grape skins has a big effect on resveratrol levels, with an approximate 10-fold increase in macerated (red) wines compared to non-macerated wines [72]. Resveratrol concentrations present in peanuts are also dependent upon numerous factors including cultivar, growing season, weather conditions, and peanut maturity [74].

Traditionally, in Chinese and Japanese medicine, resveratrol extracts taken from the roots of *P. cuspidatum* have been used as a medicine against a number of conditions including suppurative dermatitis, gonorrhoea, favus, athlete's foot and hyperlipemia [75]. Resveratrol has also been introduced into the diet through Itadori tea, which has long been used in Japan and China as a traditional herbal remedy for cardiovascular problems such as heart disease and strokes [76]. The potential benefits of resveratrol relating to cancer chemoprevention first came to light following the publication of a seminal paper by Jang and colleagues in 1997 [77]. It was in this study that the effects of resveratrol on the various stages of carcinogenesis were first explored, sparking new interest in the compound.

1.4.1 Cancer chemopreventive activity of resveratrol *in vitro* and possible mechanisms of action

In order to evaluate resveratrol as a potential chemopreventive agent, an understanding of the possible mechanisms engaged by the compound are necessary. This has led to many studies on the different targets which resveratrol may modulate, using a variety of *in vitro* cell models, including several cancer cell lines. Resveratrol has the ability to cause cell cycle arrest, trigger apoptosis, activate p53 and suppress the nuclear factor-kappa B (NF-κB) transcription factor through blocking inhibitory-kappa B (i-κB) kinase. Resveratrol has been demonstrated to have

antioxidant properties and inhibited TPA-induced free radical formation in cultured HL-60 leukaemia cells, with a half maximal inhibitory concentration (IC_{50}) of 6.2 µM [78]. In addition, resveratrol can act as an antimutagenic agent, thus preventing initiation. A brief summary of some of the mechanisms of resveratrol action *in vitro* are outlined in Table 1.1.

Mechanism	Experimental system
Inhibition of growth	Multiple cell lines
Induction of apoptosis	Leukaemia cells
Induction of p53-independent apoptosis	Colon tumour cells
Inhibition of cytochrome P450 enzymes: CYP1A1, CYP1B1, CYP3A4	Liver cells, microsomes, recombinant enzymes
Inhibition of oxygen radical formation, nitric oxide production	Macrophages
Activation of p53	Mouse epidermal cells
Activation of c-jun kinase	Mouse epidermal cells
Decrease in COX-2 expression	Mammary epithelial cells
Increase in p21/Cip1, cyclins D1, D2, E; decrease in CDKs 2, 4, 6	Epidermal carcinoma cells
Inhibition of protein kinase C activity	Gastric cells
Inhibition of protein kinase D activity	Fibroblasts
Inhibition of NF-κB activation	Monocytes, macrophages
Inhibition of NF-κB and AP-1 activation	Myeloid, lymphoid, epithelial cells
Induction of quinone reductase	Hepa 1c1c7 murine cells
Activation of NRF2	Human alveolar epithelial (A549) cells
Activation of SIRT and induction of autophagy	Human colon carcinoma (HCT-116) cells
Activation of AMPK	ER-positive and ER-negative breast cancer cells

Table 1.1 Mechanisms of resveratrol *in vitro* related to cancer chemoprevention. A summary of the key mechanisms of resveratrol action *in vitro* related to cancer chemoprevention. Adapted from [79]. Additional mechanisms may also be involved, including as yet unidentified mechanisms.

There are many additional cellular and biochemical mechanisms that resveratrol has been found to act upon. These include inhibition of cellular events associated with all stages of carcinogenesis. Some of the key *in vitro* mechanisms will be discussed in more detail in the remainder of this section.

Resveratrol inhibited the growth of HCA-7 and HT-29 colon cancer cells, with IC_{50} values of between 6 and 26 μM in one study [80]. Reduction in cell number has at least partly been attributed to the induction of apoptosis in colon cancer cells [81]. In SW480 colon cells, resveratrol in the 10 - 100 μM range caused caspase-9 and downstream caspase-3 activation and resulted in induction of apoptosis [82]. The same caspases were altered in an independent investigation [81] and caspase-3 dose-dependent activation has also been demonstrated in HT-29 cells [83]. In HCT-116 colon cancer cells caspase-6 was highlighted as being responsible for resveratrol-triggered apoptosis following resveratrol treatment [84].

In the Caco-2 adenocarcinoma cell line, resveratrol inhibited cell growth and proliferation of cells in a dose-dependent manner, at concentrations of 12.5 - 200 μM [85]. Changes in cell cycle progression were also observed, with a reduction of cells in the G2/M phase and an increase in cells in S phase. The levels of cyclin D1 and CDK 4 proteins were reduced, and in addition, resveratrol enhanced the expression of cyclin E and cyclin A [85]. An increase in expression of these cyclins is correlated with an accumulation of cells in the S phase. Similar results were obtained for the colon carcinoma cell line HCT-116 (which lacks COX protein expression), indicating that cell cycle inhibition by resveratrol in this cell line is independent of COX. When HCA-7 cells were incubated with varying concentrations of resveratrol for 48 or 96 h, COX-2 expression was downregulated. COX activity was also found to be inhibited in isolated enzyme preparations with resveratrol, providing further confirmation that alterations in cell cycle inhibition and apoptosis can occur independently of this pathway [80].

The anti-initiation activity of resveratrol has been linked to the suppression of the metabolic activation and/or induction of detoxification of carcinogens through modulation of enzymes involved either in phase I reactions (cytochrome P450 enzymes (CYP)) or phase II conjugation

reactions [86]. The ability of resveratrol to affect drug interactions was assessed by measuring the potential inhibition on specific CYP isozymes. Resveratrol marginally inhibited CYP3A4 and was a weak inhibitor of CYP2C19 [87]. In separate studies resveratrol inhibited CYP1A1 [88] and induced phase II detoxification enzymes [89]. In the latter of these studies, messenger RNA (mRNA) of three metabolizing enzymes, two isoforms of UDP-glucuronosyltransferases, UGT1A1 and UGT2B7, and a sulfotransferase, ST1E1 all increased in cells pretreated with 10 μM resveratrol for 24 h. These results were correlated with an increase in protein expression, particularly after 48 h of treatment [89].

Resveratrol can affect p53, which is one of the most important tumour-suppressor genes, and mutation or loss of p53 protein function is related to more than half of human cancers [90]. Resveratrol-induced apoptosis was only found to occur in cells expressing wild-type p53 ($p53^{+/+}$), but not p53-deficient cells ($p53^{-/-}$) [91]. These results demonstrate that resveratrol induces apoptosis through activation of p53 activity, suggesting that its anti-tumour activity may occur through the induction of apoptosis. Results from many of the *in vitro* studies support the potential benefits of resveratrol as a chemopreventive agent. Concentrations of resveratrol thought to elicit beneficial changes vary widely in these studies, but are generally between the 10 and 100 μM range [79]. Resveratrol dosing studies in animals provide a useful way of determining achievable concentrations *in vivo*, and are considered in the following section.

1.4.2 Cancer chemopreventive activity of resveratrol *in vivo* and possible mechanisms of action

To aid our understanding of cancer and the development of dietary chemopreventive agents, there has been a focus on effects in animals, particularly mouse models of carcinogenesis. Preclinical animal models allow compounds to be evaluated in a controlled environment, at relatively low cost with no threat to human safety, prior to clinical testing. The relatively short lifespan of these animals also allows rapid efficacy screening of potential agents whilst providing vital information on toxicity. Studies using the whole animal provide an integrated

system which takes into account bioavailability, metabolism and interaction with target molecules within the animal, which cannot be assessed fully using *in vitro* models. The key findings from the *in vivo* rodent studies investigating the chemopreventive effects of resveratrol on colorectal cancer are summarised in this section, and discussed further in Chapter 4.

The first published study of resveratrol reporting its anticancer effect demonstrated that it was able to interfere with all three stages of carcinogenesis, in the DMBA-induced mouse skin cancer model [77]. In this study, resveratrol inhibited the development of preneoplastic lesions and the number of tumours in mice by up to 98%, following a 25 µM twice-weekly dose for 18 weeks (applied topically) [77]. Resveratrol is more commonly administered as a component of the diet, either through supplementation of the feed, or drinking water, which can be ingested over a matter of days or weeks. The route of administration may potentially influence the concentration of resveratrol at the target site(s) of action. In a study where 8 mg/kg/day of resveratrol was administered intragastrically to 1,2-dimethylhydrazine (DMH)-induced Wistar rats, resveratrol supplementation was shown to cause a significant reduction in tumour number, incidence and size compared to control animals [92]. In addition, resveratrol significantly inhibited the development of aberrant crypt formation.

Another widely employed model of colorectal carcinogenesis for assessing chemopreventive activity in rodents includes the *Apc*$^{min+}$ mouse model. *Apc*$^{min+}$ mice have a mutation in the *APC* gene which is thought to be of central importance in the development of neoplastic growth. Therefore, the Min (multiple intestinal neoplasia) strain of laboratory mouse and its derivatives permit the study of factors that regulate the transition between normal and neoplastic growth. In a dosing study where resveratrol was administered to *Apc*$^{min+}$ mice orally through their drinking water (0.01% resveratrol in the drinking water for seven weeks), resveratrol was shown to significantly inhibit the formation of colon tumours and reduce the formation of small intestinal tumours by 70% in treated mice compared to the control groups [93]. Comparison of the expression of genes following resveratrol treatment showed that resveratrol downregulated genes that are directly involved in cell cycle progression or cell proliferation (cyclins D1 and D2, DP-1 transcription factor, and Y-box binding protein). Resveratrol also upregulated several

genes that are involved in the activation of immune cells (cytotoxic T lymophocyte Ag-4, leukaemia inhibitory factor receptor and monocyte chemotactic protein 3), highlighting the multiplicity of the molecular targets of resveratrol [93].

In a separate investigation where resveratrol was administered to male F344 rats for 100 days at a dose of 0.2 mg/kg/day (also in drinking water), there was a significant reduction in the formation of aberrant crypt foci preneoplastic lesions of the colonic mucosa [94]. An increase in the level of apoptosis was observed in isolated aberrant crypt foci compared to control animals, which was thought to contribute to the reduced growth of the foci [94]. Following supplementation of 0.2% resveratrol in the diet of *Apc*$^{min+}$ mice over a 3-week period, a 27% reduction in adenoma load was observed [80]. Furthermore, levels of PGE_2, which can stimulate tumour growth, were ~45% - 62% lower in the mucosa of treated mice compared to those mice on a control diet, suggesting a potential mechanism through which resveratrol may reduce adenoma formation. Resveratrol has also been shown to have mechanistic effects on additional targets related to tumour development, such as reducing the activity of both COX-1 and COX-2 [95]. Long-term inhibition of COX activity has been shown to significantly reduce the risk of developing cancers, and deletion of the gene responsible for encoding COX-2 in mice has a protective effect in mouse models of carcinogenesis [39].

1.5 Resveratrol clinical trials in humans

The majority of work investigating the effects of resveratrol has been undertaken in preclinical studies, whereas data describing the pharmacokinetic (PK) and pharmacodynamic (PD) effects of resveratrol in a clinical setting are less common. To determine the potential benefits of resveratrol to humans and obtain information on its distribution, metabolism and bioavailability, clinical trials in humans are necessary.

Resveratrol was first suggested as having cardiovascular health benefits based on the observation that the French have a relatively low level of heart disease despite a diet that is

high in saturated fat. [96]. It was their relatively high intake of red wine that was thought to account for these findings, and this is often referred to as the 'French paradox'. Epidemiological studies have shown an inverse correlation between red wine consumption and cardiovascular disease, or disease risk factors [96], [97]. This led to investigations into the pharmacological properties of resveratrol as a cardioprotective agent. For example, in the rabbit, resveratrol has been shown to reduce excessive aggregation of platelets which can cause blockages in veins, resulting in myocardial infarction, or stroke, in a concentration-dependent manner [98]. In feeding experiments where drinking water was supplemented with resveratrol for 15 days, there was an improved recovery in function and coronary flow of hearts isolated from rats [99]. In a clinical study involving 48 non drinkers or rare drinkers of red wine, risk factors relating to atherosclerosis, heart disease and certain inflammatory biomarkers were examined following daily consumption of 250 ml of Sicilian red wine for four weeks. The wine consumption was shown to have a positive effect on many of the risk factors measured, such as a reduction in the harmful low-density lipoprotein (LDL) [100].

Resveratrol clinical trials performed to date have aimed to investigate the potential role of resveratrol in the management of type 2 diabetes, obesity, Alzheimer's disease and cancer [101]. An up-to-date review of the current clinical trials and those which are actively recruiting can be found at http://clinicaltrials.gov/. The trials relating to the pharmacokinetics and pharmacodynamics of resveratrol, which are important for the general clinical development of resveratrol for all diseases, are discussed in section 1.5.1 and 1.5.3 respectively. The published studies of resveratrol in humans following single and multiple dosing of resveratrol are summarised in brief in Tables 1.2 and 1.3 respectively. These studies have employed a range of doses and dosing regimens, as well as a variety of resveratrol formulations for administration.

Cohort	Form of resveratrol	Resveratrol dose	Dosing schedule	Study outcome	Reference
Healthy males (12)	Delivered in white wine, white grape juice or vegetable juice.	25 mg/70 kg	Single	Resveratrol absorption was similar in all three matrices.	[102]
Healthy males (3)	Dissolved in 5 ml whisky mixed with 50 ml water.	0.03, 0.5, or 1 mg/kg	Single	Pharmacokinetic and metabolite profile.	[103]
Healthy males (3)	Delivered in grape juice (200, 400, 600 or 1200 ml).	0.32, 0.64, 0.96, or 1.92 mg	Single	Pharmacokinetic and metabolite profile.	[103]
Healthy males (3) and females (3)	^{14}C-resveratrol taken orally and intravenously.	25 mg (oral) and 0.2 mg (IV)	Single	Pharmacokinetic and metabolite profile.	[104]
Healthy males (11)	250 ml red wine.	5.38 mg	Single	Resveratrol and metabolites identified in low-density lipoprotein after moderate wine intake.	[105]
Healthy males (14) and females (11)	300 ml or 600 ml red wine, consumed after fasting, or with meals of varying lipid content.	246 µg, 480 µg, or 1.92 mg	Single	Resveratrol bioavailability was not influenced by food, or lipid content.	[106]
Healthy males (18) and females (22)	500 mg capsules.	0.5, 1.0, 2.5, or 5.0 g	Single	Pharmacokinetic and metabolite profile. Resveratrol did not cause serious adverse events.	[107]
Healthy males (9)	Dissolved in 100 ml of 15% ethanol, made up in low-fat milk to a total volume of 500 ml.	85.5 mg/70 kg	Single	Pharmacokinetic and metabolite profile. Resveratrol and its metabolites shown to have a high affinity for protein binding.	[108]
Healthy males (11)	250 ml red wine, 1 L grape juice, or 10 tablets.	14 µg/kg	Single	Bioavailability of resveratrol from wine and grape juice 6-fold higher than that from tablets.	[109]

Table 1.2 Summary of published single dosing clinical trials of resveratrol. Single dosing resveratrol clinical trials in humans. Figures in parentheses (column 1) refer to the number of participants in each study.

Cohort	Form of resveratrol	Resveratrol dose	Dosing schedule	Study outcome	Reference
Healthy males (12 young) and females (12 elderly)	Capsules.	200 mg	Single followed by multiple doses thrice daily (2 days) and a final single dose	Pharmacokinetic and metabolite profile. Resveratrol was well tolerated by young males and elderly female subjects.	[110]
Healthy males (4) and females (20)	Capsules.	250 or 500 mg	Multiple; once daily on 3 separate days	Doses of resveratrol can modulate cerebral blood flow variables.	[111]
Healthy males (20) and females (20)	Capsules.	25, 50, 100 or 150 mg	Multiple; six times/day, for 13 doses	Pharmacokinetic and metabolite profile. Resveratrol was well tolerated, but with some mild adverse events reported.	[112]
Healthy males (3) and females (5)	Capsules; taken with food, quercetin or 100 ml 5% alcohol.	2 g	Multiple; twice daily	Pharmacokinetic and metabolite profile. A high-fat meal reduced AUC and C_{max}. Resveratrol was well tolerated, although diarrhoea was frequently observed.	[113]
Male (9) and female (11) cancer patients	500 mg caplets.	0.5 or 1.0 g	Multiple; once daily for 8 days	Pharmacokinetic and metabolite profile in colon/tumour tissue removed from colorectal cancer patients.	[114]
Healthy males (11) and females (31)	500 mg caplets.	1.0 g	Multiple; once daily for 28 days	Resveratrol was shown to modulate enzyme systems involved in carcinogen activation and detoxification. Resveratrol was well tolerated.	[86]
Healthy males (10) and females (10)	300 ml sparkling wine or 200 ml either white wine or red wine.	0.357, 0.398 or 2.56 mg/day	Multiple; once daily for 28 days	Resveratrol metabolites in urine may be useful biomarkers of wine intake in epidemiological and intervention studies.	[115]

Table 1.3 Summary of published multiple dosing clinical trials of resveratrol. Multiple dosing resveratrol clinical trials in humans. Figures in parentheses (column 1) refer to the number of participants in each study.

1.5.1 Resveratrol pharmacokinetics and metabolism in humans

An understanding of the pharmacokinetics and metabolism of resveratrol through clinical studies is essential to defining appropriate human doses and evaluating its potential health impact. Additionally, this information is important for identifying clinically achievable concentrations of resveratrol/metabolites for use in preclinical mechanistic studies. Amongst the first of the pharmacokinetic investigations was that by Goldberg in 2003, which involved oral administration of resveratrol (25 mg/70 kg) to healthy male subjects (aged 25 - 45 years) in three different matrices; white wine, white grape juice and vegetable juice, in order to test its absorption [102]. Blood was taken prior to dosing and at four intervals over the first four hours after consumption (0.5, 1, 2 and 4 h). Urine was collected pre-dosing and for the 24 h post-dosing period. Highest recorded serum resveratrol/metabolite levels were achieved at 30 min post-dosing in all samples, and declined rapidly, reaching baseline levels within 4 h. Free resveratrol accounted for only a small fraction of the total dose in plasma (1.7 - 1.9%), with glucuronide and sulfate conjugates dominating the profile in both the plasma and urine. Resveratrol absorption was found to be broadly equivalent in aqueous and alcoholic matrices, but with peak resveratrol concentrations ≤ 40 nmol/l, levels were suggested to be inadequate for activity in cultured cells *in vitro* [102]. When a low dose of resveratrol (0.03 mg/kg, dissolved in whisky) was ingested with water in a separate investigation, the recovery of resveratrol in the circulating plasma suggested a rapid absorption of resveratrol in the gastrointestinal tract [103], consistent with the previous study [102].

In a more comprehensive study, the absorption, bioavailability and metabolic fate of resveratrol were followed through the use of radioisotope tracing. Radiolabelled ^{14}C-resveratrol was synthesised and administered orally to six healthy volunteers, at a dietary relevant dose of 25 mg [104]. An intravenous dose of 0.2 mg was also used to enable calculation of absolute bioavailability. Following oral dosing, the bioavailability of unchanged resveratrol was very low, due to rapid and extensive metabolism, resulting in high plasma concentrations (approximately 2 µM) of total conjugated resveratrol metabolites achieved 1 h post-dosing (for structures of metabolites, see Figure 1.7 and 1.8). A secondary peak, with a maximum concentration of

~1.3 µM was observed at 6 h post oral dosing only, indicative of enterohepatic recirculation. This secondary peak was followed by an exponential reduction in concentration of ^{14}C-labelled species. The high concentrations of radiolabelled compounds detected were largely a result of the rapid phase II metabolism of resveratrol to its various metabolites in the liver and intestines. A sulfate conjugate was detected in plasma 2 h after dosing (using fraction collection and radioactivity measurements), suggesting that sulfation could be an important process responsible for reducing the bioavailability of resveratrol. The identity of the sulfate conjugate was confirmed by incubation with aryl sulfatase, which resulted in a loss of the sulfate peak and the generation of a resveratrol peak. Despite the low systemic bioavailability of oral resveratrol, it had a very high absorption, estimated to be at least 70% [104].

In the same study, urinary analysis revealed that most of the radioactivity detected following oral dosing was recovered in the urine (53 - 85%), which is likely to be a major route of excretion of the hydrophilic resveratrol metabolite species. Liquid chromatography-mass spectrometry (LC-MS/MS) analysis was performed for samples taken from the 0 - 12 h urine collection following a larger dose of 100 mg unlabelled resveratrol. It revealed five major metabolites; two resveratrol monoglucuronides, a dihydroresveratrol monoglucuronide, a resveratrol monosulfate and a dihydroresveratrol sulfate. Sulfate conjugates accounted for approximately 24% of the dose in the urine, and glucuronides roughly half as much, with only trace amounts of resveratrol [104].

A phase I dose escalation study evaluated the safety and pharmacokinetics of 0.5, 1.0, 2.5 and 5.0 g of resveratrol administered as a single dose in healthy volunteers [107]. Plasma and urine concentrations of resveratrol and metabolites were determined by high performance liquid chromatography (HPLC-UV) and identified using LC-MS/MS. In addition, faecal samples were analysed pre- and post-dosing. The average resveratrol plasma concentration following 5 g dosing was 2.4 µM (539 ± 384 ng/ml; mean ± standard deviation (SD), n = 10), with levels of two monoglucuronides (resveratrol-3-*O*-glucuronide and resveratrol-4'-*O*-glucuronide) and resveratrol-3-*O*-sulfate three to eight-fold higher. Furthermore, the area under the plasma concentration-time curve (AUC) for these metabolites was up to 23 times greater than for

resveratrol. Additional metabolites detected were resveratrol-4'-*O*-sulfate and resveratrol disulfate, although these were relatively minor. Renal excretion of resveratrol and its metabolites was rapid, with 77% of all urinary agent-derived species excreted within 4 h following the 0.5 g dose. A secondary resveratrol peak was observed in the plasma, and a predominant amount of parent resveratrol detected in the faeces compared to the metabolites, consistent with the hypothesis that it undergoes enterohepatic circulation.

An important aspect of resveratrol pharmacokinetics is determining whether the drug reaches the proposed sites of action after oral ingestion in humans and determining the concentrations attained in target tissues [104]. Although this has been studied in detail in rodents [116], [71], it clearly presents challenges in humans.

1.5.2 Resveratrol safety and tolerability

If resveratrol is to be used as a chemopreventive agent, an important aspect for consideration is safety and establishing lack of toxicity. Comprehensive toxicological analyses have been conducted on 'high purity' resveratrol (Resvida™) in rats [117]. In a 28-day study, Resvida™ was not found to cause any adverse effects in rats at doses of 50, 150 and 500 mg/kg/day. Similarly, 90 days of Resvida™ administration at doses up to 700 mg/kg/day in rats was found to be safe. Resvida™ did not induce any adverse reproductive effects in an embryo-foetal toxicity study at a dose of 750 mg/kg/day [117]. Resvida™ was also shown to be readily absorbed, metabolised and excreted providing evidence that it is well tolerated and non-toxic. A number of separate investigations have also reported on the tolerability of resveratrol in rodents. When high doses of resveratrol were administered orally to male Sprague-Dawley rats at a dose of 20 mg/kg/day for 28 days, resveratrol did not cause any differences between control and treated groups for haematological or biochemical variables. In addition, examination of the organs at autopsy did not reveal any alterations [118].

An investigation, also in rats, evaluated toxicity following administration of significantly higher oral (gavage) resveratrol doses; 300, 1000 and 3000 mg/kg/day daily for four weeks. Adverse effects were evident, mainly at the highest dose and included increased signs of clinical toxicity, reduced final body weights and decreased food consumption. Increases in kidney weights and renal lesions were also observed. The reduced body weight gain (in females only) and elevated white cell count (in males only) was observed at the 1000 mg/kg per day dose [119]. No adverse effects were observed at the lowest dose of 300 mg/kg resveratrol per day. For a 70 kg person, this dose would equate to 21 g of resveratrol taken daily (based on a weight/weight conversion), which is considerably above doses given in resveratrol trials (Table 1.2 and Table 1.3).

There is a limited amount of information regarding resveratrol safety in humans, which has been assessed in only a small number of the clinical trials performed to date [113], [107], [120], [86], [112]. The most in-depth studies involved healthy volunteers ingesting single doses of 0.5, 1.0, 2.5 and 5.0 g of resveratrol [107]. Across all of the dose groups in the single dosing study, 58% of volunteers presented with one or more minor adverse events whilst on the trial. Out of the 40 volunteers, two showed evidence of grade 1 toxicity potentially relating to resveratrol. This included a rise in blood bilirubin in one volunteer and a rise in ALT (an enzyme involved in the metabolism of the amino acid alanine) in the second, with a return to normal the subsequent week; elevated serum levels of ALT are a sign of liver damage [107]. However, no serious adverse reactions were observed either clinically or by biochemical and haematological analyses following one-off resveratrol doses of up to 5 g resveratrol. The authors commented that the limited number of subjects did not permit a statistically valid conclusion about resveratrol safety.

In a separate investigation which recruited 42 volunteers onto a 1.0 g daily resveratrol-dosing regimen for four weeks, resveratrol was well tolerated [86]. The side effects observed were mainly mild and transient and were consistent with those observed in the trial described by Boocock *et al*. [107]. None of the clinical studies described above included a placebo control

group, and therefore it is difficult to completely attribute the effects of resveratrol ingestion to the side effects observed.

1.5.3 Resveratrol pharmacodynamics in humans

Currently, none of the clinical trials with resveratrol have exceeded more than a four-week period of dosing. Longer-term resveratrol studies are needed to assess whether resveratrol would have value as a chemopreventive agent. Indicators of a particular disease state, referred to as biomarkers can be useful in these studies. Biomarkers can be used to obtain information regarding the development and progression of cancer and help to relate results seen in clinical trials to effects on molecular and cellular pathways of action. Robust, validated biomarkers of efficacy are particularly important in the setting of chemoprevention trials/intervention studies, in which results may otherwise take several decades to obtain. Biomarkers may be discrete events such as the formation of clinically detectable colonic adenomas, or a change in a cellular or molecular marker, such as an increased cell proliferation [121].

In a phase I healthy volunteer study [120], levels of circulating insulin-like growth factor-1 (IGF-1) were measured. IGF-1 has been implicated in regulation of the malignant phenotype by its effects on cell proliferation, differentiation, and apoptosis [122]. Elevated plasma IGF levels are also associated with a greater risk/incidence of colorectal cancer in a number of studies [123], [124]. Resveratrol was found to significantly reduce circulating IGF-1 levels in healthy volunteers taking 2.5 g of resveratrol daily, suggesting that it has the potential to favourably alter cell proliferation in humans [120]. Other examples of potential biomarkers of efficacy analysed included the malondialdehyde-DNA (M_1dG) adduct, a measure of oxidatively damaged DNA, and PGE_2 reflecting perturbation of the arachidonic acid cascade, neither of which were significantly altered by resveratrol dosing in healthy volunteers [120].

The effect of pharmacological doses of resveratrol (1.0 g) taken daily for 4 weeks on drug- and carcinogen-metabolising enzymes was determined in 42 healthy volunteers [86]. The aim was to investigate any potential resveratrol interactions to assess the effects of resveratrol on drug efficacy and safety. Resveratrol was found to modulate enzyme systems involved in carcinogen activation and detoxification (CYP3A4, CYP2D6 and CYP2C9), which may be a mechanism by which resveratrol inhibits carcinogenesis [86]. However, this dose of resveratrol could potentially lead to increased adverse drug reactions or altered drug efficacy due to inhibition or induction of certain CYPs, and this warrants further investigation.

1.6 Resveratrol metabolites

Resveratrol metabolism is complex and involves several pathways. Phase I metabolism generally involves cytochrome P450s and flavin monooxygenases, which oxidise, reduce or hydrolyse resveratrol [125]. Hydrogenation of the aliphatic double bond of resveratrol has been suggested to occur in the GI tract by intestinal microflora, forming dihydroresveratrol in rats fed resveratrol [126] and in humans following red wine consumption [109]. Dihydroresveratrol sulfate and dihydroresveratrol glucuronide have also been identified in humans [104]. Metabolism by the cytochrome P450 enzyme CYP1B1 results in hydroxylation of resveratrol and the formation of piceatannol (3,3′,4,5'-tetrahydroxystilbene) [127].

A significant amount of resveratrol metabolism is through the action of phase II conjugating enzymes, resulting in sulfation and glucuronidation. Resveratrol undergoes sulfate and glucuronide conjugation by sulfotransferases (SULTs) and uridine diphosphate glucuronosyltransferases (UGTs) respectively, located primarily in the liver and intestine [128], [129]. The metabolic pathways which resveratrol can undergo are summarised in Figure 1.6.

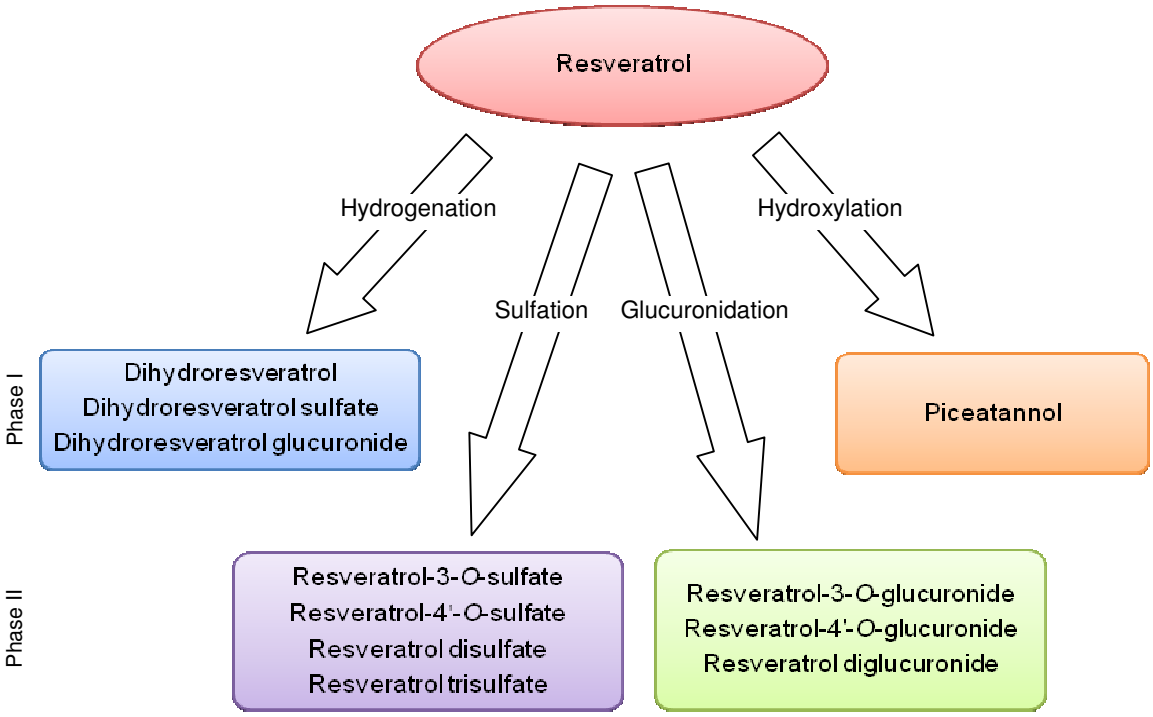

Figure 1.6 The metabolic pathways of resveratrol

The metabolic pathways of resveratrol, resulting in the formation of hydrogenated and hydroxylated phase I metabolites, via the action of intestinal bacteria and CYP(s) respectively. The major metabolite pathway generates sulfated and glucuronidated phase II metabolites via the action of sulfotransferase (SULT) and uridine diphosphate glucuronosyltransferases (UGT) enzymes. An additional metabolite formed is resveratrol sulfate glucuronide (not listed), following a combination of sulfation and glucuronidation reactions. Figure adapted from [125].

Resveratrol absorption studies in rodents show that a number of metabolites are formed after resveratrol ingestion [71], [130], [131], [132]. When rats were fed high dose resveratrol (300 mg/kg body weight) for eight weeks, metabolites detected in plasma were resveratrol-3-*O*-sulfate, resveratrol disulfates, resveratrol-3-*O*-glucuronide, and resveratrol trisulfate [71]. These have all been identified in plasma and/or urine of mammalian systems following determination by at least one of the following techniques: HPLC-UV, LC-MS/MS or nuclear magnetic resonance (NMR). The high degree of metabolism is also evident following resveratrol dosing in humans, as discussed in Section 1.5.1. The different metabolites that have been detected in humans, mice and cultured cells following resveratrol dosing are

indicated in Table 1.4. Of the metabolites shown, the most frequently occurring in human plasma are the resveratrol monosulfates and monoglucuronides [107], [86].

Based on the consistent findings from metabolism and absorption studies in animals and humans, there has been speculation about the possible contribution of resveratrol metabolites to the various activities attributed to resveratrol. A number of suggestions have been put forward to account for the potential beneficial effects of resveratrol observed despite low circulating levels [133], as outlined here.

1. Chemopreventive effects could be localised in the GI tract before resveratrol metabolism occurs [94].
2. Resveratrol metabolites may undergo enzymatic conversion back to resveratrol in target organs.
3. Enterohepatic recirculation involving biliary secretion of metabolites followed by deconjugation in the GI tract and reabsorption may account for effects in the GI tract.
4. Resveratrol metabolites could possess chemopreventive properties in their own right, which may at least in part be responsible for the observed effects.

Investigation into resveratrol metabolites is limited; however over the past 1 - 2 years, a small number of papers have been published, which examine some of the chemopreventive properties of metabolites [133], [134], [135]. The key points from these studies are discussed in more detail in the following sections.

1.6.1 Resveratrol sulfates

Absorption experiments conducted with resveratrol *in vitro* confirm findings of animal and human dosing studies. For example, incubation of Caco-2 cells with resveratrol also indicated a high level of resveratrol absorption due to efficient sulfate conjugation [136]. When human hepatocytes were incubated with resveratrol in the presence of nicotinamide adenine

dinucleotide phosphate (NADPH), resveratrol-3-*O*-sulfate and resveratrol glucuronide were produced [137]. A number of sulfotransferases (SULT1A1, 1A2, 1A3, and 2A1) have been investigated for their ability to sulfate resveratrol in ZR-75-1 and MDA-MB-231 breast cancer cell lines [138]. Reverse transcriptase-polymerase chain reaction (RT-PCR) was used for semiquantitative determination of SULT expression levels. Expression of SULT1A1 mRNA but not of the other SULTs investigated, showed a close correlation with resveratrol-3-*O*-sulfate formation, which was particularly high in ZR-75-1 and very low in MDA-MB-231 cells. Further evidence of the significant role of SULT1A1 was shown following stable transfection of MDA-MB-231 cells with SULT1A1, which showed a dramatic increase in intracellular resveratrol sulfation [138]. Evidence for a major role of SULT1A1 was also provided following incubation of human liver cytosol with resveratrol, which resulted in the formation of resveratrol-3-*O*-sulfate, resveratrol-4'-*O*-sulfate and resveratrol-3,4'-disulfate. Resveratrol-3-*O*-sulfate was almost exclusively catalysed by SULT1A1 and only to a minor extent by SULT1A2, 1A3 and 1E1, whereas resveratrol-4'-*O*-sulfate was selectively formed by SULT1A2. Resveratrol disulfate was mainly catalysed by SULT1A2 and 1A3 [139].

The structures of the various sulfate metabolites that have been identified *in vitro* and/or *in vivo* are given in Figure 1.7. In the first published investigation of the activity of resveratrol sulfates, the 3-*O*-sulfate, 4'-*O*-sulfate and 3,4'-disulfate were chemically synthesised and tested in human breast cancer cells [134]. Malignant MCF-7, MDA-MB-231, ZR-75-1 and non-malignant MCF-10A cell lines were treated with sulfates, at concentrations ranging from 1 - 350 μM. Cell growth was assessed after 48 h, at which time resveratrol-3-*O*-sulfate was found to be between ~3 - 11-fold less active than resveratrol. Resveratrol-4'-*O*-sulfate and resveratrol-3,4'-disulfate were less cytotoxic than resveratrol-3-*O*-sulfate, with the disulfate having the smallest inhibitory effect on cells [134]. These sulfate-conjugated metabolites as well as resveratrol trisulfate have been tested more comprehensively for a number of activities known to be mediated by resveratrol in an independent investigation [133]. Activities were tested in the human nasopharynx carcinoma KB cell line and in MCF-7 cells. Cell proliferation in MCF-7 cells was tested and resveratrol trisulfate and the two disulfate isomers showed a lack of activity. Resveratrol-3-*O*-sulfate was found to be the most potent metabolite toward these cells, with

52% of cells surviving following a 20 µg/ml concentration; the other sulfate derivatives had no significant effect. However, resveratrol caused the most prominent reduction, with 39% cell survival at the same concentration [133]. An additional assay compared the free radical scavenging ability and found similar levels of quenching of the 2,2-diphenyl-1-picrylhydrazyl (DPPH) free radical with both the parent and resveratrol-3-*O*-sulfate, followed by resveratrol-4'-*O*-sulfate and considerably lower effects with the disulfates, whilst the trisulfate was inactive. Quenching unstable free radicals and reducing damage to DNA by reactive oxygen species may be one of the mechanisms by which resveratrol can exert chemopreventive effects and it seems that sulfate metabolites might contribute to this effect [140].

Resveratrol has been associated with changes in the activity of NF-κB [141]. NF-κB is a transcription factor typically found in the cytoplasm in an inactive form bound to i-κB. Once activated by free radicals, inflammatory stimuli and carcinogens, NF-κB is translocated into the nucleus where it induces expression of more than 200 genes that have been shown to suppress apoptosis and induce cellular transformation, proliferation, invasion, metastasis, chemoresistance and inflammation [142]. In human colorectal carcinoma tissue NF-κB is constitutively activated and correlates with tumour progression [143]. Suppression of these specific genes through the inhibition of NF-κB activation may therefore be one of the mechanisms by which chemopreventive agents including resveratrol mediate their effects. Human embryonic kidney cells 293, which contain chromosomal integration of a luciferase reporter construct regulated by the NF-κB response element, can be used to measure NF-κB inhibition. Transcription factors can bind to the response element when stimulated by certain agents, allowing transcription of the luciferase gene. All of the metabolites retained some activity, as determined by the luciferase assay, which monitored changes occurring along the NF-κB pathway; however, potency was reduced relative to resveratrol. Of the metabolites, resveratrol-4'-*O*-sulfate was the most potent and the di- and trisulfates the least effective [133]. Both monosulfates were found to reduce activities of COX-1 and COX-2 in cells, as determined by measuring PGE_2 produced in the COX reaction via an enzyme immunoassay. However, in a separate study, inhibition of enzyme activity by resveratrol-4'-*O*-sulfate was far greater [135]. Both of these previously mentioned investigations also tested the ability of resveratrol and its

metabolites to induce quinone reductase (QR1 or QR2), a potential mechanism for cancer chemoprevention [144]. Induction of quinone reductase enzymes commonly coincides with the induction of additional phase II detoxifying enzymes. Resveratrol-3-*O*-sulfate was found to be more effective than resveratrol at increasing the expression of QR1 [133]. The function of QR2 is less well understood, however QR2 is capable of metabolically activating various quinones which can ultimately lead to cytotoxicity and cell death. Therefore, inhibition of QR2 might protect cells from harmful metabolically activated compounds that can promote DNA damage and therefore cancer. When binding of resveratrol and the monosulfates to the oxidised, free-enzyme form of QR2 was measured, no inhibition of QR2 was found by either monosulfate at concentrations of up to 100 µM, although resveratrol had activity over this concentration range [135].

Generally, resveratrol sulfates seem to be less active than parent resveratrol with increasing sulfation resulting in poorer activity. However, for some specific mechanisms sulfates are equipotent or more active than resveratrol, suggesting that they may play a role.

	Human				Mice/rats				*In vitro*
	Plasma	**Colon tissue**	**Urine**	**Faeces**	**Plasma**	**Tissues**	**Urine**	**Bile**	**Cells**
Resveratrol	✓	✓	✓	✓	✓	✓	✓	✓	✓ H, R
Resveratrol-3-*O*-sulfate	✓	✓	✓	✓	✓	✓	✓	✓	✓ H, R
Resveratrol-4'-*O*-sulfate	✓	✓	✓	✓	×	✓	×	✓	×
Resveratrol disulfate[1]	✓	✓	✓	✓	✓	✓	✓	✓	✓ H
Resveratrol trisulfate	×	×	×	×	✓	×	✓	×	×
Resveratrol-3-*O*-glucuronide	✓	✓	✓	✓	✓	✓	✓	✓	✓ H, R
Resveratrol-4'-*O*-glucuronide	✓	✓	✓	✓	×	×	×	✓	✓ H
Resveratrol diglucuronide	×	×	✓	×	×	×	×	×	✓ H
Resveratrol sulfate glucuronide	✓	✓	✓	×	×	×	×	[2]✓	×
Dihydroresveratrol	✓	×	✓	×	×	[3]✓	✓	×	[4]✓
Dihydroresveratrol sulfate	×	×	✓	×	×	×	✓	×	×
Dihydroresveratrol glucuronide	×	×	✓	×	×	×	×	×	×

Table 1.4 Resveratrol metabolites identified in humans, rodents and cells following resveratrol administration/incubation. Resveratrol metabolites identified in human and rodent biomatrices and in cells following resveratrol dosing/incubation. Human and rat cell types are denoted by letters H and R respectively. [1]Resveratrol-3,5-disulfate and resveratrol-3,4'-disulfate stereoisomers were both identified in rodent plasma and urine, but not specifically identified in humans. [2]Three sulfoglucuronide isomers were detected in bile and pefusate of rats, and very low concentrations of resveratrol diglucuronide monosulfate and resveratrol disulfate monoglucuronide identified in bile [145]. [3]Dihydroresveratrol was detected in mouse colon tissue [146] and, [4]in media supernatant following incubation of resveratrol with *Eggerthella lenta* and *Bacteroides uniformis* human anaerobic bacterial strains [147].

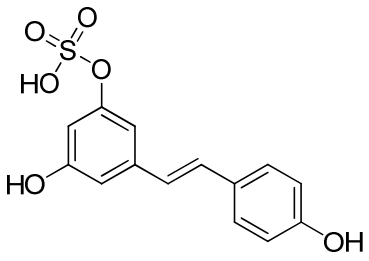

(**A**) Resveratrol-3-*O*-sulfate

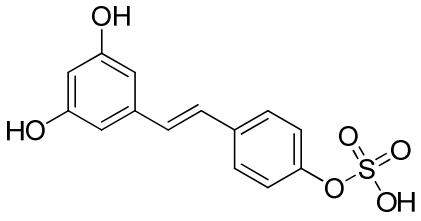

(**B**) Resveratrol-4'-*O*-sulfate

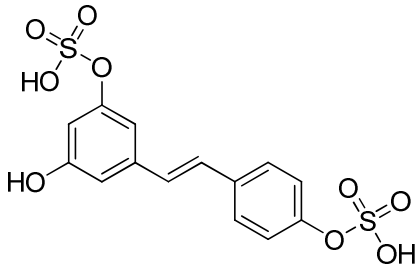

(**C**) Resveratrol-3,4'-disulfate

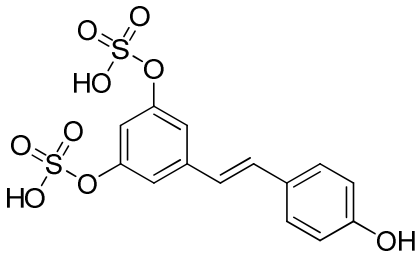

(**D**) Resveratrol-3,5-disulfate

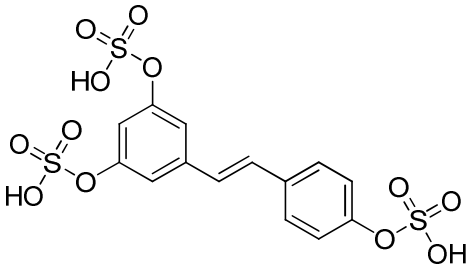

(**E**) Resveratrol trisulfate

Figure 1.7 Chemical structures of resveratrol sulfate metabolites

Structures of resveratrol-3-*O*-sulfate (**A**), resveratrol-4'-*O*-sulfate (**B**), resveratrol-3,4'-disulfate (**C**), resveratrol-3,5-disulfate, (**D**) and resveratrol trisulfate (**E**).

1.6.2 Resveratrol glucuronides

Resveratrol glucuronide formation has been shown to occur in the liver and intestine. A study investigated and reported on the ability of glucuronosyltransferase in the liver to catalyse resveratrol glucuronidation [129]. The highest rate of resveratrol glucuronidation was at pH 7, and the amounts of resveratrol glucuronide formed increased linearly with time up to at least 40 min of incubation. The hepatic rate of glucuronidation was higher than that of resveratrol sulfation measured in the same samples [129]. A separate study explored the differences in glucuronide formation following resveratrol incubation with human liver and intestinal microsomes [148]. Overall, the rate of formation for both glucuronides was higher in intestinal microsomes, and resveratrol was shown to undergo more active glucuronidation at the 3-position, which yielded resveratrol-3-*O*-glucuronide preferentially to resveratrol-4'-*O*-glucuronide. *Trans*-resveratrol has been found to undergo glucuronidation mainly by UGT1A1, UGT1A9 and UGT1A10 in human liver microsomes. The isoforms UGT1A7 and UGT1A6 could glucuronidate the compound, although at a lower extent [149]. In a more comprehensive study, glucuronidation was investigated in human microsomes prepared from liver, stomach, duodenum, four segments of the remaining small intestine and colon [150]. The two sterioisomers were glucuronidated at different rates depending on the donor and the segment from which microsomes were isolated. In liver and intestine, the formation of resveratrol-3-*O*-glucuronide predominated. However, activity toward *cis*-resveratrol glucuronidation was largely predominant in the liver, whereas *trans*-resveratrol was preferentially glucuronidated in the GI tract [150]. These data indicate the participation of different UGTs in hepatic and intestinal glucuronidation of resveratrol.

Metabolism studies in the isolated rat intestine model have shown that only small amounts of resveratrol are absorbed across the enterocytes of the jejunum and ileum unmetabolised [151]. Resveratrol glucuronide conjugates were found to be the major species detected on the serosal side (96.5% ± 4.6 of the amount absorbed), indicating the susceptibility of resveratrol to glucuronidation during transfer across the rat jejunum. The components were identified and quantified by HPLC-UV and LC-MS/MS. Enzymatic incubations of the serosal fluid with β-

glucuronidase resulted in a complete loss of the glucuronide peak when analysed by HPLC-UV providing further confirmation of metabolite identity.

The structures of the different resveratrol glucuronides, resveratrol sulfate glucuronide and the reduced metabolites of resveratrol which have been identified following resveratrol dosing are given in Figure 1.8. To our knowledge, there have been only two investigations into the properties of resveratrol glucuronides, with only one of these relating to cancer chemopreventive activity; both studies are discussed here briefly [152], [135]. In the first of the two, the activity of the resveratrol glucuronides against human immunodeficiency virus (HIV)-1 infection was investigated [152]. Resveratrol *in vitro* was found to be cytotoxic to human peripheral blood mononuclear cells (PBMCs) at concentrations of 30 µM, 90 µM and 270 µM (but not below 10 µM); however no cytotoxicity was observed for the glucuronide metabolites at these same concentrations. Resveratrol also showed strong synergistic anti human immunodeficiency virus (HIV-1) activity with the reverse transcriptase inhibitor, didanosine at 10 µM, but no effects were observed for either monoglucuronide isomer at concentrations of up to 300 µM. In a study by Calamini and colleagues, resveratrol-3-*O*-glucuronide was synthesised and tested for inhibition of COX-1 and COX-2 activity [135]. The glucuronide only weakly inhibited either enzyme.

Despite the fact that resveratrol glucuronides have been shown to be inactive *in vitro* in these assays, it is possible that they may possess other useful properties, and/or provide a renewed source of resveratrol *in vivo* because β-glucuronidase is ubiquitous in humans and could convert metabolites back to resveratrol locally or systemically [152]. Similarly, sulfate metabolites could also serve as a pool for resveratrol formation [104].

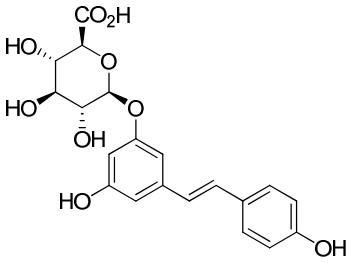

(**A**) Resveratrol-3-*O*-glucuronide

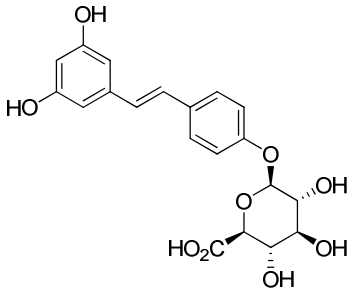

(**B**) Resveratrol-4'-*O*-glucuronide

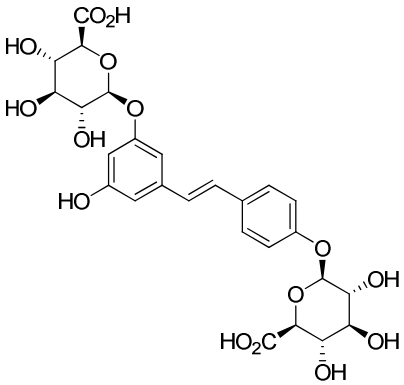

(**C**) Resveratrol diglucuronide

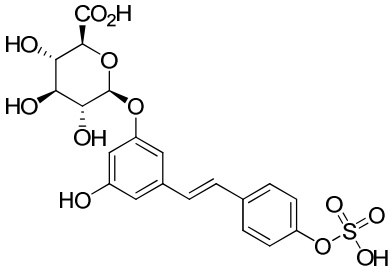

(**D**) Resveratrol sulfate glucuronide

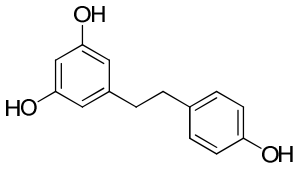

(**E**) Dihydroresveratrol

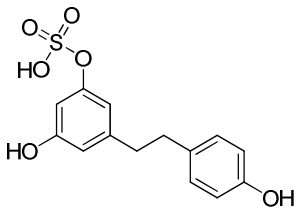

(**F**) Dihydroresveratrol sulfate

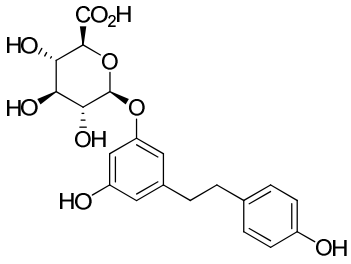

(**G**) Dihydroresveratrol glucuronide

Figure 1.8 Chemical structures of resveratrol glucuronide and hydrogenated metabolites Structures of resveratrol-3-*O*-glucuronide (**A**), resveratrol-4'-*O*-glucuronide (**B**), resveratrol diglucuronide (**C**), resveratrol sulfate glucuronide (**D**), dihydroresveratrol (**E**), dihydroresveratrol sulfate (**F**) and dihydroresveratrol glucuronide (**G**). For compounds (**D**), (**F**) and (**G**) the absolute structures have not been confirmed and those above are one of the possible isomers.

1.7 Aims and objectives

Resveratrol has demonstrated chemopreventive properties in cancer cell lines and mouse models of colorectal carcinogenesis. Resveratrol is rapidly and extensively metabolised *in vitro*, forming major metabolites including resveratrol sulfates and glucuronides, which occur at greater concentrations and cause more prolonged exposure than resveratrol in plasma and urine. It is possible that products of resveratrol metabolism may themselves have chemopreventive properties and/or act as a reservoir for resveratrol regeneration. However, their pharmacological properties have hardly been investigated. Therefore, the main objectives of this research were to assess the potential activities of resveratrol sulfate and glucuronide metabolites in cancer cell lines, and to establish whether resveratrol can be generated from resveratrol sulfates *in vitro* and *in vivo*. Pharmacologically relevant concentrations were determined from clinical trial data.

Additional aims were as follows, to obtain information on the pharmacology of metabolites:

1. To accurately quantify concentrations of resveratrol monosulfates and resveratrol monoglucuronides achieved in human plasma and colon tissue following repeat resveratrol dosing, which can be related to pharmacodynamic investigations.

2. To compare resveratrol and metabolite pharmacokinetic parameters in humans to assess the contribution of either metabolites or parent resveratrol to exposure of the body.

3. To evaluate the bioavailability of resveratrol sulfates *in vivo* and to determine their distribution in tissues to help understand amounts of metabolites present.

4. To investigate activity of resveratrol metabolites compared to resveratrol in order to improve understanding of their potential contribution to cancer chemoprevention.

Overall, this work was thought to lead to a greater understanding of the potential role of resveratrol metabolites, which will have implications for the interpretation of the activity of resveratrol in humans, particularly at sites distant from the colon. These findings may impact on resveratrol research not only for colorectal cancer, but for all diseases.

CHAPTER 2: MATERIALS AND METHODS

2.1 Materials

Chemicals were purchased from Fisher Scientific Limited (Loughborough, UK) unless stated otherwise. DMF, pyridine and DMF*SO_3 complex were ordered from Sigma-Aldrich (UK). HPLC columns and accessories were obtained from Waters Limited (Hertfordshire, UK). Cell culture materials were purchased from Greiner Bio-One Limited (Gloucestershire, UK).

HCA-7, HT-29 and HCEC cell lines were grown up from frozen cell stocks. During the course of this research, HCA-7 and HT-29 cells were obtained from the Health Protection Agency (HPA) Culture Collections, (Salisbury, UK). Paperwork received with the cell lines indicated their authenticity. HCEC cells were obtained from the Nestle Research Centre, (Lausanne, Switzerland).

2.2 Methods

2.2.1 Synthesis of resveratrol metabolites

2.2.1.1 Resveratrol monosulfates

The method of synthesis was similar to that published by Yu and colleagues [137]. Synthesis was performed under an atmosphere of nitrogen and was carried out with the supervision of Dr Robert Britton (University of Leicester).

Resveratrol was purchased from Novanat Bioresources (Shanghai, China), and included a certificate of analysis. Its purity (99.9%) was confirmed by HPLC-UV and LC-MS/MS. Resveratrol (10 g, 0.04 moles) was dried by co-evaporation from dry pyridine three times (total volume 100 ml) and then dissolved in anhydrous DMF/pyridine (3: 1, 475 ml). DMF*SO_3

complex (6.7 g, 0.04 moles) dissolved in dry DMF (25 ml) was slowly added. The resulting solution was stirred continuously at 60ºC for 4 h and then cooled to room temperature by placing on ice. Once cooled, sodium carbonate (10 g, 0.09 moles) and water (200 ml) were added and the solution reheated to 60ºC for 30 min. The solvents were evaporated *in vacuo* to leave a crude mixture of resveratrol monosulfates, resveratrol disulfate, and unreacted resveratrol. The crude reaction mixture (2 - 3 g) was dissolved in methanol (MeOH) and filtered to remove inorganic salts then silica was added (3 - 4 g). The methanol was evaporated *in vacuo* to leave dry silica with the compound adsorbed onto it, which was then purified by flash chromatography, using dichloromethane: ethanol (70: 30) with ammonium hydroxide (0.3%).

Separation of the crude mixture was monitored using normal-phase silica thin layer chromatography (TLC) aluminium-backed plates with the same mobile phase used for flash chromatography. Detection was achieved using an ultraviolet (UV) light with a wavelength of 254 nm. Fractions containing resveratrol monosulfates were combined in a round-bottomed flask and evaporated to dryness. The resulting product was checked for purity and confirmation of identity by HPLC-UV, LC-MS/MS and NMR, and stored at -80ºC.

Verification of identity:

HPLC-UV (325 nm): Two peaks at retention times of 13.4 min and 14.3 min were present, with a respective peak area ratio of 1: 3. No other peaks were detected. HPLC-UV conditions and set up are described in Section 2.2.3.1. A small amount of the mixture was purified further using column chromatography and fraction collecting on a Varian HPLC system for ^{1}H-NMR characterisation, using conditions described in Section 2.2.3.2.

LC-MS/MS: Resveratrol monosulfates were identified by single reaction monitoring (SRM) of the *m/z* 307 > 227 transition, which corresponds to loss of a sulfate group, under conditions described in Section 2.2.3.3.

^{1}H-NMR: The NMR identification provided evidence of two monosulfate isomers, these were resveratrol-4'-*O*-sulfate and resveratrol-3-*O*-sulfate which occurred in a 3: 2 ratio. The HPLC separation of the two isomers allowed individual analysis by ^{1}H-NMR, and gave the chemical shifts listed below for each monosulfate, corroborating their identities.

Resveratrol-3-*O*-sulfate:

δ_H (300 MHz; d-4 methanol) 6.66 (1H, t, *J* 2.1, C(4)-H), 6.75 (1H, m, C(6)-H), 6.77 (2H, d, *J* 8.6, C(3')-H & C(5')-H, 6.94 (2H, ABq, J_{AB} 16.3, HC=CH), 7.00 (1H, t, *J* 1.7, C(2)-H), 7.37 (2H, d, *J* 8.6, C(2')-H & C(6')-H).

Resveratrol-4'-*O*-sulfate:

δ_H (300 MHz; d-4 methanol) 6.18 (1H, t, *J* 2.1, C(4)-H), 6.48 (2H, d, *J*, 2.1, C(2)-H & C(6)-H), 6.98 (2H, ABq, J_{AB} 16.3, HC=CH), 7.28 (2H, d, *J* 8.6, C(3')-H & C(5')-H), 7.49 (2H, d, *J* 8.6, C(2')-H & C(6')-H).

2.2.1.2 Resveratrol monoglucuronides

Resveratrol-3-*O*-glucuronide and resveratrol-4'-*O*-glucuronide metabolites were synthesised by Dr Robert Britton from resveratrol *via* differential protection of the phenolic OH groups, followed by addition of glucuronic acid *via* its trichloroacetimidate. Silyl 4 and acetyl deprotection yielded the desired glucuronide as the free acid. The identity and purity of the two glucuronides were established using HPLC-UV, LC-MS/MS and ^{1}H-NMR, as outlined below.

HPLC-UV (325 nm): Injections of synthesised resveratrol-3-*O*-glucuronide and resveratrol-4'-*O*-glucuronide each produced a single peak on the HPLC, at retention times of 11.4 min and 8.7 min respectively.

LC-MS/MS: SRM of the *m/z* 403 > 227 transition, corresponding to loss of a glucuronide group confirmed the identity of both glucuronides.

^{1}H-NMR: Analysis confirmed the identity of each glucuronide isomer, by comparison with literature assignments [71].

2.2.2 Pharmacokinetics and metabolism of resveratrol in healthy volunteers following repeat resveratrol dosing

2.2.2.1 Volunteer recruitment and inclusion criteria

Application for ethical approval and volunteer recruitment for this study was conducted by Dr Victoria Brown. My role involved processing volunteer samples, developing and validating methods for sample extraction, and completing analytical analysis on samples, which allowed accurate quantitation of resveratrol levels and estimation of metabolite concentration expressed as resveratrol equivalents. In addition, once synthetic standards became available, selected volunteer samples were used for calculation of authentic metabolite concentrations in their plasma.

Forty healthy volunteers were recruited onto the multiple dosing trial of resveratrol. Half of the volunteers on the study were based in Leicester (UK) and the other half in Michigan (US). To be eligible for the trial, volunteers had to fall within the 18 - 60 year old age bracket and be able to provide a written informed consent. Individuals had to be willing to abstain from resveratrol-containing foods for a washout period of five days prior to starting on the trial, and for the duration of the trial. Laboratory tests were conducted (Haematology department, Leicester Royal Infirmary) to ensure haematological parameters and hepatic and renal functions were within the normal limits. Pregnant or lactating women, cancer patients (currently under treatment or diagnosed within the past five years), and those on chronic medications (with the exception of oral contraceptives) were all excluded from the study. Limits were also set for weekly alcohol consumption levels.

2.2.2.2 Resveratrol dosing in healthy volunteers

Volunteers on the study were required to take 29 daily oral doses of resveratrol, with at least 20 daily doses of resveratrol prior to the pharmacokinetic (PK) study day. The PK study day fell between day 20 and day 29 of resveratrol dosing. Resveratrol was administered as uncoated, immediate release caplets containing 0.5 g of resveratrol, supplied by Pharmascience Inc. (Montréal, Canada). Blood, urine and faecal samples were collected pre-dose and at time intervals post-resveratrol dosing.

Ten volunteers were recruited onto each dose level of the study at a dose escalation of 0.5, 1.0, 2.5 and 5.0 g resveratrol daily. At the end of each dose level, adverse events were discussed by the clinical team and dose escalation permitted if no serious toxicity had been established. Lack of toxicity was described as not having more than two grade II adverse events lasting for more than three days, using the National Cancer Institute Common Toxicity Criteria (Version 3.0). To determine PK parameters in plasma, the collection times for plasma were pre-dose and 0.25, 1, 1.5, 5, 12 and 24 h post-dose on the PK study day. Urine was also collected pre-dosing, and post-resveratrol dosing over 24 h on the study day at the following intervals: 0 - 2, 2 - 4, 4 - 8, 8 - 12 and 12 - 24 h.

2.2.2.3 Volunteer blood sample processing

A chart giving a brief overview of how blood samples were processed after collection from volunteers is given in Figure 2.1. As part of my project I completed the HPLC-UV and LC-MS/MS analysis for determination of resveratrol and metabolites in plasma.

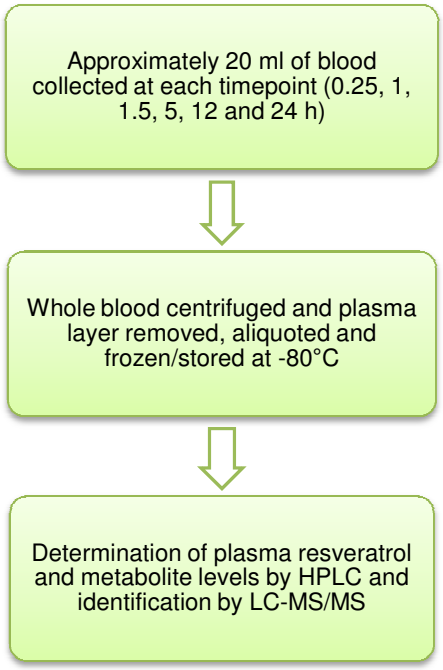

Figure 2.1 An overview of blood sample processing following collection from healthy volunteers

An overview showing how volunteer blood samples were processed, and analyses that were performed on samples.

2.2.2.4 Resveratrol and metabolite extraction method from plasma

The method of plasma analysis was identical to that previously validated and published by this laboratory [153], and used for analysis of plasma samples following consumption of single doses of resveratrol [107]. Briefly, plasma (250 µl) was acidified with concentrated hydrochloric acid (HCl, 4.4 µl), followed by the addition of methanol (250 µl), and the sample vortex-mixed (1 min), and placed at -20℃ (10 min). Samples were then centrifuged at 4℃ (15 min, 13,000 x g). The supernatant was removed and evaporated to dryness at room temperature, under a stream of nitrogen. Dried samples were reconstituted in 50: 50 methanol: water (200 µl) and vortex-mixed. Reconstituted samples were centrifuged and the supernatant transferred into suitable glass vials, and stored in a chilled autosampler (4℃) until injected onto the HPLC (100 µl). Standard curves were constructed in human plasma (obtained from the National Blood Transfusion Centre, Sheffield, UK) spiked with resveratrol standards for each analytical run.

Concentrations of metabolites were also based on standard curves of resveratrol. The HPLC method used for analysis is described in Section 2.2.3.1. For determination of authentic metabolite concentrations, the same method was used. However, standard curves of resveratrol monosulfates and resveratrol glucuronides were used to allow accurate quantitation. Pharmacokinetic parameters for resveratrol and its major metabolites were modelled using WinNonlin Version 5.3 software (Pharsight Corporation, Mountain View, California, US).

2.2.3 HPLC and LC-MS/MS systems set up and operating parameters

2.2.3.1 Waters HPLC-UV system

The HPLC system employed consisted of a Waters Alliance 2695 series separations module with column heater, refrigerated autosampler and inline degasser. Detection was by a 2487 dual wavelength UV-visible detector set to 325 nm for resveratrol and its metabolites. Empower 2 chromatography manager software was used for operating the HPLC, and collecting and analysing the data. Samples were injected onto a Waters Atlantis 3 µm C_{18} column (4.6 x 150 mm), connected to a Waters Atlantis 3 µm C_{18} guard column (4.6 x 20 mm) to prolong the column lifetime. Column and autosampler temperatures were maintained at 35°C and 4°C respectively. The flow rate was 1 ml/minute throughout. The gradient elution conditions for each injection are set out in Table 2.1. The column was re-equilibrated to 100% aqueous mobile phase (A) for 3 min prior to each injection.

Time (min)	% A	% B
	100	0
4.0	80	20
7.0	80	20
16.0	45	55
18.0	45	55
18.5	5	95
23.0	5	95
23.5	100	0
27.0	100	0

Table 2.1 Mobile phase gradient profile on the Waters HPLC-UV system. Gradient elution conditions used for the separation of resveratrol and its metabolites. The aqueous mobile phase (**A**) was made up with ammonium acetate (0.385 g, Sigma-Aldrich, UK) dissolved in 980 ml of deionised water plus 20 ml of propan-2-ol. The organic phase (**B**) consisted of 980 ml of methanol and 20 ml of propan-2-ol.

2.2.3.2 Varian ProStar HPLC-UV system

The Varian HPLC-UV system consisted of a pump (model 230), an autosampler (model 410) and UV lamp (model 310). Star Chromatography software (Version 2.0) was used for operating the HPLC. The Varian HPLC-UV system was used for preparative HPLC to separate two resveratrol monosulfates by fraction collecting. Larger amounts of compound could be injected onto the Varian machine for separation compared to the Waters HPLC, making it more suitable for this purpose. A 5 µm C_{18} Thermo Hypersil column (250 x 21.5 mm) was used for metabolite separation. The wavelength for detection was set to 325 nm and metabolite peaks at this wavelength were easily detectable at the high concentrations injected. A flow rate of 10 ml/minute was used and an injection volume between 100 – 200 µl. The gradient elution conditions for the method are set out in Table 2.2.

Time (min)	% A	% B
0	68	32
14.0	68	32
14.3	5	95
17.3	5	95
18.0	100	0
23.0	100	0

Table 2.2 Mobile phase gradient profile on the Varian HPLC-UV system. Gradient elution conditions used on the Varian HPLC for separation of resveratrol monosulfates. Mobile phase **A** consisted of 5 mM ammonium acetate, and mobile phase **B** consisted of 98% methanol. Both mobile phases contained 2% propan-2-ol.

2.2.3.3 Waters LC-MS/MS system

The LC-MS/MS chromatographic conditions were identical to those described for the HPLC analysis; however the column used was an Atlantis 3 µm C_{18} narrow bore column (2.1 x 150 mm) with a flow rate of 240 µl per minute. Identification was with SRM operated in the negative ion mode using a Waters 2695 series HPLC with a Waters Quattro Ultima Pt triple quadrupole mass spectrometer. The detailed mass spectrometry conditions were as follows:

Source Temperature and desolvation temperature: 150°C and 350°C respectively.

Entrance, collision and exit potential: 10 V, 17 V and 29 V respectively.

Capillary: 3.17 kV

Cone Voltage: 35 V

Data analysis was completed using MassLynx (Version 4.0) software.

2.2.4 Phase 1 repeat dose study of resveratrol in colorectal cancer patients

2.2.4.1 Patient recruitment and inclusion criteria

This part of the study was conducted by Dr Victoria Brown who was responsible for ethical approval and recruiting patients from Leicester hospitals onto the study. My role involved validating a method for analysing colon tissue and tumour specimens, and extraction of samples for determination of levels of resveratrol and metabolites after 8 daily doses of resveratrol.

Patients suspected of having colorectal cancer who required colorectal endoscopy for a histological diagnosis were informed about the study. Samples of blood were taken for haematological/biochemical analysis to help identify suitable patients for the study. Patients met the following eligibility criteria: histological diagnosis of colorectal adenocarcinoma, disease amenable to surgical resection; age, > 18 years; WHO performance status, 0 to 2; haemoglobin, > 10 g/dl; alanine aminotransferase and serum bilirubin, < 2.5x and < 1.5x the upper limit of normal, respectively; creatinine, < 140 µmol/l.

2.2.4.2 Clinical trial design and resveratrol dosing in colorectal cancer patients

Resveratrol dosing was discussed with participants who were asked to begin a resveratrol restricted diet until completing the study. Eligible patients (10 per group) were recruited onto a 0.5 g daily dose. Further recruitment was at a dose of 1.0 g. Patient characteristics and the medications they were taking during the course of the trial are given in Table 7.1 and 7.2 (Appendix) for the 0.5 and 1.0 g respectively. None of the patients received neoadjuvant radiotherapy or chemotherapy prior to surgery, and based on current evidence, they were not on drugs known to alter the metabolism of resveratrol. Resveratrol was administered as uncoated, immediate release caplets containing 0.5 g of resveratrol. Patients were asked to take 8 daily doses of resveratrol every evening leading up to surgical resection (day 9).

Patients took their allocated dose of resveratrol in the evening to ensure that the last dose was ingested as close to the scheduled resection time as possible, whilst still complying with nil by mouth procedures on the day of surgery. During the course of the surgery, blood samples were taken for determination of resveratrol and its metabolites in plasma. Malignant colorectal cancer tissue and non-malignant tissue were removed for analysis. Several sections of non-malignant tissue were taken relative to the tumour. Where possible, the samples collected in addition to tumour were: 5 cm proximal section, 10 cm proximal section, proximal resection margin, 5 cm distal section, 10 cm distal section and the distal resection margin (all relative to tumour).

2.2.4.3 Development of an extraction method for determining resveratrol and its metabolites in human colon tissue

To determine the concentration of resveratrol and its metabolites in colon tissue taken from colorectal patients, it was necessary to develop a method for sample extraction prior to HPLC-UV analysis. This involved establishing a suitable method of extraction that was simple, accurate and reproducible, whilst allowing a large number of samples to be processed and analysed in batches. A method which concentrated the compounds of interest, and removed impurities (e.g. proteins) before analysing on the HPLC was required.

Prior to the extraction, tissue had to be broken down and homogenised in buffer. Sections of frozen tissue were cut into smaller pieces and ground into a powder (using a pestle and mortar) with liquid nitrogen. This was found to be more effective than homogenisation with a polytron homogeniser (X-1020), due to the tough nature of the colon tissue. The powdered tissue was weighed and mixed with HEPES buffer (50 mM, pH 7.0) in a 3: 1 ratio of buffer: tissue. A smaller ratio of buffer: tissue was not possible, as the amounts of patient tissue available were often very small.

The previously validated liquid-phase extraction method employed for plasma analysis [153] was used as a starting point for extracting resveratrol and its metabolites from colon tissue. Methanol was tested as the organic phase in the extraction process. Liquid phase extractions were carried out on spiked mouse mucosal tissue homogenate, due to the absence of control human mucosa for method development. Tissue homogenate (100 µl) was extracted using an equivalent volume of methanol organic phase. The volume of concentrated hydrochloric acid added (1.75 µl) was scaled down from the plasma extraction method. Samples were vortex-mixed (1 min), placed at -20°C (10 min) and centrifuged (15 min, 13,000 x g, 4°C). Samples were evaporated under nitrogen and reconstituted in methanol: water (50: 50). Analysis by HPLC-UV produced chromatography with sharp and well-separated peaks. The absolute extraction efficiency using this method was approximately 60%.

To enable correction for losses due to extraction, various compounds with structural similarities to resveratrol, or similar chromatographic properties were injected onto the HPLC to test their suitability as an internal standard (IS). The compounds tested included *trans*-stilbene, carbamazapine, naringenin and quercetin. One of the requirements for the internal standard peak was that it needed to be well separated from the peaks of interest, and produce a sharp and distinct peak. Table 2.3 summarises the results of the HPLC-UV analysis and comments on their potential use as an internal standard using the system described previously (Section 2.2.3.1).

Compound	Ret. time	Result
trans-Stilbene	22.9	Peak eluted too late in the run
Carbamazapine	20.4	Peak eluted too closely to the 'noise' at the end of the run
Naringenin	19.3	Sharp peak with large area, eluted two min after resveratrol
Quercetin	N/A	No peak detected

Table 2.3 Compounds tested for their potential use as internal standards. Four compounds (*trans*-stilbene, carbamazapine, naringenin and quercetin) were tested for their suitability as potential internal standards. Retention time is given in minutes.

Based on these results, the compound considered to be the most suitable was naringenin. The peak was easily detectable and did not co-elute with any of the resveratrol peaks of interest. The concentration of naringenin was optimised to produce a suitable peak size following extraction that was easily detectable and could accurately reflect variations in the extraction process. A 25,000 ng/ml naringenin standard was used to spike tissue homogenate in the final extraction method used (Section 2.2.4.5). The suitability of naringenin was tested further during the method validation process.

2.2.4.4 Validation of the extraction method for determining resveratrol and its metabolites in human colon tissue

Analytical method validation is critical for the successful analysis of clinical samples. Validation ensures that a particular method used for quantitative measurement of analytes in a biological sample matrix is reliable and reproducible. A number of parameters have to be met for this validation process; these include accuracy, precision, linearity, recovery, sensitivity and stability, (based on Food and Drug Administration (FDA) guidelines; www.fda.gov). These parameters were measured using the HPLC method outlined (Section 2.2.3.1) and are described in more detail below.

2.2.4.4.1 Accuracy

Accuracy describes the closeness of mean test results obtained by the analysis method to the true value (concentration) of the compound of interest i.e. resveratrol. Three concentrations of resveratrol in the expected range for levels in clinical samples (250, 1000, 5000 ng/ml) were used for determination of interday accuracy (on three separate days), with five replicates for each concentration. For intraday accuracy the same concentrations were used, with three replicates for each concentration spiked and extracted repeatedly on the same day. Each

sample was injected once. The interday accuracy was calculated using the following formula, with the overall average taken following analysis on three separate days:

$$\text{Interday accuracy} = \frac{\text{Average concentration of spiked samples}}{\text{Concentration of spiked samples assuming 100\% recovery}} \times 100$$

Based on the figure quoted by the FDA bioanalytical method guidelines (www.fda.gov), the mean value should be within 15% of the actual value (85 - 115%). The results for the interday and intraday accuracy are given in Table 2.4, and all were within the acceptable limits.

Resveratrol conc. (ng/ml)	Interday accuracy (%)	Intraday accuracy (%)
250	107.4 ± 3.9	109.9 ± 1.0
1000	101.0 ± 0.4	94.5 ± 0.8
5000	101.2 ± 0.9	102.7 ± 0.9

Table 2.4 Interday and intraday accuracy of resveratrol measured in mouse colon tissue spiked with resveratrol. Values are the mean ± SD (n = 3) of assays conducted on three separate days (interday), or at different times during the same day (intraday).

2.2.4.4.2 Precision

Precision refers to the closeness of individual measures of the analyte when the procedure is applied repeatedly to multiple aliquots of a single homogeneous volume of a biological matrix, and is a measure of the reproducibility of the whole analytical method. Precision is expressed as the relative standard deviation (RSD), and was calculated with the following equation:

$$\text{RSD} = \frac{\text{Standard deviation of measured concentrations}}{\text{Average of measured concentrations}} \times 100$$

The same concentrations used for the determination of accuracy were tested (in triplicate) as part of the precision analysis. The interday and intraday precision results at the three concentrations measured are given in Table 2.5. The precision determined at each level should not exceed 10%, and these values were all found to be satisfactory.

Resveratrol conc. (ng/ml)	Interday precision (%)	Intraday precision (%)
250	3.61	0.90
1000	0.38	0.83
5000	0.91	0.88

Table 2.5 Interday and intraday precision of resveratrol measured in mouse colon tissue spiked with resveratrol. Values are calculated from the mean and SD (n = 3) of assays on three separate days (interday), or at different times during the same (intraday).

2.2.4.4.3 Linearity

The linearity of an analytical procedure is its ability to obtain test results which are directly proportional to the concentration of the analyte in the sample. Seven calibration curves of mouse colon tissue spiked with known concentrations of resveratrol and one concentration of naringenin were constructed. They were found to be linear over the concentration range measured (0 – 5,000 ng/ml). The average R^2 value was 0.999.

2.2.4.4.4 Recovery

Recovery was calculated by injecting solutions of neat resveratrol in 50: 50 MeOH: H_2O (50, 100, 250, 500, 1,000, 2,500 and 5,000 ng/ml) and comparing the corresponding peak areas in samples of colon tissues that were extracted (in triplicate) and analysed on the same analytical run. The average absolute recovery from seven separate runs was 56.4% ± 6.9%, whereas the

relative recovery was 95.2 ± 5.6%. Absolute resveratrol recoveries were determined based on the resveratrol peak area, whereas relative recoveries were calculated using the ratio of the internal standard areas and resveratrol peak areas.

The recovery characteristics of resveratrol and the naringenin internal standard were found to be similar and did not vary by more than 5% on any of the analytical runs. The high recoveries and small variation from separate extractions indicated that the method was suitable for these parameters.

2.2.4.4.5 Sensitivity

The limit of detection (LOD) is defined by an analyte concentration that produces a detectable signal on the HPLC, which is three times that of the background peak level, or noise (FDA bioanalytical method guidelines; (www.fda.gov)). The limit of quantitation (LOQ) describes when an analyte response is seven times greater than that of the noise. The LOD and LOQ for this method were 5 ng/ml and 10 ng/ml respectively.

2.2.4.4.6 Stability

To assess the potential for resveratrol degradation whilst samples await injection in the autosampler during the course of a batch run, samples were extracted and stored in the dark at 4ºC. Samples were not likely to be stored for more than 24 h under these conditions. Mouse colon tissue was spiked at 500 and 5000 ng/ml (n = 3 at each concentration) then extracted using established procedures (Section 2.2.4.5). Both resveratrol and the internal standard were found to be stable for at least 24 h, as determined by reinjecting samples and measuring compound levels. The average peak areas for resveratrol and internal standard, measured immediately after sample preparation compared to peak areas after 24 h did not vary by more than 5% for either compound.

Validation of the method, using the parameters discussed, showed that it was suitable to use for extracting resveratrol from colon tissue samples. Various sections of colon tissues, including tumour samples from volunteers who had taken single doses of resveratrol of 0.5 and 1.0 g for a week prior to surgical resection were analysed using the finalised method described in section 2.2.4.5.

2.2.4.5 Final validated liquid extraction method from colon tissue

The finalised tissue extraction method was as follows: frozen tissue samples were mixed with liquid nitrogen, ground and then weighed and homogenised with three parts weight per volume of HEPES buffer. Homogenate (100 µl) was acidified with concentrated HCl (1.75 µl), spiked with 25,000 ng/ml naringenin internal standard (5 µl) and extracted with methanol (100 µl). Tissue homogenate and solvent were vortex-mixed (1 min) and chilled at -20°C (10 min). Samples were centrifuged (13,000 x g, 10 min, 4°C) and the supernatant removed and evaporated to dryness under a stream of nitrogen. Samples were reconstituted in MeOH: H_2O (50: 50), (130 µl) and injected onto the HPLC (100 µl) under the conditions described previously (Section 2.2.3.1). Standard curves of resveratrol, resveratrol monosulfates and resveratrol glucuronide were constructed from homogenate of mouse mucosal scrapings and analysed under identical conditions to samples, for quantitation of concentrations.

2.2.4.6 LC-MS/MS analysis of colon tissues for metabolite identification

Tissue samples for LC-MS/MS analysis were extracted in the same way as described in Section 2.2.4.5. Conditions for mass spectrometric analysis are outlined in Section 2.2.3.3.

2.2.5 Pharmacokinetics and metabolism of resveratrol monosulfates in mice

2.2.5.1 Experimental set up and dosing

C57BL/6J adult mice (48) were purchased from Charles River Laboratories (Margate, UK) for the investigation of resveratrol monosulfate pharmacokinetics and bioavailability. Half of mice were used for intravenous (IV) dosing, and half for intragastric (IG) dosing of the monosulfates. A mixture of resveratrol-3-*O*-sulfate and resveratrol-4'-*O*-sulfate (3: 2 ratio) was given as an IV injection via the tail vein at a dose of 6 mg/kg in saline (volume of approximately 100 µl of a 1.5 mg/ml solution adjusted to individual body weight; equivalent to 4 ml/kg). The second method of administration of the mixture was by IG at a dose of 120 mg/kg in saline (volume of approximately 200 µl of a 15 mg/ml solution adjusted to individual body weight; equivalent to 8 ml/kg). Control mice received vehicle only, but were otherwise treated in the same manner and were culled at time 0.

At 5, 15, 30, 60, 120 and 360 min plus 24 h after dosing, mice (n = 3 for each time) were exsanguinated by cardiac puncture under terminal anaesthesia (halothane). Blood was collected into lithium-heparin tubes to allow determination of plasma resveratrol and metabolite levels. Blood was kept on ice until centrifugation (13,000 x g, 10 min, 4°C) and stored at -80°C until analysis. The same time points and same number of mice were used for both forms of dosing.

Mice were fasted on the morning of the experiment, and food was withheld after dosing. In the case of the 360 min and 24 h groups, access to food and water after dosing was allowed. After termination, urine was collected directly from the bladder or collected as the bladder was emptied (where possible). The small intestines and colon were flushed with phosphate buffered saline (PBS) and mucosa gently scraped and collected using a spatula. Liver, lung and pancreas were also collected for analysis of metabolite concentrations. Tissues and urine were snap frozen in liquid nitrogen and kept at -80°C until analysis.

2.2.5.2 Development of an extraction method for determining resveratrol metabolites and resveratrol in mouse plasma

The liquid extraction method used for resveratrol and metabolite determination in human plasma was assessed for its extraction efficiency of resveratrol metabolites. Methanol, acetone and acetonitrile were used as solvents. Naringenin internal standard was spiked into plasma samples to allow calculation of relative as well as absolute recoveries for resveratrol-3-*O*-glucuronide, resveratrol monosulfates and resveratrol. Due to the limited availability of control mouse plasma, control human plasma was used for the solvent optimisation. The results are provided in Table 2.6.

	Absolute recovery (%) (n = 2)				Relative recovery (%) (n = 2)			
	3-Gluc	**4′-Sulf**	**3-Sulf**	**Res**	**3-Gluc**	**4′-Sulf**	**3-Sulf**	**Res**
MeOH	56.6	50.4	50.2	52.2	114.4	101.9	101.5	95.8
Acetone	82.9	79.4	80.5	78.5	106.9	102.4	103.9	101.3
Acetonitrile	61.4	56.3	57.4	52.8	112.3	103	105.1	96.6

Table 2.6 Absolute and relative extraction efficiencies of resveratrol metabolites and resveratrol from human plasma. Efficiencies are given as percentages relative to neat injection of standards. Values are the mean of duplicate extractions completed in one experiment. Concentrations of resveratrol-3-*O*-glucuronide, resveratrol monosulfates and resveratrol in plasma were 5,000, 10,000 and 1,000 ng/ml respectively. Determination of absolute recoveries did not rely on the internal standard, whereas relative extraction efficiencies were based on peak area ratios of compounds with the internal standard.

Whereas the relative metabolite extraction efficiencies were high (> 95%) for all solvents, acetone consistently yielded the highest extraction efficiencies (both relative and absolute) and was therefore selected.

The recovery of the major sulfate and glucuronide metabolites and resveratrol was measured following extraction with acetone in spiked mouse plasma samples to ensure the method translates from human to mouse plasma. Extraction efficiencies for resveratrol-3-*O*-glucuronide, resveratrol-3-*O*-sulfate and resveratrol are given in Table 2.7.

	Plasma concentrations (ng/ml)	Absolute recovery (%) ± SD	Relative recovery (%) ± SD
3-*O*-glucuronide	25, 100, 1,000	91.5 ± 3.5	96.8 ± 1.3
3-*O*-sulfate	50, 500, 10,000	93.4 ± 3.0	105.4 ± 1.9
Resveratrol	5, 25, 250	86.1 ± 4.9	97.4 ± 9.4

Table 2.7 Extraction efficiencies of resveratrol and its metabolites in mouse plasma. Three control mouse plasma samples were spiked with low, medium and high concentrations of resveratrol-3-*O*-glucuronide, resveratrol-3-*O*-sulfate and resveratrol, (variable concentrations for each), and extracted using acetone in one experiment. The average extraction efficiency and standard deviation was calculated for each of the extracted compounds across the concentration range measured.

Standard curves were constructed in plasma and extracted using acetone. Analysis showed that detection of the metabolites and resveratrol was linear over the concentration range measured, with regression values consistently reaching 0.99, or above.

2.2.5.2.1 Finalised extraction method for determining resveratrol metabolites and resveratrol in mouse plasma

Mouse plasma (190 µl) was spiked with naringenin internal standard (10 µl, 50,000 ng/ml) and extracted using acetone (200 µl) using the same method described earlier for resveratrol extraction from plasma (Section 2.2.2.4). Following solvent evaporation under nitrogen, samples were reconstituted in 120 µl MeOH: H_2O (50: 50) and 100 µl injected onto the HPLC, using the specified method (Section 2.2.3.1).

2.2.5.3 Extraction method for determining resveratrol metabolites and resveratrol in mouse mucosa, liver, lung and pancreas

The extraction efficiencies of resveratrol and the monosulfate/monoglucuronide metabolites from mouse mucosa, liver, lung and pancreas tissues was tested using acetone, based on the high recovery from mouse plasma using this solvent. For mucosa, the relative extraction efficiencies of resveratrol-3-*O*-glucuronide, resveratrol-3-*O*-sulfate and resveratrol across a range of concentrations were between 101.2 and 119.9%, and found to be consistent. The final method used was the same as that described for analysis of mouse plasma; except that the mouse mucosa (and other tissues) were mixed with HEPES buffer (1: 3 weight to volume) prior to extraction.

Following homogenisation and extraction of liver tissue, the relative extraction efficiencies of resveratrol-3-*O*-glucuronide, resveratrol-3-*O*-sulfate and resveratrol over the concentration ranges measured were between 87% and 126.6%. The method was found to be linear over the same range measured for resveratrol and its metabolites, with regression values of 0.99, or above. Extraction efficiencies for resveratrol and its metabolites ranged from 62.4% to 127% for lung and 88% to 132% for pancreas. The extraction efficiencies within each tissue and for each compound were found to be consistent.

Typically, approximately 65 mg of mucosa, liver and lung tissue was used, with approximately 30 mg of pancreatic tissue. Injection volumes of 100 µl were used for all tissue analyses.

2.2.5.4 Extraction method for determining resveratrol metabolites and resveratrol in mouse urine

Mouse urine was diluted 20-fold and extracted (50 µl) with methanol (200 µl), using the method described for mouse plasma analysis. However, the supernatant was not dried down, and it was injected directly onto the HPLC (50 µl). A high extraction efficiency was not required as the

analysis was purely qualitative, and therefore a simple liquid extraction was used and no additional solvents were tested.

2.2.6 Cell culture

Cell lines of importance for this study include the following; HCA-7, HT-29 and HCEC cells. HCA-7 cells were established from a primary, well-differentiated, human colonic adenocarcinoma from a 58-year-old female patient and allow the study of COX-2 expression and targets for inhibition of this COX-2 activity. HT-29 cells, which are derived from colon tissue (grade II adenocarcinoma) taken from a 44-year-old Caucasian female allow the study of cellular and molecular pathways implicated in colorectal cancer. Whereas the HCA-7 and HT-29 cells are both derived from adenocarcinomas, the HCEC colon cells are derived from a healthy donor.

2.2.6.1 Resuscitating cells from frozen stocks

To grow up cells from frozen stock, cells were removed from liquid nitrogen storage and thawed in a water bath maintained at 37°C. Once thawed, cells were transferred to a Falcon tube, and media added (5 ml). The cell suspension was centrifuged using an MSE Mistral 2000 (350 x g, 3 min, room temperature) to pellet the cells, and the supernatant discarded. Cells were resuspended in fresh media (1 ml) and transferred to 75 cm^3 flasks and allowed to grow to near confluency before being passaged. Cells were grown in Dulbecco's modified Eagle's medium (high glucose) (Sigma-Aldrich, UK), which was supplemented with foetal bovine serum (50 ml, Invitrogen Ltd, Paisley, UK).

2.2.6.2 General maintenance

HCA7, HT-29 and HCEC cell lines were maintained in a CO_2 incubator under standard conditions with an atmosphere of 5% CO_2 at 37°C. Cells were passaged routinely when flasks reached approximately 80% confluency, and cells were not sub-cultured more than 35 times. In the case of HCEC cells, flasks and plates were pre-coated with coating medium (15 min at 37°C), which was removed before cells were seeded. Pre-coating media consisted of serum-free media (50 ml), 5% BSA (65 µl), collagen (0.5 ml of 0.1 mg/ml stock, Sigma-Aldrich, UK) and fibronectin from bovine serum (125 µl of 1 mg/ml stock, Sigma-Aldrich, UK). The pre-coating solution was filtered prior to use and not reused more than five times. All cell culture experiments were carried out aseptically in a laminar II flow hood.

2.2.6.3 Routine passaging of cells

To harvest flasks, media was poured off, and flasks were washed twice with PBS (5 ml). Trypsin/EDTA (diluted in PBS from stock, Invitrogen Ltd, Paisley, UK) was added to flasks (3 ml), which were left in the incubator to allow cells to detach. The strength of trypsin/EDTA used was dependent upon the cell line being harvested; 5x was used for HCA-7 cells and 2x for HT-29 and HCEC cells. Once detached, trypsin was neutralised with the addition of media (7 ml) and the suspension transferred to Falcon tubes. The cell suspension was centrifuged (350 x g, 10 min) and the supernatant discarded. Cell pellets were resuspended in fresh media (5 ml) and cell counting was performed, and cells were seeded at the required density.

2.2.6.4 Cell counting

Cells were counted using a Z2 Coulter Particle Count and Size Analyser (Beckman Coulter, High Wycombe, UK). To perform counting, an aliquot of cell suspension was mixed thoroughly

and transferred to a counting cup containing isotone (10 ml total volume) for quantification. The dilution factor was altered accordingly.

2.2.6.5 Cell proliferation curves

Initial experiments were set up to determine the most appropriate density for the duration of the experiment. Once determined, cells were seeded at densities of 6,000, 2,500 and 15,000 per well in 24-well plates for HCA-7, HT-29 and HCEC cells respectively. Five 24-well plates were set up for each cell line, for each experiment. Cells were left to adhere to the bottom of wells for a 24-hour period, after which, media was aspirated and replaced with fresh media (2 ml) containing the compounds being investigated. The final concentrations of the resveratrol monosulfate/monoglucuronide compounds were; 0 (control) 25 µM, 50 µM, 75 µM, 100 µM, 125 µM and 250 µM, with one resveratrol treatment of 10 µM. All compounds were dissolved in dimethyl sulfoxide (DMSO) to give the desired stock solutions. Stock solutions were made up fresh each time they were required. Control wells were treated with the DMSO vehicle only. The volume of DMSO in each well did not exceed 0.1% by volume, and did not affect cell growth.

Plates were left for three days post-treatment to allow the compounds to take effect before counting. One plate for each cell line was counted on a daily basis from day three (72 h) to day seven (168 h), post-addition of agents.

2.2.6.6 Metabolism study of resveratrol and resveratrol monosulfates in cells

Phenol red contained in media was found to co-elute with resveratrol during HPLC-UV analysis of media. Therefore, the metabolism of resveratrol and its metabolites in HCA-7, HT-29 and HCEC cells was investigated in cells grown in phenol free media over the course of a number of passages. The phenol free media did not contain all of the required components for the growth

of cells, and the media was therefore supplemented. Media was supplemented with sodium bicarbonate powder (1.85 g, sterile-filtered after dissolving in media, Sigma-Aldrich, UK), sodium pyruvate (100 mM, 5 ml), glutamax (200 mM, 5 ml) and foetal bovine serum (50 ml). The phenol red free media, glutamax and sodium pyruvate were purchased from Invitrogen Limited (Paisley, UK).

For each experiment, eleven 175 cm^3 flasks were seeded with 10 million cells, and three flasks seeded with 3 million cells. All flasks were left for 24 h to allow cells to adhere. After 24 h, cells were incubated with 20 ml media containing resveratrol (10 µM), resveratrol monosulfates (75 µM) or DMSO vehicle only (control). An aliquot of media was collected and flasks were harvested immediately upon treatment (time zero), and at 5 min, 15 min, 1 h, 24 h and seven days post addition of treatment. Flasks containing the DMSO vehicle were harvested at time zero and day seven only. Flasks seeded with 3 million cells were harvested on day seven. An additional flask was set up with each of the above treatments, containing media only (without cells). At the designated times, an aliquot of media was also collected from these flasks. Aliquots of media removed from flasks were immediately frozen and stored at -80ºC until analysis. Cells were harvested using the procedure mentioned previously (Section 2.2.6.3), and additional wash steps were introduced to remove the presence of any surface treatment. Pelleted cells were stored at -80ºC until analysis was performed.

2.2.6.6.1 Analysis of media for identification of resveratrol and metabolites

Media was centrifuged (10 min, 13,000 x g, 4°C) to remove any protein and cell debris, then an aliquot of the supernatant (50 µl) was injected directly onto the HPLC. Standards of resveratrol and synthesised standards of resveratrol monosulfates and resveratrol monoglucuronides were also analysed the HPLC to aid identification by comparison of retention times. The HPLC method used for analysis is provided in Section 2.2.3.1.

The metabolite identities were confirmed by LC-MS/MS as described in Section 2.2.3.3.

2.2.6.6.2 Analysis of cell pellets to determine intracellular resveratrol and metabolite concentrations

The method used for intracellular pellet analysis was based on a previously published procedure [154]. Cell pellets were frozen in liquid nitrogen three times and placed in 50°C water (approximately 1 min) after each freezing cycle. Acetone (250 µl) was added to the pellets, which were vortex mixed (3 min) and sonicated (10 min). The cell suspension was transferred to clean Eppendorf tubes and the Falcon tubes rinsed with acetone (250 µl) and the fractions combined and stored at -20°C (10 min), before centrifuging (10 min, 13,000 x g, 4°C). The supernatant was then evaporated under a stream of nitrogen. Once dried, samples were reconstituted in MeOH: H_2O (50: 50, 120 µl), centrifuged (10 min, 13,000 x g, 4°C) and the supernatant injected onto the HPLC (100 µl) using the standard HPLC method (Section 2.2.3.1). To allow quantitation of intracellular concentrations, resveratrol and monosulfates were spiked into pellets of 10 million cells, followed by extraction using the same procedure described for sample extraction. The average extraction efficiencies of resveratrol-3-*O*-sulfate, resveratrol-4'-*O*-sulfate and resveratrol spiked into cell pellets were 78.0 ± 10.7%, 80.1 ± 11.3% and 72.9 ± 16.2% respectively (mean ± SD; n = 5 different concentrations).

2.2.6.7 Cell cycle analysis

Cells were seeded into 6-well plates, at an appropriate density to ensure that wells were no more than 70% confluent at the time of harvesting (Table 2.8).

	Time of harvesting		
	24 h	**48 h**	**72 h**
HCA-7	250,000	200,000	160,000
HT-29	250,000	150,000	130,000
HCEC	120,000	100,000	65,000

Table 2.8 Cell seeding densities for cell cycle analysis. Approximate seeding densities of HCA-7, HT-29 and HCEC cells at 24 h, 48 h and 72 h.

Once seeded, cells were left to adhere for 24 h, after which time, treatments were administered. Cells were harvested at the designated times using trypsin/EDTA (1 ml), and placed in the incubator until cells detached. An equivalent volume of media was added and samples were transferred to Falcon tubes and centrifuged (5 min, 350 x g, room temperature) to pellet the cells. Media was discarded; cells were washed in PBS and resuspended using a vortex during the addition of ice-cold ethanol (2 ml, 70%). Samples were stored at 4°C and kept for a maximum of 7 days before analysis.

Samples were centrifuged (10 min, 350 x g, room temperature) prior to analysis, and the supernatant discarded. Each pellet was resuspended in PBS (800 µl), followed by the addition of RNase A (100 µl, to give a final concentration of 1 mg/ml) and propidium iodide (PI) (100 µl to give a final concentration of 50 µg/ml). Samples were incubated at 4°C overnight to aid DNA staining, and analysed on the flow cytometer (FACS Aria II, BD Bioscience) within 24 h. Analysis of results, which allowed determination of cells in each stage of the cell cycle, was completed using ModFit LT software (Version 3.2).

2.2.6.8 Annexin V-FITC assay

HCA-7, HT-29 and HCEC cells were seeded into 6-well plates at the same densities as those used in the cell cycle analysis experiment (Section 2.2.6.7). At the time of harvesting, media containing floating cells was collected into Falcon tubes. Wells were washed with PBS, followed by the addition of trypsin/EDTA (1 ml). Plates were incubated (5 min) at 37°C, and were agitated to aid cell detachment. Fresh media (1 ml) was added to each well to neutralise the trypsin, and the contents combined with the previously removed media fraction, and samples centrifuged (350 x g, 5 min, room temperature). The supernatant was discarded and replaced with fresh media (4 ml) and cells were resuspended, and incubated at 37°C (30 min). The cell suspension was centrifuged once more (350 x g, 3 min, room temperature) and the supernatant discarded. Cells were resuspended in annexin buffer (1 ml, 1x). Annexin V-FITC conjugate (4 µl) was added to samples, which were incubated in the dark at room temperature

(10 min). PI was added (1.5 µl) to give a final concentration of 1.5 µg/ml and samples incubated (1 min) prior to flow cytometry. Samples waiting to be analysed were stored on ice. Annexin buffer, Annexin V-FITC conjugate and PI were part of the Annexin V-FITC Kit, purchased from Bender MedSystems (GmbH, Vienna, Austria). Analysis was performed on a FACS Aria II flow cytometer (BD Bioscience).

2.2.6.9 Caspase-3 assay

HT-29 cells were seeded into 6-well plates at densities of 150,000 and 130,000 for 48 h and 72 h timepoints respectively, and cells were allowed to attach for 24 h prior to treatment. HCA-7 and HCEC cells were not analysed with this assay. Analysis of samples for caspase-3 staining (optimised by Mr Ankur Karmokar) involved three stages, these were; fixation, permeabilisation and indirect staining of cells.

In the fixation stage, cells were harvested as normal, and media containing floating cells was collected in separate tubes (as with the apoptosis assay), and later recombined with the trypsinised cells. Cells were fixed with the addition of ice-cold methanol (1 ml), and then stored at -20℃ (10 min). After a centrifugation step (5 min, 350 x g, room temperature), cells were washed in 3% BSA in PBS (3 g in 100 ml PBS), centrifuged (3 min, 350 x g, room temperature) and the supernatant discarded.

For permeabilisation, mild detergent (0.5% Tween 20 in PBS i.e. 100 µl of Tween 20 in 20 ml PBS) was added to samples (100 µl), which were then left to incubate at room temperature (15 min). Cells were washed with the mild detergent (1 ml), centrifuged (5 min, 350 x g, room temperature), and the supernatant discarded. The last step was repeated with 3% BSA. Samples were divided into two separate tubes to allow cell staining with either primary and secondary antibodies, or secondary antibody alone. One tube was left unstained. The primary antibody was cleaved caspase-3 rabbit monoclonal antibody (Cell Signalling, UK), and the secondary antibody was goat anti-rabbit (2 mg/ml) Alexa Fluor 594 (Invitrogen, UK). Control

(untreated) cells were not stained. Primary antibody was added to one set of tubes (10 µl) and all tubes were then incubated at room temperature in the dark (40 min). Cells were washed with the addition of 3% BSA solution and centrifuged (3 min, 350 x g, room temperature). The supernatant was discarded and this step was repeated. The secondary antibody was added to all of the samples (2 µl), with the exception of an unstained control, and samples incubated (30 min, 4°C). Two further wash steps in 3% BSA were completed, and cells were resuspended in 500 µl of 3% BSA in PBS and levels of staining determined by flow cytometry using a FACS Aria II flow cytometer (BD Bioscience).

2.2.7 Statistical analysis

Suitable statistical tests were selected to analyse the significance of experimental data, where appropriate. Differences in tissue concentrations between patients were analysed using both the Mann-Whitney U test for unpaired data and the Wilcoxon signed ranks test for paired data. The latter test was applied when comparing left and right-sided tissue samples from the same patient. These non-parametric tests assume that the data is not normally distributed as was confirmed by testing the normality using Q-Q plots.

To determine whether the change in media metabolite concentrations (without cells) over one week was significant the Student's T-test (equal variance) was applied. The same test was used for the analysis of apoptosis levels (by cleavage of caspase-3). One-Way ANOVA was used for the analysis of growth curves, cell cycle and apoptosis (by annexin V-FITC staining) experiments, which can be applied to multiple groups of data for the comparison of mean levels.

CHAPTER 3: PHARMACOKINETICS AND METABOLISM OF RESVERATROL AND RESVERATROL METABOLITES IN HUMANS

3.1 Introduction

There is an increasing body of evidence to suggest that resveratrol has the potential to impact on a variety of human diseases, including cancer. Unfortunately, the results of *in vivo* studies including those in mice [155], rats [131], rabbits [156], pigs [157] and dogs [158] do not necessarily transfer across to humans. To translate encouraging experimental findings into human benefits, information is first needed on factors such as the safety, pharmacokinetics, pharmacodynamics and efficacy of resveratrol in the clinical setting. It has been suggested that the metabolites of resveratrol may play a role in some of the beneficial effects attributed to resveratrol, and it is therefore important to investigate this further and to develop an understanding of the metabolite profiles in human plasma and tissues.

To date, the majority of clinical trials with resveratrol have involved administration of single doses. Where multiple resveratrol doses have been taken, dosing has not normally exceeded more than a 14-day period. The clinical trial conducted as part of this project involved daily dosing of resveratrol at 0.5, 1.0, 2.5 and 5.0 g, for 29 days in healthy volunteers and the analysis of plasma and urine over the course of 24 h. Among the trial objectives were to assess the safety of resveratrol and its effects on circulating levels of insulin-like growth factor-1 (IGF-1) and IGF-binding protein-3 (IGFBP-3). However, in the context of this project specifically, the aim was to determine resveratrol pharmacokinetics and accurately quantify the concentration of resveratrol and metabolites in human plasma. Plasma concentrations and pharmacokinetic parameters were determined for all metabolic species based on resveratrol extraction and UV absorption characteristics. Subsequent to this, authentic resveratrol monosulfate and monoglucuronide standards became available. Plasma levels of the major metabolites (in randomly selected volunteers) were re-analysed using the standards; these 'true' concentrations have not previously been reported, as the synthetic standards have been scarce. Both sets of data are presented in this thesis.

Colorectal cancer patients recruited onto a separate arm of the resveratrol study received eight daily doses of either 0.5 or 1.0 g of resveratrol prior to surgical resection of the colorectal malignancy. In addition to plasma, samples of colorectal tissue and tumour were collected for determination of resveratrol and metabolite concentrations. One of the aims of this part of the study was to assess whether resveratrol and its metabolites were able to reach the colon, and to determine their concentrations using metabolite standards where possible, as opposed to calculating as 'resveratrol equivalents'. Analysis of tissue levels would provide an indication of whether accumulation of the parent resveratrol and/or metabolites could occur within the colorectum, and whether concentrations reaching the tissue would be sufficient to exert beneficial effects. Neither resveratrol nor its metabolite concentrations have previously been determined in the human colon or any other tissue. Following recruitment onto this study, patient samples were collected, and analysed using a validated method. The data was recently published [159], and consistent with the healthy volunteer dosing study, resveratrol metabolite levels were reported as resveratrol equivalents. During the course of this research, the synthesised metabolite standards allowed accurate quantitation of metabolite concentrations. Both sets of data are provided for comparison in this thesis.

3.2 Resveratrol and metabolite concentrations in plasma of healthy volunteers following repeat resveratrol dosing

The average concentration of resveratrol and its major metabolites were calculated over the course of 24 h following ingestion of 0.5, 1.0, 2.5 or 5.0 g resveratrol on a day during the third week day of dosing (n = 10 volunteers per dose). Therefore, volunteers took a minimum of 21 daily doses of resveratrol before plasma samples were collected pre-dosing (on the morning of the study day) and at 0.25, 1.0, 1.5, 5, 12 and 24 h post-dosing. After this number of resveratrol doses, it was anticipated that steady-state levels might have been reached, which would allow comparisons between single and repeat resveratrol dosing. Metabolites identified by HPLC-UV were resveratrol-3-*O*-sulfate, resveratrol-4'-*O*-sulfate, resveratrol disulfate, resveratrol-3-*O*-glucuronide, resveratrol-4'-*O*-glucuronide and resveratrol sulfate glucuronide (Figure 3.1).

3.2.1 Resveratrol metabolites in plasma of healthy volunteers calculated as resveratrol equivalents

The plasma concentration versus time curves for the two monoglucuronides, two monosulfates, disulfate and resveratrol at each dose level are illustrated in Figure 3.2. Concentrations are given as resveratrol equivalents.

For all resveratrol species measured, there is an increase in the average plasma concentration, with higher resveratrol doses, irrespective of the metabolite. However, this dose-dependent increase was the least pronounced for resveratrol disulfate. In general, the metabolites had similar profiles, with rapid initial increases in concentration followed by a gradual decline, starting between 1.5 and 5 h post-dosing and continuing through to 24 h. Resveratrol disulfate appeared to be atypical compared to resveratrol and the other metabolites, as the initial increase in concentration was less marked, and at the 2.5 and 5.0 g doses, the concentration seemed to vary only slightly over 24 h. In terms of metabolites generated, two sulfate metabolites were found to be quantitatively minor products; these were resveratrol-4'-*O*-sulfate and resveratrol disulfate. Following the 0.5 g resveratrol dose, resveratrol-4'-*O*-sulfate was close to, or below the limit of detection in the majority of volunteers, and therefore these data could not be plotted. As shown by the peak plasma concentration achieved, the two glucuronides and resveratrol-3-*O*-sulfate were dominant; compared to these, resveratrol concentrations were relatively low (Figure 3.2). Maximum peak concentrations of resveratrol were observed at an average time of 1 h post-dosing across all doses levels, which is slightly earlier than for the metabolites.

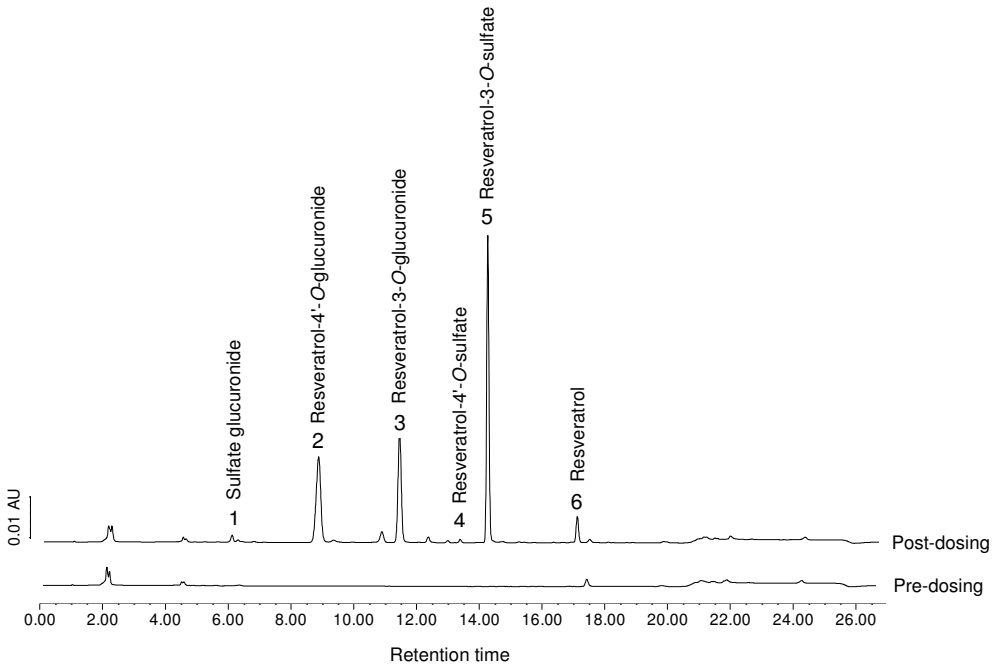

Figure 3.1 Typical HPLC-UV human plasma chromatograms pre- and post-resveratrol dosing

HPLC-UV chromatograms of plasma taken from a healthy volunteer prior to resveratrol ingestion (bottom line), compared to the same volunteer's plasma sample 1 h post-dosing with 1.0 g of resveratrol. Designated peaks are resveratrol sulfate glucuronide (**1**), resveratrol-4'-*O*-glucuronide (**2**), resveratrol-3-*O*-glucuronide (**3**), resveratrol-4'-*O*-sulfate (**4**), resveratrol-3-*O*-sulfate (**5**) and resveratrol (**6**) identified by comparison of retention times with synthesised standards, where available and confirmed by LC-MS/MS. Resveratrol disulfate was not detected in this volunteer, but normally elutes at approximately 9.2 min.

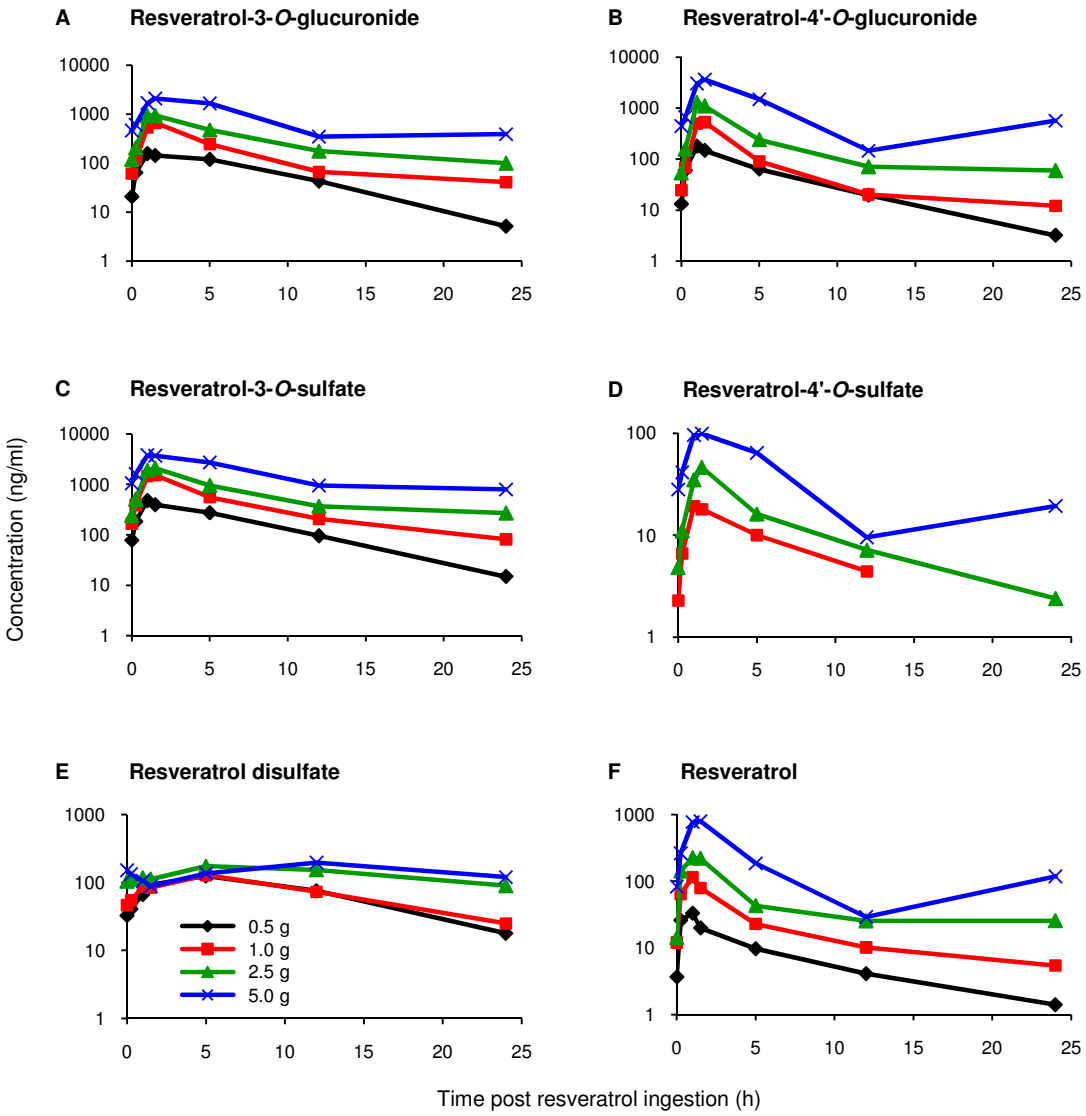

Figure 3.2 Resveratrol and metabolite profiles in plasma of healthy volunteers after repeat resveratrol dosing

Average resveratrol and metabolite concentrations (as resveratrol equivalents) in plasma taken from healthy volunteers receiving 0.5, 1.0, 2.5 or 5.0 g of resveratrol for 21 - 28 days. Values plotted are the mean C_{max} values from 10 volunteers per dose group. (**A**), (**B**), (**C**), (**D**), (**E**) and (**F**) show data for the major metabolites; these are resveratrol-3-*O*-glucuronide, resveratrol-4'-*O*-glucuronide, resveratrol-3-*O*-sulfate, resveratrol-4'-*O*-sulfate, resveratrol disulfate and parent resveratrol respectively. For resveratrol-4'-*O*-sulfate (**D**), the majority of average C_{max} concentrations at the 0.5 g dose level and at 24 h on the 1.0 g dose level were close to, or below the limit of quantitation (LOQ), and therefore were not plotted.

Comparison of the maximum concentrations attained for each metabolite and resveratrol, averaged across each dose group indicates that resveratrol-3-*O*-glucuronide and resveratrol-3-*O*-sulfate reached the highest C_{max} values, followed by resveratrol-4'-*O*-glucuronide (3886, 4172 and 2323 ng/ml respectively) at the 5.0 g dose level (Figure 3.3). For the major metabolites, C_{max} values ranged from 2323 to 4172 ng/ml at the highest dose, and concentrations across all doses were between 2.4 and 12.9-fold greater than for parent resveratrol. The extent of resveratrol-4'-*O*-sulfate formation was low, with average C_{max} concentrations consistently below those attained for resveratrol. Resveratrol disulfate also reached average C_{max} levels similar to, or below those for resveratrol (259 and 967 ng/ml respectively) following 5.0 g resveratrol dosing. There was a large variation in C_{max} between individuals within the same dose group and this was evident for all species. The CV for the C_{max} concentrations ranged from 46 - 88%, 48 - 107%, 35 - 51% and 54 - 89% for resveratrol-4'-*O*-glucuronide, resveratrol-3-*O*-glucuronide, resveratrol-3-*O*-sulfate and resveratrol respectively.

When plotted versus dose, the total extent of exposure, or average area under the curve (AUC_{last}) for resveratrol, the two glucuronides and resveratrol-3-*O*-sulfate increased in a broadly dose-proportional manner (Figure 3.4). The two glucuronides had comparable AUC_{last} levels, whereas resveratrol-3-*O*-sulfate had the highest AUC_{last} values at each of the dose levels, with resveratrol having the lowest. At the 5.0 g dose the AUC_{last} value for resveratrol-3-*O*-sulfate was 38,900 ng·h/ml, which is ~9-fold higher than for parent resveratrol (4121 ng·h/ml).

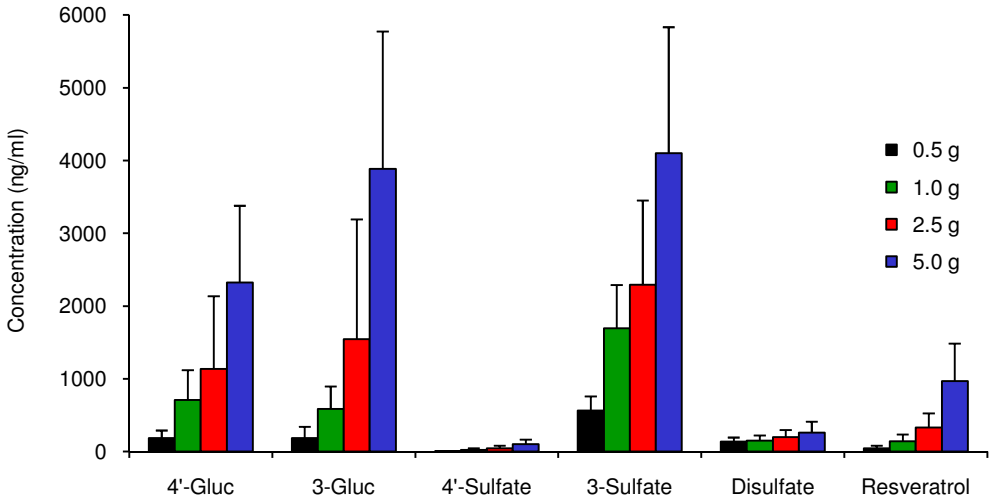

Figure 3.3 Average C_{max} of resveratrol and its metabolites in plasma following repeat resveratrol dosing in healthy volunteers

Plasma C_{max} values shown are the mean + SD of 10 healthy volunteers per dose after 21 - 28 days of resveratrol. Metabolite concentrations are calculated based on resveratrol standard curves and are therefore estimates. CV for resveratrol, resveratrol-4'-*O*-glucuronide, resveratrol-3-*O*-glucuronide and resveratrol-3-*O*-sulfate ranged from 54 - 89%, 46 - 88%, 48 - 107% and 35 - 51% respectively.

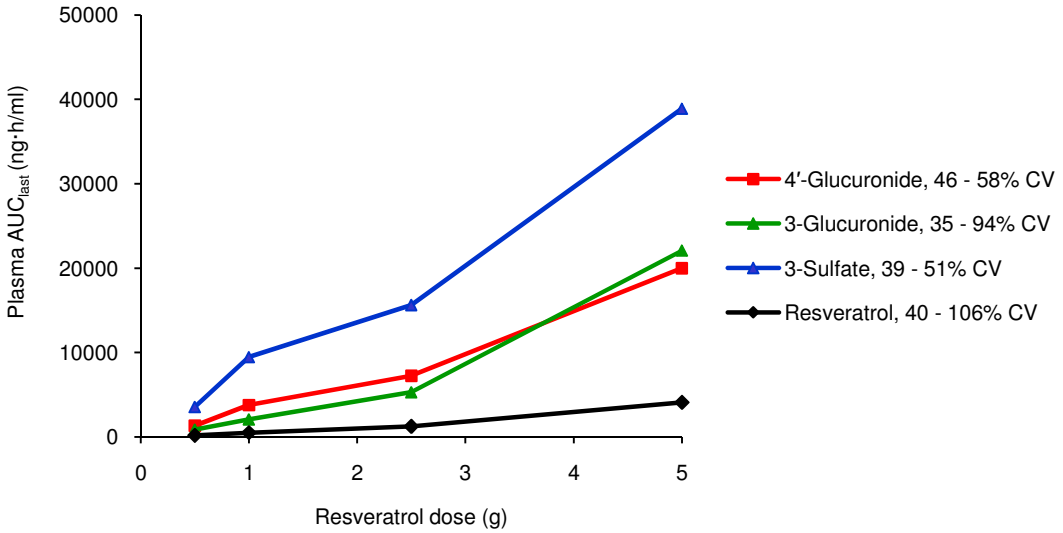

Figure 3.4 Average AUC_{last} of resveratrol and its major metabolites in plasma following repeat resveratrol dosing in healthy volunteers

Plasma AUC_{last} values shown for resveratrol, resveratrol-4'-*O*-glucuronide, resveratrol-3-*O*-glucuronide and resveratrol-3-*O*-sulfate are the mean of 10 healthy volunteers per dose after 21 - 28 days of resveratrol. Percentage CV values are provided in the key.

3.2.2 Resveratrol metabolite concentrations in plasma calculated using metabolite standards

The metabolite concentrations originally calculated in the repeat-dose resveratrol study described in Section 3.2 and published by Brown *et al*. [120], were based on the assumption that recovery characteristics and the relationship between peak area and concentration (i.e. their extinction coefficients) were the same for resveratrol and its metabolites. Resveratrol metabolites are not commercially available. Therefore, metabolite concentrations were given as resveratrol equivalents which could lead to over or under estimation of true concentrations. During the course of the study, authentic monoglucuronide and monosulfate standards were synthesised in-house, making it possible to accurately quantify the 'real' concentrations in the human samples.

To enable comparison of metabolite concentrations in plasma after repeat resveratrol dosing, three volunteers were randomly selected from each dose level for analysis. For each set of volunteer samples, plasma concentrations were calculated as resveratrol equivalents based on an extracted resveratrol standard curve. Authentic glucuronide concentrations were based on the extraction of a standard curve of resveratrol-4'-*O*-glucuronide, and resveratrol monosulfate concentrations based on standard curves of a mixture of the two isomers. Resveratrol and metabolite standard curves were extracted simultaneously with volunteer samples. Although the profiles remain the same qualitatively (Figure 3.5A and Figure 3.5B), it is clear that the metabolite concentrations are much higher when calculated using the authentic standards at every dose level. The average plasma C_{max} concentrations for the glucuronide and both monosulfates (in ng/ml) were approximately 4.7 and 3.9-fold higher, respectively, when calculated using authentic standards (Figure 3.6). Using the same set of data, the AUC_{inf} was recalculated with the WinNonlin software. Taking the 0.5 g dose level as an example, the AUC_{inf} values for the monoglucuronide and monosulfate metabolites were calculated using the resveratrol and authentic standard curves (Figure 3.7). The increase in AUC_{inf} concentrations for the monoglucuronides and monosulfates were also approximately 4.7 and 4-fold higher respectively when recalculated using authentic standards.

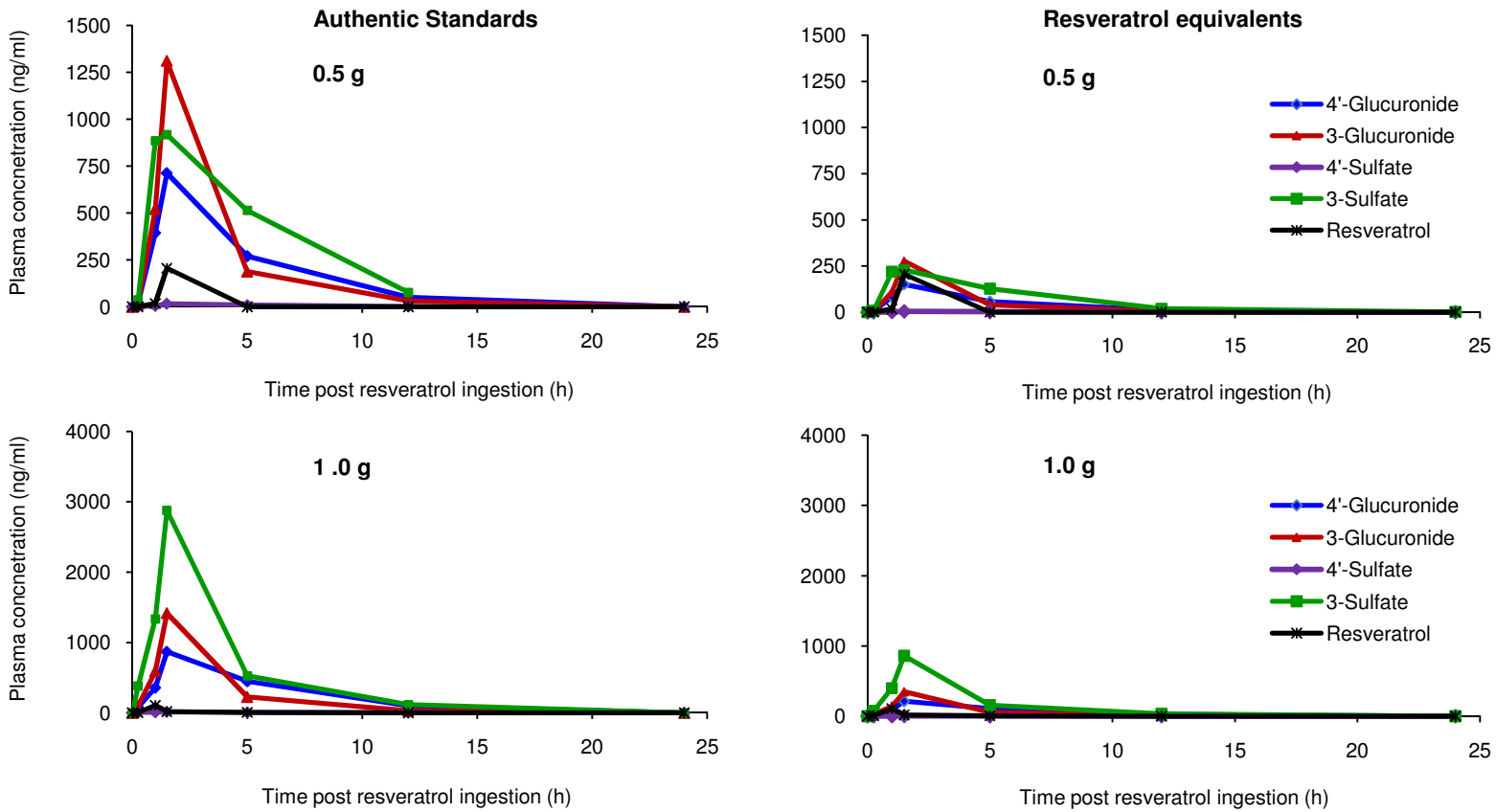

Figure 3.5A Representative resveratrol and metabolite concentration profiles in plasma of healthy volunteers on the 0.5 and 1.0 g dose level

Representative profile of resveratrol and its metabolites in plasma taken from random volunteers (one volunteer per dose, with one plasma sample extracted per timepoint) following repeat resveratrol dosing of 0.5 and 1.0 g in healthy volunteers measured over a 24 h period. Metabolites were calculated using authentic resveratrol-4'-*O*-glucuronide and resveratrol monosulfate metabolite standards (left) and as resveratrol equivalents (right).

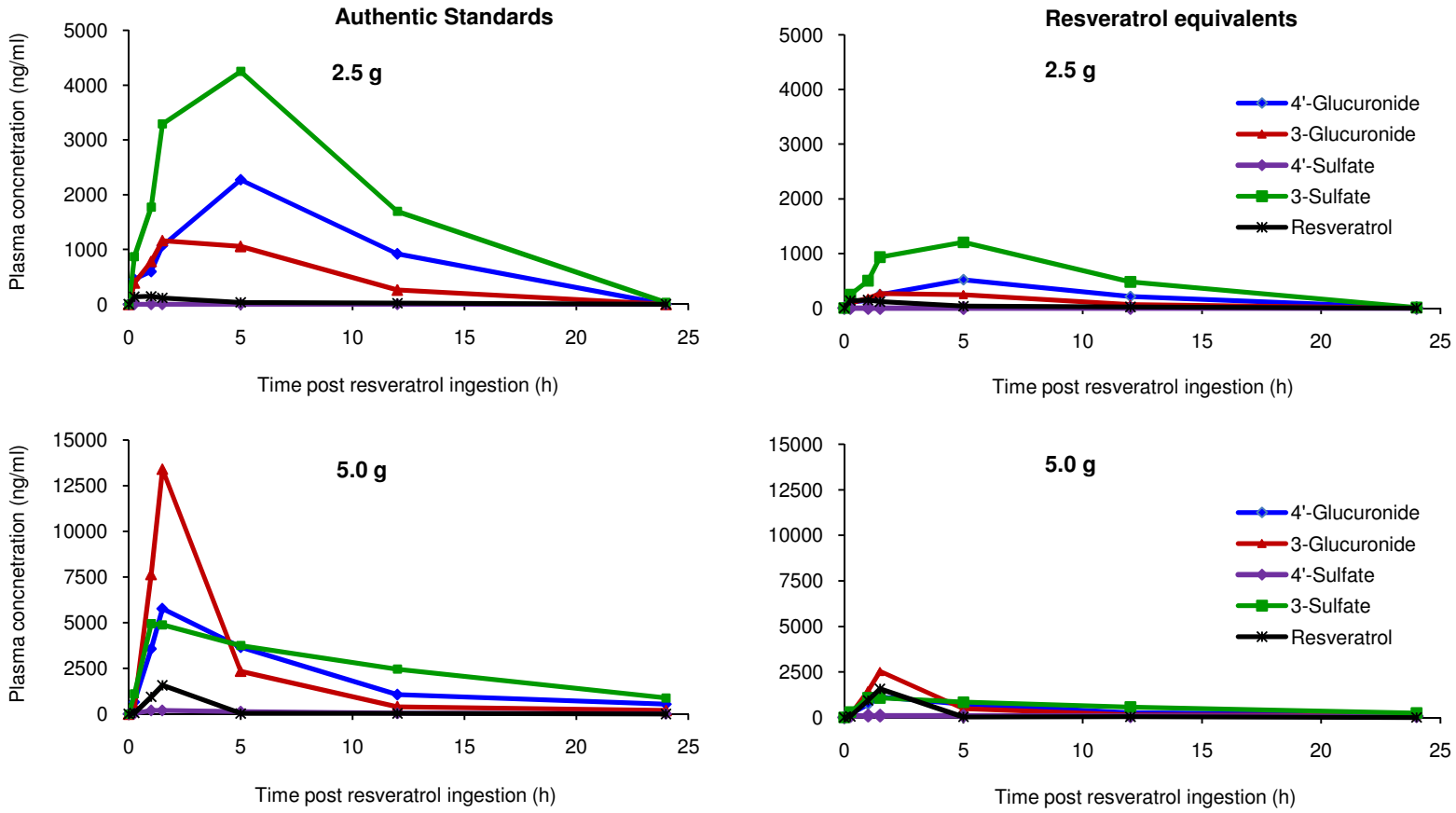

Figure 3.5B Representative resveratrol and metabolite concentration profiles in plasma of healthy volunteers on the 2.5 and 5.0 g dose level

Representative profile of resveratrol and its metabolites in plasma taken from random volunteers (one volunteer per dose, with one plasma sample extracted per timepoint) following repeat resveratrol dosing of 2.5 and 5.0 g in healthy volunteers measured over a 24 h period. Metabolites were calculated using authentic resveratrol-4'-*O*-glucuronide and resveratrol monosulfate metabolite standards (left) and as resveratrol equivalents (right).

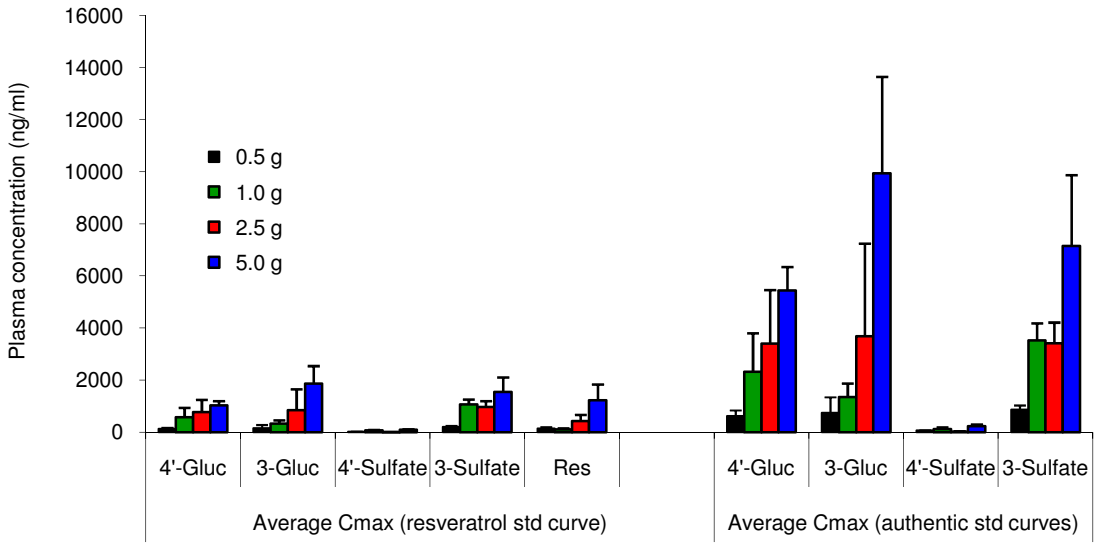

Figure 3.6 Metabolite plasma C_{max} concentrations based on resveratrol equivalents and authentic metabolite standards

Comparison of average plasma C_{max} concentrations in three healthy volunteers, receiving daily doses of 0.5, 1.0, 2.5 or 5.0 g resveratrol for 21 - 28 days, based on resveratrol equivalents (left), and authentic metabolite standards (right). Values shown are the mean + SD of 3 volunteers selected at random from each dose level.

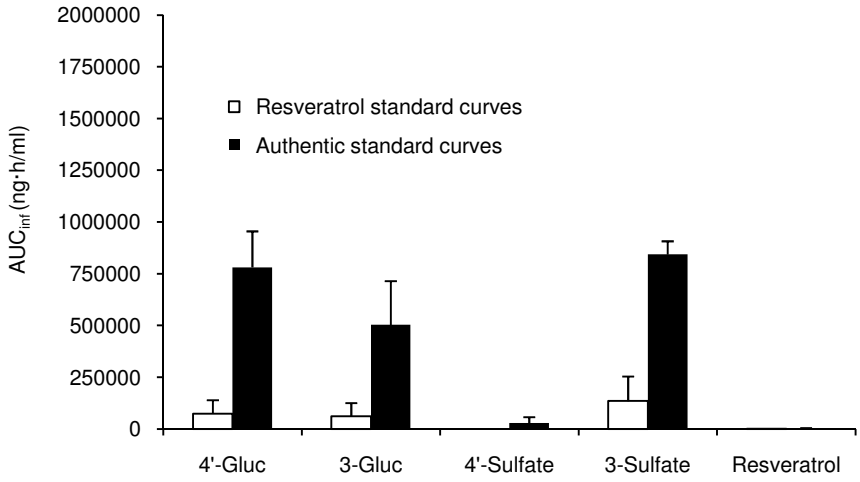

Figure 3.7 Metabolite plasma AUC_{inf} concentrations based on resveratrol equivalents and authentic metabolite standards

Comparison of average AUC_{inf} in three healthy volunteers receiving daily doses of 0.5 g resveratrol for 21 - 28 days based on resveratrol equivalents (clear bars), and authentic metabolite standards (black bars). Values shown are the mean + SD of 3 volunteers selected at random from the 0.5 g dose level.

3.3 Repeat resveratrol dosing study in colorectal cancer patients

Twenty patients with colorectal cancer were recruited onto the study by Dr Victoria Brown. Eleven of these patients were female and nine were males, and their ages ranged from 46 - 83 years. Patients (10 per dose level) ingested 0.5 or 1.0 g of resveratrol for eight days prior to resection of their tumour. The final resveratrol capsule was taken on the evening prior to surgery. The majority of patients (60%) underwent surgery the following morning, with the remainder during the afternoon. Up to seven different pieces of colon tissue were removed at proximal and distal regions to the tumour tissue (5 cm and 10 cm away and at the resection margins). The collection of these normal specimens was dependent upon tumour location and length of the colon section that was removed. Therefore, it was not always possible to obtain the 5 and 10 cm sections from each patient. Normal and malignant (tumour) tissues were analysed for the presence of resveratrol and its metabolites.

There were differences in the staging and location of tumours that were resected from patients. In total, 21 tumours were removed, as one patient presented with two tumours; one in the caecum (right-side), and the other in the sigmoid colon (left-side). Both tumours were removed during the course of the same operation. The locations of the 21 tumours removed from the colon of the patients are shown in Figure 3.8. Blood was also taken pre-dosing, and during the surgery to allow analysis of plasma resveratrol and metabolite levels.

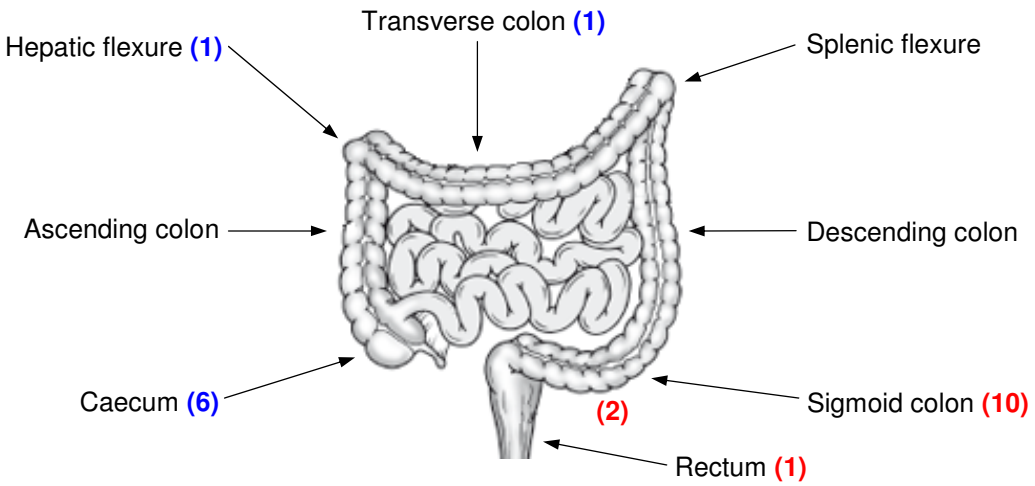

Figure 3.8 Anatomy of the human colon and location of resected colorectal cancers

The location of tumours resected from 20 colorectal cancer patients receiving either 0.5 or 1.0 g of resveratrol for eight days. In total, 21 tumours were removed from 20 patients, as one patient presented with two synchronous left and right-sided tumours. Values given in parentheses indicate the total number of tumours that were removed from each section. Numbers in blue indicate right-sided tumours, whereas numbers in red indicate left-sided tumours.

3.3.1 Resveratrol and metabolite concentrations in colon tissue samples

In addition to parent resveratrol (described below), a number of metabolites were detected and quantified in the colon tissue of patients on both dose levels, these were resveratrol-3-*O*-sulfate, resveratrol-4'-*O*-sulfate, resveratrol disulfate, resveratrol-3-*O*-glucuronide, resveratrol-4'-*O*-glucuronide and a sulfate glucuronide. Whereas the previously published concentration values for these metabolites were calculated as resveratrol equivalents (Table 7.3 and 7.4; Appendix), the data presented here (and summarised in Table 3.1 and 3.2) give authentic resveratrol-3-*O*-sulfate and resveratrol-4'-*O*-sulfate concentrations. Resveratrol disulfate concentrations have also been based on monosulfate standards. Concentrations of the isomeric monoglucuronides were extrapolated from quantitation of three sets of random patients per dose group (analysed with resveratrol monoglucuronide standards). Projected concentrations for the different tissue sections and those across each dose group were determined this way, and samples analysed from each dose group were assumed to be representative of all patients. Finally, the sulfate glucuronide concentrations were also recalculated based on resveratrol-4'-*O*-glucuronide standards. Individual metabolite concentrations are described in Section 3.3.2 onwards.

Colorectal tissue resveratrol concentrations were originally calculated using standard curves of the compound, and therefore were not adjusted in any way, and these levels are summarised here (Table 3.1 and Table 3.2). Concentrations of resveratrol measured in each tissue sample were plotted as individual points (in scatter plots) to show the variation within different sections of tissue and between tumour and proximal/distal tissues taken from the same patient. The scatter plots also allow comparisons to be made between different individuals. There did not appear to be an obvious trend in resveratrol concentrations detected in specific tissue types, although there were higher resveratrol concentrations achieved in tissues proximal to the tumour (at the 1.0 g dose; Figure 3.9B). Tumour tissue concentrations, as indicated by symbols in red, did not seem to follow a pattern. Following the 0.5 g dose, resveratrol concentrations in tissues originating in the left side of the colon, from different patients were broadly similar in terms of the mean concentrations reached and the (relatively narrow)

distribution within individual tissues (Figure 3.9A). The highest mean resveratrol concentration (in left-sided tissues where levels were detected) was achieved in patient C110, with 1.62 nmol/g of tissue.

With an increasing dose from 0.5 to 1.0 g, there were higher resveratrol levels detected within the tissues. In tumour tissue at the low dose, the mean concentration achieved was 8.3 ± 6.1, whereas following the 1.0 g dose the corresponding concentration was 94 ± 89 nmol/g. Maximum concentrations in tumour reached 15.0 and 195 nmol/g at the 0.5 and 1.0 g dose respectively. Where the highest resveratrol concentrations were detected, there was also a large variation within different tissues sections removed from the same patient, indicating the high intra-individual variability. For example, in patient C223, who was recruited onto the 1.0 g dose level, the tumour tissue resveratrol concentration was 186 nmol/g of tissue. In the same patient, two out of three sections of tissue located distally to the tumour had lower resveratrol concentrations with one higher (272 nmol/g). In contrast, the proximal tissue sections had resveratrol concentrations up to 20-fold above those found in the tumour tissue, ranging from 1146 to 3774 nmol/g - the highest observed resveratrol tissue level across all of the samples analysed. Mean resveratrol concentrations across all tissues in this patient were 1253 ± 1600 nmol/g.

Furthermore, there was found to be a prominent increase in the magnitude of tissue concentrations originating from the right-side of the colon as compared to the left for a given dose (3.9B and D versus 3.9A and C respectively). This trend was found to occur in all sections of tissue, including tumours. The difference in concentrations within the colorectal tissue based on the anatomical region is described further in Section 3.3.5.

0.5 g Resveratrol	Left-sided (n = 7)			Right-sided (n = 3)		
	Proximal to tumour	Tumour	Distal to tumour	Proximal to tumour	Tumour	Distal to tumour
Resveratrol	0.67 ± 0.72 (0 - 3.01)	0.63 ± 0.69 (0 - 1.80)	0.48 ± 0.47 (0 - 1.04)	18.6 ± 17.4 (0 - 45.9)	8.3 ± 6.1 (3.11 - 15.0)	4.9 ± 4.8 (1.95 - 13.5)
Resveratrol-3-*O*-glucuronide	0.19 ± 0.43 (0 - 1.22)	0	0.13 ± 0.38 (0 - 1.14)	137.7 ± 200.6 (0 - 506.7)	1.2 ± 2.0 (0 - 3.5)	1.02 ± 0.74 (0 - 1.50)
Resveratrol-4'-*O*-glucuronide	0.27 ± 0.54 (0 - 1.49)	0.16 ± 0.42 (0 - 1.10)	0.45 ± 0.69 (0 - 1.58)	12.7 ± 17.9 (0 - 45.1)	0.46 ± 0.80 (0 - 1.39)	0
Resveratrol disulfate	1.43 ± 2.28 (0 - 6.43)	0.99 ± 1.70 (0 - 3.84)	3.6 ± 7.7 (0 - 21.7)	20.2 ± 24.9 (0 - 54.7)	1.9 ± 1.9 (0 - 3.71)	0.29 ± 0.63 (0 - 1.41)
Resveratrol-3-*O*-sulfate	1.03 ± 1.24 (0 - 4.95)	0.50 ± 1.10 (0 - 2.96)	1.3 ± 2.0 (0 - 6.13)	70.8 ± 102.5 (0 - 268.7)	5.5 ± 4.1 (0.93 - 7.10)	3.83 ± 0.69 (1.37 - 2.17)
Resveratrol-4'-*O*-sulfate	0.08 ± 0.19 (0 - 0.79)	0.27 ± 0.49 (0 - 1.26)	0.05 ± 0.14 (0 - 0.45)	2.1 ± 3.0 (0 - 8.18)	0.26 ± 0.46 (0 - 0.79)	0.08 ± 0.19 (0 - 0.42)
Resveratrol sulfate glucuronide	27.3 ± 33.3 (0 - 97.8)	20.5 ± 25.4 (0 - 55.3)	32.1 ± 63.5 (0 - 192.9)	71.1 ± 76.6 (0 - 237.7)	8.1 ± 12.6 (0 - 22.6)	0

Table 3.1 Average resveratrol and metabolite concentrations in sections of human colon and tumour tissue after 0.5 g repeat resveratrol dosing

Concentration of resveratrol and its metabolites in normal tissue (proximal or distal to the tumour) and tumour tissue in colorectal cancer patients who received 0.5 g resveratrol for eight days (in nmol/g of tissue). Concentrations are separated for left-sided (splenic flexure, descending colon, sigmoid colon, and rectum) and right-sided (caecum, ascending colon and hepatic flexure) tumour and tissues. Monosulfate concentrations in all patient samples are calculated using resveratrol-3-*O*-sulfate and resveratrol-4'-*O*-sulfate standards. Glucuronide concentrations are determined based on extraction of selected patient samples (3 sets per dose) and calculated using resveratrol-4'-*O*-glucuronide standards, whereas resveratrol disulfate and resveratrol sulfate glucuronide concentrations are based on resveratrol sulfate and resveratrol-4'-*O*-glucuronide standard curves respectively. Values are the mean ± SD of seven samples from tissues on the left side and three from the right side, with one tumour sample and between one and three normal tissue samples per patient. The range is given in brackets.

1.0 g Resveratrol	Left-sided (n = 6)			Right-sided (n = 5)		
	Proximal to tumour	Tumour	Distal to tumour	Proximal to tumour	Tumour	Distal to tumour
Resveratrol	1.21 ± 1.33 (0 - 5.23)	2.1 ± 3.3 (0.3 - 8.7)	2.1 ± 3.3 (0.3 - 9.4)	674 ± 1303 (10.1 - 3774)	94.1 ± 89.2 (12.7 - 195)	62.5 ± 76.2 (10.7 - 272)
Resveratrol-3-*O*-glucuronide	0.30 ± 0.35 (0 - 0.98)	0	0.45 ± 0.46 (0 - 1.14)	17.3 ± 27.5 (0 - 81.3)	1.2 ± 1.12 (0 - 2.96)	1.33 ± 1.30 (0 - 5.18)
Resveratrol-4'-*O*-glucuronide	0.69 ± 0.66 (0 - 1.95)	0.61 ± 0.75 (0 - 1.68)	0.85 ± 0.77 (0 - 2.16)	2.7 ± 3.0 (0 - 8.5)	0.85 ± 1.26 (0 - 2.85)	1.3 ± 1.2 (0 - 3.8)
Resveratrol disulfate	0	0	0	0.99 ± 1.67 (0 - 5.85)	0	0.14 ± 0.46 (0 - 1.56)
Resveratrol-3-*O*-sulfate	0.81 ± 0.79 (0 - 2.41)	0.23 ± 0.41 (0 - 1.01)	1.6 ± 2.0 (0 - 5.7)	117.7 ± 207.3 (6.8 - 638.0)	21.5 ± 32.3 (2.4 - 78.0)	10.1 ± 5.3 (2.6 - 19.0)
Resveratrol-4'-*O*-sulfate	0	0.07 ± 0.02 (0 - 0.44)	0	4.2 ± 4.0 (0 - 13.1)	6.7 ± 11.3 (0 - 26.7)	1.4 ± 1.2 (0 – 3.0)
Resveratrol sulfate glucuronide	31.2 ± 7.7 (17.1 - 43.7)	33.1 ± 8.1 (18.7 - 40.6)	40.3 ± 27.5 (7.3 - 82.9)	43.4 ± 34.6 (16.6 - 151.4)	46.6 ± 20.5 (26.2 - 81.0)	29.4 ± 9.2 (15.4 - 47.0)

Table 3.2 Average resveratrol and metabolite concentrations in sections of human colon and tumour tissue after 1.0 g repeat resveratrol dosing

Concentration of resveratrol and its metabolites in normal tissue (proximal or distal to the tumour) and tumour tissue in colorectal cancer patients who received 1.0 g resveratrol for eight days (in nmol/g of tissue). Concentrations are separated for left-sided (splenic flexure, descending colon, sigmoid colon, and rectum) and right-sided (caecum, ascending colon and hepatic flexure) tumour and tissues. Monosulfate concentrations in all patient samples are calculated using resveratrol-3-*O*-sulfate and resveratrol-4'-*O*-sulfate standards. Glucuronide concentrations are estimated based on extraction of selected patient samples (3 sets per dose) with resveratrol-4'-*O*-glucuronide standards, whereas resveratrol disulfate and resveratrol sulfate glucuronide concentrations are based on resveratrol sulfate and resveratrol-4'-*O*-glucuronide standard curves respectively. Values are the mean ± SD of six samples from tissues on the left side and five from the right side, with one tumour sample and between one and three normal tissue samples per patient. The range is given in brackets.

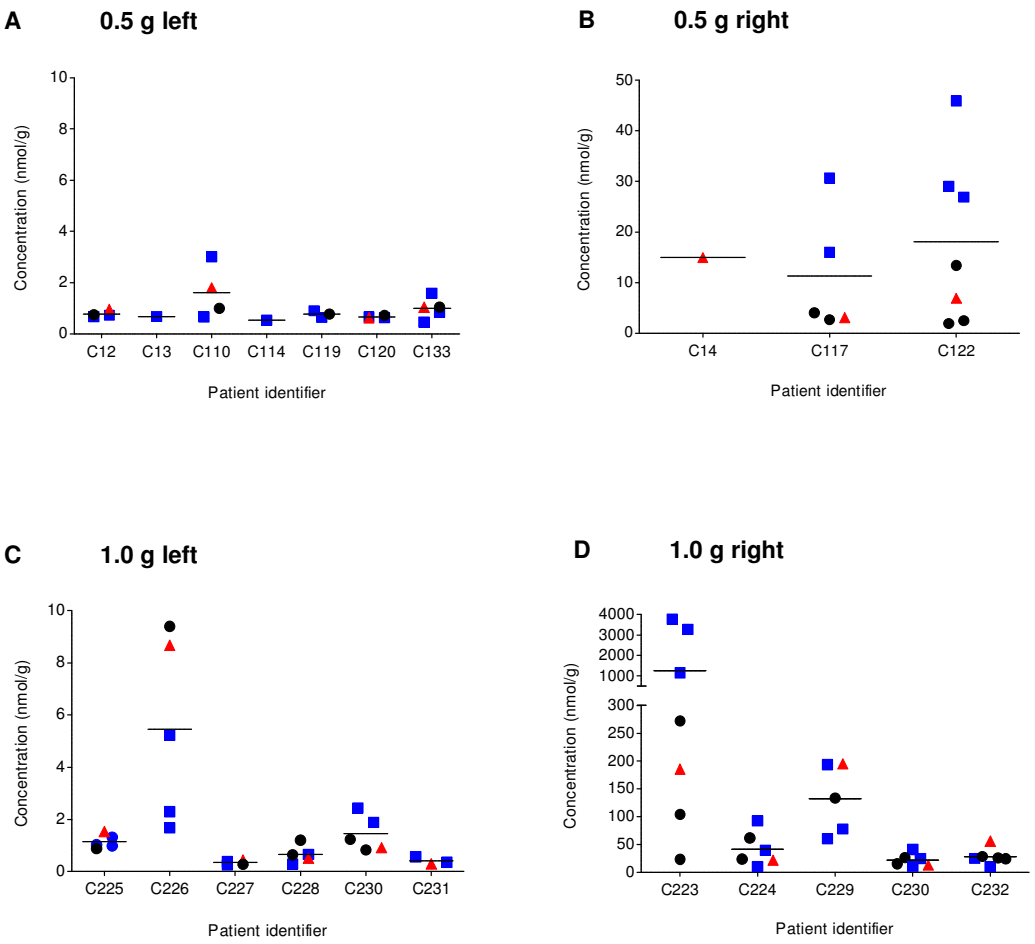

Figure 3.9 Scatterplots of resveratrol concentrations in sections of human colon and tumour tissue after resveratrol daily dosing

Resveratrol concentrations in sections of colon and tumour tissue taken from colorectal cancer patients, who received either 0.5 g (**A** and **B**), or 1.0 g resveratrol for eight days (**C** and **D**). (**A**) and (**C**) show concentrations in left-sided tissues, and (**B**) and (**D**) show concentrations in right-sided tissues. Symbols in blue, black and red represent tissue proximal to the tumour, distal to tumour and tumour tissue respectively. Samples where the concentrations were below the LOQ have not been included in the graphs. Horizontal bars indicate the mean tissue concentrations, across sections where resveratrol was detected. A break in the y-axis has been incorporated in (**D**) for clarity. Significance was tested using the Mann-Whitney U test. Resveratrol levels in tissues originating from the right-side of patients were significantly higher than those from the left-side at both the 0.5 and 1.0 g dose ($P \leq 0.0005$ for both). Levels achieved following the 1.0 g dose were also significantly elevated compared to concentrations generated at the 0.5 g dose; this was the case for both left ($P = 0.029$) and right-sided ($P \leq 0.0005$) tissues.

3.3.2 Resveratrol sulfate concentrations in tissue samples, expressed as resveratrol equivalents and authentic concentrations

Values previously reported by our group [114] presented metabolite concentrations in colon tissues as resveratrol equivalents, based on the assumption that recovery characteristics and relationship between peak area ratio and concentration were the same for resveratrol and its metabolites. At the same time, and in order to obtain a more accurate indication of the levels of resveratrol monosulfate metabolites achievable in human colon tissue, authentic monosulfate metabolites were also used to quantify concentrations. Both sets of standard curves were extracted simultaneously with all patient colon tissues and used for quantification (Figure 3.10).

The recalculated concentrations, based on authentic standard curves, were on average 1.7-fold higher for the resveratrol sulfates than the published estimated values. In patient C223, where the highest concentration of sulfates were detected, the authentic concentration was 185 ± 273 nmol/g rather than 107 ± 156 nmol/g of tissue. Using the recalculated (authentic) sulfate concentrations, the range of concentrations found in different sections of patient tissue were plotted, to assess the intra and inter-patient distribution (Figure 3.11). As shown for resveratrol, there was a clear difference in the concentrations of resveratrol-3-*O*-sulfate detected in tissues taken from the left and right-side of the colon. Whereas, the mean sulfate concentration (indicated by horizontal bars) across all tissues and patients was approximately 1.6 ± 1.5 nmol/g in tissues originating in the left-side, the corresponding value on the right was 37.7 ± 78.0 nmol/g following repeated dosing. Following the 0.5 g resveratrol dosing, there did not appear to be a clear pattern for concentrations in the different tissue sections either proximally or distally located in relation to the tumour, or within the tumour tissue itself (Figure 3.11).

Unlike resveratrol-3-*O*-sulfate, resveratrol-4'-*O*-sulfate was a minor metabolite, and in left-sided tissues following both doses, concentrations were not found to exceed a mean concentration of 0.27 ± 0.49 nmol/g. Resveratrol disulfate was also a minor metabolite in tissues, and in the tumour tissue, the disulfate was generally close to, or below the LOQ (Table 3.1 and 3.2).

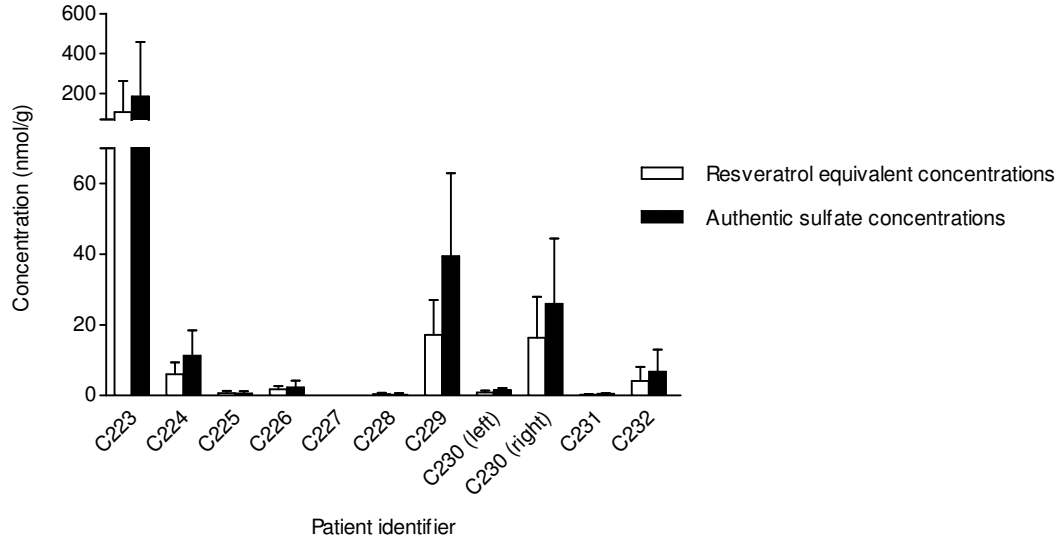

Figure 3.10 Resveratrol-3-*O*-sulfate concentrations in human colon tissues based on resveratrol equivalents and authentic standards

Average resveratrol-3-*O*-sulfate concentrations in non-malignant and tumour tissue removed from the colon of patients receiving 1.0 g of resveratrol daily for eight days. Concentrations are presented as resveratrol equivalents (clear bars) and as authentic resveratrol-3-*O*-sulfate concentrations (black bars), calculated based on standard curves of the metabolite. Sulfate standard curves were analysed alongside resveratrol standard curves and with all patient samples. Values are the mean of 3 to 7 sections of colon tissue (including tumour tissue) per patient. A break in the y-axis has been incorporated for clarity.

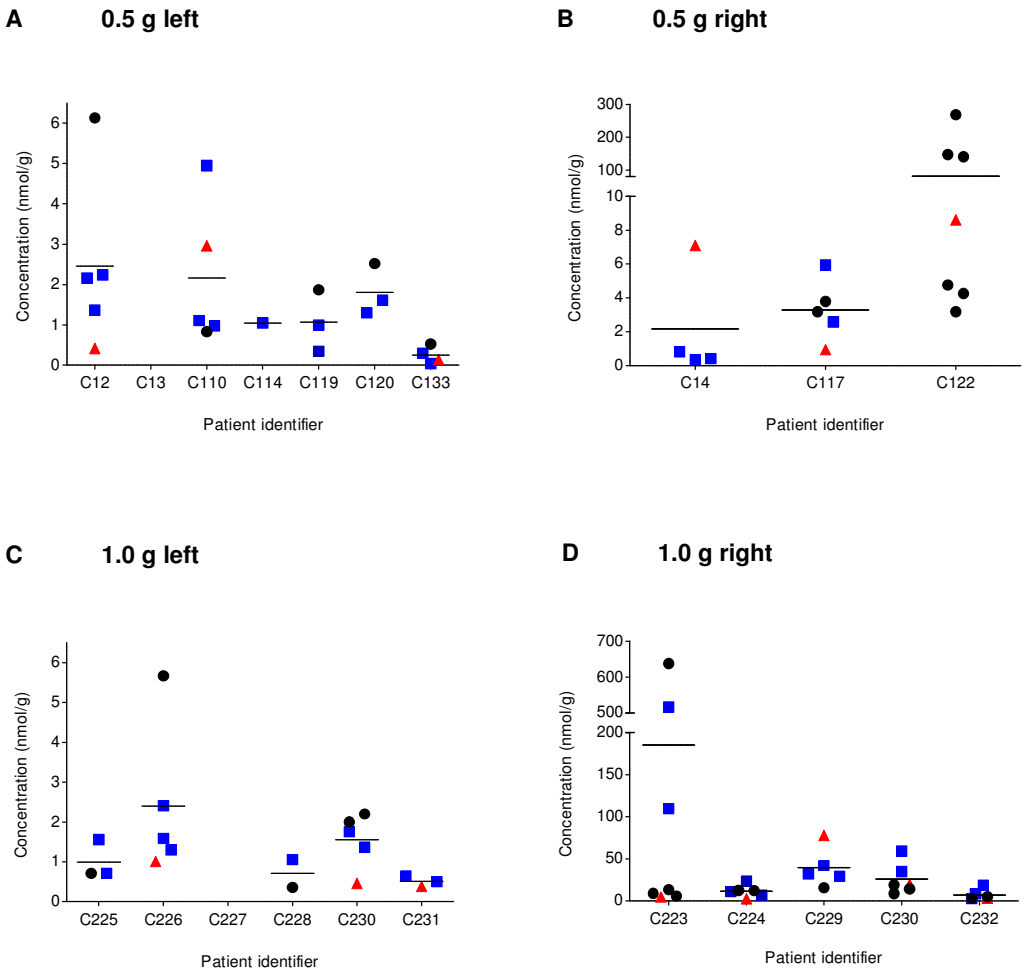

Figure 3.11 Scatterplots of resveratrol-3-*O*-sulfate concentrations in sections of human colon and tumour tissue after daily resveratrol dosing

Resveratrol-3-*O*-sulfate concentrations in sections of colon and tumour tissue taken from colorectal cancer patients, who received either 0.5 g (**A** and **B**), or 1.0 g resveratrol for eight days (**C** and **D**). (**A**) and (**C**) show concentrations in left-sided tissues, and (**B**) and (**D**) show concentrations in right-sided tissues. Symbols in blue, black and red represent tissue proximal to the tumour, distal to tumour and tumour tissue respectively. Samples where the concentrations were below the LOQ have not been included in the graphs. Horizontal bars indicate the mean tissue concentrations, across sections where resveratrol was detected. A break in the y-axis has been incorporated in (**B**) and (**D**) for clarity. Significance was tested using the Mann-Whitney U test. Resveratrol-3-*O*-sulfate levels in tissues originating from the right-side of patients were significantly higher than those from the left-side at both the 0.5 and 1.0 g dose ($P \leq 0.0005$ for both). There was no significant difference between levels achieved following the two different doses in tissues originating from the left side ($P = 0.864$). In right-sided tissues however, there was a significant difference between levels achieved at the two doses ($P = 0.012$).

3.3.3 Resveratrol sulfate glucuronide concentrations in tissue samples

In colon tissues, the sulfate glucuronide conjugate was found to consistently reach high levels in the majority of patients; it was a prominent metabolite in five out of ten patients on the 0.5 g dose and nine out of ten patients on the 1.0 g dose. Interestingly, the differences between left and right-sided concentrations observed for parent resveratrol and all of the other metabolites were not apparent for the sulfate glucuronide, with similar concentrations being achieved regardless of anatomical region (Figure 3.12A and C versus 3.12B and D). For example, following the 1.0 g dose, the sulfate glucuronide concentration (calculated as resveratrol equivalents) was 21 ± 9 and 24 ± 16 nmol/g (mean ± SD; n = 10 patients) across all left and right-sided tissue samples, respectively. Furthermore, the increase in dose did not correlate with higher tissue concentrations. Due to the lack of an authentic sulfate glucuronide standard, the concentrations plotted represent resveratrol equivalents, and are therefore approximations.

3.3.4 Resveratrol glucuronide concentrations in tissue samples, expressed as resveratrol equivalents and authentic concentrations

For the determination of authentic glucuronide tissue levels, concentrations of the two glucuronides were based on the extraction of resveratrol-4'-*O*-glucuronide spiked into tissue, and extracted alongside patient samples. Authentic glucuronide concentrations were calculated in samples from three randomly selected patients from the 0.5 g dose and another three sets from the 1.0 g dose (Figure 3.13), and used to estimate concentrations across all patients (Table 3.1 and 3.2). Three patient subsets from within each dose group were assumed to be representative of all samples, and were not major outliers. Glucuronide concentrations based on the authentic standards were found to be on average 1.6-fold greater than values calculated using the resveratrol standard curves; concentrations detected were consistently higher at both the 0.5 and 1.0 g dose level in the samples analysed.

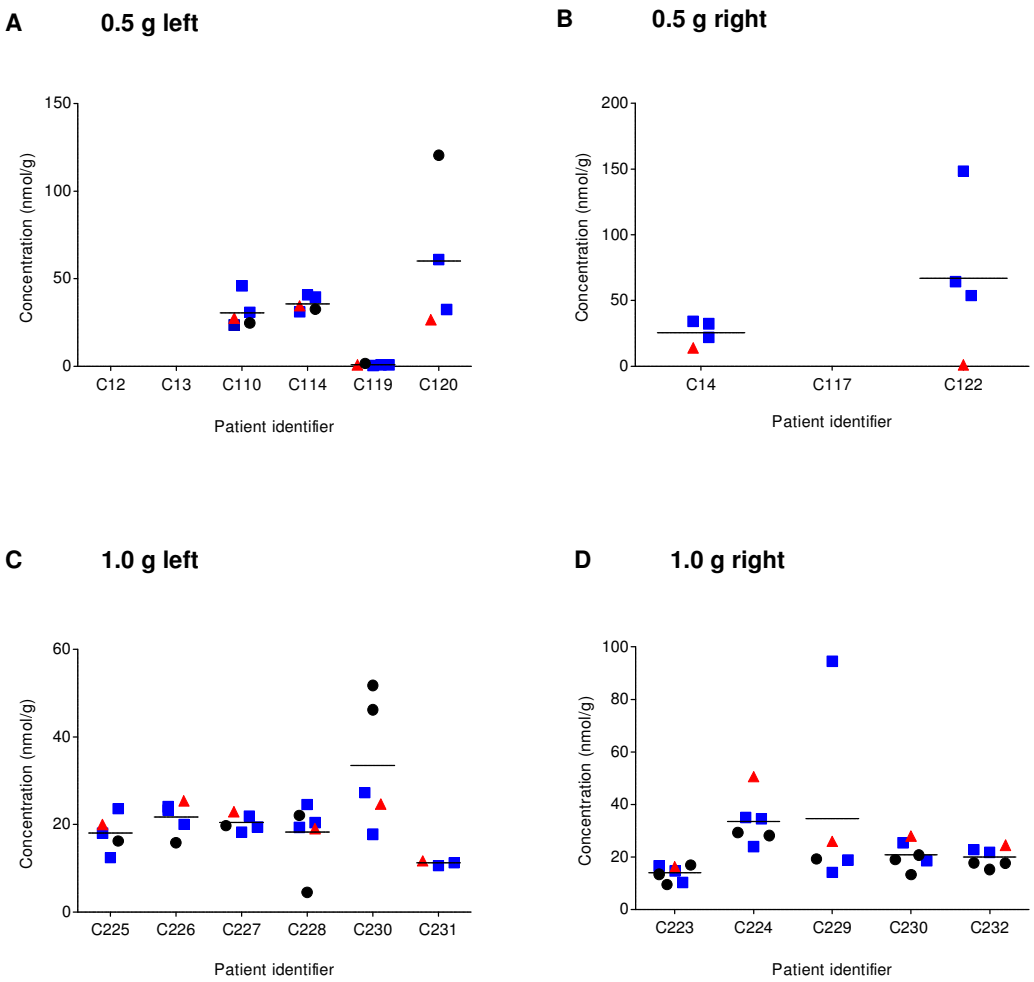

Figure 3.12 Scatterplots of resveratrol sulfate glucuronide concentrations in sections of human colon and tumour tissue after daily resveratrol dosing

Resveratrol sulfate glucuronide concentrations calculated as resveratrol equivalents in sections of colon and tumour tissue taken from colorectal cancer patients, who received either 0.5 g (**A** and **B**), or 1.0 g resveratrol for eight days (**C** and **D**). (**A**) and (**C**) show concentrations in left-sided tissues, and (**B**) and (**D**) show concentrations in right-sided tissues. Symbols in blue, black and red represent tissue proximal to the tumour, distal to tumour and tumour tissue respectively. Samples where the concentrations were below the LOD have not been included in the graphs. Horizontal bars indicate the mean tissue concentrations, across sections where the sulfate glucuronide was detected. Significance was tested using the Mann-Whitney U test. Resveratrol sulfate glucuronide levels in tissues originating from the right-side of patients were not significantly higher than those from the left-side at either the 0.5 or 1.0 g dose ($P = 1$ and $P = 0.862$ respectively). There was also no significant difference between levels achieved following the 0.5 and 1.0 g dose in tissues originating from either the left side or right side ($P = 0.099$ and $P = 0.071$ respectively).

A Resveratrol-4'-*O*-glucuronide

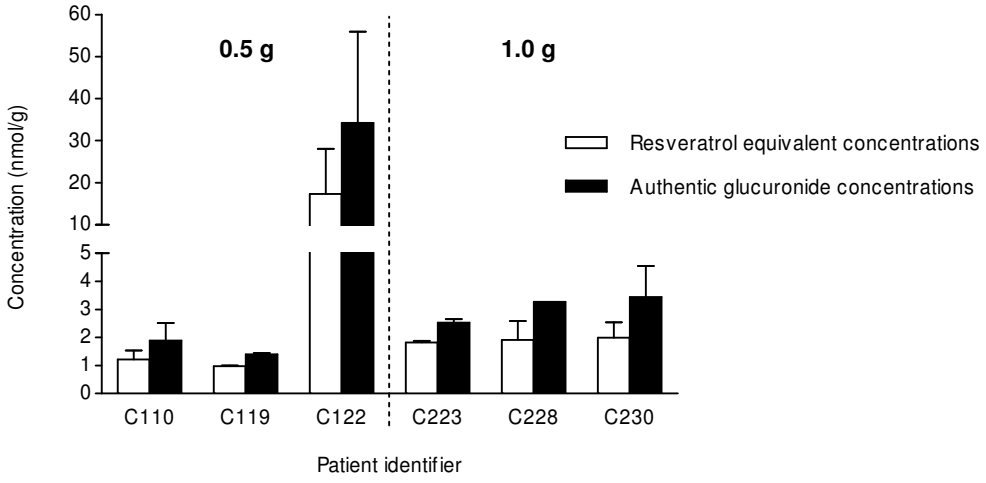

B Resveratrol-3-*O*-glucuronide

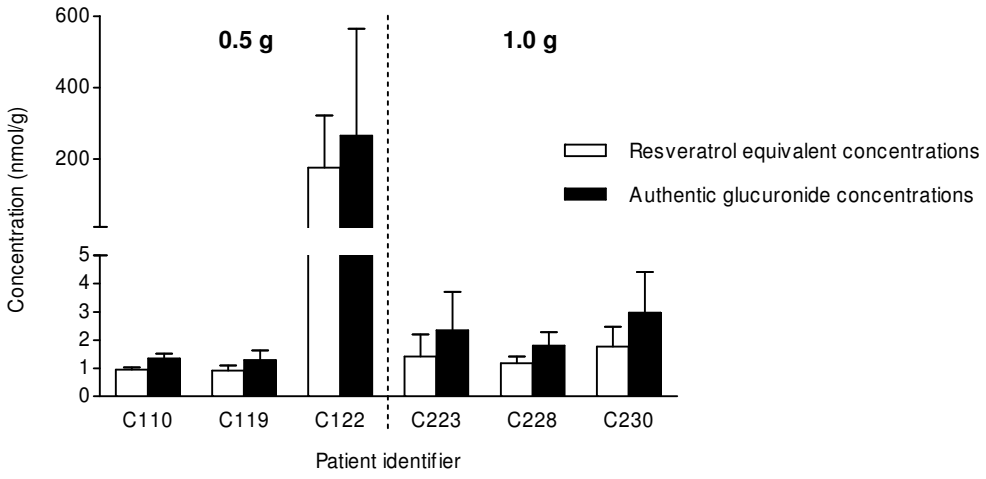

Figure 3.13 Average resveratrol glucuronide concentrations in sections of human colon and tumour tissue after resveratrol dosing

Average resveratrol-4'-*O*-glucuronide (**A**) and resveratrol-3-*O*-glucuronide (**B**) concentrations in non-malignant and tumour tissue removed from the colon of patients receiving 0.5 or 1.0 g of resveratrol for eight daily doses. A random set of patients were chosen to represent each group as a whole. Patient identifiers beginning with 'C1' indicate recruitment onto the 0.5 g dose, whereas identifiers starting with 'C2' indicate participants on the 1.0 g dose level. Concentrations are presented as resveratrol equivalents (clear bars) and as authentic resveratrol glucuronide concentrations (black bars), calculated based on standard curves of the metabolite. Values are the mean of 3 to 7 sections of colon tissue (including tumour tissue). A break in the y-axis has been incorporated for clarity.

3.3.5 Variation in tissue resveratrol and metabolite concentrations with localisation

The tissue concentrations of resveratrol and all metabolites detected apart from the sulfate glucuronide seemed to be related to the site at which the tumour was located, i.e. whether it originated on the left or right side of the colon. Concentrations detected in colon tissues originating from the right side of patients were higher than those from the left side. The left-right variation described is clearly illustrated for resveratrol and resveratrol-3-*O*-sulfate in tumour tissue (Figure 3.14). There were greater concentrations achieved for both parent and metabolite with a dose escalation from 0.5 to 1.0 g in the right-sided tumours, whereas this did not appear to be the case with the tumours originating on the left. The differences in concentrations achieved between the two sides of the colon were exemplified by a colorectal cancer patient who presented with two synchronous left and right-sided tumours (Figure 3.15). Analysis of similar sections of non-malignant tissue relative to the tumour, and tumour itself removed from either side of the colon, revealed marked differences in the concentrations (true values) found within the tissues. This was apparent for both resveratrol and resveratrol-3-*O*-sulfate (Figure 3.15). In the tumours, concentrations of resveratrol and true values of resveratrol-3-*O*-sulfate on the right-side were 14-fold and 43-fold greater, respectively, than those in left sided samples. Resveratrol concentrations observed in this particular patient were similar to those for resveratrol-3-*O*-sulfate.

The glucuronide and disulfate concentrations were also found to follow a similar pattern, with greater tissue levels achieved on the right. However, in contrast to resveratrol and the other metabolites, the sulfate glucuronide concentrations in this patient were found to be higher in left compared to right-sided tissues, with concentrations of 33.5 ± 14.7 and 20.9 ± 5.2 nmol/g of tissue respectively. This difference was, however, not statistically significant ($P = 0.465$; Wilcoxon signed ranks test) and may be due to the variation between samples.

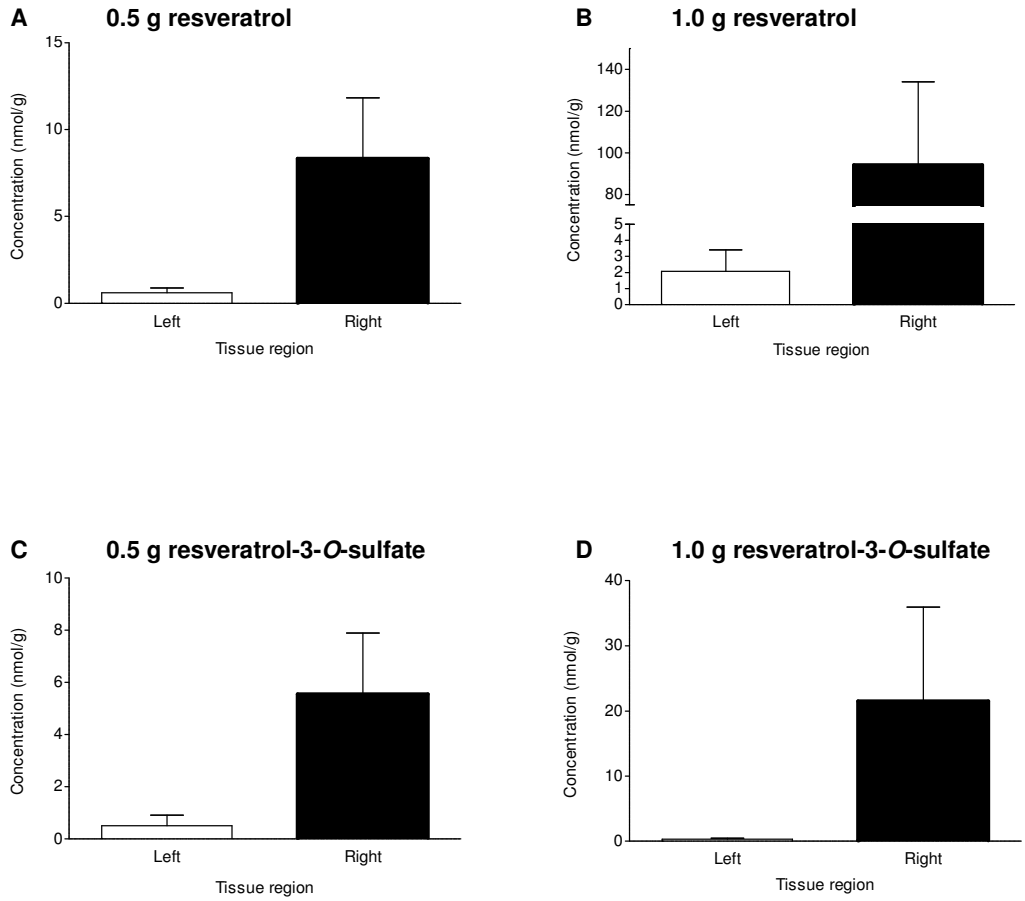

Figure 3.14 Comparison of average resveratrol and resveratrol-3-*O*-sulfate concentrations in left versus right-sided tumour tissues after resveratrol dosing

Average resveratrol (**A** and **B**) and authentic resveratrol-3-*O*-sulfate concentrations (**C** and **D**) in tumour tissue taken from colorectal cancer patients receiving 0.5 g (**A** and **C**) and 1.0 g (**B** and **D**) resveratrol for eight days. Values are the mean + SD of seven tumour tissues removed from the left side of patients and three from the right side following 0.5 g resveratrol dosing. At the 1.0 g dose level, values are the mean + SD of six tumour tissues removed from the left side of patients and five from the right side. A break in the y-axis has been incorporated in (**B**) for clarity. Significance was tested using the Mann-Whitney U test. Resveratrol levels in tumour tissues originating from the right-side of patients were significantly higher than those from the left-side at both the 0.5 and 1.0 g dose (*P = 0.017* and *P = 0.004* respectively). There was no significant difference between levels achieved following the 0.5 and 1.0 g dose in tissues originating from either the left side or right side (*P = 0.534* and *P = 0.053* respectively). Resveratrol-3-*O*-sulfate levels in tumour tissues originating from the right-side of patients were significantly different to those from the left-side at both the 0.5 and 1.0 g dose (*P = 0.025* and *P = 0.004* respectively). There was no significant difference between levels achieved following the two doses in tissues originating from either the left or right side (*P = 0.836* and *P = 0.786* respectively).

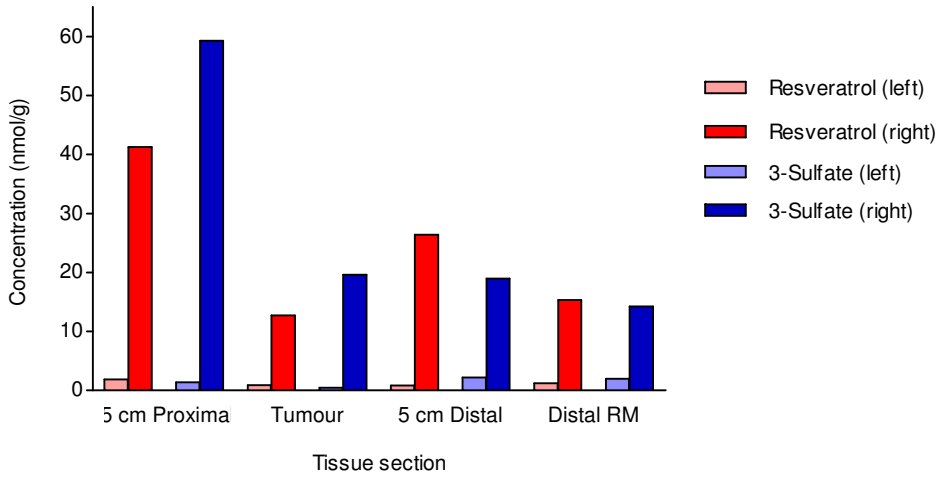

Figure 3.15 Comparison of resveratrol and resveratrol-3-*O*-sulfate concentrations in left versus right-sided sections of human colon and tumour tissue after resveratrol dosing

Concentrations of resveratrol and authentic resveratrol-3-*O*-sulfate in normal colon and tumour tissue of patient C230, who presented with two synchronous tumours (one left-sided and one right-sided), who received 1.0 g resveratrol daily for eight days. Normal tissue samples were taken at a distance of 5 cm proximal or distal from the tumour and from the distal resection margin (RM) in comparable sections of tissue from either side of the colon.

3.3.6 Identification of resveratrol and metabolites in patient plasma and tissues by HPLC-UV and LC-MS/MS

In addition to the removal of tumour and tissues, blood was also drawn from patients during the course of the operation, and their plasma was analysed by HPLC-UV to determine the concentration of resveratrol and any metabolites formed. This enabled direct comparison of plasma and tissue levels in the same patient, which has never been done before. Pre- and post-dosing patient plasma samples were compared, and in the majority of samples, only metabolites were detected in the plasma, with resveratrol levels close to or below the LOQ (Table 3.3). These results are expected, considering the time elapsed between ingestion of the last resveratrol dose and collection of plasma during surgery, which ranged from 11 - 21 h (with a mean of 17.8 h). Also as expected, higher concentrations of metabolites (as resveratrol equivalents) were detected in plasma at the 1.0 g dose compared to the 0.5 g dose. At the higher dose, the sulfate glucuronide conjugate was found to be the most prominent, reaching concentrations 37-fold higher than the monosulfates (assuming equal extraction characteristics), with mean concentrations of 22.3 ± 10.1 nmol/ml. However, based on the earlier findings in Section 3.2.1, the authentic concentrations of the metabolites would be greater than those given here (Table 3.3). In contrast to the profile found in patient plasma, the volunteer plasma varied, with the sulfate glucuronide being a minor metabolite (Figure 3.1).

The identity of metabolites in the patient plasma and tissues were determined by comparison of retention times with synthesised standards of the monosulfates and monoglucuronides using HPLC-UV. However, to further confirm their identities and also to characterise those metabolites where standards were not available, LC-MS/MS was used. Mass spectrometry analysis involved monitoring the relevant multiple reaction monitoring (MRM) transitions of specific mass to charge ratios (*m/z*). A mixture of standards was also used to aid identification of metabolite transitions. Analysis by mass spectrometry is more informative and specific compared to comparison of peak retention time, as it provides definitive evidence of parent compound and their metabolite molecular weights, based on their mass to charge ratios. For the sulfate glucuronide, the transitions monitored corresponded to loss of the individual sulfate

(*m/z* 483 > 404) and glucuronide moieties (*m/z* 483 > 308) and loss of both groups (*m/z* 483 > 227). All of these transitions produced abundant ions from a characteristic fragmentation pattern; however, the *m/z* 483 > 227 transition produced the strongest signal. In plasma and tissues, metabolites identified were resveratrol sulfate glucuronide, resveratrol disulfate (*m/z* 387 > 227; corresponding to loss of both sulfates), resveratrol monoglucuronide (*m/z* 403 > 227; loss of the glucuronide), resveratrol monosulfate (*m/z* 307 > 227; loss of the sulfate), resveratrol trisulfate (*m/z* 467 > 227; loss of three sulfates) and resveratrol diglucuronide (*m/z* 579 > 403 and *m/z* 579 > 227; corresponding to loss of either one or both glucuronides). In addition, parent resveratrol was also identified in tissues and plasma by its characteristic fragmentation (*m/z* 227 > 184) (Figure 3.16B). Also provided in the figure is a typical HPLC-UV chromatogram displaying the various metabolites (and parent) found in the tissue of a patient who had received 1.0 g of resveratrol for eight days, and another who had refrained from taking resveratrol for seven days prior to resection (Figure 3.16A).

Based on the identification of resveratrol metabolites, a number of pathways for resveratrol metabolism to its various metabolites were confirmed (Figure 3.17). Resveratrol can undergo sulfation, glucuronidation, or a combination of the two. The positions of metabolite groups for the disulfate, diglucuronide and sulfate glucuronides were not determined.

	Plasma concentration (nmol/ml)	
	0.5 g	**1.0 g**
Resveratrol	< LOQ	< LOQ
Resveratrol-3-*O*-glucuronide	< LOQ	0.24 ± 0.13 (0.07 - 0.50)
Resveratrol-4'-*O*-glucuronide	0.04 ± 0.06 (0 - 0.16)	0.24 ± 0.17 (0.05 - 0.57)
Resveratrol disulfate	0.31 ± 0.20 (0 - 0.59)	0.60 ± 0.81 (0.17 - 2.86)
Resveratrol-3-*O*-sulfate	0.13 ± 0.15 (0 - 0.52)	0.59 ± 0.41 (0.17 - 1.33)
Resveratrol-4'-*O*-sulfate	< LOQ	< LOQ
Resveratrol sulfate glucuronide	13.4 ± 16.5 (0 - 34.9)	22.3 ± 10.1 (6.67 - 36.3)

Table 3.3 Concentration of resveratrol and its metabolites in patient plasma. Concentrations of resveratrol and its metabolites in plasma of colorectal cancer patients who received 0.5 or 1.0 g of resveratrol for eight days (as resveratrol equivalents). Values are the mean ± SD of 10 patients per dose level, with the lower and upper range given in parentheses. LOQ refers to samples where concentrations were below the limit of quantitation, which were 0.02, 0.05 and 0.05 nmol/ml for resveratrol, resveratrol-3-*O*-glucuronide and resveratrol-4'-*O*-sulfate respectively. Time from oral administration of resveratrol to the time of plasma collection ranged from 11 - 21 h (mean of 17.8 h).

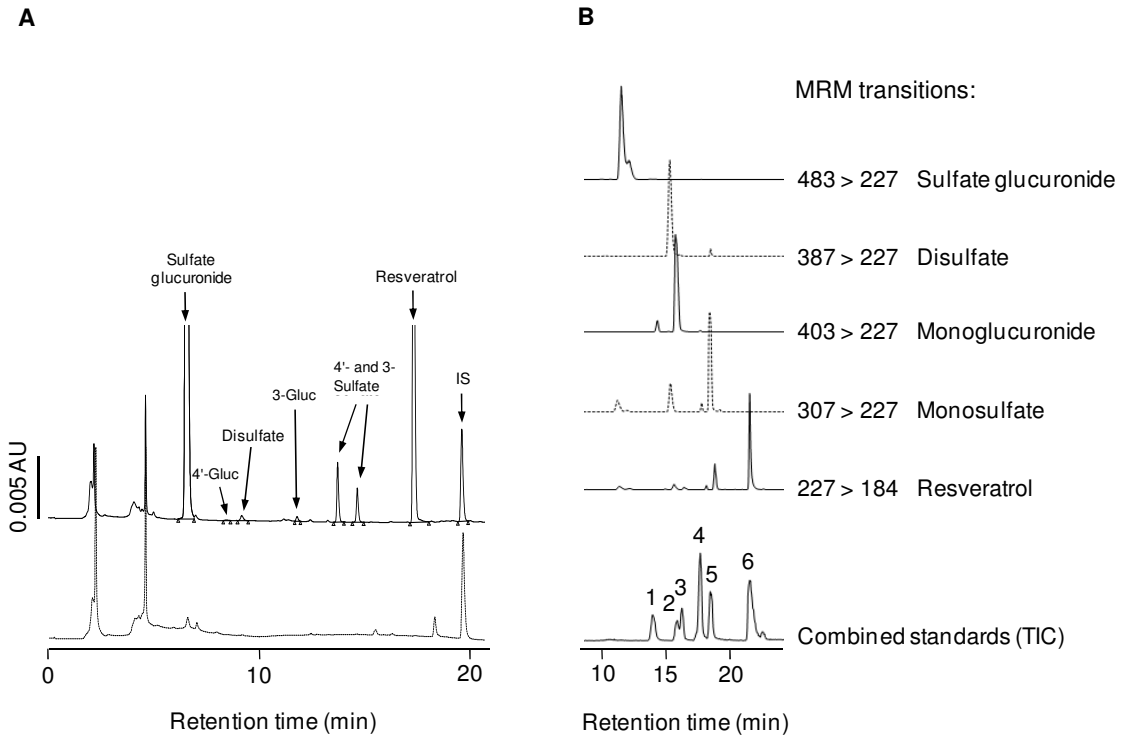

Figure 3.16 Human tumour tissue HPLC-UV chromatograms pre- and post-resveratrol dosing and mass spectrometry MRM transitions

HPLC-UV chromatogram (**A**) and mass spectrometry MRM transitions (**B**) in tumour tissue taken from a colorectal cancer patient who received 1.0 g of resveratrol for eight days. In Figure (**A**), the dotted line (bottom) is an extracted tissue sample from a patient who refrained from taking resveratrol during the seven days before resection. Figure (**B**) shows the individual MRM transitions of resveratrol metabolites in the sample, and the combined total ion current (TIC) for a mixture of standards. The numbers above peaks correspond to metabolites as follows; resveratrol-4'-*O*-glucuronide (**1**), resveratrol-3-*O*-glucuronide (**2**), dehydrated resveratrol glucuronide (**3**), (which was not in any samples), resveratrol-4'-*O*-sulfate (**4**), resveratrol-3-*O*-sulfate (**5**), and resveratrol (**6**). Figure adapted from [114].

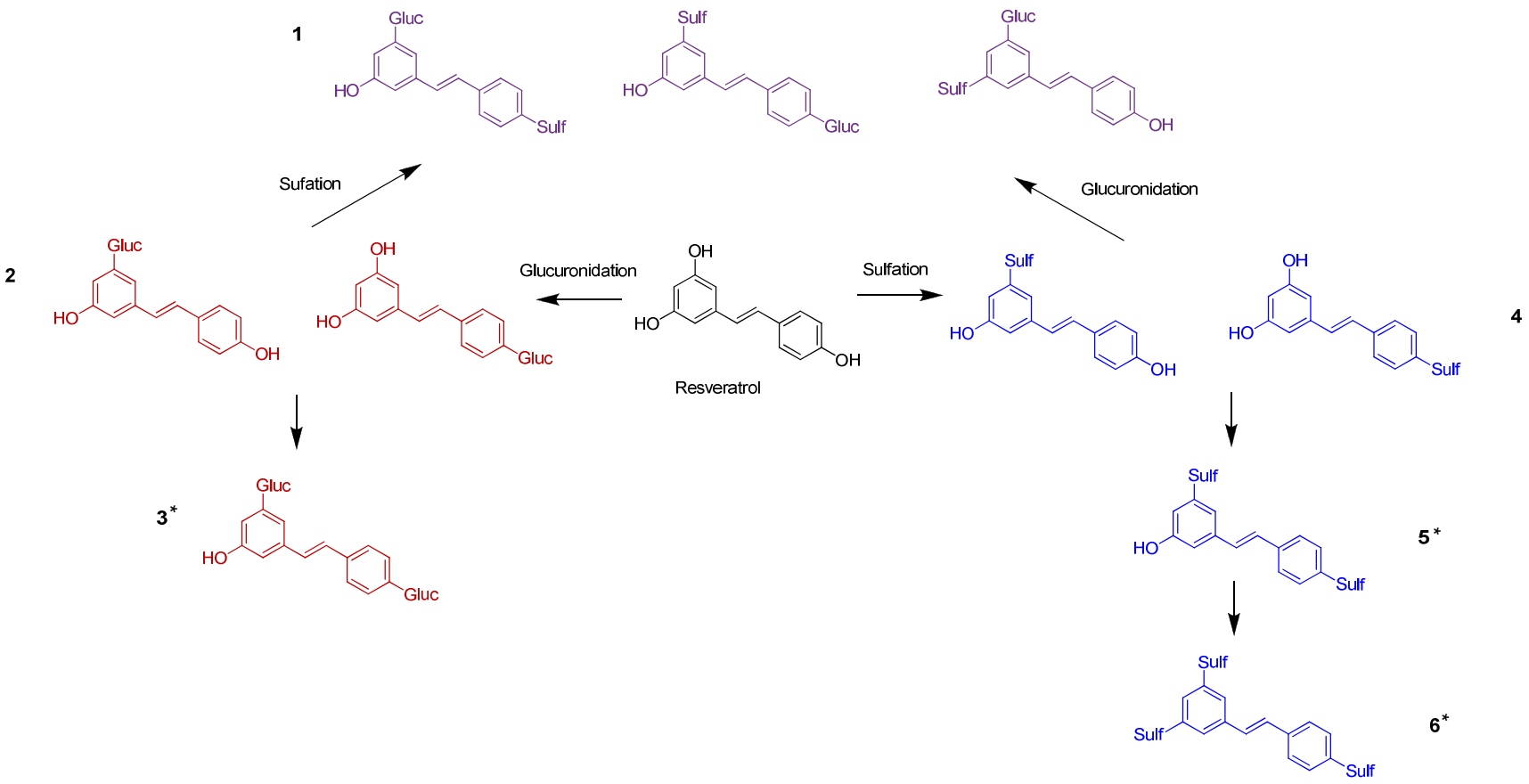

Figure 3.17 Metabolic pathway of resveratrol in human plasma and colon tissue

The metabolites detected in human plasma and colon tissue of colorectal cancer patients, and their pathways of formation from resveratrol. Metabolites detected were resveratrol sulfate glucuronide(s) (**1**), resveratrol monoglucuronides (**2**), resveratrol diglucuronide (**3**), resveratrol monosulfates (**4**), resveratrol disulfates(s) (**5**), and resveratrol trisulfate (**6**). Blue, red and purple represent sulfates, glucuronides and sulfate glucuronides respectively. Specific metabolite positions were not determined for sulfate glucuronide, disulfate or diglucuronide metabolites. Resveratrol triglucuronide was not detected. Asterisks indicate metabolites characterised, but not quantified in tissues.

3.4 Discussion

Resveratrol has been shown to possess many useful properties, including those relevant to cancer chemoprevention. However, following ingestion the polyphenol undergoes extensive metabolism, with conjugation initially occurring in the small intestine by phase II drug-metabolising enzymes [160]. The net result of the first-pass metabolism of resveratrol is that the sulfate and glucuronide metabolites predominate in the plasma of humans and mice [107], [137]. Conjugation of resveratrol to generate these metabolites is a common detoxification step, which restricts exposure to the parent compound, by conversion to more hydrophilic components that can be readily excreted from the body. For the non-absorbed fraction and the fraction re-excreted in the bile, metabolism is by the colonic microflora in mouse models [161]. The change in resveratrol structure due to its metabolism is likely to result in altered pharmacological and physiological properties, which may affect distribution patterns within tissues and cells compared to the parent and consequently efficacy in target organs. The distribution profiles of metabolites reaching plasma and colon tissue in humans were determined in this part of the study.

Clinical trials of resveratrol in humans have shown that following a single dose, the quantities of the major metabolites in plasma are greater than those of resveratrol, with differences in some of their pharmacokinetic characteristics [104], [108]. In the repeat resveratrol dosing study carried out here, resveratrol plasma concentrations were accurately quantified over time in healthy volunteers, whereas metabolite concentrations were initially reported as resveratrol equivalents. At a later stage of the project metabolite standards became available enabling more accurate determination of metabolite levels. An additional aim was to determine whether resveratrol and its metabolites could be found within resected human normal colon and tumour tissue removed from colorectal cancer patients taking resveratrol daily, and if so, at what concentrations. These data would help to provide information on future dosing strategies. They would also identify a more relevant range of metabolite concentrations for use in *in vitro* experiments, to help determine their potential activity in relation to chemoprevention (discussed in Chapter 5).

In this repeat dosing resveratrol study, plasma resveratrol and metabolite levels were measured by HPLC-UV in pre-dose samples and at 0.25, 1.0, 1.5, 5, 12 and 24 h post-dose on a day between the 21st and the 28th day of resveratrol ingestion. During the planning of the study, this was considered to be a suitable duration to attain steady-state. The pharmacokinetic profile over the 24 h period was similar to that seen following individual doses at the same level, with a rapid initial increase in plasma concentration followed by a gradual decline [107]. The same metabolites were also identified in both studies, with resveratrol-3-*O*-glucuronide, resveratrol-4'-*O*-glucuronide and resveratrol-3-*O*-sulfate dominating in the plasma. To calculate plasma metabolite concentrations following resveratrol dosing more accurately, standards of the sulfate and glucuronide metabolites were synthesised and these were used to construct standard curves in plasma, which allowed quantitation of metabolite levels. A set of samples selected at random were re-extracted so that 'authentic' C_{max} and AUC values could be determined across the four resveratrol dose levels. In the repeat-dose study, resveratrol-3-*O*-sulfate, resveratrol-4'-*O*-glucuronide and resveratrol-3-*O*-glucuronide had C_{max} values (as resveratrol equivalents) up to 5-fold and 13-fold greater for the glucuronides and sulfates respectively, as compared to resveratrol. When the average C_{max} plasma concentrations were recalculated using resveratrol sulfate and glucuronide standard curves, their respective concentrations were 3.9 and 4.7-fold higher than those determined using resveratrol standard curves.

Therefore, when resveratrol-3-*O*-sulfate average C_{max} plasma concentrations for the 5.0 g dose were reported to average 4,172 ng/ml (18 µM), the mean concentration was more likely to be in the region of ~16,300 ng/ml (53 µM). Similarly, for resveratrol-3-*O*-glucuronide, the average C_{max} value based on the resveratrol standard curve was 3,886 ng/ml (17 µM); the corresponding concentration using the glucuronide standard curve would be approximately 18,300 ng/ml (45.2 µM). One likely explanation for this difference is that the metabolites possess different UV absorbance coefficients to those of resveratrol. The extraction method used for the plasma analysis was developed and optimised specifically for resveratrol, with the UV absorbance set to 325 nm [153]. One of the metabolites of resveratrol, dihydroresveratrol, which has been detected in mouse mucosa [146], and human urine [104] following resveratrol dosing, has been shown to have a peak lambda maximum of 276 nm. Also, the absorbance values for given

concentrations of the metabolites are different to the parent. The absorbance maxima for the monosulfates and monoglucuronides have been reported as 291 and 297 nm respectively [71]. The extraction efficiencies of resveratrol, its monosulfates and resveratrol-3-*O*-glucuronide were determined in human plasma; however efficiencies were not found to vary by more than 10%, and are therefore unlikely to account entirely for the differences.

Another parameter that was found to be greater for the resveratrol conjugates was the area under the plasma concentration versus time curve (AUC). In the case of resveratrol-3-*O*-sulfate, total exposure to the metabolite (as resveratrol equivalents) exceeded those of their parent by up to 20-fold at the 0.5 g dose. When based on the resveratrol standards, the AUC was also underestimated for the glucuronides and sulfate metabolites. Following calculation with metabolite standards, AUC values for these respective metabolites were approximately 5- and 4-fold higher respectively, compared to using resveratrol standards. Therefore, based on the re-extracted samples with metabolite standards, the AUC_{all} for resveratrol-3-*O*-sulfate could be as much as 80-fold higher than that for resveratrol. The increase in the C_{max} and AUC_{all} both indicate an even greater total extent of exposure and higher peak concentration compared to metabolite levels calculated as resveratrol equivalents.

The rapid and extensive metabolism seen in this study was consistent with findings by Walle *et al*. [104], who showed that the oral bioavailability of unchanged resveratrol was almost zero, following a 25 mg dose, but high concentrations of resveratrol metabolites were present. Another study involved oral administration of resveratrol (25 mg/70 kg) in healthy male subjects (aged 25 - 45 years) in three different matrices; white wine, white grape juice and vegetable juice, in order to test their absorption [102]. Blood was taken prior to dosing and at four intervals over the first four hours of consumption (0.5, 1.0, 2 and 4 h). Urine was collected pre-dosing and for the 24 h post-dosing period. Highest recorded serum resveratrol/metabolite levels were achieved at 30 min post-dosing in all volunteers, and these were found to decline rapidly, reaching baseline levels within 4 h. Free resveratrol accounted for only a small fraction of the total dose in plasma (1.7 - 1.9%). In contrast, the glucuronide and sulfate conjugates dominated in both the plasma and urine.

Since the publication of these early studies, a number of recent clinical trials have confirmed these findings following multiple dosing of authentic resveratrol [112], [86]. One common feature of the pharmacokinetic studies is the large inter-individual variation which exists between volunteers, including those recruited onto the same dose level. Consistent with this, a large variation in the PK parameters such as AUC, C_{max} and average plasma concentration was observed in the present multiple dosing resveratrol study. For example, within each dose group, the CV was commonly more than 50% for the average C_{max} concentrations (Figure 3.3). Similarly, large variations in the C_{max} values (as indicated by CV values > 40%) were reported in a study comparing PK parameters in young and elderly individuals following a single 200 mg resveratrol dose followed by thrice daily dosing for two days [110]. One of the main findings of this study was that despite a relatively high dose (200 mg), and short dosing interval (8 h), plasma concentrations of resveratrol were below concentrations shown to have activity *in vitro* (> 1000 ng/ml). Interestingly, the resveratrol kinetic profile was independent of age and gender [110].

The large variability in PK parameters for resveratrol and its metabolites, observed in these studies is likely to be related to a combination of many factors. For example, the resveratrol doses were not adjusted for body weight and did not take body mass index (BMI) into account. Although there was no correlation with either sex or age in the previously mentioned study [110], the sample size for each group was relatively small, and larger scale studies might have a higher likelihood of picking up any potential differences. When soy containing both genistein and daidzein was ingested by men and women, there were differences in the metabolism and disposition between the sexes [162]. For example, in women recoveries of conjugates of genistein and daidzein in urine were 24% and 66% of the amounts ingested, respectively, whilst in men the corresponding figures were 15% and 47% respectively. A progressive decrease in urinary excretion of genistein and daidzein was observed in women but not in men during the study [162]. The activity of several CYP isozymes, including CYP2C19, CYP2D6 and CYP2E1 and the conjugating enzymes involved in drug metabolism may be variable in men and women [163].

Kinetics of the formation of two monosulfate and resveratrol disulfate metabolites has been investigated using human liver cytosol [139]. Incubation in the presence of human recombinant SULTs demonstrated that resveratrol-3-*O*-sulfate production was almost exclusively catalysed by SULT1A1 and only to a minor extent by SULT 1A2, 1A3 and 1E1. Resveratrol-4'-*O*-sulfate was selectively formed by SULT1A2, whereas formation of the disulfate was shown to be catalysed by SULT 1A2 and 1A3 [139]. Using human microsomes prepared from stomach, duodenum, four segments of the small intestine and colon and derived from Caco-2 and PD-7 cell lines, resveratrol-3-*O*-glucuronide and resveratrol-4'-*O*-glucuronide were generated following incubation with resveratrol [150]. Among the UGT's that are known to be expressed in the GI tract, the isoforms UGT1A1, 1A6, 1A8, 1A9 and 1A10 were active in glucuronidating resveratrol, demonstrating the importance of the GI tract in the first pass metabolism of resveratrol [150]. The extent of metabolism that occurs has also been shown in human cellular systems, such as the Caco-2 model; this is discussed in more detail in Chapter 5, which explores specifically cellular metabolism and *in vitro* metabolism of resveratrol and its metabolites.

In a small-scale study with eight healthy volunteers, the pharmacokinetic and metabolic profile of resveratrol was found to be significantly altered when consumed with a high-fat breakfast. AUC and C_{max} values decreased by 45% and 46% respectively when compared with a standard breakfast [113]. Additional components in the diet have also been shown to affect the rates of resveratrol metabolism. For instance, the polyphenolic agent quercetin, as well as many flavonoids present in wine, fruits and vegetables can inhibit both glucuronidation [129] and sulfation of resveratrol [128]. Sulfation has been found to be more susceptible to inhibition by flavonoids [128]. Inhibition of sulfation and glucuronidation may be a possible way of increasing the bioavailability of resveratrol. However, it is unlikely that diet would have influenced PK parameters in the current study, as volunteers took resveratrol on an empty stomach and were fasted prior to the collection of the majority of blood samples on the sampling day.

In one study, the plasma content of UGT1A1 protein was analysed in volunteers who received 85.5 mg of piceid/70 mg body weight. This was to determine whether the formation of

glucuronides was related to the plasma UGT1A1 protein content, since this enzyme catalyses the reaction [108]. Protein levels, measured by western blotting, reached a maximum at 4 - 6 h after piceid administration, which corresponded with a peak concentration achieved after 6 h. The authors concluded that the induction of UGT1A1 protein expression was correlated with resveratrol glucuronide formation. In the repeat resveratrol dose study here, and as part of further investigations, the UGT1A1 protein levels could be measured to re-enforce the findings above. If there was a correlation, baseline protein expression could be measured in future volunteers and/or patients as an indicator of resveratrol doses which should be administered.

Although glucuronidation and sulfation of resveratrol has been described as the dominant form of metabolism, based on findings by Walle *et al*., it has been suggested that reduced dihydroresveratrol conjugates, in addition to highly polar unknown products may account for as much as 50% of an oral resveratrol dose. Colonic bacterial metabolism may account for more metabolism of the parent compound than previously thought. Confirmation of this type of metabolism has come from radioisotope studies revealing the presence of polar early-eluting radiolabelled species in plasma analysed by HPLC-UV. Reduced dihydroresveratrol conjugates have been detected in the plasma and urine of humans [109] and also in plasma of rats [164], [126]. Interestingly, the incubation of resveratrol with 43 strains of commonly-related animal or human bacterial species identified eleven that were capable of transforming at least 20% of the resveratrol. Three major metabolites were formed, resveratroloside, piceid and dihydroresveratrol [147]. This type of metabolism may not necessarily be picked up using traditional HPLC-UV reverse phase methods such as that used in the present study, as the metabolites would be more polar than the sulfate and glucuronide metabolites. Therefore, it is possible that these metabolites elute earlier in the solvent front, or are not sufficiently retained on the column. The analytical method used in this project would probably require further optimisation to allow detection of these metabolites and potentially any other phase I metabolites. A possible suggestion for further work would be to alter the absorbance wavelength of detection, as well as changing the HPLC gradient system to maximise chances of detecting these less-well characterised metabolites.

As well as the pharmacokinetics and metabolism of resveratrol, an additional aspect for consideration is resveratrol safety and tolerability. Resveratrol safety has been assessed in only a small number of human studies [107], [113], [86], [112]. In the single dosing study administration of resveratrol (0.5 g - 5.0 g) was found to be well-tolerated [107]. However, following the same doses taken daily for 29 days in the present study, 28 of the 40 volunteers reported one or more adverse events while on the trial, with the majority of these on the highest two doses [120]. The most common side effect was gastrointestinal, particularly diarrhoea, nausea, and abdominal pain, all of which occurred only in individuals taking in excess of 1.0 g per day. Consistent with these findings, in another trial resveratrol taken twice-daily at a dose of 2 g was well-tolerated, although diarrhoea was frequently observed [113]. Patients administered another plant polyphenol, flavopiridol, also experienced diarrhoea as a side effect [165]. A mechanism that has been suggested to account for this relates to modulation of cyclic AMP (cAMP). Resveratrol stimulated cAMP-dependent Cl^- secretion in T84 colon cancer cells and mouse jejunal epithelial membrane, which would result in increased entry of water into the gut, hence providing evidence that it could potentially induce secretory diarrhoea in this way [166]. In a separate study, effects of pharmacologic doses of resveratrol on drug- and carcinogen-metabolizing enzymes were assessed [86]. Volunteers who received 1.0 g resveratrol daily for four weeks and had low baseline levels of glutathione S-transferase (GST) and UGT1A1 were found to have elevated levels of these enzymes post-dosing. Both are responsible for drug and carcinogen metabolism. Inhibition of CYP enzymes was observed, including CYP3A4 and CYP2C9, which are responsible for metabolising a broad range of drugs [86]. Therefore, enzyme inhibition could lead to elevated plasma resveratrol concentrations and increased likelihood of toxicity, and further investigations are required. In addition to inhibition of CYP3A4, an independent study also indicated that resveratrol marginally inhibited CYP2C19, although resveratrol-3-*O*-sulfate was not found to inhibit any of the five CYP enzymes investigated [87]. Based on the findings in volunteers repeatedly taking resveratrol, it has been suggested that doses lower than 1.0 g of resveratrol should be considered in future clinical trials [86].

As a result of the high degree of metabolism that resveratrol undergoes, alternatives to enhance its bioavailability have been investigated. For example, a variety of resveratrol analogues have been synthesised and tested for their ability to engage properties germane to cancer chemoprevention, and their metabolism has been explored in mice [167]. In a different study, glucosyl groups were added to resveratrol to increase its solubility and the analogues were shown to have a better *in vivo* retention [168]. The work on resveratrol analogues has been discussed in more detail in Chapter 5. Formulations of resveratrol now exist which are optimised for slow release, and provide a colon-specific delivery system of resveratrol, thus increasing the bioavailability at the potential sites of action. Another modification to increase resveratrol bioavailability has been to supplement it with 5% rice bran phylate (commercially known as Longevinex), and to micronise [169].

An important requirement for a potential chemopreventive agent is that it must be capable of reaching the target organ(s), where it can elicit an effect. To investigate whether resveratrol can reach its potential target tissue, it was administered to colorectal cancer patients for eight days prior to surgical resection. Resveratrol and six metabolite concentrations were quantified in tumour and non-malignant tissue; these were resveratrol-3-*O*-sulfate, resveratrol-4'-*O*-sulfate, resveratrol-3-*O*-glucuronide, resveratrol-4'-*O*-glucuronide, resveratrol disulfate and resveratrol sulfate glucuronide. As with the repeat dosing study in healthy volunteers, concentrations of metabolites were initially calculated as resveratrol equivalents and this data has been published [159]. Authentic concentrations of resveratrol-3-*O*-sulfate and resveratrol-4'-*O*-sulfate were subsequently calculated in all of the patient tissues using the respective resveratrol sulfate standards. Glucuronide concentrations across the range of patients were estimated based on the analysis of three patients per dose, chosen at random using authentic standard curves. Sulfate glucuronide concentrations were also based on the glucuronide standard curves. Resveratrol disulfate concentrations were based on resveratrol monosulfate standard curves. Resveratrol and metabolite concentrations have not previously been measured in the human colon.

In the current study resveratrol concentrations detected within the colon were very variable following either dose, with mean (± SD) concentrations of 18.6 ± 17.4 nmol/g and values ranging from 0 - 45.9 nmol/g in non-malignant tissue on the 0.5 g dose (Table 3.1). Similarly after 1.0 g resveratrol, resveratrol reached 674 ± 1,303 nmol/g (mean ± SD), with levels ranging from 10.1 - 3,774 nmol/g (Table 3.2). The average concentrations were calculated across tissue sections taken from all patients on both dose levels, and sections where concentrations were below the LOQ, were treated as zero. Authentic metabolite concentrations found within the colon following the 1.0 g resveratrol dose were generally below those for resveratrol. However, at the 0.5 g dose, resveratrol concentrations were more comparable to true levels of metabolites including for resveratrol-3-*O*-sulfate and resveratrol-3-*O*-glucuronide. Resveratrol sulfate glucuronide concentrations (calculated as glucuronide equivalents) were above those for resveratrol at both doses, apart from in right-sided tissues obtained from patients on the higher dose. This metabolite consistently reached high levels, and on the 1.0 g dose, average concentrations of at least 19 nmol/g of tissue were detected in all sections analysed. Mean sulfate glucuronide concentrations in left-sided and right-sided tumour tissue on the 1.0 g dose were 21 and 29 nmol/g respectively. Metabolite concentrations detected within normal tissues generally seemed to be higher than in tumour tissue, which might suggest differential levels of uptake. However, the wide variability and limited number of samples, particularly for tumour sections compared to normal mucosa, makes it difficult to draw firm conclusions regarding the uptake in malignant and non-malignant tissue. The high degree of inter-individual variability in tissue levels may be due to those factors considered previously (for the variation in plasma levels), including age, sex, BMI, enzyme expression/activity and ethnicity. Across the 20 patients in this study, the mean age range on the 0.5 and 1.0 g dose was 60 - 80 and 46 - 83 years respectively, with corresponding BMI ranges of 17.4 - 29.2 and 22.8 - 27.6 kg/m^2. Resveratrol doses here were not adjusted in any way, as has been done for resveratrol delivery in some other trials [108], [102], [103].

Metabolite levels have been related to the presence of specific cell membrane transporters in rats [170] and mice [146]. Resveratrol was shown to enter enterocytes by passive diffusion, where a high level of conjugation metabolism occurred; these conjugates were then secreted

back into the intestinal lumen via breast cancer resistance protein (BCRP) and multidrug resistance protein transporters (MRP2) [170]. The contrasting levels found on the left and right side of the colon could be related to a differential uptake or transport mechanisms in varying regions of colonic tissue. Levels of the MRP2 protein in rats (responsible for resveratrol metabolite transport, and in particular for resveratrol glucuronides) had a pronounced reduction in the intestine from proximal to distal regions [171]. The increased absorption might also be related to the colonic conditions on the right side of the colon, where the liquid environment facilitates the uptake from partially digested material, compared to the semi-solid environment on the left. The variable drug uptake of quinine was measured in the human colon following treatment with lactulose and codeine which varied the stool water content [172]. Greater plasma quinine concentrations were achieved in those individuals on the lactulose treatment arm, which had the effect of increasing stool water content and allowing greater absorption.

Further evidence for the differential levels comes from studies of curcumin, a constituent of the spice turmeric, which has been shown to reduce adenoma burden in rodent models of colorectal carcinogenesis. In a phase I study with curcumin in colorectal cancer patients, an increased uptake of the dietary constituent curcumin in normal mucosa from the caecum and ascending colon compared to normal mucosa from the transverse, splenic flexure, and descending colon has been described [173]. In patients who had received a single dose of curcumin, the concentration of curcumin measured was 21.7 ± 8.2 and 6.8 ± 3.7 nmol/g in the right and left colon respectively (n = 4 patients). However, this difference was not reflected by curcumin levels in tumour tissue originating from different sites of the bowel. Concentrations in malignant tissue following ingestion of curcumin at repeated doses of 3.6 g/day resulted in maximum mean concentrations of 7.7 ± 1.8 nmol/g of tissue [173], below those seen for resveratrol. Another important finding of the curcumin study was that although curcumin sulfate and curcumin glucuronide were detected in mucosa, quantitatively they contributed to only a very minor extent to the overall colorectal load of curcumin-derived species. In contrast, resveratrol and metabolite concentrations here encompassed a wider range, with greater C_{max} concentrations.

These investigations all support the findings from the colorectal tissue study here, where the concentrations of resveratrol and its metabolites (with the exception of the sulfate glucuronide) were higher in tissues originating from the caecum and hepatic flexure (right-side) as compared to those originating in the sigmoid colon and rectum (left-side). This variation in tissue concentration between different regions was reinforced by patient C230, where marked differences between tissues taken from opposite sides of the colon were found. Not consistent with this left-right pattern of distribution were the sulfate glucuronide concentrations, for which broadly similar concentrations were found on both sides on the colon. One possible explanation for this might be that once formed, this conjugate is more stable and less likely to undergo deconjugation and excretion.

Unpublished data from our research group show that ingestion of a single dietary achievable dose of 5 mg [^{14}C]-resveratrol, can generate detectable levels in human colon tissue, at concentrations above those in plasma [174]. Concentrations of resveratrol-derived species in malignant tissue were similar to colonic mucosa, reaching 1.80 ± 2.79 pmol/mg. In the normal colon, levels in mucosa were approximately 5 - 9-times higher than in the adjacent muscle, possibly due to topical [^{14}C]-resveratrol. A useful addition to the current study would have been to analyse resveratrol and metabolite levels in the outer muscle layer (serosa) and the inner luminal surface (mucosa) separately. This would have enabled us to determine whether delivery route to the gastrointestinal tract is due to systemic or topical distribution.

The resveratrol concentrations in patient plasma samples taken at the time of surgery were close to or below the LOQ, consistent with the rapid metabolism of resveratrol. These findings are expected, based on the results of healthy volunteer pharmacokinetic data analysed at similar times post resveratrol dosing [107]. Mean plasma concentrations (all based on resveratrol standards) of the two glucuronide species at the 1.0 g dose were identical (0.24 nmol/ml). Resveratrol-4'-*O*-sulfate concentrations were at the limit of quantitation, whereas resveratrol disulfate and resveratrol-3-*O*-sulfate were present at concentrations over double those for the glucuronides. Consistent with the findings in tissues, resveratrol sulfate glucuronide was the major plasma metabolite at both doses with 22.3 ± 10.1 nmol/ml at the

1.0 g dose level. However, in plasma of healthy volunteers this metabolite was normally a minor metabolite. Despite the low circulating plasma resveratrol concentrations, levels similar to those found within tissue sections removed at the same time have been shown to exert beneficial activity *in vitro* [80]. Furthermore, when resveratrol was administered to *Apc*$^{min+}$ mice, a model of colon cancer, a reduction in adenoma number was apparent relative to control mice on a standard diet [155]. Concentrations in the gastrointestinal tract of these mice reached 36 nmol/g - levels that can be achieved in humans after 0.5 and 1.0 g doses (Table 3.1 and 3.2 respectively).

Information on the effect that resveratrol and its metabolites have on potential biomarkers of carcinogenesis is also necessary, to further our understanding of possible mechanisms of action. Biomarkers may be used to monitor effectiveness of intervention. In a phase I pilot clinical trial, the effects of resveratrol and freeze-dried grape powder on a key signalling pathway involved in colon cancer initiation, the Wnt pathway, was evaluated [175]. Expression of a panel of Wnt target genes was measured by microarray, and grape-powder containing low concentrations of resveratrol in combination with other bioactive components was found to inhibit the Wnt pathway in normal colonic mucosa, as indicated by a reduction in the expression of Wnt target genes. Results from the repeat dose resveratrol study in healthy volunteers, suggested that plasma IGF-1, which influences malignant development was down-regulated following resveratrol consumption [120]. A small reduction in Ki-67, a tissue cell proliferation marker, was found to occur following resveratrol dosing in colorectal cancer patients in the study here, however the data does not form part of this project [114].

The low resveratrol bioavailability seen in the repeat resveratrol dose investigations here is consistent with many *in vivo* studies in animals and humans, which also confirm its rapid and extensive metabolism [137], [104]. The results presented here show that resveratrol metabolites are found to dominate in the plasma following resveratrol dosing in both healthy volunteers and colorectal cancer patients. However, metabolite concentrations, which have previously been reported as resveratrol equivalents in at least four published studies, do not reflect the realistic concentrations that may be attained in plasma and tissue. Plasma

resveratrol sulfate and glucuronide concentrations were considerably higher than those for resveratrol, although tissue resveratrol concentrations were similar to, or above those for metabolites, suggesting that accumulation could occur. The observed levels may well be within the range at which they have the ability to exert beneficial effects, particularly for resveratrol sulfate glucuronides. As suggested in a number of studies, resveratrol metabolites may act as an inactive pool of resveratrol, and result in the delivery of resveratrol to various sites within the body following deconjugation by sulfatase or glucuronidase enzymes. This will be investigated both *in vivo* and in *in vitro* in the following chapters.

CHAPTER 4: PHARMACOKINETICS AND METABOLISM OF RESVERATROL SULFATES IN MICE

4.1 Introduction

In the previous chapter, the formation of sulfate and glucuronide metabolites following resveratrol ingestion in humans was investigated. Metabolite concentrations in plasma were shown to greatly exceed those of resveratrol, and tissues metabolite concentrations of resveratrol sulfate glucuronide at the 0.5 g dose were consistently higher than for resveratrol. It has been suggested by several authors ([71], [137], [156], [79], [152], [104]) that the metabolites could act as a reservoir of resveratrol, which may become available at various sites within the body following the action of sulfatases and glucuronidases, thereby prolonging the beneficial effects of the parent compound. In order to address this point, the plasma and tissues (mucosa, liver, pancreas and lung) of mice were analysed by HPLC-UV, following IV and IG dosing of a synthesised mixture of resveratrol monosulfates. The mixture consisted of resveratrol-3-*O*-sulfate and resveratrol-4'-*O*-sulfate in a 3: 2 ratio respectively, (as determined by NMR analysis). Pharmacokinetics and bioavailability of resveratrol has been carried out in mice and is well established. Therefore, for the purposes of this study, dosing was only completed with the mixture of the sulfate metabolites. Analysis of the plasma and tissues following sulfate dosing would help determine if resveratrol formation was possible *in vivo*, and whether this was restricted to certain tissues within the body. Mouse urine was also analysed to allow identification of the excretory products of resveratrol monosulfates. Additional aims involved investigation of the tissue distribution of the sulfates and any other metabolites formed, and determination of PK parameters of the sulfates and resveratrol (where found). Finally, the administration of both IV and IG doses would allow calculation of the bioavailability of the sulfate mixture in plasma. To our knowledge, the bioavailability of any resveratrol metabolite has not been investigated previously and their potential conversion to resveratrol *in vivo* has not been explored.

4.2 Characterisation of resveratrol monosulfate pharmacokinetics in mouse plasma

The IV and IG doses administered to the mice were 6 mg/kg and 120 mg/kg, respectively, with doses adjusted according to body weight. The doses were selected based on estimations that they would generate levels sufficient in plasma and tissues to be detected [137], [156]. The IV dose used was lower, as the entire amount would enter the circulation directly without any losses, and therefore be detected more readily. As mentioned previously, the sulfate mixture consisted of resveratrol-3-*O*-sulfate and resveratrol-4'-*O*-sulfate in a 3: 2 ratio. Separation of the two isomers is extremely time consuming, and the preparative HPLC used for this process would result in a low yield. Therefore, it was decided to conduct the initial studies in this project with the mixture, which could be produced in sufficient quantities. In human plasma and colorectal tissue samples following resveratrol dosing, resveratrol-3-*O*-sulfate is the more prominent metabolite, as discussed in Chapter 3.

In order to optimise the time points for the PK experiment, an initial pilot animal study was conducted. Mice (n = 3 per treatment group, n = 2 for control group) were dosed with 6 mg/kg or 120 mg/kg by either IV or IG, respectively, and exsanguinated under terminal anaesthesia at 5, 30 and 60 min. Initial data (not shown) indicated a rapid rise in plasma concentration of resveratrol sulfates at 5 min post-dose for both routes of administration, with lowest concentrations evident at 60 min. It was therefore decided to include a number of shorter sampling time points to maximise the PK information obtained from the full experiment. Mice were exsanguinated post-dosing at 5, 15, 30, 60, 120, 360 min, and 24 h. Control mice receiving vehicle only were culled at t = 0.

4.2.1 Mouse plasma profile following resveratrol sulfate dosing by IV and IG routes

Blood was collected by cardiac puncture under terminal anaesthesia at the specified sampling times, and plasma was isolated as described in Section 2.2.5.1, then subject to extraction and HPLC-UV analysis (page 62). In addition to resveratrol-3-*O*-sulfate and resveratrol-4'-*O*-sulfate

in the plasma, a total of three additional metabolites were identified by HPLC-UV following monosulfate dosing. These were resveratrol-3-*O*-glucuronide, resveratrol disulfate and resveratrol sulfate glucuronide. Resveratrol was also detected at low levels (as outlined later in this section). A typical chromatogram showing the profile in plasma following IG dosing with the sulfates compared to control plasma is illustrated in Figure 4.1. Although the same metabolites were found to occur following IG and IV dosing over the 24 h measurement period, there were quantitative differences in the PK characteristics depending on the route of sulfate administration (Figure 4.2). Concentrations in the plasma were calculated using standard curves of authentic resveratrol monosulfates (a mixture of the two isomers), and resveratrol-3-*O*-glucuronide. When detected, resveratrol concentrations were determined based on a standard curve of the parent compound.

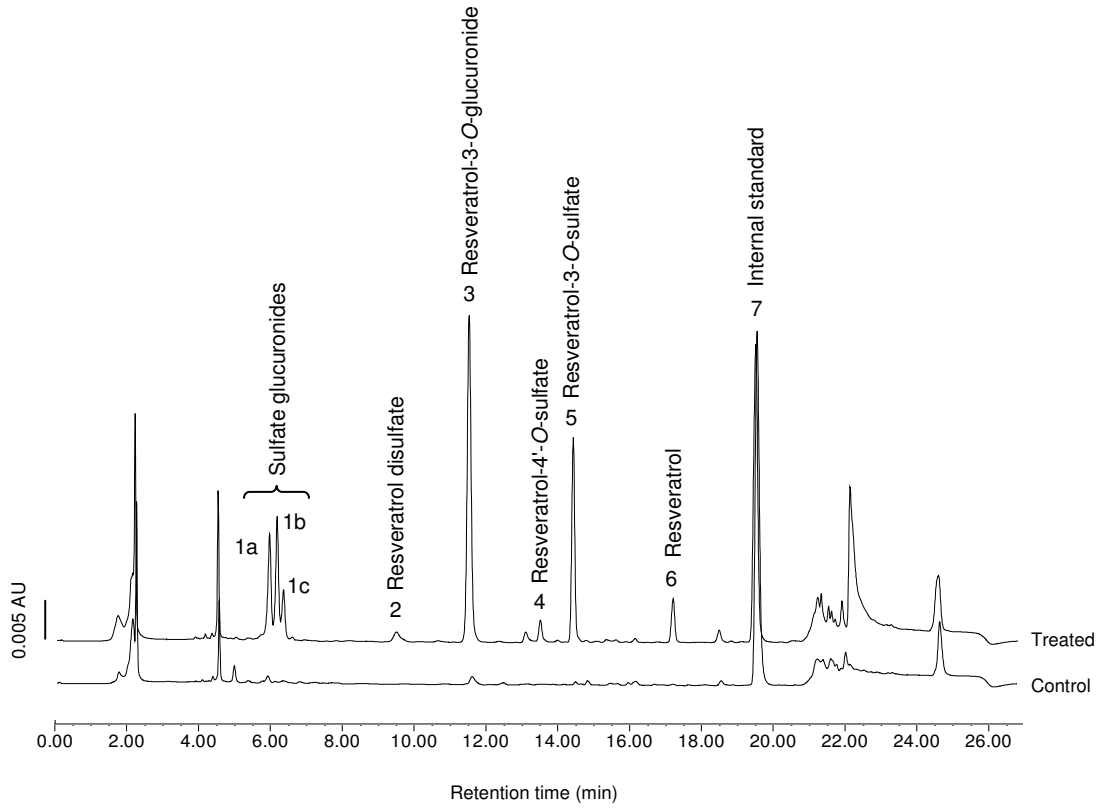

Figure 4.1 Typical HPLC-UV chromatogram of mouse plasma following IG dosing of resveratrol-3-*O*-sulfate and resveratrol-4'-*O*-sulfate (3: 2 ratio)

HPLC-UV chromatograms of plasma taken from mice receiving saline vehicle only (bottom line), or 120 mg/kg resveratrol sulfates (by IG) obtained 1 h post-dosing (top line). Designated peaks are resveratrol sulfate glucuronides (**1a, 1b** and **1c**), resveratrol disulfate (**2**), resveratrol-3-*O*-glucuronide (**3**), resveratrol-4'-*O*-sulfate (**4**), resveratrol-3-*O*-sulfate (**5**) and resveratrol (**6**) identified by comparison of retention time with synthesised standards, where available and confirmed by LC-MS/MS. Peak (**7**) is the internal standard naringenin.

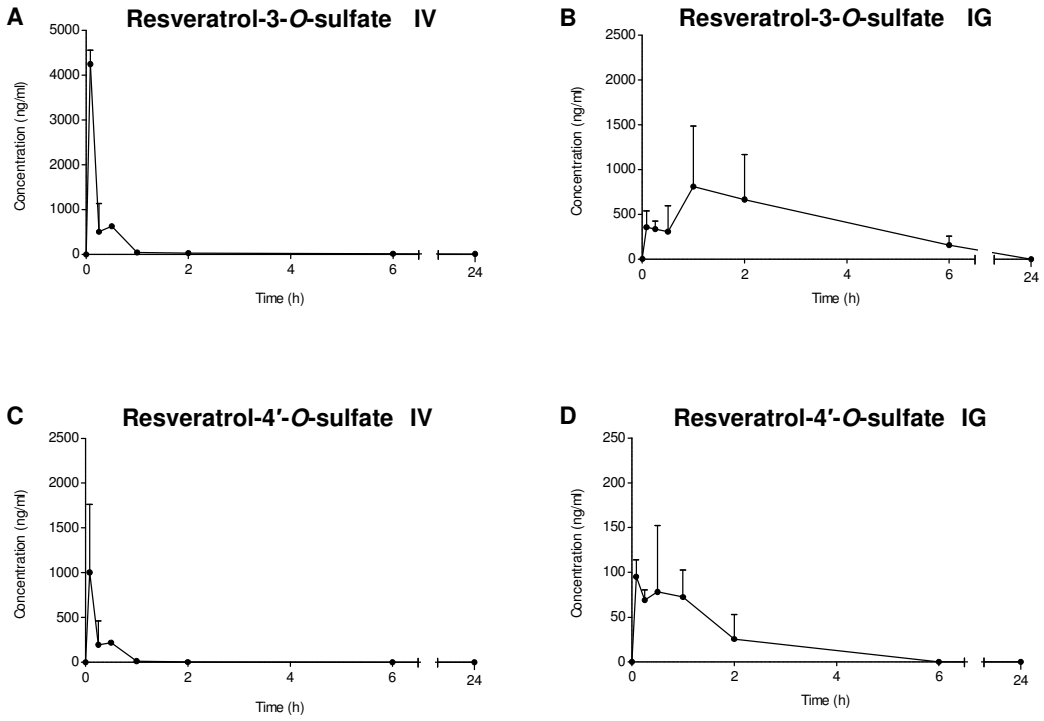

Figure 4.2 Concentrations of resveratrol monosulfates in mouse plasma following IV and IG monosulfate dosing

Concentrations of resveratrol-3-*O*-sulfate in mouse plasma over 24 h following IV (**A**) and IG dosing (**B**) of 6 and 120 mg/kg of resveratrol monosulfates respectively. Resveratrol-4'-*O*-sulfate plasma concentration profiles following the same two routes of administration are shown in (**C**) and (**D**) respectively. Values for each point are the mean + SD of three mice per group. Note the break in the x-axis between 6 and 24 h.

Despite the fact that a higher dose of sulfates was given by the IG route, plasma resveratrol-3-*O*-sulfate concentrations were found to reach a higher C_{max} concentration following IV dosing; average values were 4250 ± 310 ng/ml compared to 809 ± 680 ng/ml for IG. Furthermore, the time at which the maximum concentration was achieved i.e. T_{max}, was found to be earlier following IV dosing; as would be expected (5 min compared to 1 h). The plasma T_{max} for resveratrol-4'-*O*-sulfate was also found to occur at 5 min after the IV dose with C_{max} concentrations more than 10-fold greater following IV dosing relative to the oral route. The AUC_{all}, which gives a better indication of total exposure, was calculated for both monosulfate metabolites, using WinNonlin software (version 5.3). Whereas the AUC_{all} was higher for resveratrol-4'-*O*-sulfate following IV compared to IG dosing (266.2 and 173.9 ng/ml/h respectively), the opposite was true for the major sulfate metabolite; resveratrol-3-*O*-sulfate AUC_{all} values after IV and IG dosing were 1295 and 4250 ng/ml/h respectively. Figures 4.2A and B show that it took a longer time to reach the maximum concentration of this metabolite after oral administration. At 6 h and 24 h post-dosing resveratrol-4'-*O*-sulfate was not detected following either route of administration. For resveratrol-3-*O*-sulfate low levels still persisted at 24 h after the IV dosing route (12.4 ± 8.7 ng/ml), whereas the 6 h time point was the last where levels were seen after IG dosing (158 ± 98 ng/ml).

As mentioned previously, a number of metabolites were generated after both forms of dosing. Resveratrol sulfate glucuronide was the most prominent metabolite after IV injection (Figure 4.3A, C and E; 1a, 1b and 1c), and was also a major metabolite for the oral route. Three polar peaks eluted very close together (Figure 4.1; peaks 1a, 1b and 1c) and these were assigned as sulfate glucuronide isomers based on their retention times. Structures were confirmed using LC-MS/MS (Section 4.6). It was not possible to distinguish which of these were derived from the 3-*O*-sulfate and 4'-*O*-sulfate. Three possible sulfate glucuronide conjugates structures may be formed (Figure 4.3G).

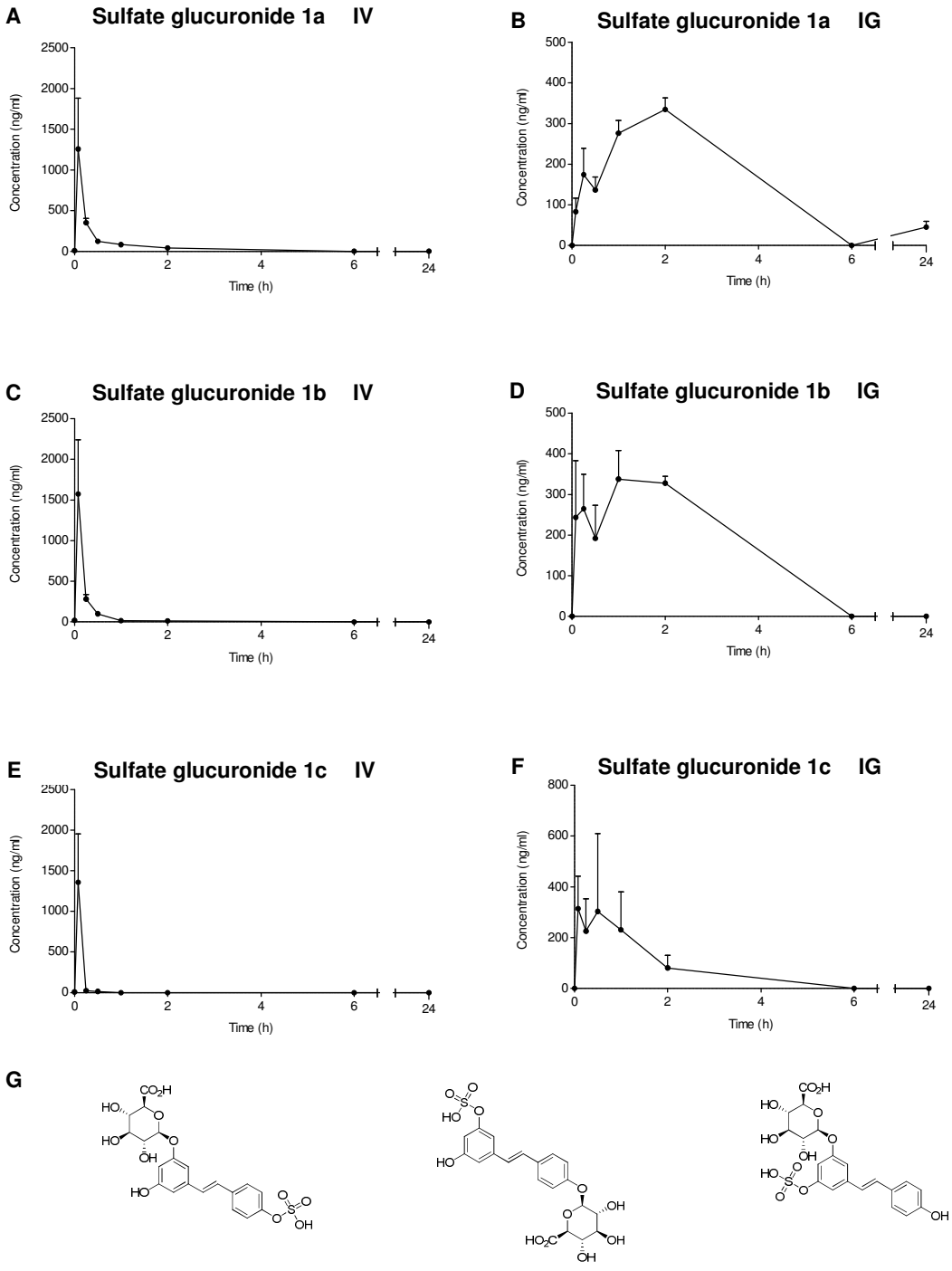

Figure 4.3 Concentrations of resveratrol sulfate glucuronide isomers in mouse plasma following IV and IG monosulfate dosing, and their structures

Concentrations of resveratrol sulfate glucuronide isomers (**1a**, **1b** and **1c**) formed in mouse plasma over 24 h following IV (**A**, **C** and **E**) and IG dosing (**B**, **D** and **F**) of 6 and 120 mg/kg resveratrol monosulfates respectively (calculated using a standard curve of resveratrol-3-*O*-sulfate). The specific peaks assigned as 1a, 1b and 1c are indicated in Figure 4.1. Values for each point are the mean + SD of three mice per group. Note the break in the x-axis between 6 and 24 h. The three isomeric structures are given in (**G**).

Resveratrol-3-*O*-glucuronide was the most abundant metabolite formed in the plasma after IG dosing, and reached maximum average concentrations of 4064 ± 500 ng/ml at 2 h (Figure 4.4B). Furthermore, concentrations of this metabolite greatly exceeded those of resveratrol-3-*O*-sulfate and resveratrol-4'-*O*-sulfate, where C_{max} levels were 809 ± 680 ng/ml (1 h) and 95 ± 19 ng/ml (5 min) respectively. The resveratrol-3-*O*-glucuronide concentration generated was almost 20-fold greater than that achieved following IV administration. The resveratrol-4'-*O*-glucuronide isomer was not detected in any of the plasma samples analysed. This is consistent with findings in Wistar rats given oral doses of resveratrol [71]. The formation of the glucuronides might result from deconjugation of the monosulfates to resveratrol and conjugation with the glucuronide moiety (preferentially at the 3- position).

Resveratrol disulfate, although detected following both routes, was present in only a small number of samples. After IV dosing, it was detectable at 5 and 15 min only, whereas after IG dosing, it was present at 30, 60 and 120 min time points. Importantly, resveratrol was detected in the plasma following both routes of dosing, although these were often close to, or below the LOQ after IV dosing. Following IG dosing (Figure 4.4C), the levels of resveratrol produced were below the LOQ during the first 30 min. The C_{max} was reached at 2 h (132 ± 142 ng/ml), in comparison to 12.9 ± 21.8 after IV dosing at 6 h. There was a high degree of variability in the concentrations detected in plasma, which accounted for the large standard deviations calculated, for example, at the 2 h time point after IG dosing, concentrations of resveratrol generated ranged between 31 and 294 ng/ml in the three mice.

The bioavailability of the resveratrol sulfates in plasma was calculated using the formula:

$$\text{Bioavailability} = \frac{AUC_{inf}\ \text{oral dose x IV dose}}{AUC_{inf}\ \text{IV dose x oral dose}} \times 100$$

The bioavailability of resveratrol-3-*O*-sulfate and resveratrol-4'-*O*-sulfate in plasma was calculated separately as 13.7% and 3.0%, respectively. The overall bioavailability of the two sulfates in plasma was 12.2%.

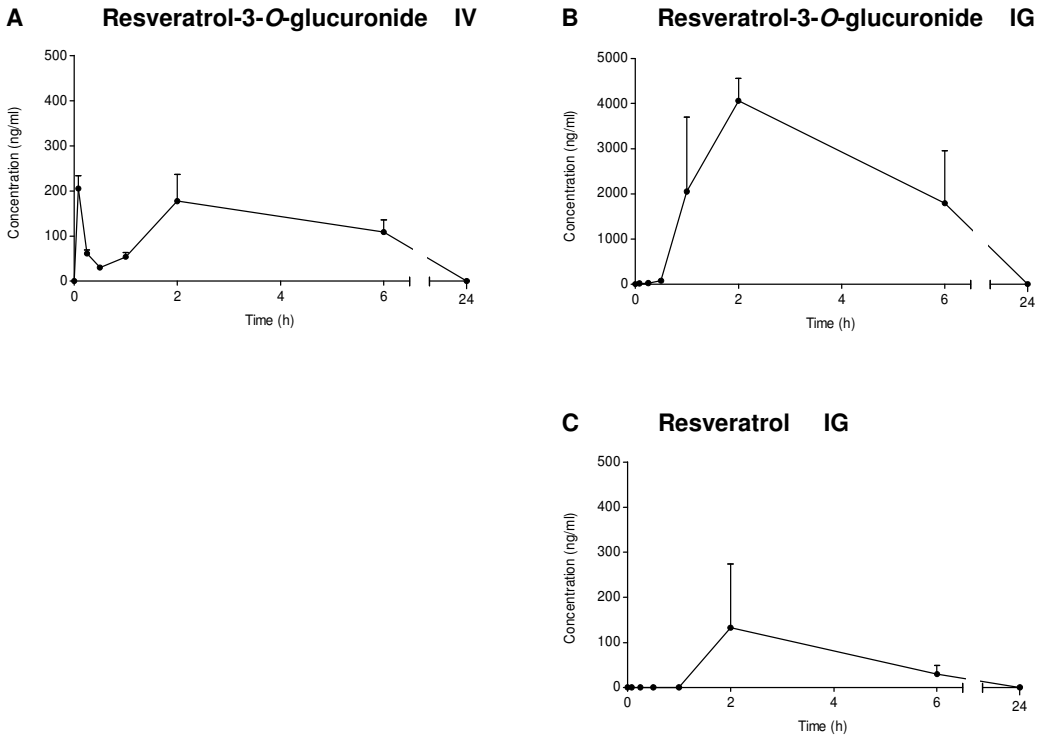

Figure 4.4 Concentrations of resveratrol-3-*O*-glucuronide and resveratrol in mouse plasma following IV and IG monosulfate dosing

Concentrations of resveratrol-3-*O*-glucuronide in mouse plasma over 24 h following IV (**A**) and IG dosing (**B**) of 6 and 120 mg/kg resveratrol monosulfates respectively. The resveratrol concentration profile following sulfate administration by IG only is shown in (**C**) as it was not possible to construct an equivalent curve after IV dosing, where the majority of samples were below the LOQ. Values for each point are the mean + SD of three mice per group. Note the break in the x-axis between 6 and 24 h.

4.3 Characterisation of resveratrol monosulfate pharmacokinetics in mouse tissues

4.3.1 Mouse mucosa profile following resveratrol sulfate dosing by IV and IG routes

Small intestine and colon mucosal scrapings were collected from all mice following exsanguinations. The mucosa was homogenised in buffer and analysed for the presence of sulfates and other metabolites. A representative HPLC-UV chromatogram showing the metabolite profile in mucosa after IG dosing (compared to control) is illustrated in Figure 4.5. For resveratrol-3-*O*-sulfate, the C_{max} was achieved quickly, at the first sampling time of 5 min, and reached an average concentration of 1,229 ± 688 nmol/g following the IG dose (Figure 4.6B). After IV dosing, it took slightly longer to reach the C_{max} in the mucosa, (0.5 h), and a lower concentration was attained (70.6 ± 31.8 nmol/g). AUC_{all} for resveratrol-3-*O*-sulfate was also higher following the IG compared to IV route, reaching 2,112 and 279 nmol/g/h respectively. For resveratrol-4'-*O*-sulfate, a similar pattern was observed between the two dosing regimens, with AUC_{all} values of 339 and 3 nmol/g/h (Figure 4.6). However, a smaller proportion of the total dose of this metabolite was seen after IV dosing, compared to IG dosing.

A number of additional metabolites were also formed from the monosulfates; these were resveratrol disulfate, resveratrol-3-*O*-glucuronide and resveratrol sulfate glucuronide. Resveratrol disulfate concentrations (Figure 4.6E and F) reached comparable levels following both routes of administration. Maximum concentrations achieved were 12.8 ± 8.5 and 17.3 ± 4.6 after IV and IG dosing, with respective T_{max} of 0.5 and 1 h. Similar to the findings in plasma, three sulfate glucuronide metabolite peaks were present at the retention time between 6.0 - 6.3 minutes, which were not fully resolved from one another; the levels of each isomer were determined separately over time (Figure 4.7). Concentrations of the third isomer (peak 1c) were found to be the most prominent after both dosing routes.

Maximal concentrations of the 3-*O*-glucuronide were in the region of 100-fold greater after IG dosing compared to IV, with a relatively long presence in the mucosa (Figure 4.8A and B). After 6 h post administration of the IV and oral doses, concentrations within the mucosa were 0.90 ±

0.46 and 99.1 ± 41.1 nmol/g respectively. Interestingly, resveratrol was detected in the mucosa following both IV and IG sulfate administration; however, tissue levels were found to be variable. The concentrations were approximately 10-fold higher after the IG dose, with C_{max} values of 14.9 ± 7.0 and 1.5 ± 0.7 nmol/g, reached at 0.25 h (for both) after IG and IV dosing respectively. Resveratrol was still detectable 6 h post administration with both routes of drug delivery (Figure 4.8C and D). Many of the differences described above may be related to the variable doses administered.

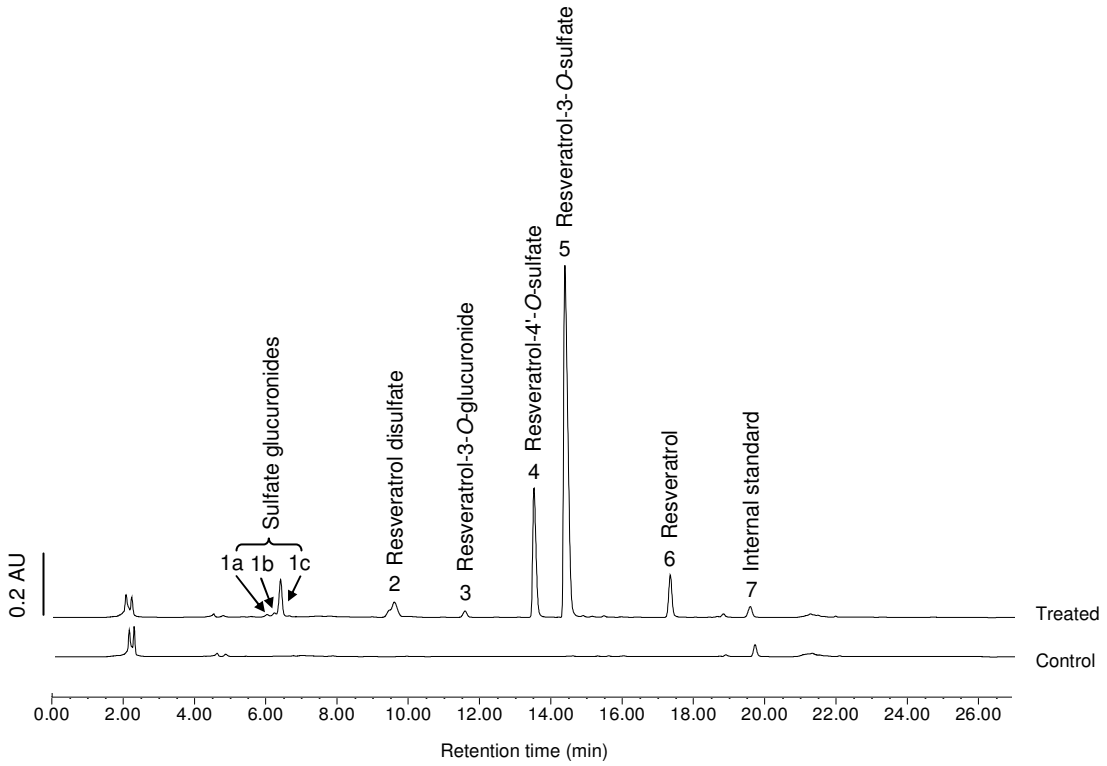

Figure 4.5 Typical HPLC-UV chromatogram of mouse mucosa extracts following IG dosing of resveratrol-3-*O*-sulfate and resveratrol-4'-*O*-sulfate

HPLC-UV chromatograms of mucosa taken from mice receiving saline vehicle only (bottom line), or 120 mg/kg resveratrol sulfates (by IG) taken 1 h post-dosing (top line). Designated peaks are resveratrol sulfate glucuronides (**1a, 1b** and **1c**), resveratrol disulfate (**2**), resveratrol-3-*O*-glucuronide (**3**), resveratrol-4'-*O*-sulfate (**4**), resveratrol-3-*O*-sulfate (**5**) and resveratrol (**6**) identified by comparison of retention times with synthesised standards, where available and confirmed by LC-MS/MS. Peak (**7**) is the internal standard naringenin.

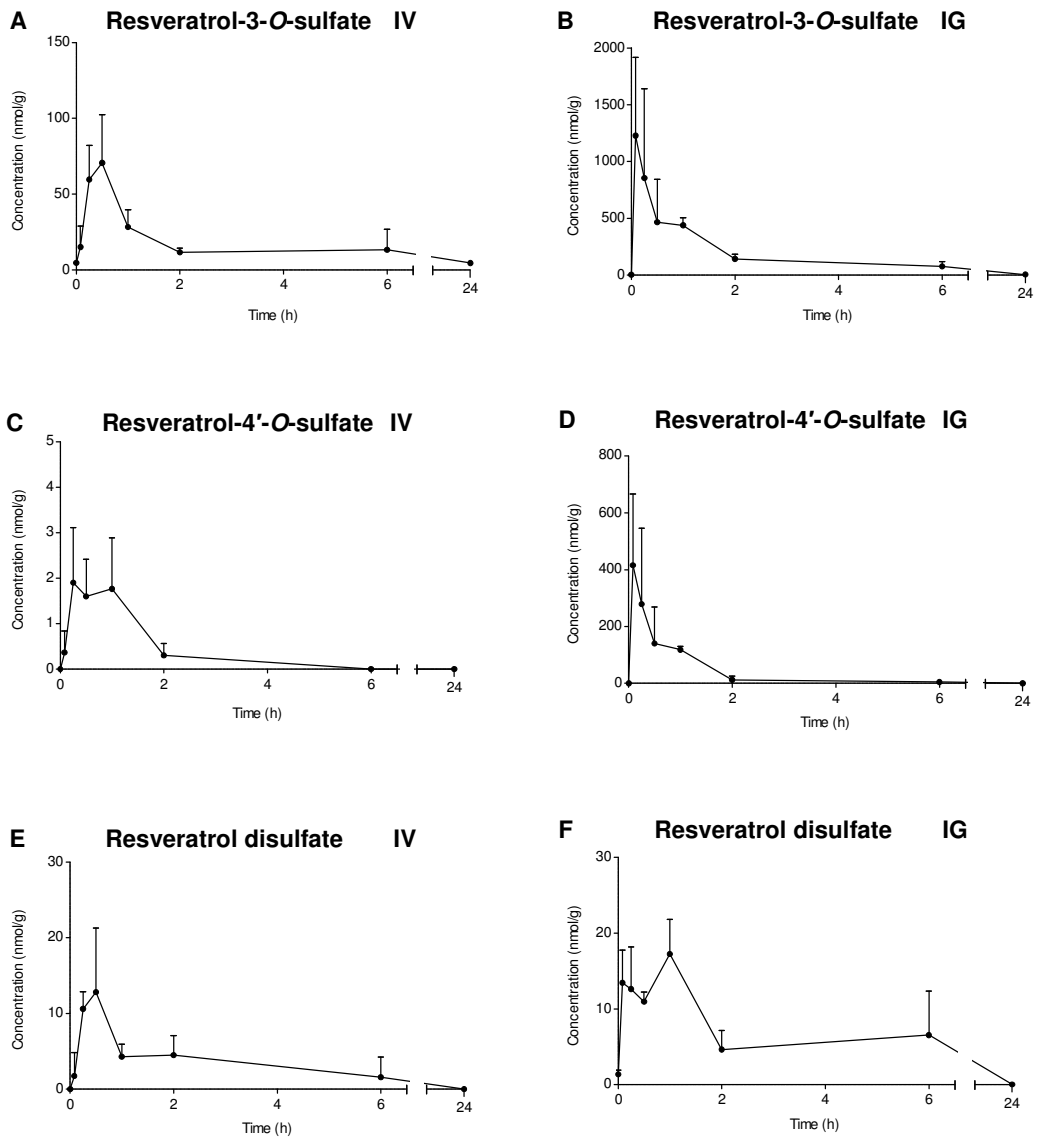

Figure 4.6 Concentrations of resveratrol monosulfates and disulfate in mouse mucosa following IV and IG monosulfate dosing

Concentrations of resveratrol-3-*O*-sulfate in mouse mucosa over 24 h following IV (**A**) and IG dosing (**B**) of 6 and 120 mg/kg of resveratrol monosulfates respectively. Resveratrol-4'-*O*-sulfate concentration profiles following the same two routes of administration are shown in (**C**) and (**D**) and those for resveratrol disulfate are shown in (**E**) and (**F**) respectively. Resveratrol disulfate concentrations were calculated using a standard curve of resveratrol-3-*O*-sulfate. Values for each point are the mean + SD of three mice per group. Note the break in the x-axis between 6 and 24 h.

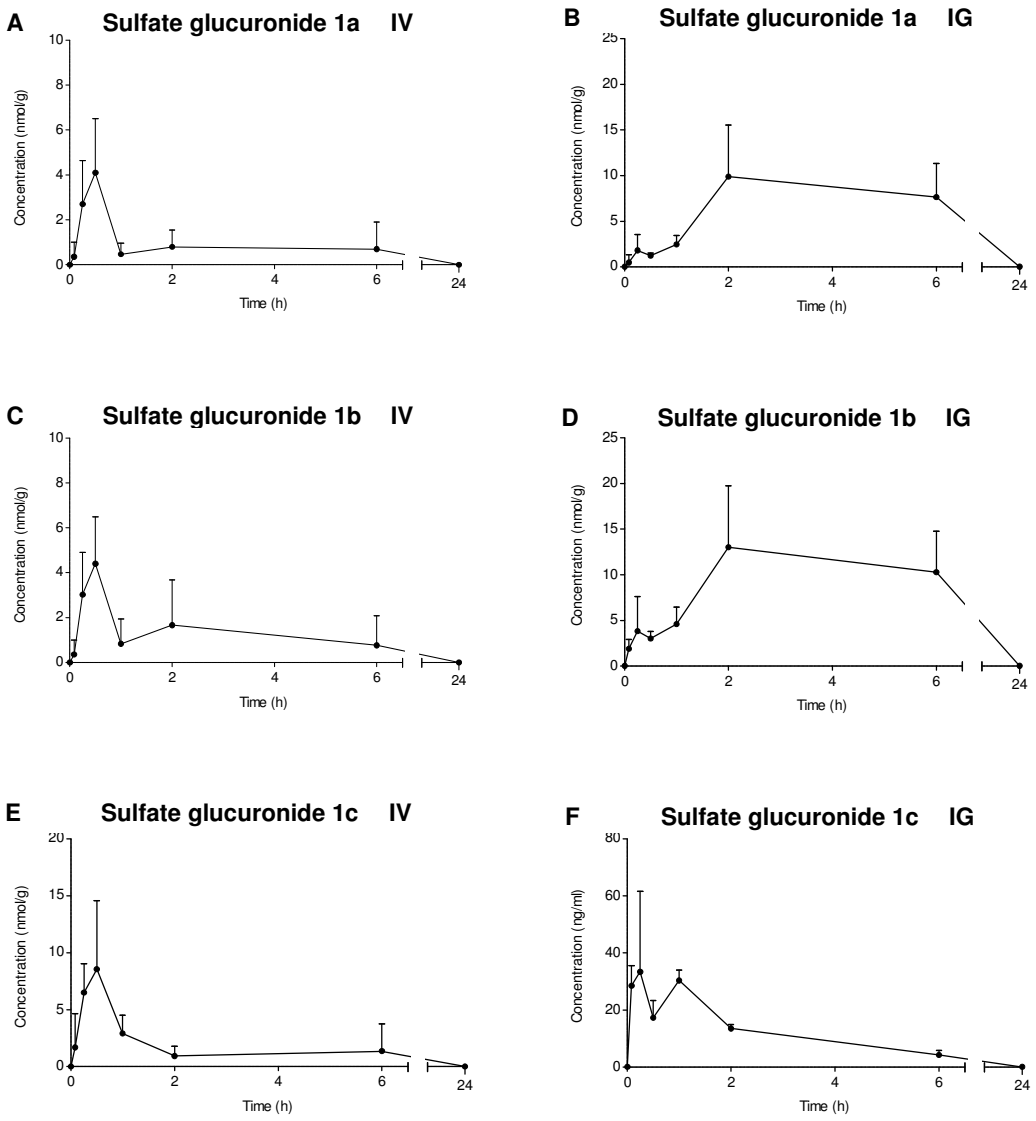

Figure 4.7 Concentrations of resveratrol sulfate glucuronides in mouse mucosa following IV and IG monosulfate dosing

Concentrations of resveratrol sulfate glucuronide isomers (**1a**, **1b** and **1c**) formed in mouse mucosa over 24 h following IV (**A**, **C** and **E**) and IG dosing (**B**, **D** and **F**) of 6 and 120 mg/kg resveratrol monosulfates respectively (calculated using a standard curve of resveratrol-3-*O*-sulfate). The specific peaks assigned as **1a**, **1b** and **1c** are indicated in Figure 4.5. Values for each point are the mean + SD of three mice per group. Note the break in the x-axis between 6 and 24 h.

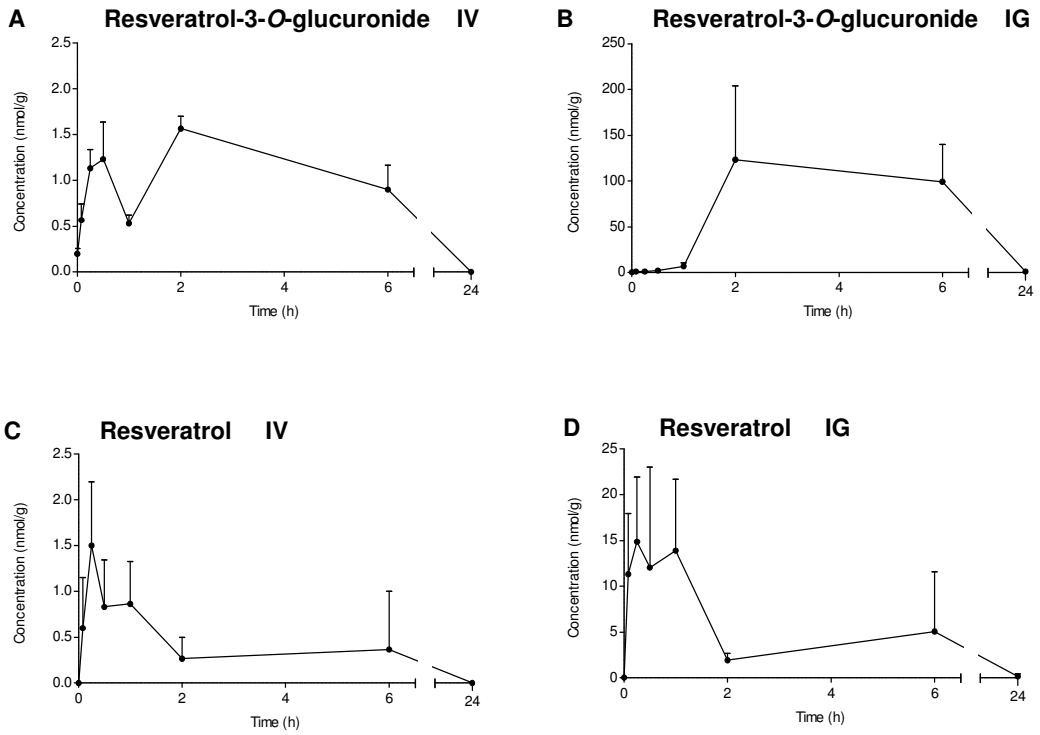

Figure 4.8 Concentrations of resveratrol-3-*O*-glucuronide and resveratrol in mouse mucosa following IV and IG monosulfate dosing

Concentrations of resveratrol-3-*O*-glucuronide in mouse mucosa over 24 h following IV (**A**) and IG dosing (**B**) of 6 and 120 mg/kg resveratrol monosulfates respectively. Resveratrol concentration profiles following the same two routes of administration are shown in (**C**) and (**D**) respectively. All concentrations were calculated using authentic standards. Values for each point are the mean + SD of three mice per group. Note the break in the x-axis between 6 and 24 h.

4.3.2 Mouse liver profile following resveratrol sulfate dosing by IV and IG routes

Liver tissues were homogenised in HEPES buffer and extracted for HPLC-UV analysis as described in Section 2.2.5.3. Example chromatograms of liver extracts following IG dosing of the sulfates and extracts from control mouse liver are shown in Figure 4.9.

In addition to the two monosulfates, parent resveratrol was also found in liver tissue following oral and IV dosing as illustrated by Figure 4.10. Concentrations of resveratrol-4'-*O*-sulfate reached C_{max} values of 1.2 ± 0.6 and 2.1 ± 1.7 nmol/g after IV and IG dosing respectively, and were considerably lower than resveratrol-3-*O*-sulfate. Although the C_{max} was higher for the major sulfate following the IV route, (58.9 ± 17.0 compared to 35.5 ± 8.8 nmol/g), the AUC_{all} was far greater after IG dosing, reaching 457 nmol/g/h compared with 61 nmol/g/h after the IV dose. After IG dosing there was an initial rise in the 3-*O*-sulafte concentration, which dipped at 30 min and increased at 2 h, to the C_{max} level. The concentration was similar when measured at 6 h, but by 24 h, both sulfates were no longer detected. Similar patterns of metabolism were found for resveratrol sulfate glucuronides, resveratrol-3-*O*-glucuronide and resveratrol disulfate following IG dosing, with an increase up to 2 h, and plateau between 2 to 6 h (Figure 7.1 and 7.2; Appendix). With IV dosing, the metabolite concentrations increased sharply, with early T_{max} values, followed by a rapid clearance from the liver tissue.

Resveratrol concentrations in the liver were within the same concentration range irrespective of dosing route (Fig 4.10E and F). Resveratrol reached an average C_{max} of 3.2 ± 0.7 nmol/g at the earliest sampling time of 5 min following IV dosing; levels then declined rapidly, falling to an average of 0.1 ± 0.1 nmol/g at 6 h. After IG dosing, average resveratrol C_{max} (2.8 ± 0.4 nmol/g) was achieved at 2 h, and these levels persisted until 6 h.

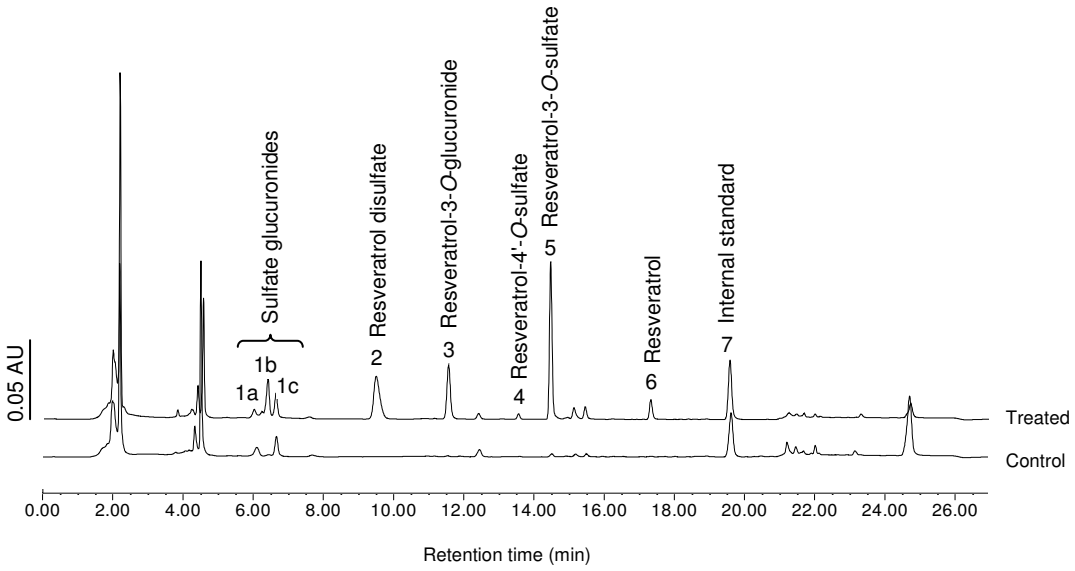

Figure 4.9 Typical HPLC-UV chromatogram of mouse liver extracts following IG dosing of resveratrol-3-*O*-sulfate and resveratrol-4'-*O*-sulfate

HPLC-UV chromatograms of mouse liver extracts taken from mice receiving saline vehicle only (bottom line), or 120 mg/kg resveratrol sulfates (by IG) taken 1 h post-dosing (top line). Designated peaks are resveratrol sulfate glucuronide isomers (**1a**, **1b** and **1c**), resveratrol disulfate (**2**), resveratrol-3-*O*-glucuronide (**3**), resveratrol-4'-*O*-sulfate (**4**), resveratrol-3-*O*-sulfate (**5**) and resveratrol (**6**) identified by comparison of retention times with synthesised standards, where available and confirmed by LC-MS/MS. Peak (**7**) is the internal standard naringenin.

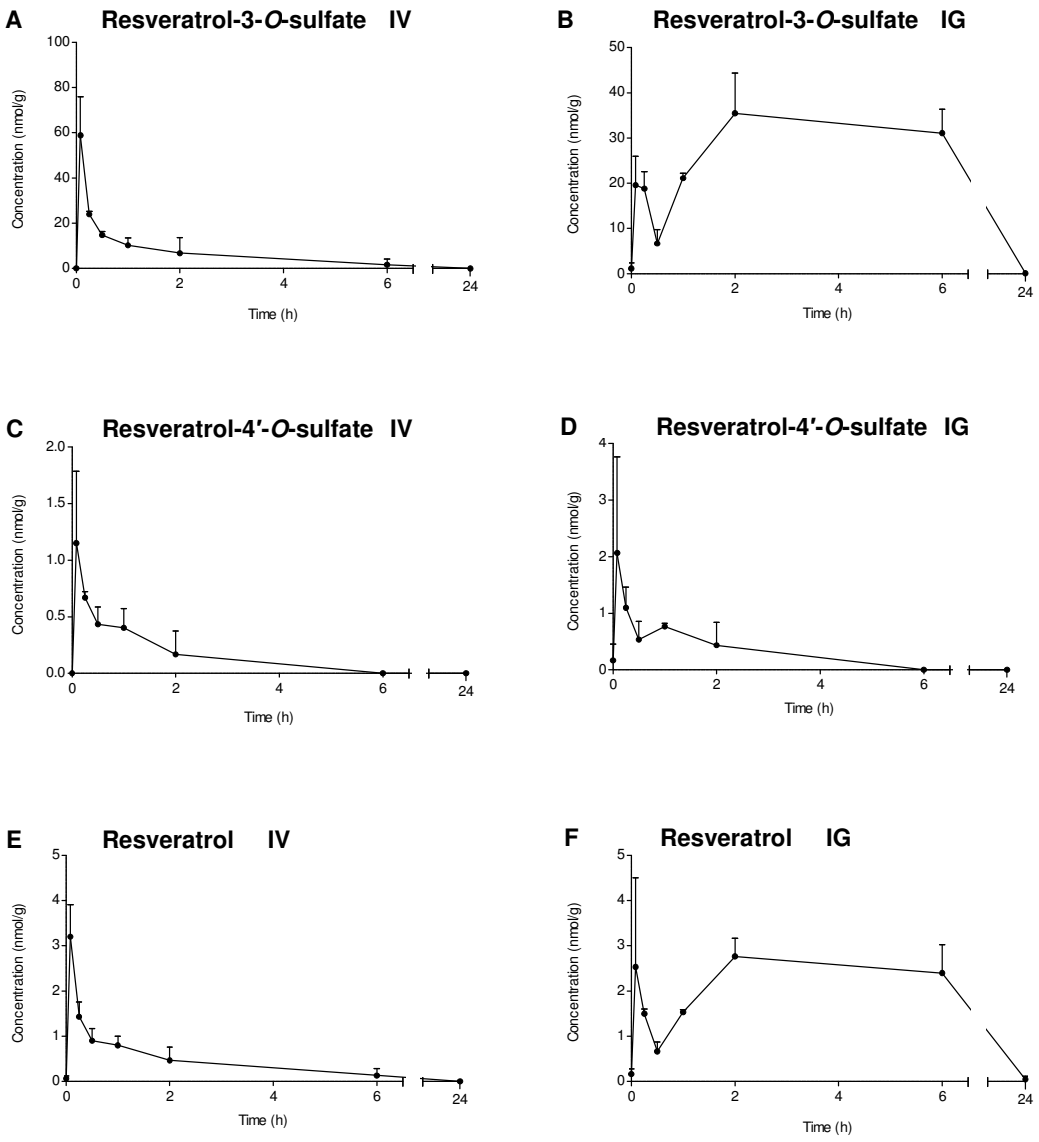

Figure 4.10 Concentrations of resveratrol monosulfates and resveratrol in mouse liver following IV and IG monosulfate dosing

Concentrations of resveratrol-3-*O*-sulfate in mouse liver over 24 h following IV (**A**) and IG dosing (**B**) of 6 and 120 mg/kg resveratrol monosulfates respectively. Resveratrol-4'-*O*-sulfate concentration profiles following the same two routes of administration are shown in (**C**) and (**D**) and those for resveratrol are shown in (**E**) and (**F**) respectively. Values for each point are the mean + SD of three mice per group. Note the break in the x-axis between 6 and 24 h.

4.3.3 Mouse lung and pancreas profiles following resveratrol sulfate dosing by IV and IG routes

Mouse lung and pancreas were also analysed in order to determine the extent of resveratrol sulfate distribution in tissues after sulfate dosing. The HPLC-UV chromatograms in lung and pancreas extracts of mice dosed with monosulfates are shown in Figure 4.11A and B respectively.

Resveratrol monosulfates and resveratrol were detected in the lung tissue after both forms of dosing (Figure 4.12). The AUC_{all} for resveratrol-3-*O*-sulfate after IV and IG administration was 1.4 and 29.5 nmol/g/h respectively, with approximately 10-fold lower values of the 4'-*O*-sulfate for both routes. Resveratrol concentrations, although detected after IV dosing, were only above the LOQ at 5 min. However, it was still possible to calculate the average C_{max} values, which were 0.32 ± 0.02 and 2.2 ± 3.9 after the IV and IG dose respectively. AUC_{all} could only be determined after IG dosing, and was 1.1 nmol/g/h.

Of the metabolites previously reported in plasma, resveratrol-3-*O*-glucuronide was detected in the lung tissue of mice culled at the earliest time point of 5 min, only after IV dosing. Higher levels of this metabolite were detected in IG samples (Figure 7.3; Appendix). Resveratrol disulfate was absent in all samples, and resveratrol sulfate glucuronide was a minor metabolite, detectable in only a small number of samples after the IG route. Of all the organs analysed, the fewest metabolites were detected in pancreatic tissue. In addition to the monosulfates (Figure 4.13), resveratrol-3-*O*-glucuronide was present after IG administration only (Figure 7.4; Appendix). The monosulfates had AUC_{all} values and C_{max} concentrations of a similar order of magnitude as those in lung tissue. Consistent with the other tissues, much higher AUC values were achieved after IG dosing, with a longer residence time, as indicated by the time at which the last measurable concentration was achieved (T_{last}). Average resveratrol C_{max} concentrations were 0.31 ± 0.33 and 1.8 ± 3.2 nmol/g after IV and IG dosing respectively. As resveratrol was only observed at levels above LOQ at 5 min after IV dosing, the AUC_{all} could only be calculated after IG dosing, and reached 1.62 nmol/g/h.

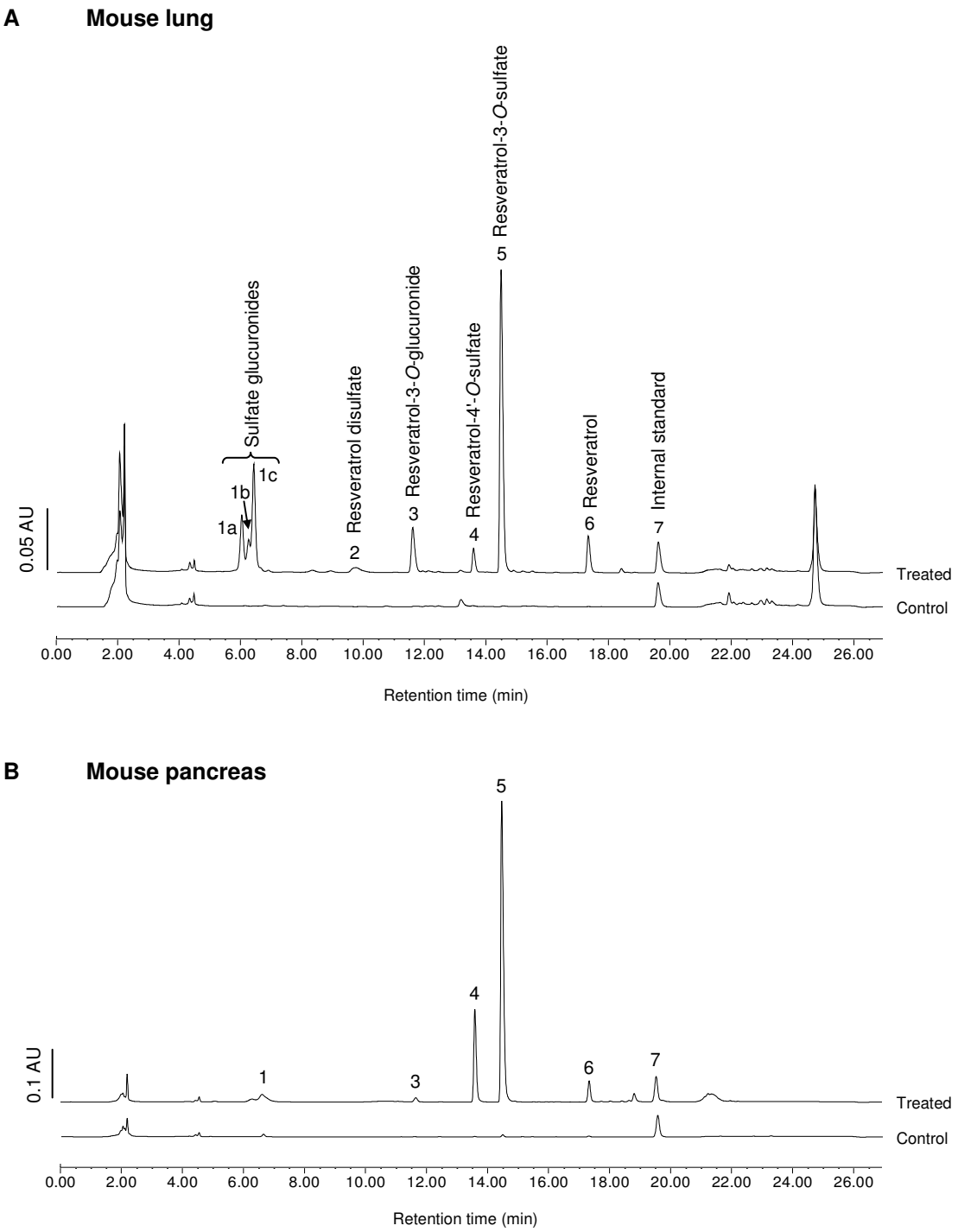

Figure 4.11 Typical HPLC-UV chromatogram of mouse lung and pancreas extracts following IG dosing of resveratrol-3-*O*-sulfate and resveratrol-4'-*O*-sulfate

HPLC-UV chromatograms of lung (**A**) and pancreas (**B**) taken from mice receiving saline vehicle only (bottom line in each figure), or 120 mg/kg resveratrol sulfates (by IG) taken 0.5 h post-dosing (top line in each figure). Designated peaks are resveratrol sulfate glucuronide isomers (**1a**, **1b** and **1c**), resveratrol disulfate (**2**), resveratrol-3-*O*-glucuronide (**3**), resveratrol-4'-*O*-sulfate (**4**), resveratrol-3-*O*-sulfate (**5**) and resveratrol (**6**) identified by comparison of retention times with synthesised standards, where available and confirmed by LC-MS/MS. Peak (**7**) is the internal standard naringenin.

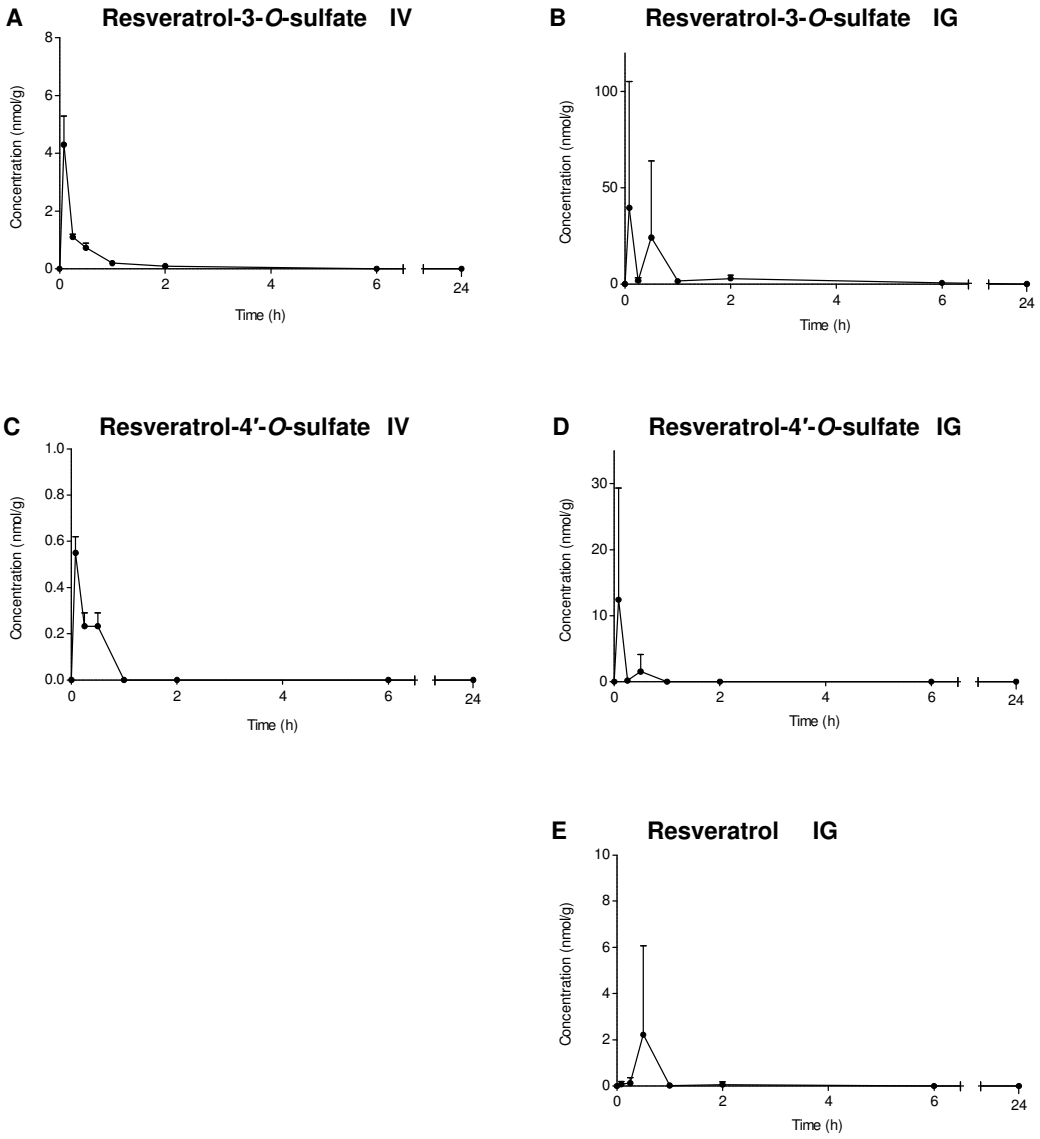

Figure 4.12 Concentrations of resveratrol monosulfates and resveratrol in mouse lung following IV and IG monosulfate dosing

Concentrations of resveratrol-3-*O*-sulfate in mouse lung over 24 h following IV (**A**) and IG dosing (**B**) of 6 and 120 mg/kg resveratrol monosulfates respectively. Resveratrol-4'-*O*-sulfate concentration profiles following the same two routes of administration are shown in (**C**) and (**D**). The resveratrol profile following sulfate administration by IG dosing only is shown in (**E**), as it was not possible to construct an equivalent curve after IV dosing, where the majority of samples were below the LOQ. Values for each point are the mean + SD of three mice per group. Note the break in the x-axis between 6 and 24 h.

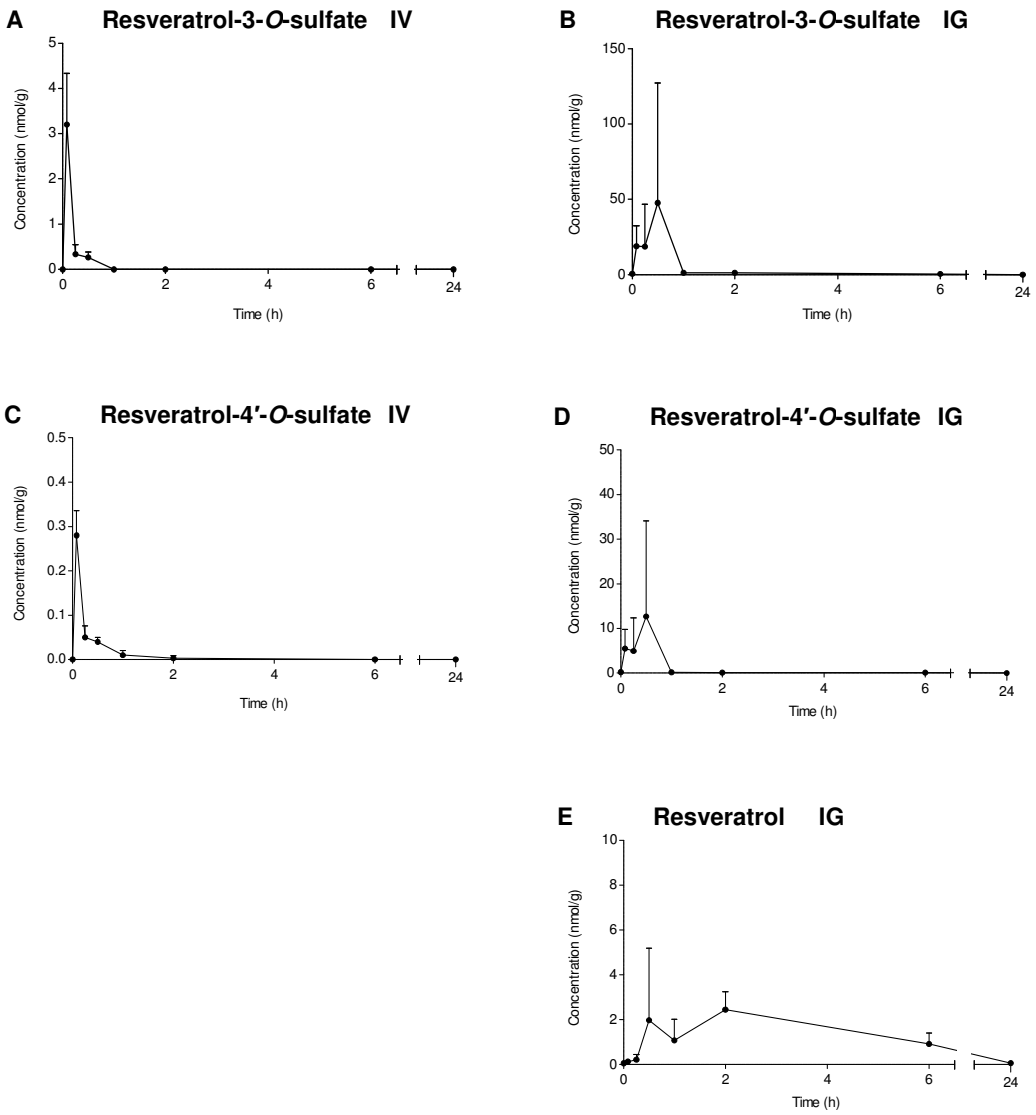

Figure 4.13 Concentrations of resveratrol monosulfates and resveratrol in mouse pancreas following IV and IG monosulfate dosing

Concentrations of resveratrol-3-*O*-sulfate in mouse pancreas over 24 h following IV (**A**) and IG dosing (**B**) of 6 and 120 mg/kg resveratrol monosulfates respectively. Resveratrol-4'-*O*-sulfate concentration profiles following the same two routes of administration are shown in (**C**) and (**D**). The resveratrol profile following sulfate administration by IG dosing only is shown in (**E**), as it was not possible to construct an equivalent curve after IV dosing, where the majority of samples were below the LOQ. Values for each point are the mean + SD of three mice per group. Note the break in the x-axis between 6 and 24 h.

4.4 Comparison of resveratrol monosulfate and resveratrol pharmacokinetic parameters in plasma and tissues following IV and IG dosing

The PK parameters in mouse plasma and each of the tissues analysed (liver, lung, mucosa and pancreas) have been summarised for resveratrol-3-*O*-sulfate, resveratrol-4'-*O*-sulfate and resveratrol (Table 4.1). These were not calculated for resveratrol sulfate glucuronide, resveratrol disulfate or resveratrol-3-*O*-glucuronide as the main focus was on the bioavailability and characteristics of the sulfates and the formation of resveratrol.

For both sulfates and resveratrol, the greatest overall exposure to tissues, as indicated by AUC_{all}, was in mouse mucosa. The proportion of total resveratrol-3-*O*-sulfate that was detected in tissues including the mucosa, liver, lung and pancreas was 81.5%, 17.9%, 0.4% and 0.2% respectively, after IV dosing. The respective proportions of the 3-*O*-sulfate detected in these tissues were almost identical after IG dosing (80.2%, 17.3%, 1.1% and 1.3%). By comparison, exposure to resveratrol-4'-*O*-sulfate of tissues after IG dosing was highest in the mucosa (96.8%), with low levels detected in the liver (0.7%) and tissues analysed. After the IV dose, there was a larger proportion of the 4'-*O*-sulfate present in the liver (26.9%), and lower levels than those after IG dosing in the mucosa (67.7%). Pancreas and lung both had low concentrations of resveratrol-4'-*O*-sulfate.

Of the tissues, pancreas and lung were also shown to have the lowest resveratrol C_{max} concentrations after IV and IG dosing. Resveratrol exposure to tissues was also less than that observed in the mucosa and liver. The amount of resveratrol in the mucosa and liver accounted for 68% and 30% respectively of the total tissue AUC_{all} exposure. Analysis of all of the tissues rather than just the selected set here, would have allowed a more accurate tissue distribution to be determined.

A Resveratrol-3-*O*-sulfate

	T_{max} (h)		C_{max} (nmol/g)		T_{last} (h)		AUC_{all} (nmol/g/h)		Cl_{obs} (ml/min/kg)		V_D (L)	
	IV	**IG**	**IV**	**IG**	**IV**	**IG**	**IV**	**IG**	**IV**	**IG**	**IV**	**IG**
Plasma	0.083	1	4,250	809	24	6	1,295	4,250	46.3	282	0.022	
Liver	0.083	2	58.9	35.5	6	24	61.4	457				
Lung	0.083	0.083	4.3	39.6	2	6	1.4	29.5				
Mucosa	0.5	0.083	70.6	1,229	24	24	279	2,112				
Pancreas	0.083	0.5	3.2	47.7	0.5	6	0.58	34.7				

B Resveratrol-4'-*O*-sulfate

	T_{max} (h)		C_{max} (nmol/g)		T_{last} (h)		AUC_{all} (nmol/g/h)		Cl_{obs} (ml/min/kg)		V_D (L)	
	IV	**IG**	**IV**	**IG**	**IV**	**IG**	**IV**	**IG**	**IV**	**IG**	**IV**	**IG**
Plasma	0.083	0.083	1,004	95	2	2	266	174	150	4601	0.613	
Liver	0.083	0.083	1.2	2.1	2	2	1.25	2.3				
Lung	0.083	0.083	0.6	12.4	0.5	0.5	0.19	2.2				
Mucosa	0.25	0.083	1.9	415	2	6	3.14	339				
Pancreas	0.083	0.5	0.3	12.7	0.25	2	0.06	6.9				

C Resveratrol

	T_{max} (h)		C_{max} (nmol/g)		T_{last} (h)		AUC_{all} (nmol/g/h)		Cl_{obs} (ml/min/kg)		V_D (L)	
	IV	**IG**	**IV**	**IG**	**IV**	**IG**	**IV**	**IG**	**IV**	**IG**	**IV**	**IG**
Plasma	6	2	12.9	132	6	6	N/A	658				
Liver	0.083	2	3.2	2.8	6	24	3.98	36				
Lung	0.083	0.5	0.32	2.2	0.083	2	N/A	1.1				
Mucosa	0.25	0.25	1.5	14.9	6	24	6.51	82				
Pancreas	0.083	0.5	0.31	1.8	0.083	2	N/A	1.6				

Table 4.1 Resveratrol monosulfate and resveratrol PK parameters in mouse plasma and tissues. Resveratrol-3-*O*-sulfate (**A**), resveratrol-4'-*O*-sulfate (**B**) and resveratrol (**C**) PK parameters in mouse plasma and tissues following IV and IG dosing of resveratrol sulfates at 6 mg/kg and 120 mg/kg respectively. Parameters were calculated on an average of 3 tissues per group using WinNonlin software. Plasma concentrations are expressed in ng/ml for C_{max} and ng/h/ml for AUC_{all}. Tissue concentrations are given in nmol/g, which are equivalent to µM values. Cl_{obs} (in ml/min/kg) and V_D (in L) are the plasma clearance and volume of distribution respectively.

4.5 Mouse urine analysis following IG resveratrol sulfate dosing

Mouse urine pre- and post-IG dosing was analysed using HPLC-UV (Figure 4.14) to allow identification of metabolites that were renally excreted. Whereas no resveratrol-related species were detected in the control and 5 min urine samples, large quantities were detected at 30 and 60 min post-dosing. The metabolites detected were resveratrol sulfate glucuronide, resveratrol disulfate, resveratrol-3-*O*-glucuronide, in addition to parent resveratrol-3-*O*-sulfate and resveratrol-4'-*O*-sulfate. Resveratrol was not detected in any of the urine samples analysed.

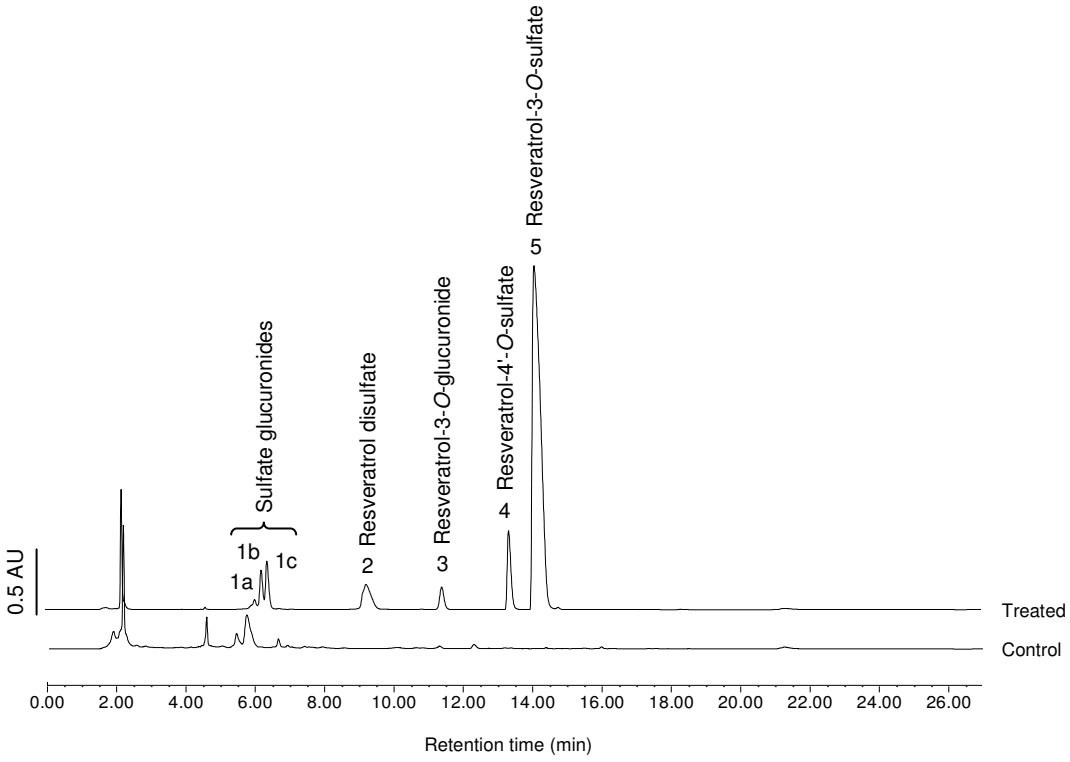

Figure 4.14 Typical HPLC-UV chromatogram of mouse urine following IG dosing of resveratrol-3-*O*-sulfate and resveratrol-4'-*O*-sulfate

HPLC-UV chromatograms of mouse urine taken from mice receiving saline vehicle only (bottom line), or 120 mg/kg resveratrol sulfates (by IG) taken 0.5 h post-dosing (top line). Urine samples were diluted 20-fold prior to extraction. Designated peaks are resveratrol sulfate glucuronide isomers (**1a**, **1b** and **1c**), resveratrol disulfate (**2**), resveratrol-3-*O*-glucuronide (**3**), resveratrol-4'-*O*-sulfate (**4**) and resveratrol-3-*O*-sulfate (**5**) identified by comparison of retention times with synthesised standards, where available and confirmed by LC-MS/MS.

4.6 Characterisation of resveratrol and metabolites in mouse matrices by LC-MS/MS

In order to further confirm the identity of the metabolites recovered in the mouse plasma, urine and tissues following IG dosing, particularly those where no standards were available, LC-MS/MS was used. Samples were analysed using MRM to monitor the characteristic fragmentations of the major metabolites in the negative ion mode (see Section 2.2.3.3 for more details) (Figure 4.15).

The LC-MS/MS results confirmed the assignments made on the basis of retention time by HPLC-UV analysis. In plasma, peaks undergoing transitions with *m/z* of 483 > 227 (loss of a sulfate and glucuronide), 387 > 227 (loss of a sulfate), 403 > 227 (loss of a glucuronide), 307 > 227 (loss of a monosulfate) and 227 > 184 were present, which correspond to resveratrol sulfate glucuronide, resveratrol disulfate, resveratrol monoglucuronide, resveratrol monosulfate and resveratrol respectively. In plasma and mucosa, resveratrol-3-*O*-glucuronide was detected, but not the 4′-*O*-glucuronide isomer, which is consistent with findings from the HPLC-UV analysis. Resveratrol peaks of high intensity were present in both plasma and mucosa.

Samples of mouse liver, lung, pancreas and urine taken from mice which had received the mixture of resveratrol sulfates by the IG route, were also extracted and analysed by LC-MS/MS. The same transitions as those used for plasma and mucosa were monitored. Resveratrol sulfate glucuronide was not detected in either lung or pancreas, and resveratrol disulfate was not detected in the latter. Whereas a resveratrol peak was observed in plasma and all tissues, there was none detected in the mouse urine sample, although the four metabolites mentioned above were (data not shown).

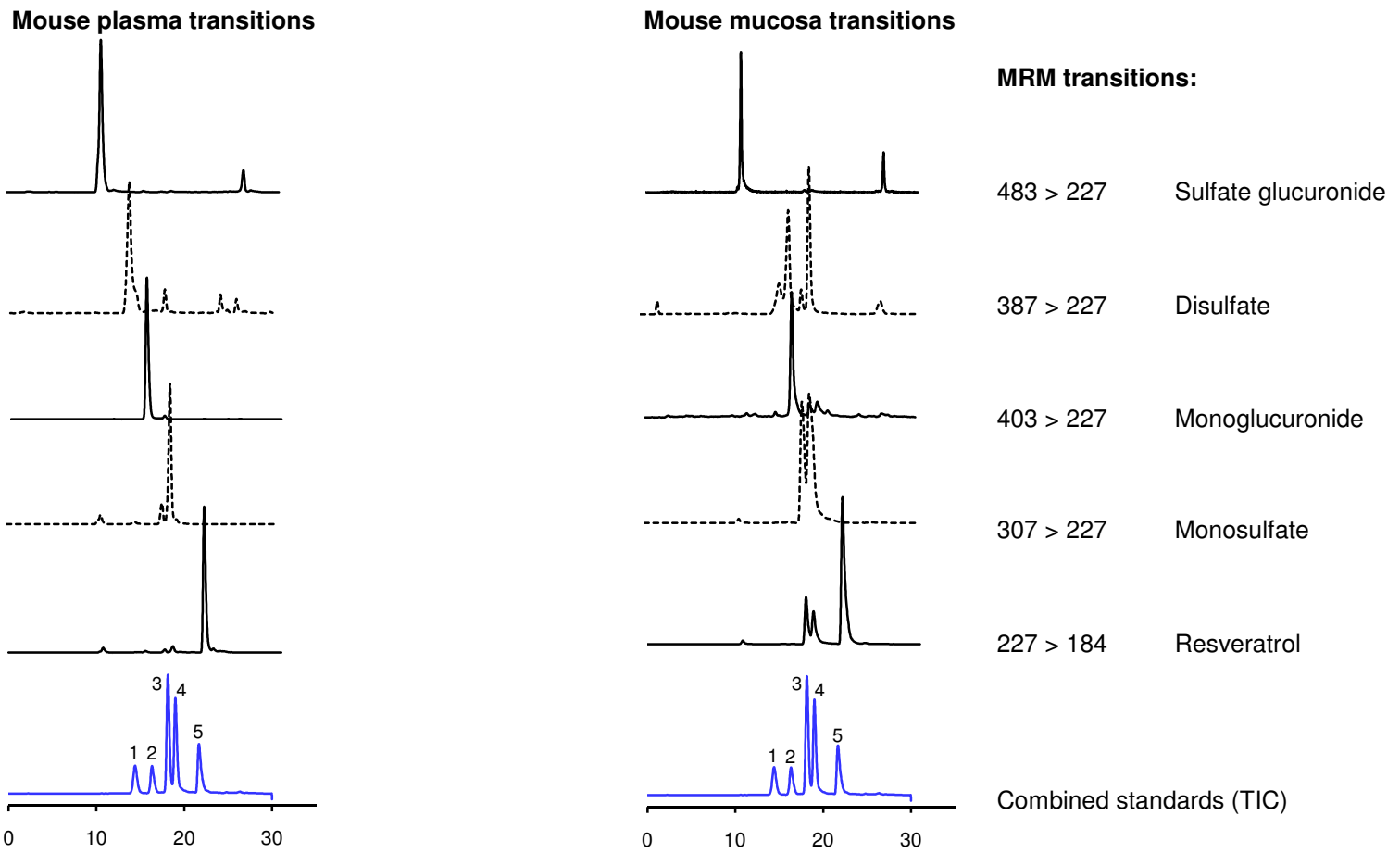

Figure 4.15 LC-MS/MS multiple reaction monitoring (MRM) transitions in mouse plasma and mucosa following IG monosulfate dosing

Identification of resveratrol metabolites in mouse plasma and mucosa following dosing with 120 mg/mg of resveratrol monosulfates by IG. The total ion current from a mixture of authentic standards is also shown for comparison. The mixture consisted of resveratrol-4'-*O*-glucuronide (**1**), resveratrol-3-*O*-glucuronide (**2**), resveratrol-4'-*O*-sulfate (**3**), resveratrol-3-*O*-sulfate (**4**) and resveratrol (**5**). Resveratrol and all of the metabolites shown in the transitions above were detected in the mouse plasma and mucosa.

4.7 Discussion

In previously published studies the distribution and bioavailability of resveratrol in tissues has been investigated in rodents following IV and/or IG dosing of the compound [156], [116], [155], [71], [132]. The formation and distribution of the glucuronide and sulfate conjugates have also been explored after both routes of resveratrol administration. However, as yet, resveratrol metabolites have not been administered and evaluated in animals. In this study, resveratrol sulfates were synthesised and given to mice, by IV and IG routes, to allow an estimation of bioavailability and to determine their tissue distribution after direct administration. Analysis of plasma and various tissues would also provide an indication of whether resveratrol sulfates could be converted to resveratrol in target organs, as has been proposed by a number of investigators [71], [137], [156], [79], [152], [104].

After dosing with the monosulfate mixture by IV and IG routes, the metabolites in plasma were identified as resveratrol-3-*O*-glucuronide, resveratrol disulfate and resveratrol sulfate glucuronide. Sulfate and glucuronide metabolites have previously been identified in plasma of rodents receiving resveratrol in their diet [71], [155], and via IV [137], [131] and IG routes [103], [132], [131]. However, resveratrol sulfate glucuronides have not been identified in mouse plasma before, although there was evidence of their presence in bile and perfusate of Wistar rats following 20 µM resveratrol perfusions in isolated livers [145]. In patient colon tissues and plasma, resveratrol sulfate glucuronide was demonstrated to be a major metabolite after resveratrol dosing (as discussed in Chapter 3; Section 3.3.3 and 3.3.6) [114]. In the mouse plasma here, it was found to be prominent, with C_{max} and total peak exposures (AUC_{all}) greater than for resveratrol-4'-*O*-sulfate. Three early-eluting sulfate glucuronide peaks were detected and these might correspond to the isomers that can be formed, which are resveratrol-3-*O*-sulfate-4′-*O*-glucuronide, resveratrol-3-*O*-glucuronide-4′-*O*-sulfate and resveratrol-3-*O*-glucuronide-5-*O*-sulfate [145]. The sulfate glucuronide isomers could be formed primarily by glucuronidation of the administered monosulfates. Deconjugation to resveratrol and reconjugation of both sulfate and glucuronide groups could also occur, although probably to a lesser degree. Co-eluting sterioisomers resveratrol-3,5-disulfate and resveratrol-3,4'-disulfate

were identified in plasma of rats fed with 300 mg resveratrol per kg bodyweight for eight weeks [71]. In the sulfate dosing study here, a disulfate was identified; however, standards of the two disulfate isomers would be needed to determine whether both isomers were actually present.

The majority of investigations with resveratrol dosing in rodents, have identified resveratrol glucuronide as being a prominent metabolite. In both this study, and that by Wenzel *et al*. [71] in rats, the 4'-*O*-glucuronide isomer was absent and only resveratrol-3-*O*-glucuronide was formed. The identity of resveratrol-3-*O*-glucuronide in the present study was confirmed by comparison of retention times with authentic synthesised standards, in addition to using LC-MS/MS. In terms of the newly formed plasma metabolite concentrations, resveratrol-3-*O*-glucuronide had the highest AUC_{all} following IG dosing and reached a C_{max} of 4064 ± 500 ng/ml at 2 h, whereas sulfate glucuronide generation was more marked after IV dosing. Analysis of plasma showed that the C_{max} for resveratrol-4'-*O*-sulfate achieved following IV dosing (1004 ± 760 ng/ml) was considerably greater than after IG dosing (95 ± 19 ng/ml), despite the 20-fold lower dose administered by IV. These differences might be expected, as the whole dose enters the blood stream immediately with IV dosing, and therefore is not subject to any losses due to incomplete absorption or metabolism in the GI tract. In a mouse study where the plasma concentrations were compared after a 20 mg/kg resveratrol dose via intraperitoneal (IP) and IG dosing routes, higher concentrations of resveratrol, glucuronide and sulfate metabolites were reached after IP dosing [137]. Resveratrol-3-*O*-sulfate was the most abundant metabolite in plasma, reaching concentrations of approximately 13 µM at 15 min. Concentrations of resveratrol-3-*O*-glucuronide at this time were 5 µM, and by 1 h post-dosing both metabolites and resveratrol were no longer detectable. When resveratrol was administered orally at a dose of 10 mg/kg, the resveratrol sulfate AUC was slightly higher than that for the glucuronide (12,600 and 11,600 ng/h/ml respectively) [131]. In a study where resveratrol was administered to rats intraperitoneally at a dose of 15 mg/kg, only the sulfate and glucuronide metabolites were shown to be formed, with observable plasma metabolite levels after one minute, consistent with the extremely rapid metabolism of resveratrol [132]. However, unlike the previously mentioned studies, resveratrol glucuronide was shown to be the predominant conjugate, suggesting that differences in the extent of sulfation and glucuronidation may occur

and that they are both major metabolic pathways. One possible explanation for the variable metabolism seen in these studies could be related to the species difference.

When the mixture of sulfates were given in the experiments here, resveratrol-3-*O*-sulfate reached plasma T_{max} later after IG dosing (1 h compared to 5 min after IV injection) and was detectable at 24 h after the IV route only. Resveratrol-4'-*O*-sulfate was not detected in plasma after 2 h irrespective of dosing regimen. This might be due to the lower levels of the 4'-*O*-sulfate metabolite that were administered, resulting in a more rapid clearance from the body. Therefore, modification of sampling times may result in improved detection of this metabolite. The difference in these parameters might also be related to the bioavailability of the two monosulfates. Although a mixture of the sulfates was administered, the bioavailability of the metabolites was calculated separately, which allowed comparisons to be made. Whereas the overall bioavailability of the sulfates in plasma was approximately 12%, for resveratrol-3-*O*-sulfate and resveratrol-4'-*O*-sulfate the respective values were 14% and 3%. The lower plasma bioavailability of resveratrol-4'-*O*-sulfate might indicate why this metabolite is absent in plasma of humans following a diet high in resveratrol [71]. Resveratrol-4'-*O*-sulfate was also shown to be a minor metabolite in human plasma after resveratrol doses of up to 5 g were consumed as either a single [107], or repeated dose (Chapter 3; Section 3.2). The bioavailability of resveratrol was not assessed in mice in the current study. However, it has been calculated in rats following an oral and IV dose of 50 mg/kg and 15 mg/kg respectively and was found to be 38% bioavailable [130]. The percentages of the resveratrol and glucuronide exposure that were due to enterohepatic circulation (calculated using bile-donor and recipient rats) were almost identical (25% and 24% respectively). Similar doses (50 mg/kg and 10 mg/kg) were used in another bioavailability study also in rats, and resveratrol bioavailability was calculated to be 30% [131]. The higher bioavailability of resveratrol compared to that of the metabolites (calculated in this study) might be expected as resveratrol is less polar and can therefore be absorbed more readily. Resveratrol was also administered in a solution of hydroxypropyl β-cyclodextrin, in the first study [130] compared to saline for the sulfates as part of this research, potentially making it more bioavailable. Lipophilic compounds tend to be more permeable, and in addition, they are normally more rapidly and extensively metabolized. There are comprehensive data to suggest

that despite its high absorption, resveratrol has a low oral bioavailability [104], [146]. Absorption of resveratrol was estimated to be at least 70% in one study in humans, with oral bioavailability of unchanged resveratrol (as established from plasma data), close to zero [104]. Bioavailability is influenced by many properties, including the rate and extent of absorption and systemic clearance. For resveratrol, the time taken to reach a maximum concentration in plasma of rats was very rapid with a T_{max} of 10 min after 2 mg/kg and 240 mg/kg resveratrol [176], [155], quicker than with the oral dose of the sulfates in mice here.

One of the primary aims of this study was to determine if it was possible for resveratrol formation to occur from the sulfate metabolites *in vivo*. Plasma analysis showed that resveratrol was detectable after both forms of dosing, although values were not consistently high enough to plot and AUC_{all} could not be quantified after IV dosing. The amount of resveratrol as a fraction of the systemically available monosulfates was calculated after IG dosing as 12.9% (of the combined monosulfate AUC_{all}). The occurrence of resveratrol in the plasma indicates that resveratrol conversion may occur from the metabolites *in vivo*, and at measurable levels in plasma. The presence of resveratrol and additional metabolites in the systemic circulation suggests that deconjugation of the sulfate, and reconjugation can occur to form new metabolites. This is discussed in more detail in relation to resveratrol tissue concentrations below.

The analysis of tissues following sulfate dosing showed that the same metabolites were present as those found in plasma. The C_{max} concentrations in the mucosa were drastically higher after IG dosing (as opposed to IV) for both monosulfates. The AUC_{all} was ~8-fold and 108-fold greater for resveratrol-3-*O*-sulfate and resveratrol-4'-*O*-sulfate respectively, after the IG dose. After IG administration, the dose (dissolved in saline) enters the stomach, from where it can pass into the small intestine and colon. Of all the tissues analysed, the highest levels of the monosulfates were reached in the mucosal scrapings from these regions, after both dosing routes. These findings are consistent with studies in which the tissue distribution of resveratrol in rodents was determined in rats and mice after oral administration of [^{3}H] and [^{14}C]-resveratrol, respectively [177], [116]. In the rat study, [^{3}H]-resveratrol-derived radioactivity was highest in

the gastrointestinal tract when measured at both post-dosing times of 2 and 18 h [177]. When [^{14}C]-resveratrol was administered, the highest radioactivity levels were detected in the duodenum at all of the time points measured (1.5, 3 and 6 h) [116]. After monosulfate dosing here, the time taken for the sulfates to reach the mucosa was found to be extremely rapid. This was particularly obvious after IG dosing, where the T_{max} was at the earliest sampling time of 5 min, compared to 30 min following IV dosing (for resveratrol-3-*O*-sulfate), and was likely to be due to the direct delivery into the stomach. For IV dosing there would be a time lag associated with distribution and equilibration in different tissue compartments. Interestingly, the mucosa was also shown to have high concentrations of resveratrol-3-*O*-glucuronide (at 2 h and 6 h after IG dosing), and additional metabolites formed were resveratrol disulfate and resveratrol sulfate glucuronide. The 3-*O*-glucuronide concentrations at these time points might suggest that their presence is related to hepatic metabolism rather than localised enzyme activity alone. When resveratrol was administered orally to rats at a dose of 60 mg/kg daily, the glucuronide and sulfate metabolites were minor, reaching 3.40 ± 1.29 nmol/g and 0.44 ± 0.23 nmol/g respectively in the colon 24 h after the final (49th) dose [146]. The specific glucuronide isomer was not identified, but is most likely to have been resveratrol-3-*O*-glucuronide as this has been the major glucuronide detected in rodent studies following resveratrol dosing [71], [137]. In a very recent investigation, the enzyme kinetic profiles of the formation of resveratrol-3-*O*-glucuronide and resveratrol-4'-*O*-glucuronide by liver microsomes from humans, dogs and rodents were compared. In mouse and rat liver microsomes, resveratrol was almost exclusively conjugated to form the 3-*O*-glucuronide, whereas human and dog livers also glucuronidated resveratrol at the 4' position (in a 5:1 ratio for the respective glucuronides) [178]. In the study by Alfaras *et al*. above, the most abundant metabolite found in the rat colon was dihydroresveratrol (303 ± 35 nmol/g) followed by the glucuronide [146]; in the present study however, dihydroresveratrol was not detected, possibly because the method was not optimised for its detection.

The high glucuronide concentrations in the mucosa after IG sulfate dosing here, indicates the importance of the gastrointestinal tract in the accumulation of this metabolite. Glucuronide formation in the mucosa is also likely to be due to the action of deconjugating enzymes on the

sulfates, followed by glucuronidation. Higher concentrations of this metabolite were detected in the colon compared to the plasma. Enterohepatic circulation may also have a role in the redelivery of metabolites to the mucosa where they can undergo deconjugation to parent resveratrol and reconjugation. Resveratrol absorption and metabolism has been investigated in the jejunum in an isolated rat small intestine model [151]. Only small amounts of resveratrol were absorbed across the jejunum and ileum unmetabolised and the major compound detected on the serosal side was the glucuronide conjugate. The processes that take place in the intestine have been investigated in a separate study, also using intestinal perfusion models [170]. Specifically, the role of ATP-binding cassette transporters MRP2 and BCRP (located in the apical membranes of enterocytes), in the secretion of the glucuronide and sulfate metabolites was investigated using specific inhibitors [170]. The jejunum was perfused with resveratrol in the presence, or absence of the ATPase inhibitor, dinitrophenol. Although the absorption of resveratrol did not change, the efflux rates of intracellularly formed glucuronide and sulfate were significantly inhibited by 51% and 44% respectively. Piperine, which modifies the rate of glucuronidation by lowering the endogenous UDP-glucuronic acid content, and by inhibiting transferase activity, also reduced the amount of the glucuronide secreted back to the intestinal lumen, but not the sulfate or resveratrol [170]. These data confirm the involvement of an ATP-dependent transporter in the efflux of resveratrol metabolites, but not resveratrol itself. When the bioavailability of resveratrol was assessed in a rat perfusion model, absorbed resveratrol was conjugated yielding resveratrol glucuronide, which was also found to be the main luminal metabolite [179]. The importance of metabolite efflux of the conjugates has also been proven using transgenic knockout mice (BCRP1$^{-/-}$ and MRP3$^{-/-}$). When BCRP1$^{-/-}$ mice were given resveratrol orally, the contents of the intestine showed reductions of 71% and 97% of glucuronide and sulfate respectively relative to wild-type mice, and plasma AUC of metabolites increased, consistent with a lower efflux from enterocytes [180]. These results indicate that BCRP1 is predominantly responsible for intestinal excretion of sulfates, and to a lesser extent the glucuronides. In mice lacking MRP3, there was a 10-fold lower plasma level of resveratrol-3-*O*-glucuronide compared to concentrations in control mice, and this was accompanied by a similar reduction in urinary excretion [181]. The expression of transporters along the length of the intestine in mice has been shown to vary. Following incubation of the

intestine with parent 4-methylumbelliferone, the efflux rates of its metabolite conjugate were followed, and its extrusion to the serosal side was found to be greatest in the duodenum, which gradually decreased to the distal segment in wild-type mice [182]. The presence of both UDP-glucuronosyltransferases and sulfotransferases also in the intestine of mice, have been shown to be region specific [183]. These studies all support the role of specific metabolite transporters in the gastrointestinal tract, which affect the bioavailability, tissue distribution and elimination of resveratrol and its metabolites.

The specific tissues analysed following resveratrol sulfate dosing were selected to allow determination of concentrations in internal tissues distant from the GI tract, which is the major site of absorption. The liver was analysed as it has an important role in metabolism. There is some evidence to suggest that resveratrol has growth-inhibitory efficacy against pancreatic cells, and the pancreas may therefore be an important target for chemoprevention. In liver tissue following sulfate dosing, the AUC values for the monosulfates were above those in any other tissue, with the exception of the mucosa. This is similar to findings in mice fed with oral doses of resveratrol, in which the AUC (determined by HPLC analysis) was highest in intestinal and colonic mucosa followed by the liver [155]. Autoradiography of mice that received [^{14}C]-resveratrol revealed that the liver had some of the highest deposition of [^{14}C] [116]. In the present monosulfate dosing study, after the IG dose, resveratrol-3-*O*-sulfate in the liver accounted for 17.3% of the tissue (AUC) levels, with the majority found in the mucosa (80.2%). By comparison, there was a minimal accumulation of resveratrol-4'-*O*-sulfate in the liver (0.7%), and most of the tissue dose was present in the mucosa (96.8%). This suggests the liver may play only a minor role in the conversion/detoxification of resveratrol-4'-*O*-sulfate.

After the sulfate dosing in mice, the liver monosulfate concentrations were higher after the IG route. Metabolites detected in this tissue were the sulfate glucuronides, resveratrol disulfate and resveratrol-3-*O*-glucuronide. In studies where resveratrol has been administered to rodents, sulfate and glucuronide metabolites have been present in liver, with levels above those for other organs analysed [177], [155], [132], [71]. The specific metabolite isomers were not assigned in all but the latter study [71], where the two monosulfate isomers and resveratrol-3-*O*-

glucuronide were identified. However, resveratrol disulfate and resveratrol sulfate glucuronides were not detected, although they were after monosulfate dosing in the present investigation. The variable metabolite profiles might be related to differences in metabolism of the mixture of sulfates compared to resveratrol, or in the methods of extraction and/or chromatographic conditions used.

Like the intestine, the liver has been shown to be a site where there is a high level of enzyme activity and extensive metabolism can occur [139]. Resveratrol itself was detected in both locations after monosulfate dosing by IV, with AUC_{all} values of 6.5 and 4.0 nmol/g/h for mucosa and liver respectively. The respective figures after IG dosing in mucosa and liver were 82.1 and 36.3 nmol/g/h, and were the highest across all of the tissues analysed. The resveratrol AUC_{all} in liver following IG dosing (36.3 nmol/g/h) exceeded that of resveratrol-4'-*O*-sulfate in the same tissue (2.3 nmol/g/h), indicating a much greater presence. Resveratrol was also detected in lung and pancreas, following both dosing routes, although the AUC could not be calculated after the IV route because concentrations were too low. Of the total resveratrol tissue distribution (AUC), the amount in mucosa accounted for 68%, liver 30% and lung and pancreas 1.1% and 1.6% respectively. The fraction of resveratrol from the total observed monosulfates AUC_{all} was also calculated for each tissue after IG dosing. The percentage of resveratrol in the lung, mucosa and pancreas ranged from 3.4 - 3.9%, whereas in the liver, resveratrol accounted for 7.9% of the total AUC_{all} of the sulfates, suggesting a higher degree of sulfate deconjugation.

Resveratrol could reach the tissues either systemically or through a localised conversion by sulfatase enzymes, or a combination of the two. Based on the percentage of resveratrol (as a fraction of the tissue sulfate AUC), the amount in the liver (7.9%) was more than in the other tissues, which might indicate a local conversion, like that seen with oestrone sulfate. The oestrone sulfatase enzyme appears to be the enzyme primarily responsible for intra-tissue oestrone production in hormone-dependent breast carcinomas [184]. It is possible that the resveratrol concentrations observed are affected by expression of the sulfatases, which may vary in different organs and locations within the body. The gastrointestinal tract, liver and

kidneys possess high levels of phase II metabolising activities [185] including sulfatases, which is consistent with this finding.

From the mucosa, absorption may occur across the gut barrier into the bloodstream. Sulfate metabolites can be subjected to phase II metabolism with further conversions occurring in the liver where enterohepatic recirculation and transport in the bile may result in some recycling back to the small intestine [186]. Therefore, it is possible that the sulfate metabolites administered may undergo a small amount of conversion to resveratrol, which then becomes sulfated/glucuronidated, and is once again deconjugated to the parent. Hence, resveratrol formation in this way may follow a cyclic process, which allows the effects of resveratrol to be sustained over a longer period of time than previously thought. The data from this study supports a role for resveratrol sulfates contributing to the amount of resveratrol within tissues, which may result in an increase in efficacy due to resveratrol formation. Therefore, in studies where the resveratrol tissue concentrations have been determined, at least some of the observed resveratrol may be derived from metabolites. Resveratrol was shown to be present in the plasma, mucosa, and liver and to a lesser extent, the lung and pancreas in this study. At the low concentrations of resveratrol observed in the lung and pancreas following the oral dose of resveratrol sulfates, quantities may still be sufficient to exert beneficial effects, caused by subtle changes at the cellular level. For example, unpublished data from our research group show that resveratrol administration to mice at a dose of 0.07 mg/kg body weight can significantly alter 5′-AMP-activated protein kinase (AMPK) levels, which has been linked to the growth and/or survival of some cancer cells [187].

In previous studies, the urine from rats has been analysed for metabolite and resveratrol determination following a resveratrol-rich diet containing 50 mg and 300 mg of resveratrol per kg body weight per day for eight weeks [71]. Resveratrol was identified in urine from both, although levels were lower at the 50 mg dose level. Metabolites identified were resveratrol-3-*O*-sulfate (but not resveratrol-4'-*O*-sulfate), resveratrol disulfate, resveratrol-3-*O*-glucuronide and resveratrol trisulfate. In this monosulfate study, despite the large quantities administered and recovered in the urine, there was no resveratrol present, nor was it detected by LC-MS/MS after

either route of administration. Resveratrol trisulfate was also not detected. Urine is a major excretory route for resveratrol metabolites, although very little unchanged resveratrol is excreted via the urine. [188]

The earlier mentioned study by Asensi *et al*., which focussed on the bioavailability of resveratrol after oral dosing, used a sulfate donor 3′-phosphoadenosine-5′-phosphosulfate-[^{35}S] to label resveratrol sulfate [156]. This was isolated and identified using LC-MS/MS and *in vitro* synthesised [^{35}S]-labelled resveratrol sulfate was administered intraportally to rats and the radioactive elimination followed in the urine. A large proportion of the radioactivity was recovered in the 24 h urine of the rats (73 ± 9%); however resveratrol sulfate was not detected by LC-MS/MS. The authors suggested that sulfatase activity had degraded the conjugate [156].

A resveratrol metabolite, dihydroresveratrol can be formed by the hydrogenation of the aliphatic double bond of resveratrol by intestinal flora. It has been suggested to be a major metabolite, and has been identified in rat [126], [189] and human urine [104] after resveratrol dosing. Dihydroresveratrol sulfates were also recovered in the urine of both species. Neither metabolites were detected in the mouse urine, or other plasma/tissue samples in the present study; however the method was not optimised for its detection (as discussed in Chapter 3) and appropriate transitions were not monitored by LC-MS/MS. It has been reported that the reduced metabolite loses its UV absorption properties at 306 nm, the optimum wavelength used for resveratrol detection, thus it was only by LC-MS/MS that it could be recognised as accounting for an appreciable fraction of the dose [104]. A method of analysis of dihydroresveratrol in rat plasma was developed and validated to allow quantitation after oral administration of 60 mg/kg dihydroresveratrol to Sprague-Dawley rats [164]. Dihydroresveratrol was extensively metabolised, and 30 min after its administration, the concentrations of its glucuronide and sulfate conjugates were 38- and 6-fold higher respectively than the parent.

One of the limitations of this study is that the sulfates were given as a mixture, and therefore it is not possible to identify which metabolite is responsible for conversion to resveratrol. It may be that there is a preferential conversion of one metabolite over the other. However, the fact that

there is more of the resveratrol-3-*O*-sulfate present suggests that it is likely to occur with this metabolite. The presence of sulfates and resveratrol in all of the tissues provides evidence that they are all sites where the sulfates can potentially exert their effects, or at least act as a source for resveratrol generation. In the mucosa and liver tissues where the highest resveratrol levels were found, there was a continuous exposure over at least 6 hours. Therefore, resveratrol may undergo repeated conjugation and deconjugation, thereby prolonging its beneficial activity at these sites within the body. Although this has not been demonstrated previously with resveratrol *in vivo*, there is evidence to suggest that this type of cycling can occur with oestrogen sulfatase in human breast carcinoma [184]. As part of further investigations, a useful additional experiment would be to do the same dosing with resveratrol glucuronide to allow determination of its bioavailability and tissue distribution. In order to evaluate the role of metabolites in the regeneration of resveratrol further, it would be interesting to determine whether the glucuronides can also undergo deconjugation liberating resveratrol and if so, whether this follows the same pattern as seen with the sulfates. If conversion is under the influence of sulfatases for the sulfates, differences in the glucuronidase enzyme expression could result in an altered resveratrol tissue distribution to that seen after sulfate administration. The bioavailability and tissue distribution of resveratrol and its metabolites is the result of a complex interaction of transporters and enzyme activities in the different tissues and requires further investigation.

CHAPTER 5: ACTIVITY, UPTAKE AND METABOLISM OF RESVERATROL METABOLITES AND RESVERATROL IN COLON CELLS

5.1 Introduction

Resveratrol has been the focus of extensive *in vitro* investigation in recent years for its beneficial properties, including its potential as a cancer chemopreventive agent. It may have the ability to delay or reverse the onset of cancer [77], and as a natural compound present in the diet, this makes it a prime candidate for evaluation. A comprehensive list of the studies on resveratrol over the past few decades has been compiled [101]. The variety of biological and pharmacological activities outlined in this review [101], occur despite the low systemic bioavailability [156], [104] and rapid clearance of resveratrol, due to extensive sulfation and glucuronidation in the liver and intestine [134]. However, in contrast to parent resveratrol, there has only been a limited amount of information published on resveratrol metabolites, despite their prevalence both in rodent models and humans in *vivo*. It is possible that resveratrol metabolites may themselves possess useful chemopreventive properties, which warrants further study.

This part of the investigation aimed firstly to determine whether resveratrol metabolites, specifically resveratrol monosulfates and monoglucuronides have any growth inhibitory properties in colorectal cancer cell lines by measuring cell proliferation, and secondly to explain any potential changes. To achieve this, the cellular uptake and metabolism of monosulfate metabolites and resveratrol were investigated in cells and in media following incubation with the compounds. Intracellular monosulfate and resveratrol concentrations were measured in two malignant and one non-malignant colon epithelial cell line; HCA-7, HT-29 and HCEC respectively. Another aim was to establish if conversion of the sulfate metabolites to parent resveratrol could occur in cells, as this may be responsible for any potential reduction in cancer cell proliferation. In addition, cell cycle analysis, apoptosis and caspase-3 assays were completed as part of further investigation. To our knowledge, the effects of resveratrol metabolites have not been assessed in the cell lines used here.

5.2 Effect of resveratrol monosulfates on cell proliferation

5.2.1 Cell growth curves

Cell proliferation assays can be used to evaluate proliferation and cytotoxicity of cultured mammalian cells. One of the assays available for measuring this is the ATPLite™ assay, which provides an indirect measure of viable cells by measuring the emitted light following reaction of adenosine triphosphate (ATP) with D-luciferin. The emitted light is proportional to the amount of ATP, which is present in all metabolically active cells. A more direct, but lengthier approach is to count the number of live cells following treatment using a coulter counter. Both methods were tested, however the ATPLite™ assay was found to be unsuitable for the compounds being evaluated since resveratrol and its sulfate metabolites caused interference by reducing the amount of light emitted. Resveratrol has been reported to potently inhibit firefly luciferase activity [190]. Therefore, direct cell counting was used throughout.

Colorectal HCA-7, HT-29 and HCEC cells were treated with varying concentrations of a mixture of resveratrol-3-*O*-sulfate and resveratrol-4'-*O*-sulfate (3: 2 ratio), and one concentration of resveratrol (10 µM) as a positive control, in order to assess their potential anti-proliferative effects. Concentrations of sulfates (25 - 250 µM) and resveratrol tested were based on levels reached in the human colon after ingestion of resveratrol, as described in Chapter 3.

5.2.2 Proliferation of HCA-7 cells

The concentration-dependent change in HCA-7 cell number following resveratrol monosulfate exposure is illustrated (Figure 5.1A). There was a general increase in cell number for all treatment groups over the course of seven days. However, greater monosulfate concentrations resulted in a bigger reduction in cell number relative to control cells incubated with vehicle only. This was most pronounced with the highest concentration of resveratrol monosulfates (250 µM). This exposure caused a comparable reduction in cell number as 10 µM of resveratrol.

The differences in cell number relative to solvent treated control samples were calculated as percentage change on day three and day seven, (Figure 5.1B and Figure 5.1C respectively). On day three, all treatments caused a reduction in the number of cells present. With the exception of 25 µM, the lowest concentration of monosulfates, this was significant for all treatment groups *(P ≤ 0.0005)*. When cells were counted after seven days post-treatment, all groups remained significantly different to the control *(P ≤ 0.0005)*, including the 25 µM incubation which also now contained significantly lower cell numbers. In this particular cell line resveratrol caused the biggest reduction in proliferation over the concentration ranges examined, with just 28 ± 4.5% cells remaining at day 7 relative to control cell counts. The percentage change in cell number at each concentration was used to create a line of best fit (data not shown). This allowed the IC_{50} value for the monosulfates in HCA-7 cells to be determined, which was 131 ± 10.2 µM on day seven (mean ± SD; n = 3 experiments in triplicate).

5.2.3 Proliferation of HT-29 cells

Proliferation of HT-29 cells following resveratrol monosulfate treatment was assessed in exactly the same way as described above (Section 5.2.2). As the concentration of monosulfates in the media increased, there was a corresponding reduction in cell number (Figure 5.2A). The highest monosulfate concentration (250 µM) caused an almost total inhibition of cell growth; however, there was still a small increase in cell number observed over the course of the week. On day three post-treatment (Figure 5.2B), the reduction in cell number compared to control incubation was significant for all of the treatment groups *(P ≤ 0.0005)*, but slightly less so following treatment with 25 µM of monosulfates *(P = 0.031)*.

On day seven (Figure 5.2C), 250 µM of monosulfates caused a large reduction in cell proliferation, with 6.5 ± 2.9% of cells remaining relative to control cells. Resveratrol (10 µM) did not have as strong an effect as it did in HCA-7 cells, only causing an equivalent reduction in proliferation to monosulfates between the range of 25 - 50 µM. Differences in cell numbers

observed between control and treatment groups were all significant on day seven *(P ≤ 0.0005)* with the exception of 25 µM monosulfates. The IC_{50} for the mixture of monosulfates in the HT-29 cell line was calculated to be 67.8 ± 8.4 µM on day seven post-treatment, indicating these cells are more sensitive than the HCA-7 cell line to resveratrol sulfates.

5.2.4 Proliferation of HCEC cells

Resveratrol sulfates were also tested in the HCEC cell line. Figure 5.3A shows a representative growth curve following resveratrol monosulfate and resveratrol dosing in HCEC cells. None of the monosulfate concentrations used had a significant effect on the number of cells present. However, when treated with 10 µM of resveratrol there was a highly significant reduction on both day three and day seven *(P ≤ 0.0005*, Figure 5.3B and Figure 5.3C respectively*)*; the number of cells remaining on these days was 74.6 ± 4.4% and 67.8 ± 9.3% respectively, relative to control cells (100%). No IC_{50} values for the monosulfates could be calculated over the concentration range tested because of the lack of activity.

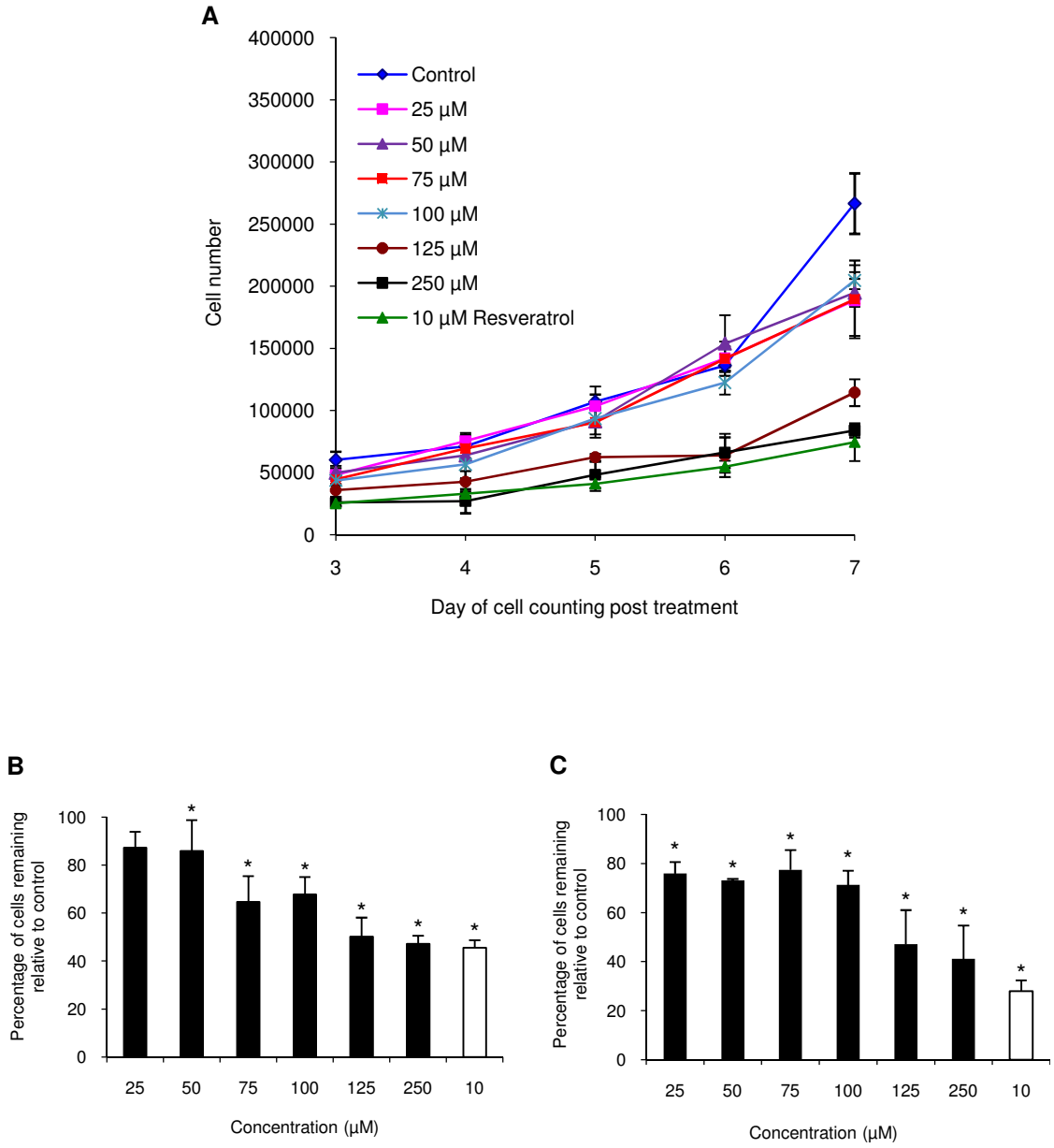

Figure 5.1 Change in HCA-7 cell proliferation following treatment with resveratrol monosulfates and resveratrol

Typical dose response curve of HCA-7 cells following treatment with a mixture of resveratrol-3-*O*-sulfate and resveratrol-4'-*O*-sulfate (3: 2). Resveratrol (10 µM) and DMSO vehicle (0.1% volume) served as positive and negative controls respectively. Data are the mean ± SD for one experiment in triplicate (**A**). Percentage of HCA-7 cells remaining relative to control cells (set as 100%) following resveratrol monosulfate (black bars) or resveratrol treatment (10 µM, clear bars) after three days (**B**) and seven days (**C**). Data for (**B**) and (**C**) are the mean + SD for three independent experiments performed in triplicate. *$P \leq 0.0005$ for all treatment groups on day three and day seven, with the exception of 25 µM on day three *($P = 0.069$)*, compared to control (One-Way ANOVA). The IC_{50} on day seven was 131.6 ± 10.2 µM.

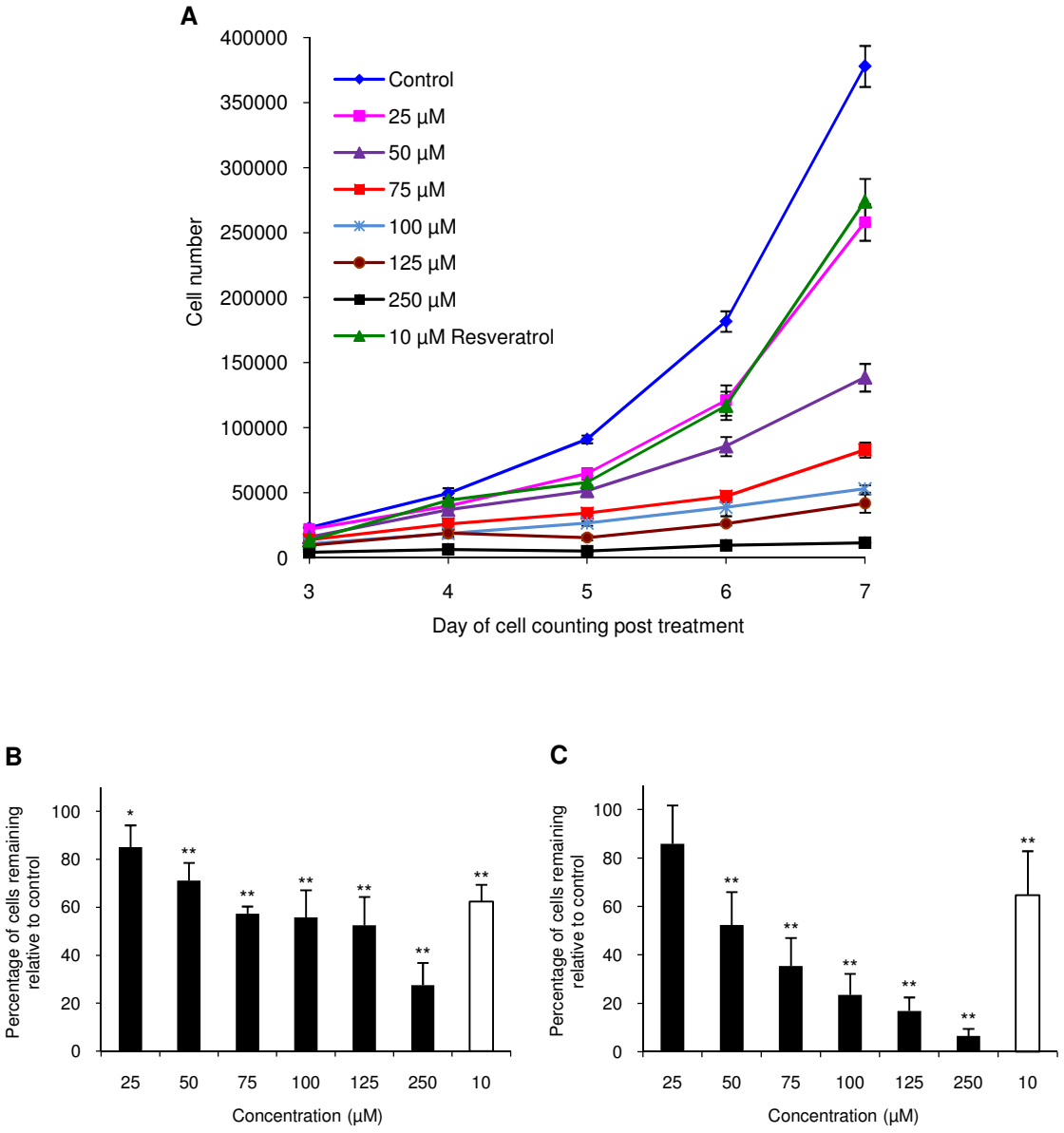

Figure 5.2 Change in HT-29 cell proliferation following treatment with resveratrol monosulfates and resveratrol

Typical dose response curve of HT-29 cells following treatment with a mixture of resveratrol-3-*O*-sulfate and resveratrol-4'-*O*-sulfate (3: 2). Resveratrol (10 µM) and DMSO vehicle (0.1% volume) served as positive and negative controls respectively. Data are the mean ± SD for one experiment in triplicate (**A**). Percentage of HT-29 cells remaining relative to control cells (set as 100%) following resveratrol monosulfate (black bars) or resveratrol treatment (10 µM, clear bars) after three days (**B**) and seven days (**C**). Data for (**B**) and (**C**) are the mean + SD for three independent experiments performed in triplicate. $*P < 0.05$ and $**P \leq 0.0005$ compared to control (One-Way ANOVA). The IC_{50} on day seven was 67.8 ± 8.4 µM.

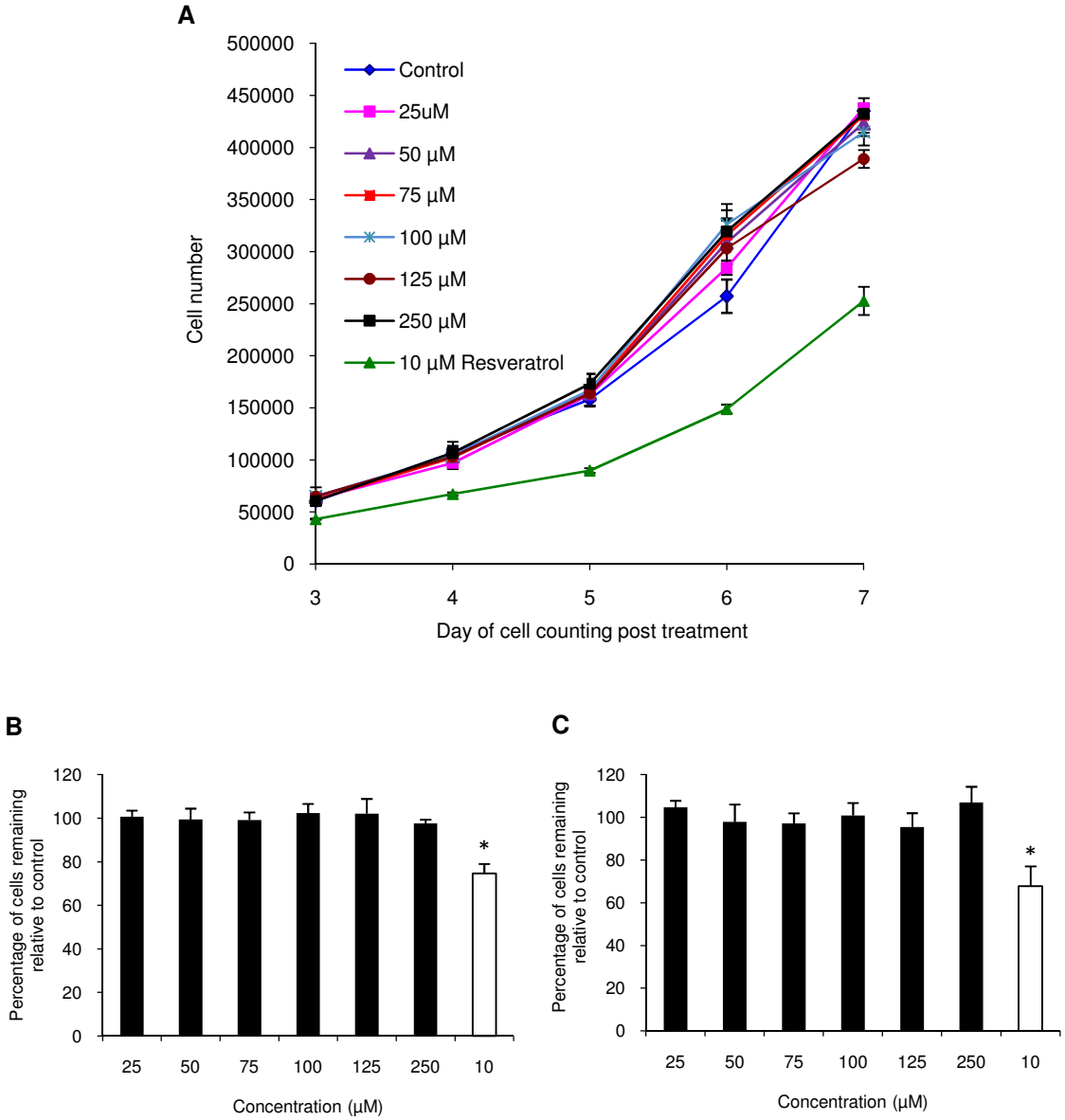

Figure 5.3 Change in HCEC cell proliferation following treatment with resveratrol monosulfates and resveratrol

Typical dose response curve of HCEC cells following treatment with a mixture of resveratrol-3-*O*-sulfate and resveratrol-4'-*O*-sulfate (3: 2). Resveratrol (10 µM) and DMSO vehicle (0.1% volume) served as positive and negative controls respectively. Data are the mean ± SD for one experiment in triplicate (**A**). Percentage of HCEC cells remaining relative to control cells (set as 100%) following resveratrol monosulfate (black bars) or resveratrol treatment (10 µM, clear bars) after three days (**B**) and seven days (**C**). Data for (**B**) and (**C**) are the mean + SD for three independent experiments performed in triplicate. *$P \leq 0.0005$ for 10 µM resveratrol compared to control on day three and day seven (One-Way ANOVA). The IC_{50} could not be calculated due to lack of effect over the concentration range examined.

5.3 Effect of resveratrol glucuronides on cell proliferation

5.3.1 Proliferation of HCA-7 and HT-29 cells following incubation with resveratrol-3-*O*-glucuronide

Two resveratrol glucuronide isomers were also screened for their ability to inhibit cancer cell growth, using the cell proliferation assay. The effects of resveratrol-3-*O*-glucuronide and resveratrol-4'-*O*-glucuronide on HCA-7 and HT-29 cell numbers was measured on day three and day seven post-treatment. A full dose response curve was not completed due to the limited amount of the synthesised standards available.

On day three post-treatment with resveratrol-3-*O*-glucuronide there was a significant reduction in HCA-7 cell numbers relative to control with glucuronide concentrations of 100 µM and above (Figure 5.4A). However, the highest glucuronide concentration did not have the same magnitude of an effect as 10 µM of resveratrol (with approximately 75% and 54% of cells remaining relative to control following the respective treatments). On day seven post-treatment, none of the glucuronide exposures caused a significant change in cell number relative to control. Cells incubated with resveratrol remained significantly different, with a 56.6 ± 9.6% reduction in cell number compared to control cells (Figure 5.4B).

In HT-29 cells on day three post-treatment, resveratrol-3-*O*-glucuronide caused a significant reduction in cell number for all treatment groups, with the exception of 25 and 50 µM (Figure 5.4C). The reduction in cell number following 250 µM of the 3-*O*-glucuronide was approximately 20% compared to untreated cells. On day seven the reduction in cell numbers was no longer significant for any of the glucuronide concentrations tested, apart from 250 µM which reduced numbers by only ~10% (Figure 5.4D); this reduction was less significant and less marked than with 10 µM resveratrol, which decreased cell numbers by approximately 25%.

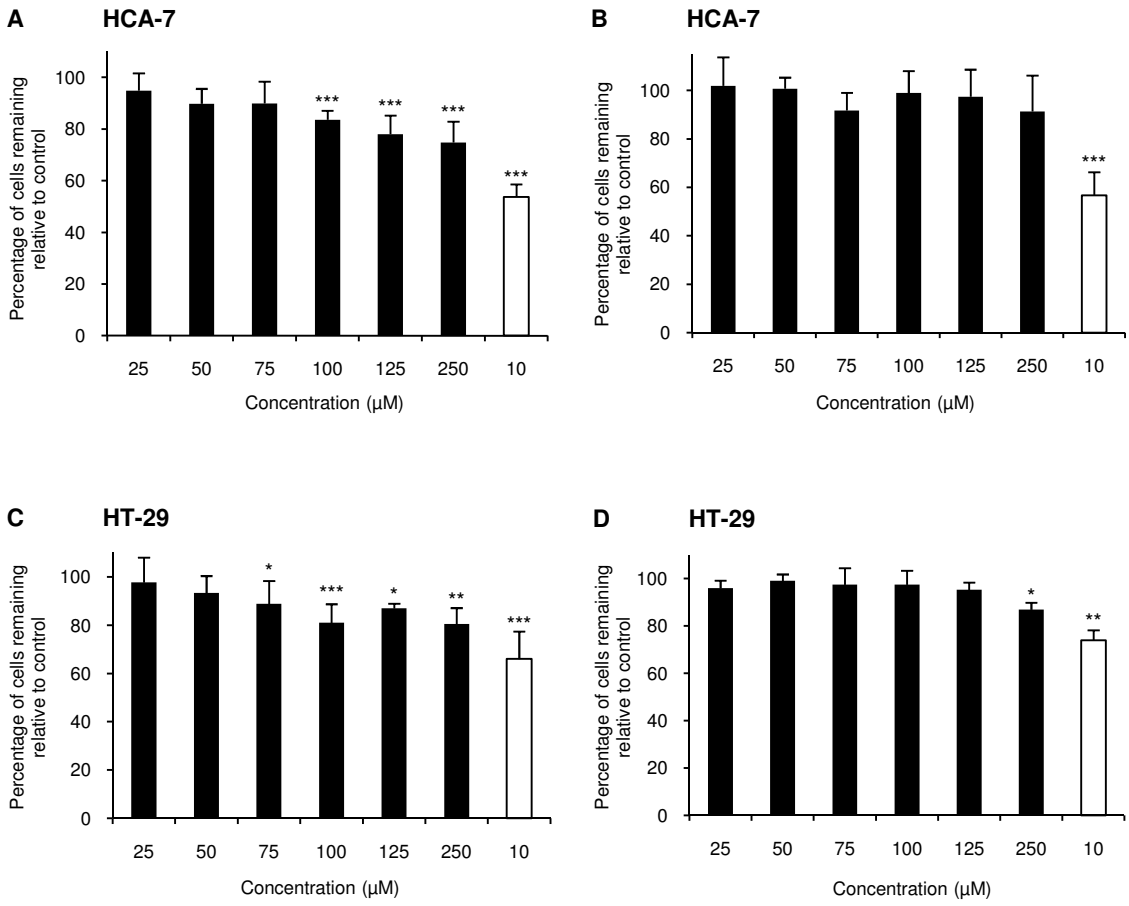

Figure 5.4 Change in HCA-7 and HT-29 cell proliferation following treatment with resveratrol-3-*O*-glucuronide and resveratrol

Percentage of HCA-7 cells remaining relative to control cells following treatment with resveratrol-3-*O*-glucuronide, or resveratrol (10 μM) after three days (**A**) and seven days (**B**). Change in cell proliferation in HT-29 cells following the same treatments after three days (**C**) and seven days (**D**) is also shown. Data are the mean + SD shown for three independent experiments performed in triplicate. *$P \leq 0.05$, **$P \leq 0.005$ and ***$P \leq 0.0005$ compared to control (One-Way ANOVA).

5.3.2 Proliferation of HCA-7 and HT-29 cells following incubation with resveratrol-4'-*O*-glucuronide

Resveratrol-4'-*O*-glucuronide was not found to cause a significant reduction in the number of HCA-7 cells relative to control on either day three (Figure 5.5A) or day seven post-treatment (Figure 5.5B) for any of the treatment groups. As observed previously, resveratrol treatment caused a significant reduction *($P \leq 0.05$)* on both days, with 60.8 ± 8.5 and 52.7 ± 4.7% cells remaining relative to control.

In HT-29 cells exposed to resveratrol-4'-*O*-glucuronide, 100 and 125 µM (but not 250 µM) caused a significant reduction in cell number relative to control cells on day three post-treatment (Figure 5.5C). After seven days of treatment, these groups were no longer significantly different to control (Figure 5.5D). The only group to reach significance was the 250 µM glucuronide treatment group.

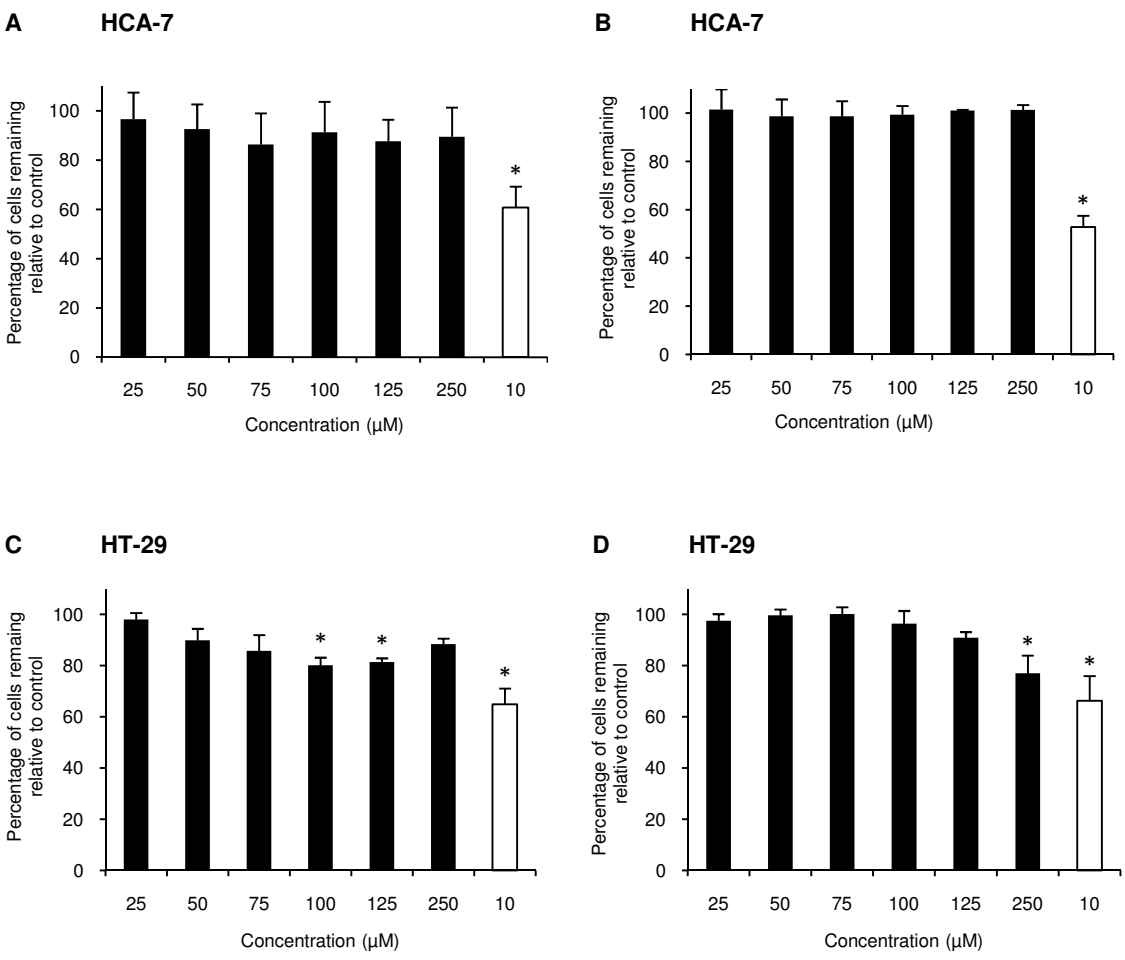

Figure 5.5 Change in HCA-7 and HT-29 cell proliferation following treatment with resveratrol-4'-*O*-glucuronide and resveratrol

Percentage of HCA-7 cells remaining relative to control cells following treatment with resveratrol-4'-*O*-glucuronide, or resveratrol (10 μM) after three days (**A**) and seven days (**B**). Change in cell proliferation in HT-29 cells following the same treatments after three days (**C**) and seven days (**D**) is also shown. Data are the mean + SD shown for three independent experiments performed in triplicate. *$P \leq 0.0005$, compared to control (One-Way ANOVA).

5.4 Uptake and metabolism of resveratrol monosulfates and resveratrol in cells

Unlike the resveratrol glucuronides which caused little or no effect on proliferation with significant reductions of less than 20% only apparent at concentrations of 75 µM and above, the resveratrol sulfates had a more pronounced effect on cell proliferation. Therefore, further studies focussed on the mixture of sulfate metabolites only.

There was a differential response in proliferation in the cell lines treated with sulfates, with reduced proliferative capacity in the HT-29 and HCA-7 cell lines only. In contrast, incubation with resveratrol caused a reduction in cell number in all three cell lines. Differences in cellular uptake, and metabolism were examined as possible explanations for the cell specific responses observed. The mixture of resveratrol sulfates was incubated with each of the cell types (in phenol free media to prevent interfering phenol peaks during HPLC-UV analysis), and aliquots of media were collected at various timepoints, up to seven days post-incubation (Section 2.2.6.6.1). Cell pellets were also harvested for determination of intracellular monosulfate concentrations and to examine whether conversion of monosulfates to resveratrol was occurring *in vitro*. For comparison, analysis of cell pellets and media was also carried out in the same way following incubation with resveratrol.

Initially, the concentrations of the monosulfates and resveratrol were measured in media in the absence of cells to assess stability over the incubation period of seven days. Authentic standards were not available to quantify all metabolite concentrations, and therefore following incubation of sulfates and resveratrol with cells, the proportions of each metabolite in media and within cells were determined at each timepoint. Concentrations of resveratrol and monosulfates in media and cells were quantified by HPLC-UV, using the respective standard curves for accurate determination (data provided in Section 5.4.2).

5.4.1 Media analysis following incubation of resveratrol monosulfates or resveratrol without cells

The stability of resveratrol monosulfates without cells was measured over the duration of one week using 75 µM of the sulfate mixture, which was similar to the IC_{50} in HT-29 cells (68 µM). The same concentrations were used for cell incubation experiments described in subsequent sections, to allow direct comparisons to be made. Resveratrol (10 µM) was used for cell incubations (as a positive control), and therefore the same concentration was used here. Spiked media was kept in flasks under an atmosphere of 5% CO_2 at 37°C in an incubator under identical conditions to those used for all cell incubations. No change in concentration was observed for resveratrol-3-*O*-sulfate in the media without cells over seven days (Figure 5.6). There was a slight but significant reduction (*P = 0.01*; Student's T-test) in resveratrol-4'-*O*-sulfate over the same duration, from a starting concentration of 20.4 ± 1.1 to 16.4 ± 1.1 µM on day seven, suggesting this may be the less stable of the two isomers. Resveratrol was not detected in the media. When resveratrol (10 µM) was spiked into media without cells, it was either detected at very low levels at 24 h, or not at all (data not presented). No resveratrol was detected on day seven post-incubation.

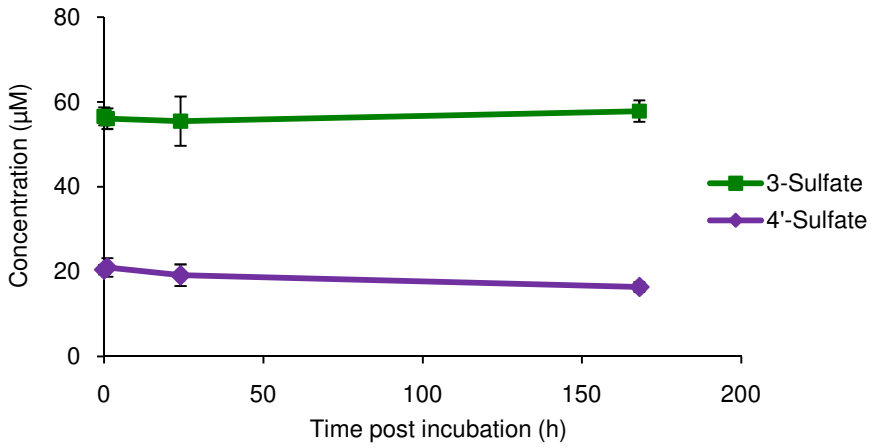

Figure 5.6 Stability of resveratrol monosulfates in media

Concentrations of resveratrol-3-*O*-sulfate and resveratrol-4'-*O*-sulfate detected following incubation of a mixture of monosulfates (75 µM) in media (without cells) maintained under standard conditions at 37ºC over one week. Data points are the mean ± SD shown from three independent experiments.

5.4.1.1 Media analysis following incubation of resveratrol monosulfates or resveratrol with HCA-7 cells

Following incubation of resveratrol monosulfates with HCA-7 cells, media supernatant was analysed by HPLC-UV (Figure 5.7A). There was a steady fall in the amount of resveratrol-3-*O*-sulfate detected in media over the course of seven days, where it initially accounted for 73.8 ± 0.3% of total resveratrol-related species and 36 ± 5% after one week (Figure 5.8). The reduction in resveratrol-4'-*O*-sulfate over the same period was similar to that observed in media without cells (Figure 5.6). Additional metabolites were detected in the media, which became more prominent from 24 h onwards. The proportions of each metabolite including resveratrol (where present), were calculated on day seven. The two monosulfates accounted for 57.8%, and the major metabolite formed from the monosulfates was resveratrol sulfate glucuronide, which reached a maximal concentration on day seven (33.3%), followed by resveratrol disulfate (4.8%), resveratrol-4'-*O*-glucuronide (3.6%) with only minor amounts of resveratrol-3-*O*-glucuronide (0.4%).

When media was spiked with resveratrol in the presence of cells, it was not detectable after 24 h (Figure 5.9). Corresponding with the reduction in resveratrol concentration, there was an increase in the metabolites detected. Resveratrol-4'-*O*-glucuronide was the dominant metabolite (66.5% of total resveratrol species), followed by resveratrol-3-*O*-glucuronide (21.2%) and resveratrol-3-*O*-sulfate (10.2%) at 24 h post-treatment, with broadly similar proportions on day seven. A typical HPLC-UV chromatogram following incubation of HCA-7 cells with resveratrol is illustrated (Figure 5.7D).

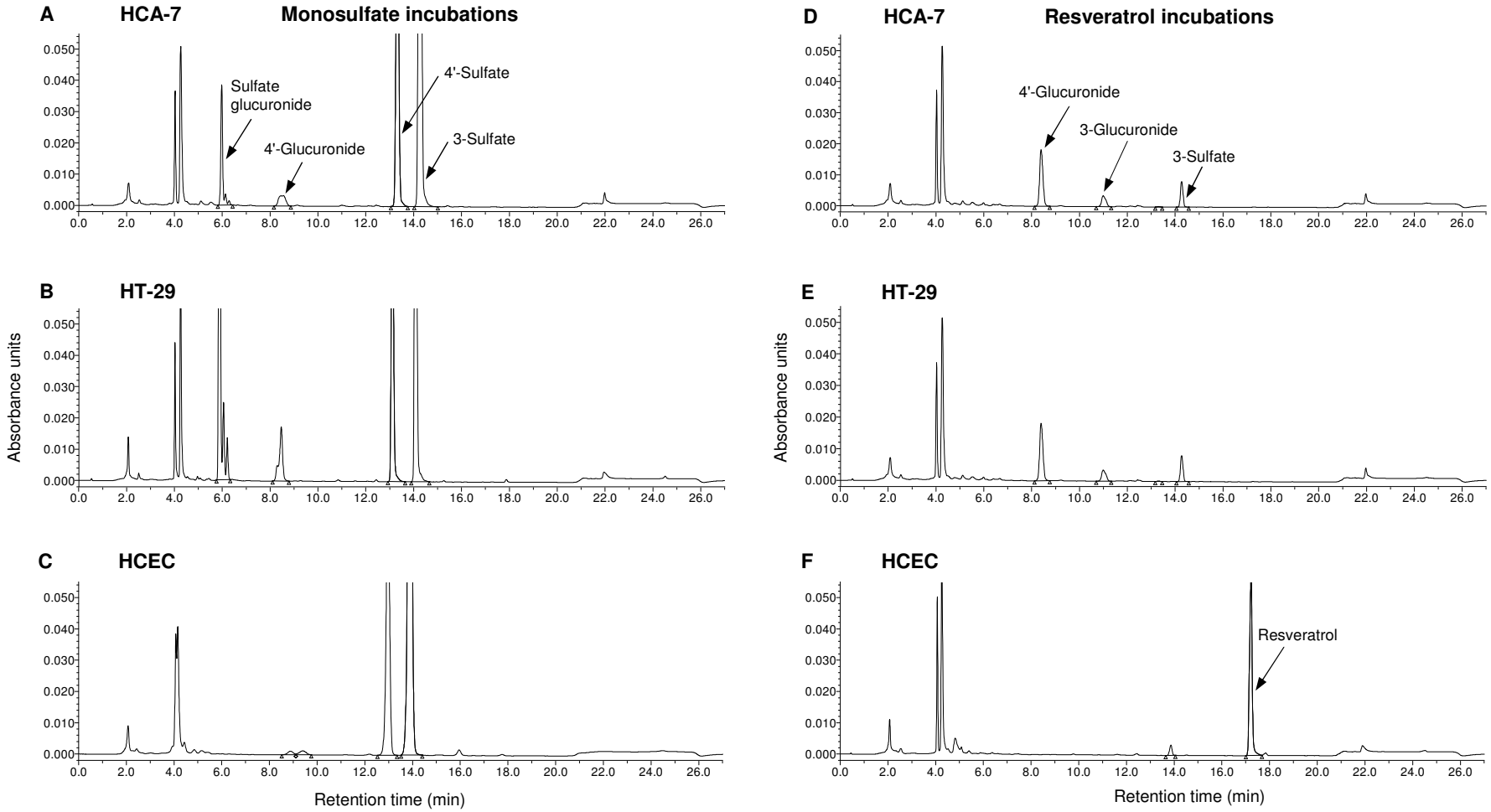

Figure 5.7 Representative media HPLC-UV profiles following cell incubations with resveratrol monosulfates or resveratrol

Representative media HPLC-UV profiles following incubation of a mixture of 75 µM resveratrol-3-*O*-sulfate and resveratrol-4'-*O*-sulfate (3: 2), or resveratrol (10 µM) with HCA-7, HT-29, and HCEC cells for 24 h. (**A**), (**B**) and (**C**) represent monosulfate incubation in HCA-7, HT-29, and HCEC cells respectively. (**D**), (**E**) and (**F**) represent resveratrol incubation in HCA-7, HT-29 and HCEC cells respectively. Note; maximum peak height in Figure (**A**), (**B**) and (**C**) exceeds 0.050 absorbance units due to higher media concentrations.

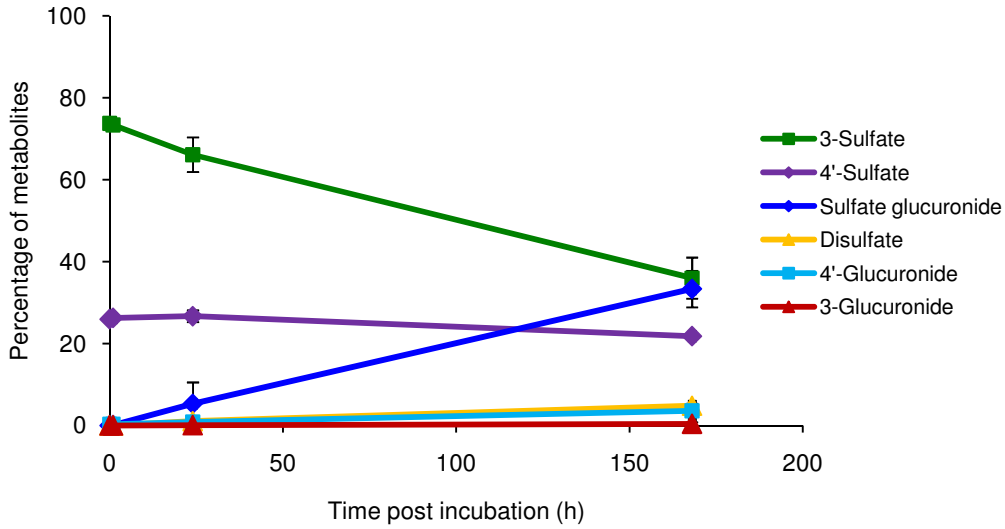

Figure 5.8 Metabolite profile in media following incubation of resveratrol monosulfates with HCA-7 cells

Resveratrol derivatives detected in media following incubation of a mixture of 75 µM resveratrol-3-*O*-sulfate and resveratrol-4'-*O*-sulfate (3: 2) with HCA-7 cells over seven days, expressed as percentage of total resveratrol species per timepoint. Data are the mean ± SD of three independent experiments.

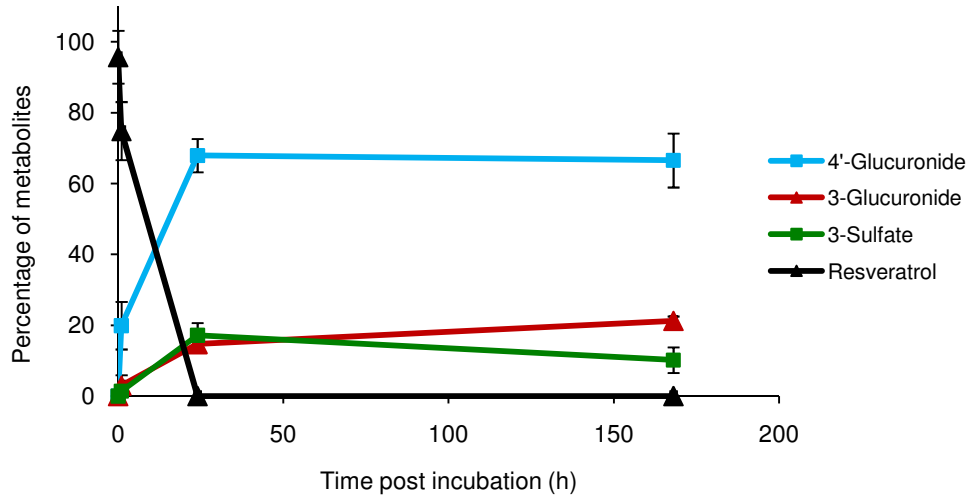

Figure 5.9 Metabolite profile in media following incubation of resveratrol with HCA-7 cells

Resveratrol derivatives detected in media following incubation of 10 µM resveratrol with HCA-7 cells over seven days, expressed as percentage of total resveratrol species per timepoint. Data are the mean ± SD of three independent experiments.

5.4.1.2 Media analysis following incubation of resveratrol monosulfates or resveratrol with HT-29 cells

A similar pattern of metabolism as that seen with HCA-7 cells was observed in media spiked with monosulfates and incubated with HT-29 cells (Figure 5.10). In terms of new resveratrol-related species generated, resveratrol sulfate glucuronide was the most prominent at 24 h (Figure 5.7B), comparable to the proportion of resveratrol-4'-*O*-sulfate remaining in the media (29.9% and 24.6% respectively). However, resveratrol-3-*O*-sulfate was still the most prevalent at this time accounting for 43.0% of all derivatives detected. The 4'-*O*- and 3-*O*-sulfates dropped in concentration over the course of seven days at varying rates, with a much more rapid reduction of resveratrol-3-*O*-sulfate (73.4 ± 0.5% falling to just 3.0 ± 1.6% at the latter time point). In contrast, there was an increase in the formation of resveratrol-3-*O*-glucuronide, resveratrol-4'-*O*-glucuronide and resveratrol disulfate over seven days; these derivatives comprised 0.5%, 3.2% and 7.0% of total resveratrol-related species respectively on day seven, with the sulfate glucuronide accounting for 75% of the total.

Following resveratrol incubation with HT-29 cells, resveratrol disappearance was rapid, with very low levels (less than 0.2%) detected at 24 h (Figure 5.11 and Figure 5.7E). At this timepoint, resveratrol-4'-*O*-glucuronide dominated in the media corresponding up to 75.5% of all resveratrol species followed by resveratrol-3-*O*-glucuronide (13.9%) and resveratrol-3-*O*-sulfate (6.4%). The proportion of glucuronide metabolites remained similar on day seven. The profile was similar to that observed with the HCA-7 cells, with possibly more rapid metabolism occurring in this cell line.

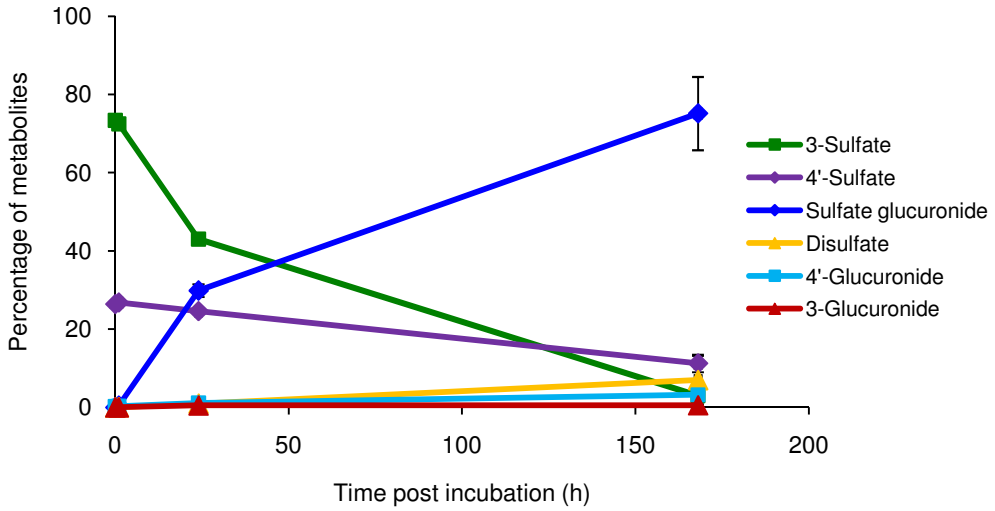

Figure 5.10 Metabolite profile in media following incubation of resveratrol monosulfates with HT-29 cells

Resveratrol derivatives detected in media following incubation of a mixture of 75 µM resveratrol-3-*O*-sulfate and resveratrol-4'-*O*-sulfate (3: 2) with HT-29 cells over seven days, expressed as percentage of total resveratrol species per timepoint. Data are the mean ± SD of three independent experiments.

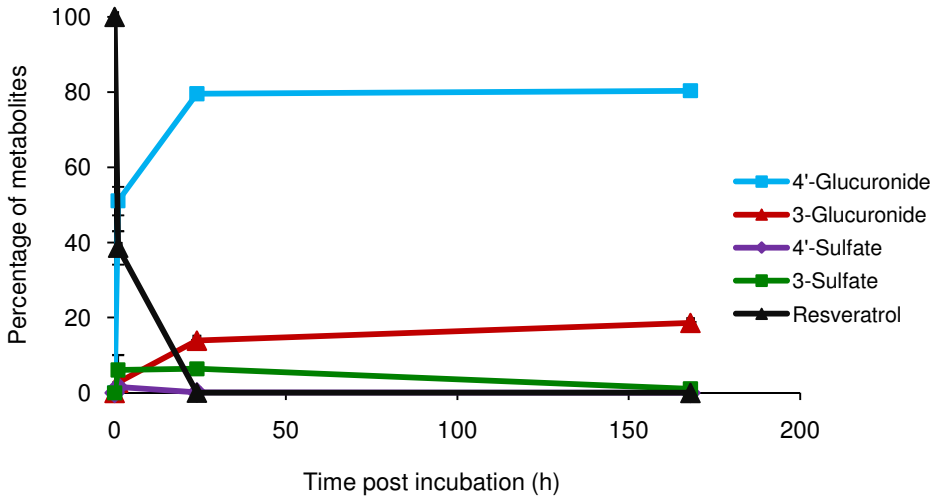

Figure 5.11 Metabolite profile in media following incubation of resveratrol with HT-29 cells

Resveratrol derivatives detected in media following incubation of 10 µM resveratrol with HT-29 cells over seven days, expressed as percentage of total resveratrol species per timepoint. Data are the mean ± SD of three independent experiments.

5.4.1.3 Media analysis following incubation of resveratrol monosulfates or resveratrol with HCEC cells

In media incubated with sulfates and HCEC cells (Figure 5.12), there was no observed reduction in resveratrol-3-*O*-sulfate concentration. With resveratrol-4'-*O*-sulfate, there was a similar amount of loss with and without the presence of cells (Figure 5.6) on day seven (17% compared to 20% respectively). A small amount of resveratrol disulfate was formed in the presence of cells, reaching a maximum of 3.2% of total resveratrol species present on day seven.

There was a much more gradual reduction in the resveratrol concentration following incubation with HCEC cells (Figure 5.13), compared to both HCA-7 and HT-29 cell lines. As the concentration of resveratrol fell, a corresponding increase in the amount of resveratrol-3-*O*-sulfate was detected. Only minor amounts of resveratrol-4'-*O*-sulfate were formed. By day seven only resveratrol-3-*O*-sulfate was present. Typical HPLC-UV chromatograms of media following sulfate and resveratrol incubation are illustrated in Figure 5.7C and F respectively.

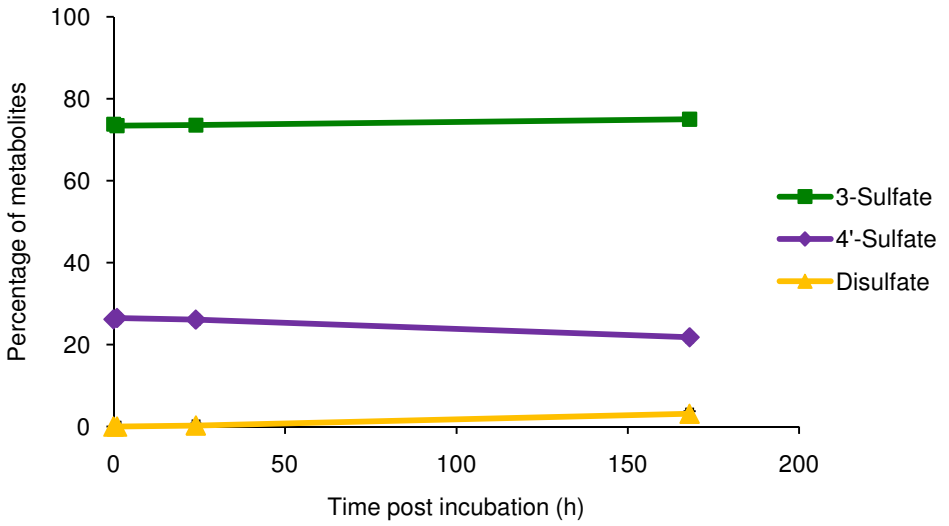

Figure 5.12 Metabolite profile in media following incubation of resveratrol monosulfates with HCEC cells

Resveratrol derivatives detected in media following incubation of a mixture of 75 µM resveratrol-3-*O*-sulfate and resveratrol-4'-*O*-sulfate (3: 2) with HCEC cells over seven days, expressed as percentage of total resveratrol species per timepoint. Data are the mean ± SD of three independent experiments.

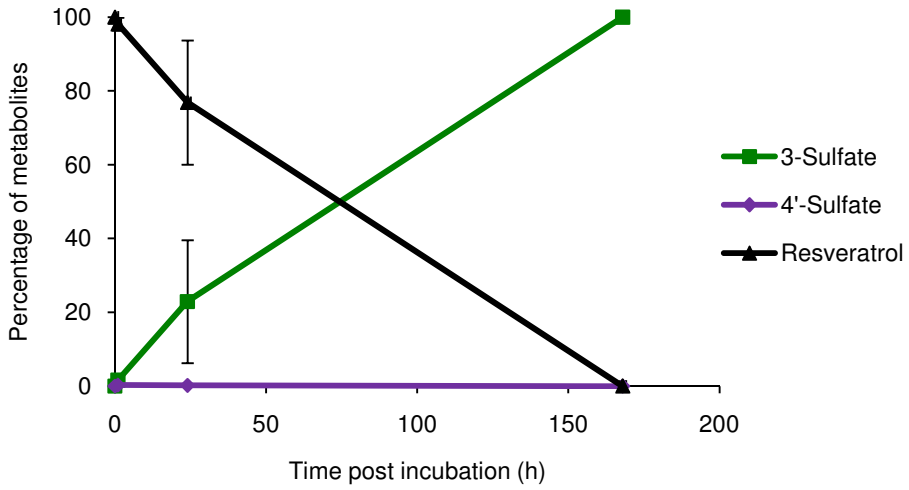

Figure 5.13 Metabolite profile in media following incubation of resveratrol with HCEC cells

Resveratrol derivatives detected in media following incubation of 10 µM resveratrol with HCEC cells over seven days, expressed as percentage of total resveratrol species per timepoint. Data are the mean ± SD of three independent experiments.

5.4.2 Determination of species in media and cells following incubation of HCA-7 cells with resveratrol monosulfates or resveratrol

Following incubation spiked with either resveratrol sulfates, or resveratrol, cells were washed thoroughly, harvested and the pellets lysed and extracted to allow determination of intracellular content. Additional earlier times were incorporated for cell pellet analysis (compared to media), to maximise chances of detecting intracellular levels. Typical HPLC-UV chromatograms of the intracellular pellets following extraction and analysis are illustrated (Figure 5.14).

5.4.2.1 HCA-7 cell pellet and media analysis following incubation with resveratrol monosulfates

For each timepoint over the course of the experiment (0, 5 min, 15 min, 1 h, 24 h and 168 h), the proportion of total resveratrol species within cells were determined (Figure 5.15). The most abundant metabolite found within the HCA-7 cells following sulfate incubation was resveratrol-3-*O*-sulfate and was seen at all sampling times. At 24 h, resveratrol-3-*O*-sulfate accounted for 86% of total resveratrol species found within the cells. Resveratrol-4'-*O*-sulfate was the next most abundant molecule, corresponding to 7.5% of the total at 24 h. Also at this time, there was 3.5% of resveratrol-4'-*O*-glucuronide and a combined total of 1% of resveratrol sulfate glucuronide and resveratrol-3-*O*-glucuronide. This contrasted with the relatively high sulfate glucuronide levels seen in the media. The proportion of the sulfates and resveratrol at the timepoints measured remained largely unaltered over seven days, whereas the disulfate and sulfate glucuronide were more abundant at earlier timepoints (Figure 5.15). Resveratrol was detected intracellulary at low levels at all times, and standard curves of the parent, resveratrol-3-*O*-sulfate and resveratrol-4'-*O*-sulfate allowed determination of their respective concentrations within cells and in media. Resveratrol reached a maximum concentration of 0.05 ± 0.02 ng/mg of cells 24 h after incubation with the monosulfates (Figure 5.16A). The concentrations of both monosulfates which cells were exposed to reached higher intracellular levels. The increase in the intracellular sulfate concentration was rapid, with resveratrol-3-*O*-sulfate reaching a

maximum concentration of 3.2 ± 2.4 ng/mg of cells at 15 min (Figure 5.16A). This concentration fell between 15 min and 1 h and increased slightly up to 2.2 ± 1.1 at 24 h. Between 24 h and 168 h, the concentration dropped by approximately 20%. Resveratrol-4'-*O*-sulfate intracellular concentration followed a similar pattern, but was consistently lower, reaching a C_{max} concentration of 0.22 ± 0.18 ng/mg of cells at 15 min.

Consistent with the increase in intracellular monosulfate concentrations, amounts of resveratrol-3-*O*-sulfate in media decreased rapidly from 56.4 ± 3.1 µM at time of spiking, to 47.6 ± 1.1 µM at 24 h (Figure 5.16B). This level continued to drop further to 26.3 ± 3.9 µM on day seven. The concentration of resveratrol-4'-*O*-sulfate fell only slightly, from an initial concentration of 19.8 ± 1.2 to 15.8 ± 0.8 µM on day seven respectively. This did not vary substantially from the resveratrol-4'-*O*-sulfate concentration observed in media without cells over the same period (Figure 5.6).

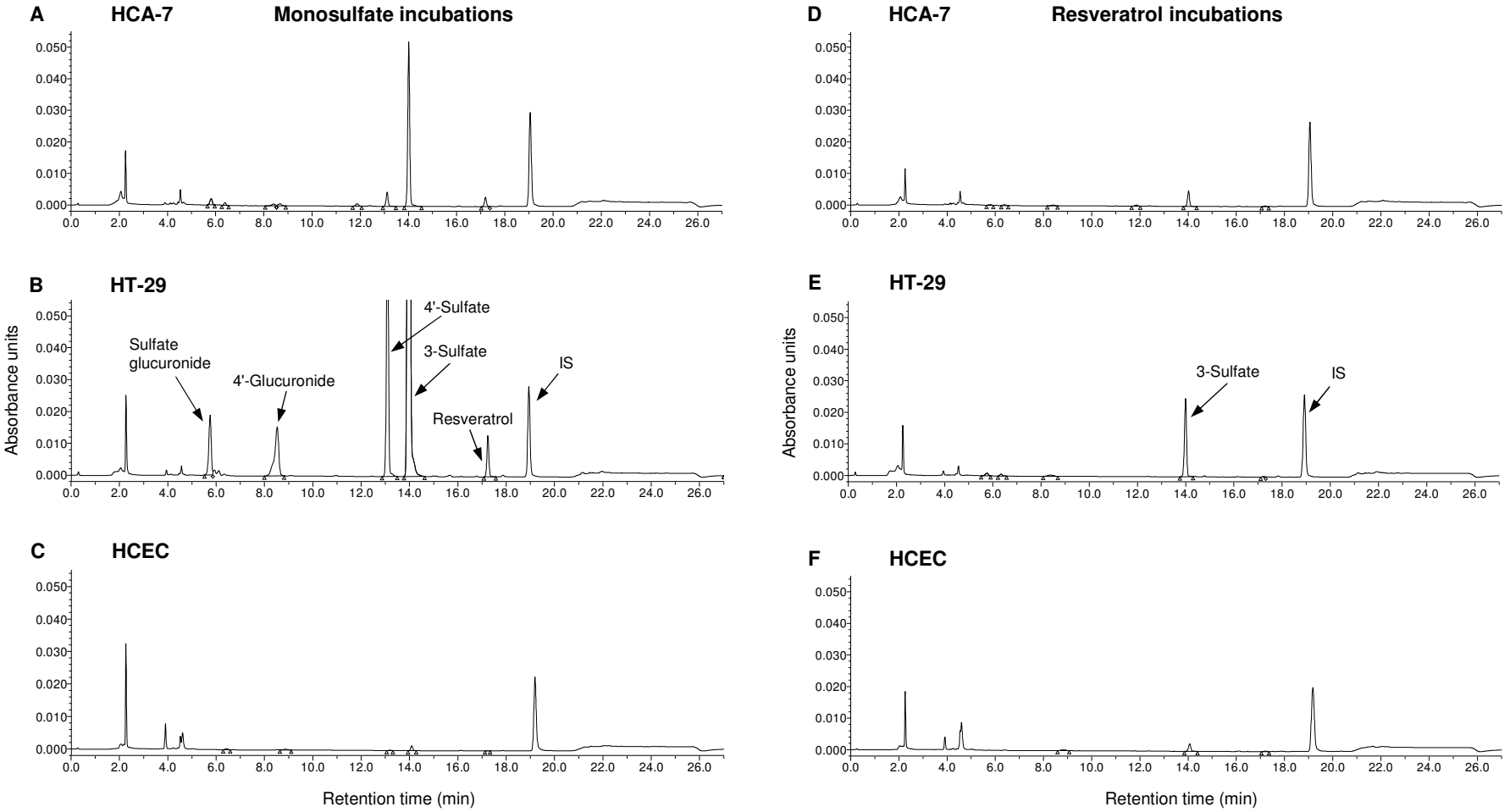

Figure 5.14 Representative intracellular pellet HPLC-UV profiles following incubation with resveratrol monosulfates or resveratrol

Intracellular pellet profiles following incubation of a mixture of 75 µM resveratrol-3-*O*-sulfate and resveratrol-4'-*O*-sulfate (3: 2), or resveratrol (10 µM) with HCA-7, HT-29 and HCEC cells for 24 h. (**A**), (**B**) and (**C**) represent monosulfate incubation in HCA-7, HT-29 and HCEC cells respectively. (**D**), (**E**) and (**F**) represent resveratrol incubation in HCA-7, HT-29 and HCEC cells respectively. Note; maximum peak height in Figure (**B**) reaches 0.50 absorbance units due to higher intracellular concentration.

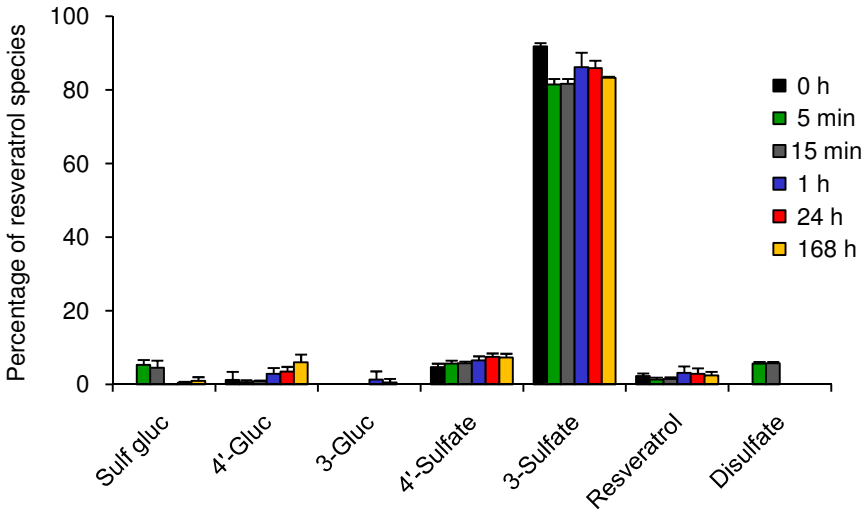

Figure 5.15 Proportion of resveratrol species in HCA-7 cells following incubation with resveratrol monosulfates

Resveratrol derivatives detected in HCA-7 cells following incubation with a mixture of resveratrol-3-*O*-sulfate and resveratrol-4'-*O*-sulfate (75 µM) over seven days, expressed as percentage of total resveratrol species per timepoint. Data shown are the mean + SD from three independent experiments.

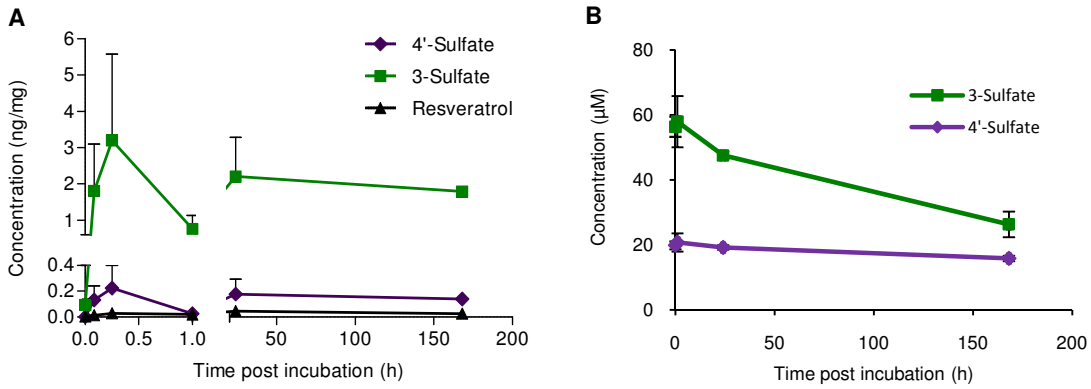

Figure 5.16 Concentrations of resveratrol and monosulfates in HCA-7 cells and loss in media following incubation with resveratrol monosulfates

Concentrations of monosulfates and resveratrol in HCA-7 cell pellets over seven days, following incubation with a mixture resveratrol-3-*O*-sulfate and resveratrol-4'-*O*-sulfate (75 µM) (**A**). Loss of resveratrol monosulfates detected in media following incubation with the same mixture over seven days (**B**). Data shown are the mean + and ± SD from three independent experiments for (**A**) and (**B**) respectively. Note the break in the x and y-axis in **A**.

5.4.2.2 HCA-7 cell pellet and media analysis following incubation with resveratrol

In resveratrol-treated HCA-7 cells, resveratrol and a number of metabolites were identified (Figure 5.17). The highest levels of resveratrol were detected at 15 min of incubation, where the average concentration reached 0.01 ng/mg of cells (Figure 5.18). Resveratrol was rapidly metabolised by the cells, resulting in a greater concentration of resveratrol-3-*O*-sulfate (0.33 ± 0.23 and ng/mg), than parent resveratrol at 15 min. Additional metabolites formed from resveratrol included the sulfate glucuronide and resveratrol-3-*O*-glucuronide, which were only detected at the two earliest timepoints, whilst the disulfate and resveratrol-4'-*O*-sulfate were absent altogether (Figure 5.17). Resveratrol-4'-*O*-glucuronide was the most prevalent resveratrol species present at 1 h (80.5% of total metabolites/resveratrol detected); however, at 24 h, resveratrol-3-*O*-sulfate had replaced the 4'-*O*-glucuronide as the major derivative observed (91.7%). In media spiked with resveratrol only (without cells), resveratrol could not be detected after 24 h (data not plotted), possibly due to its protein binding [191].

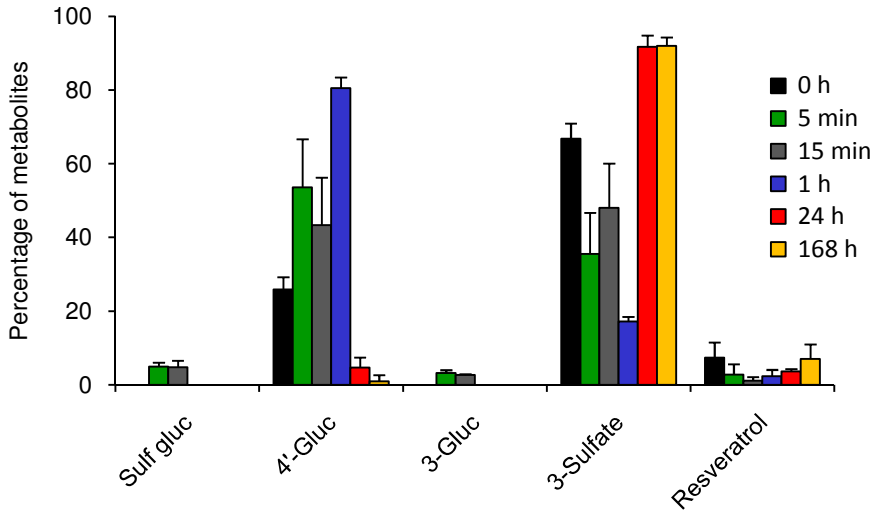

Figure 5.17 Proportion of resveratrol species in HCA-7 cells following incubation with resveratrol

Resveratrol derivatives detected in HCA-7 cells following incubation with resveratrol (10 µM) over seven days, expressed as percentage of total resveratrol species per timepoint. Data shown are the mean + SD from three independent experiments.

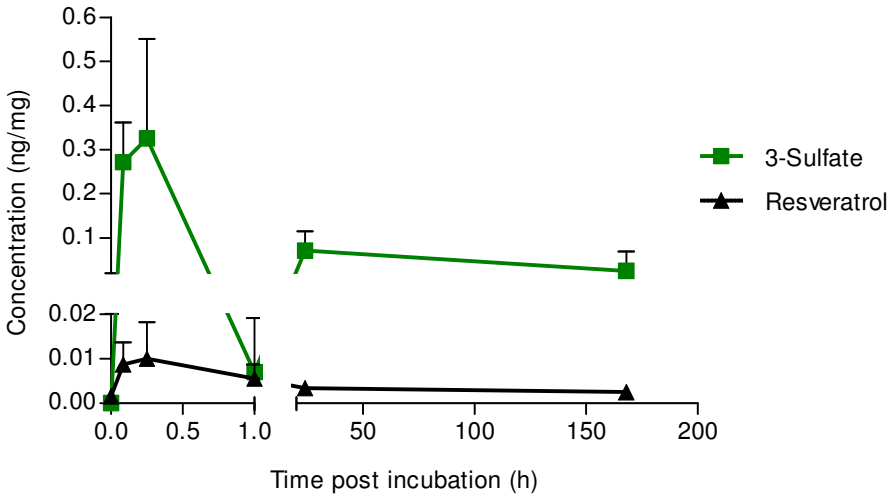

Figure 5.18 Resveratrol species in HCA-7 cells following incubation with resveratrol

Concentration of resveratrol-3-*O*-sulfate and resveratrol detected in HCA-7 cell pellets following incubation with 10 µM resveratrol over seven days. Data shown are the mean + SD from three independent experiments. Note the break in the x and y-axis.

5.4.3 Determination of species in media and cells following incubation of HT-29 cells with resveratrol monosulfates or resveratrol

5.4.3.1 HT-29 cell pellet and media analysis following incubation with resveratrol monosulfates

Resveratrol-3-*O*-sulfate was the major metabolite detected within the HT-29 cell pellets at all of the timepoints following incubation with the monosulfate mixture (Figure 5.19). This was followed by resveratrol-4'-*O*-sulfate. The relative percentages of metabolites varied considerably between 24 h and 168 h over the period measured. Whereas at 24 h resveratrol-3-*O*-sulfate accounted for 83% of the total species present, on day seven this had fallen to 45%. Resveratrol-4'-*O*-glucuronide and resveratrol-4'-*O*-sulfate, which made up 4.5 and 9.1% of the total, respectively, at 24 h, were more prominent on day seven, with each accounting for approximately 25% of the total species. Resveratrol was detectable at all timepoints and reached a C_{max} of 0.16 ± 0.05 ng/mg of cells at 24 h (Figure 5.20A). Resveratrol monosulfate metabolites reached substantially higher concentrations in the HT-29 cell pellets, with resveratrol-3-*O*-sulfate being the major molecule following monosulfate incubation. After 1 h of incubation, resveratrol-3-*O*-sulfate was detected at a concentration of 6.3 ± 2.7 ng/mg. Maximal concentrations of both resveratrol-3-*O*-sulfate and resveratrol-4'-*O*-sulfate occurred at 24 h at 14.6 ± 3.6 and 1.8 ± 1.5 ng/mg, respectively.

When media spiked with monosulfates was incubated in the presence of HT-29 cells, the concentration of resveratrol-3-*O*-sulfate dropped from an initial 53.5 ± 7.0 µM to 29.4 ± 2.4 µM at 24 h (Figure 5.20B). By day seven, the concentration had fallen further to 2.4 ± 0.9 µM. Resveratrol-4'-*O*-sulfate concentration also decreased over the course of 24 h from 19.2 ± 2.3 µM to 16.7 ± 1.5 µM. On day seven, the concentration detected in media was 6.9 ± 1.3 µM, which is far lower than that detected in media without cells under identical conditions (Figure 5.6).

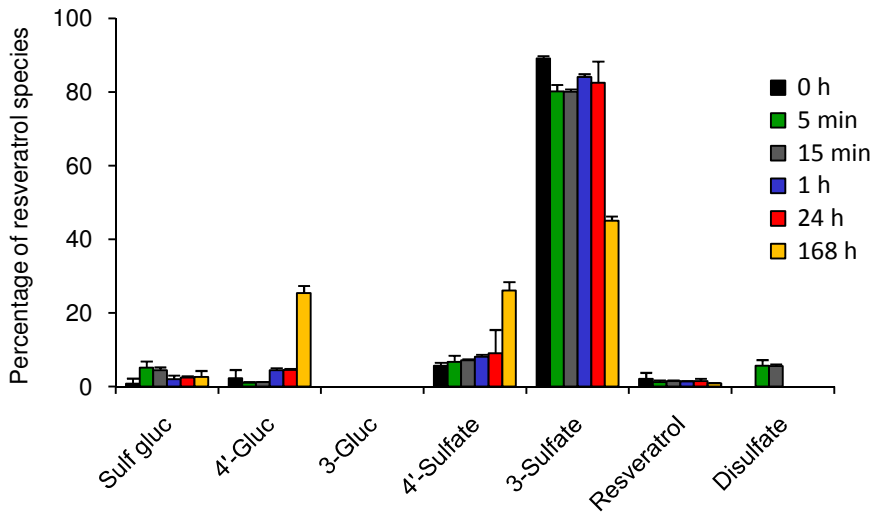

Figure 5.19 Proportion of resveratrol species in HT-29 cells following incubation with resveratrol monosulfates

Resveratrol derivatives detected in HT-29 cells following incubation with a mixture of resveratrol-3-*O*-sulfate and resveratrol-4'-*O*-sulfate (75 µM) over seven days, expressed as percentage of total resveratrol species per timepoint. Data shown are the mean + SD from three independent experiments.

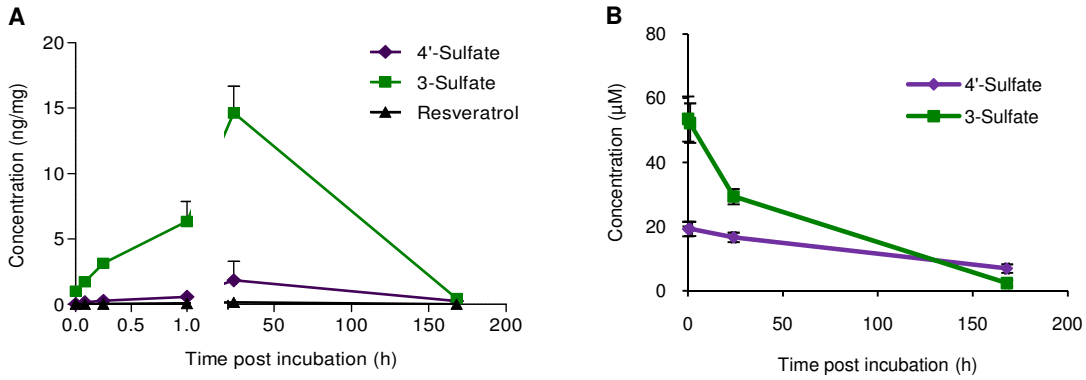

Figure 5.20 Concentrations of resveratrol and monosulfates in HT-29 cells and loss in media following incubation with resveratrol monosulfates

Concentrations of monosulfates and resveratrol in HT-29 cell pellets over seven days, following incubation with a mixture resveratrol-3-*O*-sulfate and resveratrol-4'-*O*-sulfate (75 µM) (**A**). Note the break in the x-axis. Loss of resveratrol monosulfates detected in media following incubation with the same mixture over seven days (**B**). Data shown are the mean + and ± SD from three independent experiments for (**A**) and (**B**) respectively.

5.4.3.2 HT-29 cell pellet and media analysis following incubation with resveratrol

The metabolic profile following incubation of resveratrol with HT-29 cells (Figure 5.21) closely resembled the profile described in HCA-7 cells (Figure 5.17). Resveratrol disappearance was extremely rapid, as was the formation of resveratrol-4'-*O*-glucuronide and resveratrol-3-*O*-sulfate. Resveratrol in cells reached a maximum concentration of 0.02 ± 0.01 ng/mg at 1 h, compared to far greater resveratrol-3-*O*-sulfate concentrations at the same time (0.36 ± 0.24 ng/mg) (Figure 5.22). This was the dominant metabolite formed, and unlike resveratrol, persisted at higher concentrations for longer. In addition to the 3-*O*-sulfate, lower levels of resveratrol-4'-*O*-glucuronide were detected in cell pellets as early as 5 min post-incubation, but this derivative accounted for only a negligible amount after 1 h indicating that it is removed from cells and/or it is metabolised further.

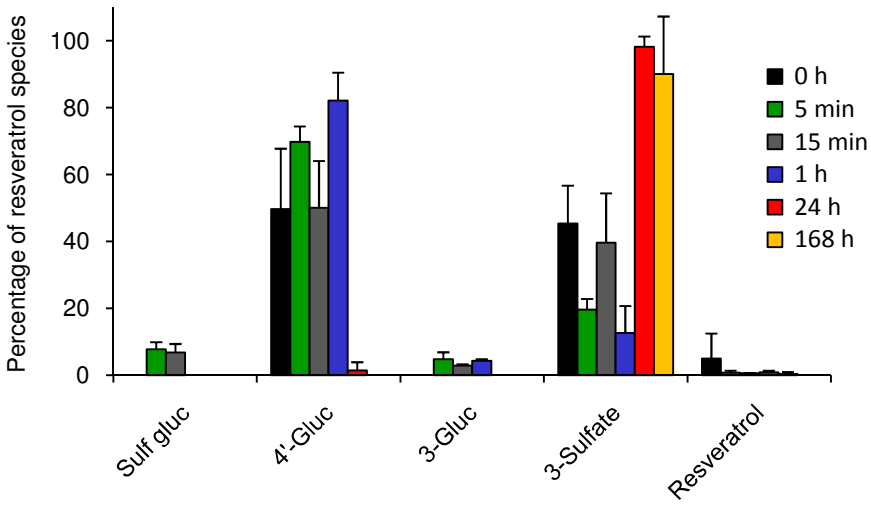

Figure 5.21 Proportion of resveratrol species in HT-29 cells following incubation with resveratrol

Resveratrol derivatives detected in HT-29 cells following incubation with resveratrol (10 µM) over seven days, expressed as percentage of total resveratrol species per timepoint. Data shown are the mean + SD from three independent experiments.

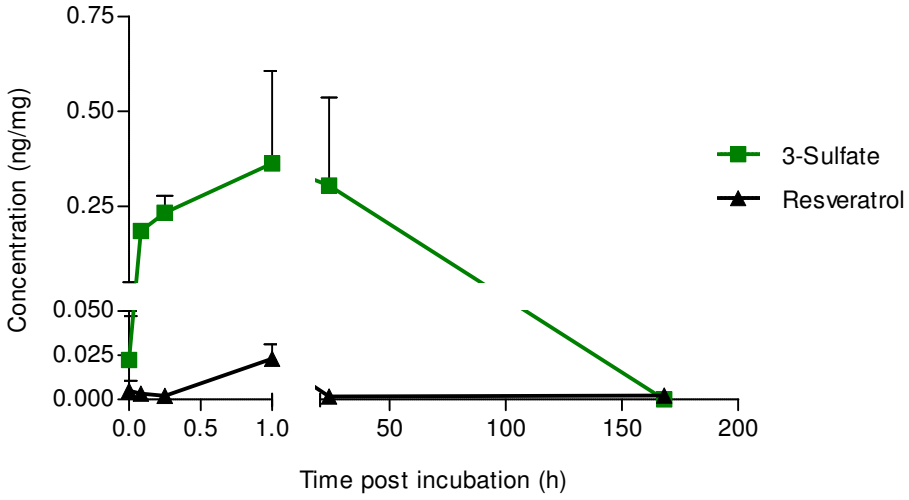

Figure 5.22 Concentrations of resveratrol and resveratrol-3-*O*-sulfate in HT-29 cells following incubation with resveratrol

Concentration of resveratrol-3-*O*-sulfate and resveratrol detected in HT-29 cell pellets following incubation with 10 µM resveratrol over seven days. Data shown are the mean + SD from three independent experiments. Note the break in the x and y-axis.

5.4.4 Determination of species in media and cells following incubation of HCEC cells with resveratrol monosulfates or resveratrol

5.4.4.1 HCEC cell pellet and media analysis following incubation with resveratrol monosulfates

Metabolite and resveratrol levels in the HCEC cell pellets were generally difficult to detect after incubation with the monosulfates (Figure 5.14C) and close to or below the limit of quantitation (0.001 - 0.005 ng/mg), particularly at the later harvesting times. Therefore, the concentrations could not be quantified, and there was a large variability in the percentage data for this cell line (Figure 5.23). Following incubation of HCEC cells with resveratrol monosulfates, resveratrol-3-*O*-sulfate was the major species detected. Some sulfate-glucuronide and resveratrol-4'-*O*-glucuronide were present, however, these were not detected before the 1 h sampling time.

The resveratrol-3-*O*-sulfate concentration in media was not found to vary over the course of seven days when incubated in the presence of HCEC cells (Figure 5.24). Resveratrol-4'-*O*-sulfate decreased slightly over seven days from an initial concentration of 19.5 ± 2.7 to 16.2 ± 1.2 µM on day seven. This was similar to the reduction observed following incubation of monosulfates in media without cells (Figure 5.6).

5.4.4.2 HCEC cell pellet and media analysis following incubation with resveratrol

Following incubation of HCEC cells with resveratrol, resveratrol-3-*O*-sulfate was the main metabolite generated, with small amounts of resveratrol-4'-*O*-glucuronide present (Figure 5.25). The C_{max} for resveratrol-3-*O*-sulfate concentration was reached earlier than for resveratrol (5 min compared to 1 h), with respective concentrations of 0.08 ± 0.05 ng/mg and 0.02 ± 0.05 ng/mg at these times (Figure 5.26). After seven days, neither resveratrol nor its 3-*O*-sulfate metabolite were detected in pellets.

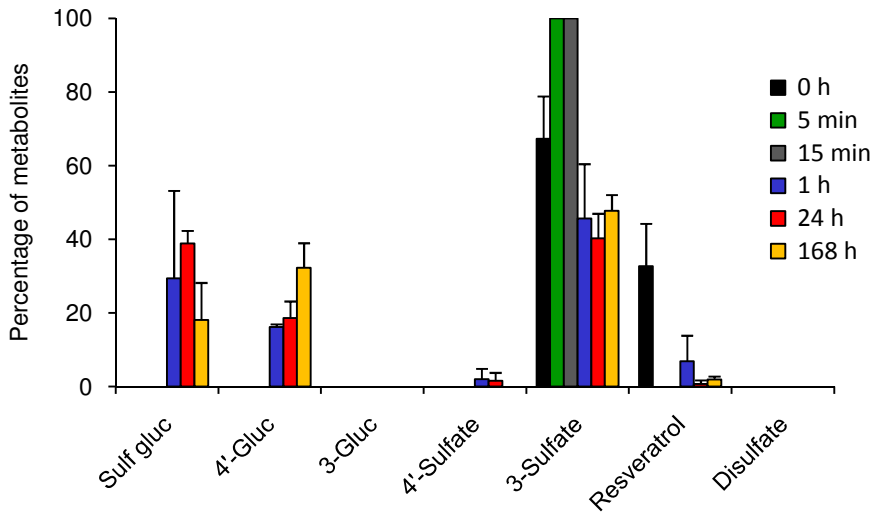

Figure 5.23 Proportion of resveratrol species in HCEC cells following incubation with resveratrol monosulfates

Resveratrol derivatives detected in HCEC cells following incubation with a mixture of resveratrol-3-*O*-sulfate and resveratrol-4'-*O*-sulfate (75 µM) over seven days, expressed as percentage of total resveratrol species per timepoint. Data shown are the mean + SD from three independent experiments.

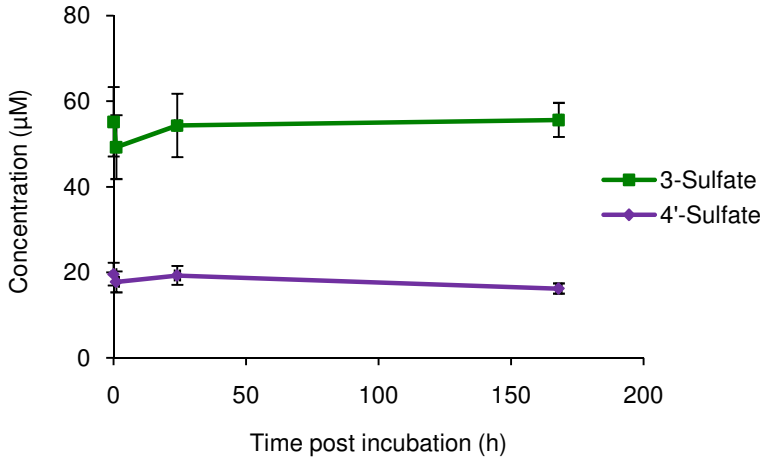

Figure 5.24 Media concentration of resveratrol monosulfates following incubation with HCEC cells

Loss of resveratrol monosulfates detected in media following incubation a mixture of resveratrol-3-*O*-sulfate and resveratrol-4'-*O*-sulfate (75 µM) over seven days. Data shown are the mean ± SD from three independent experiments.

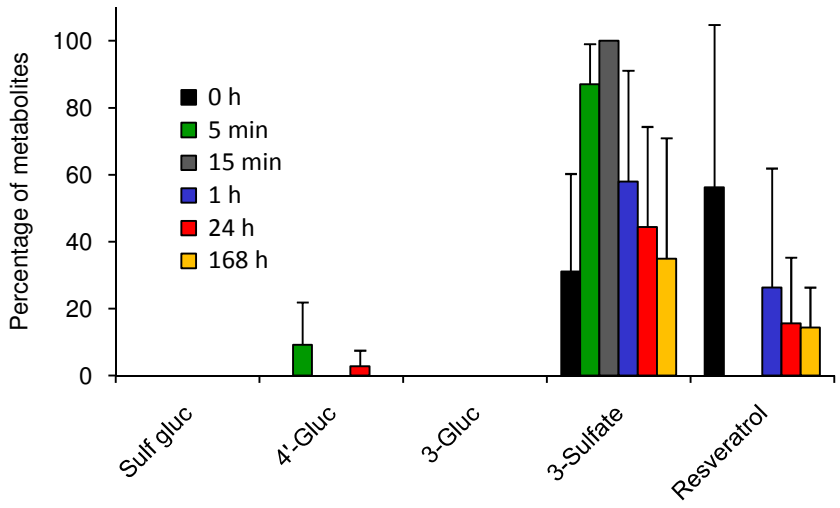

Figure 5.25 Proportion of resveratrol species in HCEC cells following incubation with resveratrol

Resveratrol derivatives detected in HCEC cells following incubation with resveratrol (10 µM) over seven days, expressed as percentage of total resveratrol species per timepoint. Data shown are the mean + SD from three independent experiments.

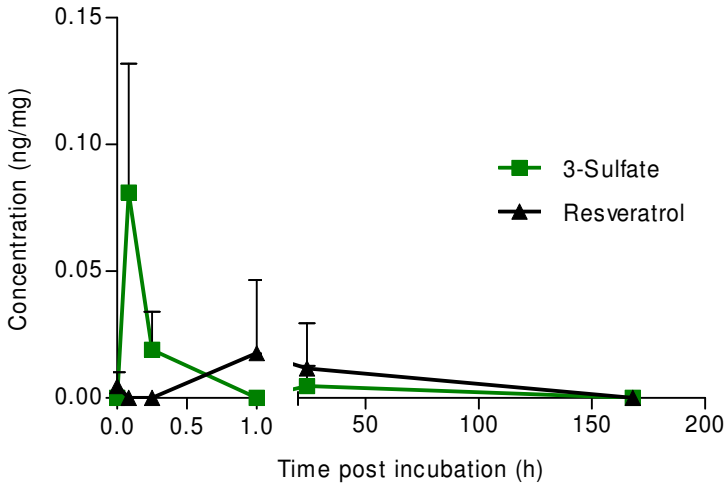

Figure 5.26 Concentrations of resveratrol and resveratrol-3-*O*-sulfate in HCEC cells following incubation with resveratrol

Concentration of resveratrol-3-*O*-sulfate and resveratrol detected in HCEC cell pellets following incubation with 10 µM resveratrol over seven days. Data shown are the mean + SD from three independent experiments. Note the break in the x-axis.

5.4.5 Summary of resveratrol monosulfate and resveratrol concentrations in cells

The 24 h timepoint was selected to compare concentrations detected within cells. This timepoint was chosen as concentrations of resveratrol derivatives were generally high. The sulfate and resveratrol intracellular concentration data from this timepoint for each of the cell lines is shown in Table 5.1 for comparison.

	HCA-7			HT-29			HCEC		
	4'-Sulf	**3-Sulf**	**Res**	**4'-Sulf**	**3-Sulf**	**Res**	**4'-Sulf**	**3-Sulf**	**Res**
75 µM Sulfate mixture	0.18 ± 0.12	2.21 ± 1.07	0.05 ± 0.02	1.84 ± 1.45	14.64 ± 3.55	0.16 ± 0.05	LOD	BLQ	BLQ
10 µM Res	LOD	0.07 ± 0.04	BLQ	LOD	0.30 ± 0.23	BLQ	LOD	BLQ	BLQ

Table 5.1 Resveratrol and resveratrol monosulfate concentrations in colon cells at 24 h. Concentration of resveratrol monosulfates and resveratrol in HCA-7, HT-29 and HCEC cells incubated in the presence of either a mixture of resveratrol-3-*O*-sulfate and resveratrol-4'-*O*-sulfate (75 µM), or 10 µM resveratrol, measured 24 h post-incubation. Values are the mean ± SD of three independent experiments, with concentrations given in ng/mg of cells. LOD indicates levels below the limit of detection (0.0003 ng/mg). BLQ indicates samples below the limit of quantitation, which fall within the range of 0.001 - 0.005 ng/mg of cells.

The data shows that the highest intracellular concentrations achieved were in HT-29 cells following incubation with resveratrol sulfates. For resveratrol-4'-*O*-sulfate, resveratrol-3-*O*-sulfate and resveratrol, these were approximately 10-, 7- and 3-fold greater respectively than the concentrations achieved in the HCA-7 cells following identical exposure to sulfates. Higher concentrations of resveratrol were detected following monosulfate dosing compared to resveratrol dosing in both HCA-7 and HT-29 cell lines. However, this may be due to the higher concentrations of sulfates compared to resveratrol used in the incubations. In HT-29 cells following resveratrol dosing, 4-times more resveratrol was detected compared to HCA-7 cells. HCEC cells contained the lowest intracellular concentrations, with levels either below the limit of quantitation (BLQ), or not detectable. In the monosulfate-treated cells, the intracellular resveratrol concentrations were highest in HT-29 cells with lower levels in HCA-7 and HCEC

cells (and almost absent in the latter). The intracellular resveratrol concentrations corresponded to the level of anti-proliferative activity in the cell lines.

A comparison of the intracellular resveratrol concentrations in the cell lines following incubation with resveratrol (10 µM) or sulfates (75 µM) across all timepoints analysed is illustrated (Figure 5.27). The results show that resveratrol was rapidly metabolised and reached C_{max} concentrations at, or before 1 h of incubation with resveratrol in all of the cell lines. In contrast, resveratrol presence is more prolonged after cell incubations with monosulfates. The exception is in the HCEC cell after monosulfate dosing, where resveratrol concentrations could not be quantified as they were BLQ or below the LOD.

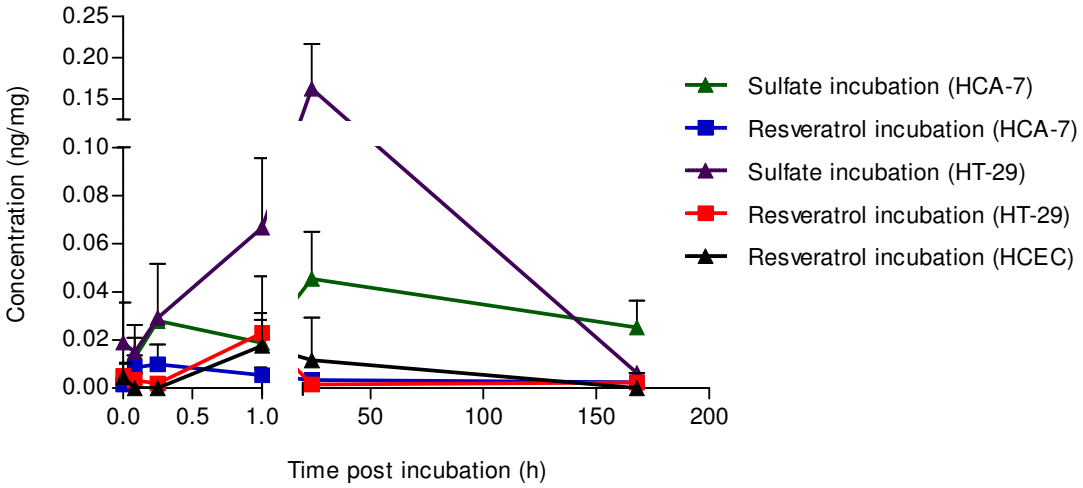

Figure 5.27 Concentrations of resveratrol in HCA-7, HT-29 and HCEC cells following incubation with resveratrol monosulfates and resveratrol

Concentration of resveratrol detected in HCA-7, HT-29 and HCEC cell pellets following incubation with a mixture of resveratrol-3-*O*-sulfate and resveratrol-4'-*O*-sulfate (75 µM) or resveratrol (10 µM) over seven days. Resveratrol concentrations in HCEC cells following monosulfate treatment could not be plotted as concentrations were not quantifiable. Data shown are the mean + SD from three independent experiments. Note the break in the x and y-axis.

5.4.6 Identification of metabolites in media by LC-MS/MS

The identity of the metabolites detected in media incubates from each of the cell types were confirmed by LC-MS/MS to backup the assignments made on the basis of chromatographic properties and comparison of retention times with authentic synthetic standards. This was particularly important for those metabolites where standards were not available. To analyse media samples taken on day seven post-incubation, MRM was employed to measure the characteristic fragmentation of the major metabolites in negative ion mode. Media from all three cell lines was analysed in this way, however, the transitions of media derived from incubation of monosulfates with HCA-7 cells have not been displayed. The two most extreme media profiles in terms of maximal and minimal amounts of metabolites detected by HPLC-UV were HT-29 and HCEC cells respectively, and are illustrated in Figure 5.28.

There were major differences in the metabolites detected following resveratrol monosulfate incubation in the media collected from the two different cell incubations. Resveratrol monosulfates were found in media from all three cell lines, as characterised by the transition *m/z* 307 > 227, which corresponds to loss of a sulfate group, and also resveratrol disulfate (*m/z* 387 > 227, loss of two sulfate groups). Metabolites identified in media grown with HT-29 cells, but not HCEC cells were, resveratrol-3-*O*-glucuronide and resveratrol-4'-*O*-glucuronide (*m/z* 403 > 227, loss of a glucuronide moiety) and resveratrol sulfate glucuronide (*m/z* 483 > 227). (Figure 5.28 and Table 5.2). The same transitions were detected in HCA-7 cells as for HT-29 cells (Table 5.2). Transitions shown for the HCEC cell media, for example in the *m/z* 227 > 184, displayed multiple peaks due to the monosulfates also undergoing the same transition as resveratrol.

The major sulfate glucuronide peak detected in media of HT-29 cells was isolated by HPLC; the appropriate fraction was collected and analysed by LC-MS/MS to provide definitive identification. This was identified unambiguously using the transitions; *m/z* 483 > 404 (loss of a sulfate), *m/z* 483 > 307 (loss of a glucuronide), *m/z* 483 > 227 (loss of both) (Figure 5.29).

Resveratrol was not detected in any of the samples of media on day seven post-treatment regardless of incubation or cell type. Resveratrol monosulfates were present after both forms of treatment, in all three cell lines. Following incubation of the monosulfates with HCA-7 and HT-29 cells, all of the four major metabolites were detected (resveratrol sulfate glucuronide, resveratrol disulfate, resveratrol monoglucuronide and monosulfate) in the media. In contrast, media taken from HCEC cells incubated with monosulfates had neither sulfate glucuronide nor monoglucuronides; unchanged resveratrol monosulfates dominated in the media, with some disulfate also detected.

Resveratrol disulfate and monosulfates were present in media of HCA-7 and HT-29 cells incubated with resveratrol. Only the monosulfates were present in media taken from HCEC cells following the same treatment.

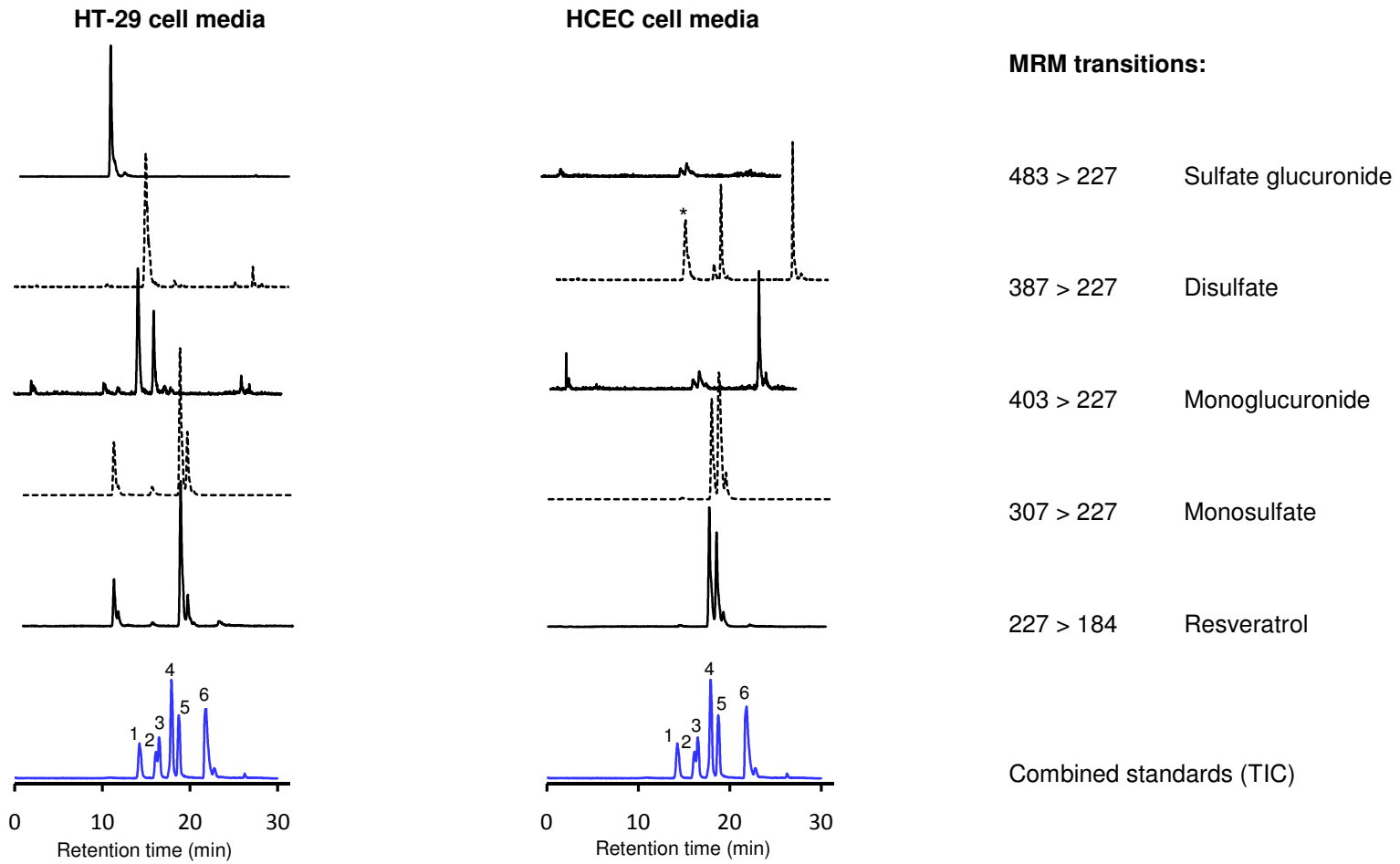

Figure 5.28 Representative LC-MS/MS MRM ion chromatograms of media spiked with resveratrol monosulfates and incubated with HT-29 or HCEC cells

Representative LC-MS/MS MRM ion chromatograms of media spiked with resveratrol monosulfates and incubated with either HT-29 or HCEC cells for seven days. The total ion current from the analysis of a mixture of authentic standards is also shown for comparison. The mixture consisted of resveratrol-4'-*O*-glucuronide (**1**), resveratrol-3-*O*-glucuronide (**2**), dehydrated resveratrol glucuronide (exhibits the transition 385 > 227 and was not present in the media samples) (**3**), resveratrol-4'-*O*-sulfate (**4**), resveratrol-3-*O*-sulfate (**5**) and resveratrol (**6**). The resveratrol disulfate peak in the HCEC media is indicated by an asterisk.

		Sulfate glucuronide	Disulfate	Monoglucuronide	Monosulfate	Resveratrol
	Incubation	**483 > 227**	**387 > 227**	**404 > 227**	**307 > 227**	**227 > 184**
HCA-7	**Monosulfates**	✓	✓	✓	✓	×
	Resveratrol	×	×	✓	✓	×
	Control	×	×	×	×	×
HT-29	**Monosulfates**	✓	✓	✓	✓	×
	Resveratrol	×	×	✓	✓	×
	Control	×	×	×	×	×
HCEC	**Monosulfates**	×	✓	×	✓	×
	Resveratrol	×	×	×	✓	×
	Control	×	×	×	×	×

Table 5.2 The presence or absence of resveratrol derivatives in media incubated with colon cells. LC-MS/MS MRM of transitions for the detection of resveratrol metabolites and resveratrol in media treated with monosulfates or resveratrol and incubated with HCA-7, HT-29 or HCEC cells for seven days.

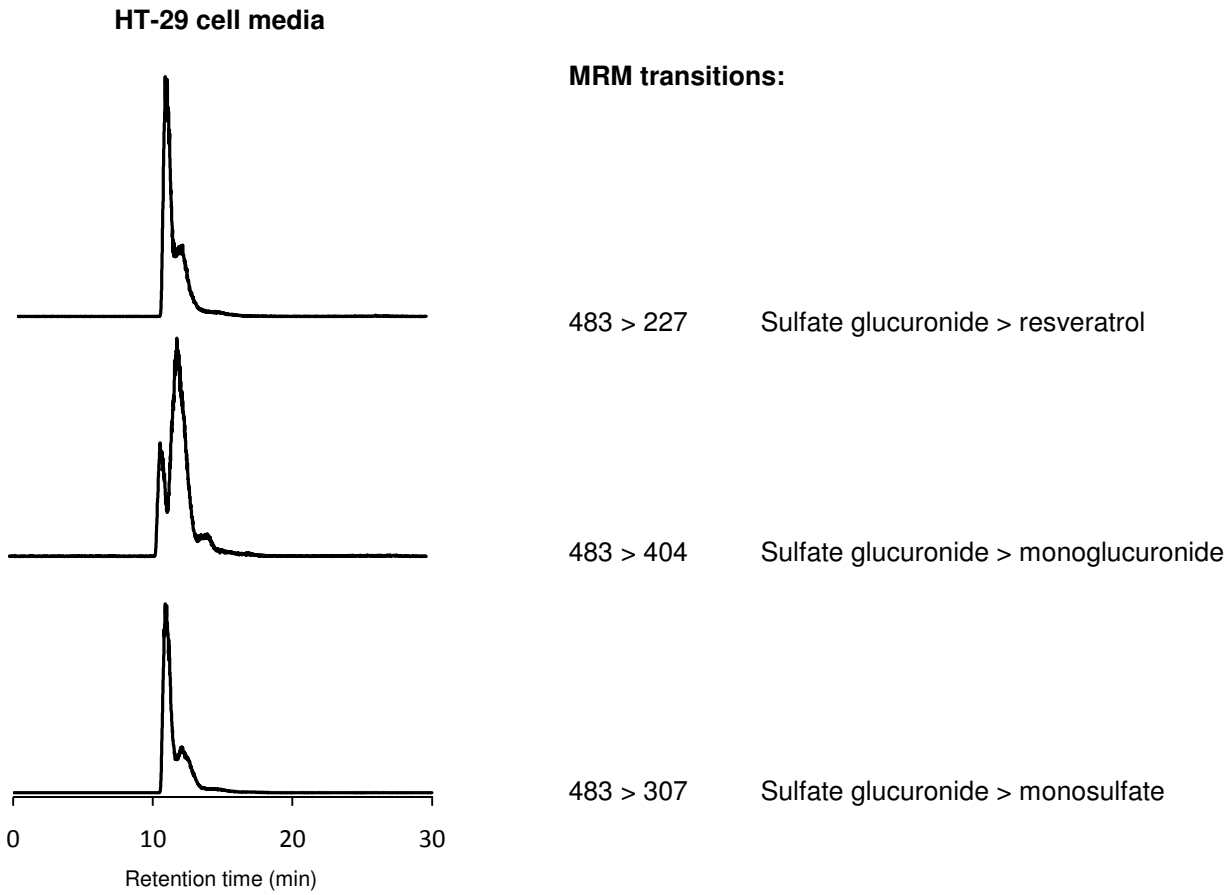

Figure 5.29 LC-MS/MS MRM analysis of an HPLC fraction for the identification of resveratrol sulfate glucuronide in media

The HPLC fraction containing resveratrol sulfate glucuronide was generated in media spiked with monosulfates and incubated with HT-29 cells for seven days. Transitions monitored were 483 > 227, 483 > 404 and 483 > 307, which indicated a loss of a sulfate and glucuronide group, loss of a sulfate group and loss of a glucuronide group respectively.

5.5 Investigation into the action of resveratrol monosulfates in cells

A number of analyses were undertaken to try and explain the processes which may have mediated the reduction in cell number described in Section 5.2, and to determine whether the cells became cytostatic, or apoptotic and/or necrotic. The first method used was cell cycle analysis to determine if the cells were arrested in a particular phase of the cell cycle.

5.5.1 Cell cycle analysis

Cells naturally undergo division and replication. The series of events leading up to this can be categorised by a number of phases. In a given population, cells will be distributed among three major phases of the cell cycle: G0 - G1 phase, S-phase, and G2 - M phase. Cell cycle analysis is a method of determining which stages of the cycle cells are at.

Cell cycle analysis was performed on all three cell lines to ascertain the effects of resveratrol sulfates. HCA-7, HT-29 and HCEC cells were treated with two concentrations of resveratrol (5 and 10 µM) or two concentrations of sulfates (75 and 250 µM), and harvested at 24, 48 and 72 h post-treatment. Cells were fixed in ethanol and the DNA stained by the addition of PI 24 h prior to analysis by flow cytometry.

5.5.1.1 Cell cycle analysis in HCA-7 cells

In the HCA-7 cells, the profiles of control untreated cells were generally similar across the different timepoints analysed (Figure 5.30). With control cells at 24, 48 and 72 h, the majority of cells were present in the G0 - G1 phase, followed by the S-phase, with a small proportion in the G2 - M phase. At the higher concentrations of both resveratrol and sulfates, there was a shift in the profile, with more cells in the S-phase of the cycle. With resveratrol treatment this increase was only significant at 24 h *($P \leq 0.01$*; One-Way ANOVA*)* and only at the higher concentration of

resveratrol (10 µM). The observed increase in the number of cells in the S-phase following 250 µM sulfate dosing (relative to control) was also highly significant at 24 h *(P ≤ 0.002*; One-Way ANOVA*)*. At 48 h this difference remained and was accompanied by a reduction in the cells at both G0 - G1, and G2 - M *(P ≤ 0.002* and *P ≤ 0.05* respectively). With the same treatment, a small reduction in percentage of cells in G2 - M was also observed at 24, and 72 h compared to control, but this difference was not significant. Similarly, the slight differences in the profiles of the cells with 250 µM sulfates at 72 h post-treatment were not found to differ significantly from control suggesting the cells were returning to their normal distribution.

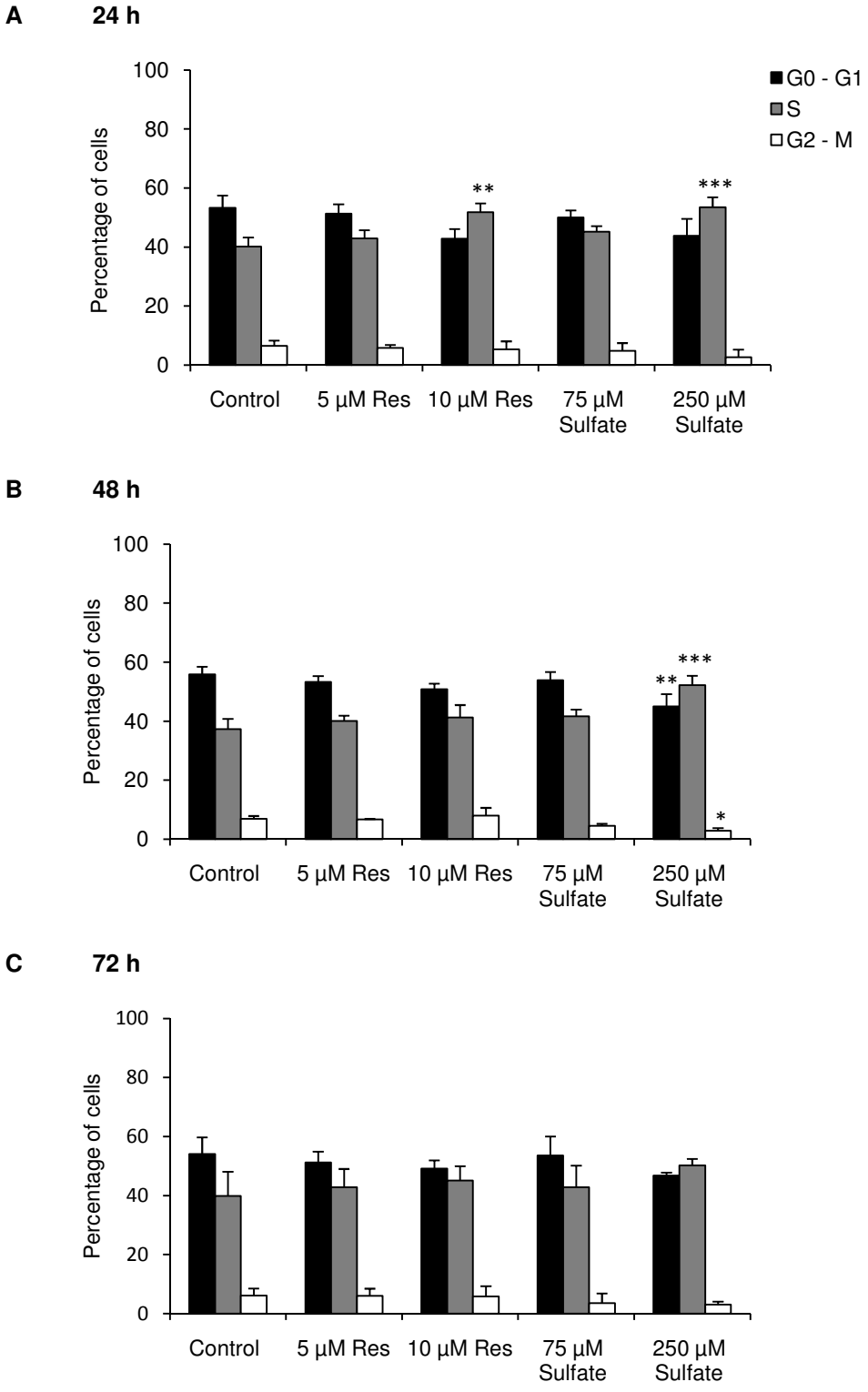

Figure 5.30 Distribution of HCA-7 cells in stages of the cell cycle following incubation with resveratrol and resveratrol monosulfates

Percentage of HCA-7 cells in each stage of the cell cycle at 24, 48 and 72 h post-treatment with 5 and 10 µM of resveratrol and 75 and 250 µM of resveratrol sulfates. Asterisks indicate level of significance following One-Way ANOVA analysis (*$P \leq 0.05$, **$P \leq 0.01$, ***$P \leq 0.002$).

5.5.1.2 Cell cycle analysis in HT-29 cells

In the HT-29 cells (Figure 5.31), there were similar changes in response to treatment as to those described for HCA-7 cells. However, following resveratrol dosing there was no significant alteration in the percentage of cells at each stage compared to control at any of the three timepoints. The biggest change was observed after treatment with 250 µM of the sulfates where the proportion of cells in the S-phase increased significantly relative to control at 24, 48 and 72 h ($P \leq 0.05$, $P \leq 0.05$ and $P \leq 0.01$, respectively; One-Way ANOVA). Following 75 µM of sulfate treatment there was a slight increase in S-phase and reduction in G0 - G1 relative to control. However, neither of these changes were found to be significant at any of the time intervals.

5.5.1.3 Cell cycle analysis in HCEC cells

Unlike the HCA-7 and HT-29 cells, no significance was reached in HCEC cells (Figure 5.32) following exposure to 250 µM of sulfate at any of the timepoints. At 24 h post-treatment, the proportion of cells in all the treated groups remained very similar to those recorded in control cells. At 48 h and 72 h, 10 µM resveratrol treated cells gave a significantly different profile to control cells, with an increase in the number of cells in the G0 - G1 phase ($P \leq 0.01$ and $P \leq 0.002$ respectively; One-Way ANOVA). At 72 h, also with 10 µM resveratrol, there was a significant reduction in the number of cells in the S-phase of the cycle ($P \leq 0.002$).

As the changes observed in the HCA-7 and HT-29 cells following cell cycle analysis were not thought to be sufficient to cause the extent of reduction in cell number outlined in Sections 5.2.2 and 5.2.3 respectively, an apoptosis assay was used to determine whether cells were undergoing apoptosis or necrosis.

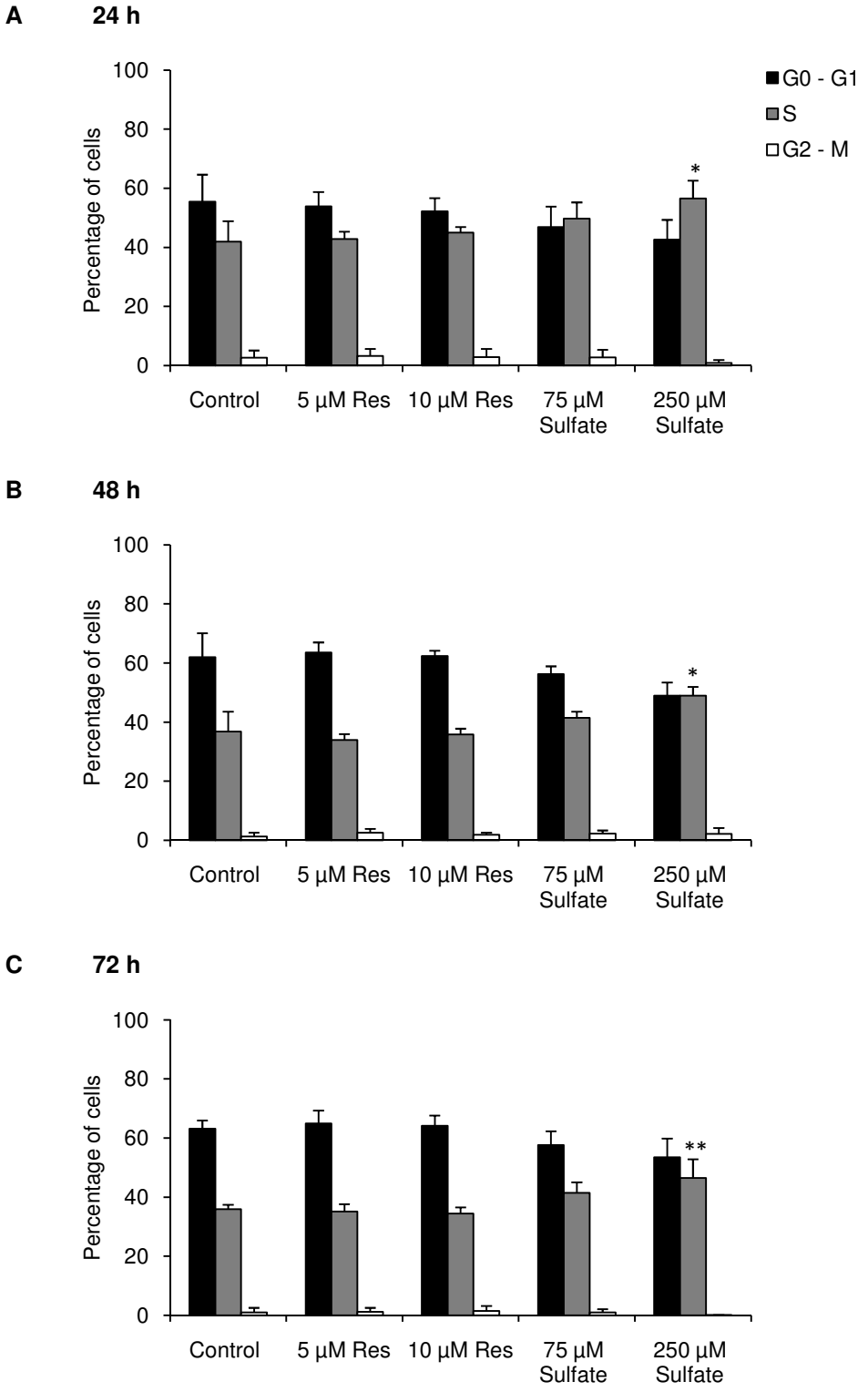

Figure 5.31 Distribution of HT-29 cells in stages of the cell cycle following incubation with resveratrol and resveratrol monosulfates

Percentage of HT-29 cells in each stage of the cell cycle at 24, 48 and 72 h post-treatment with 5 and 10 µM of resveratrol and 75 and 250 µM of resveratrol sulfates. Asterisks indicate level of significance following One-Way ANOVA analysis (*$P \leq 0.05$, **$P \leq 0.01$).

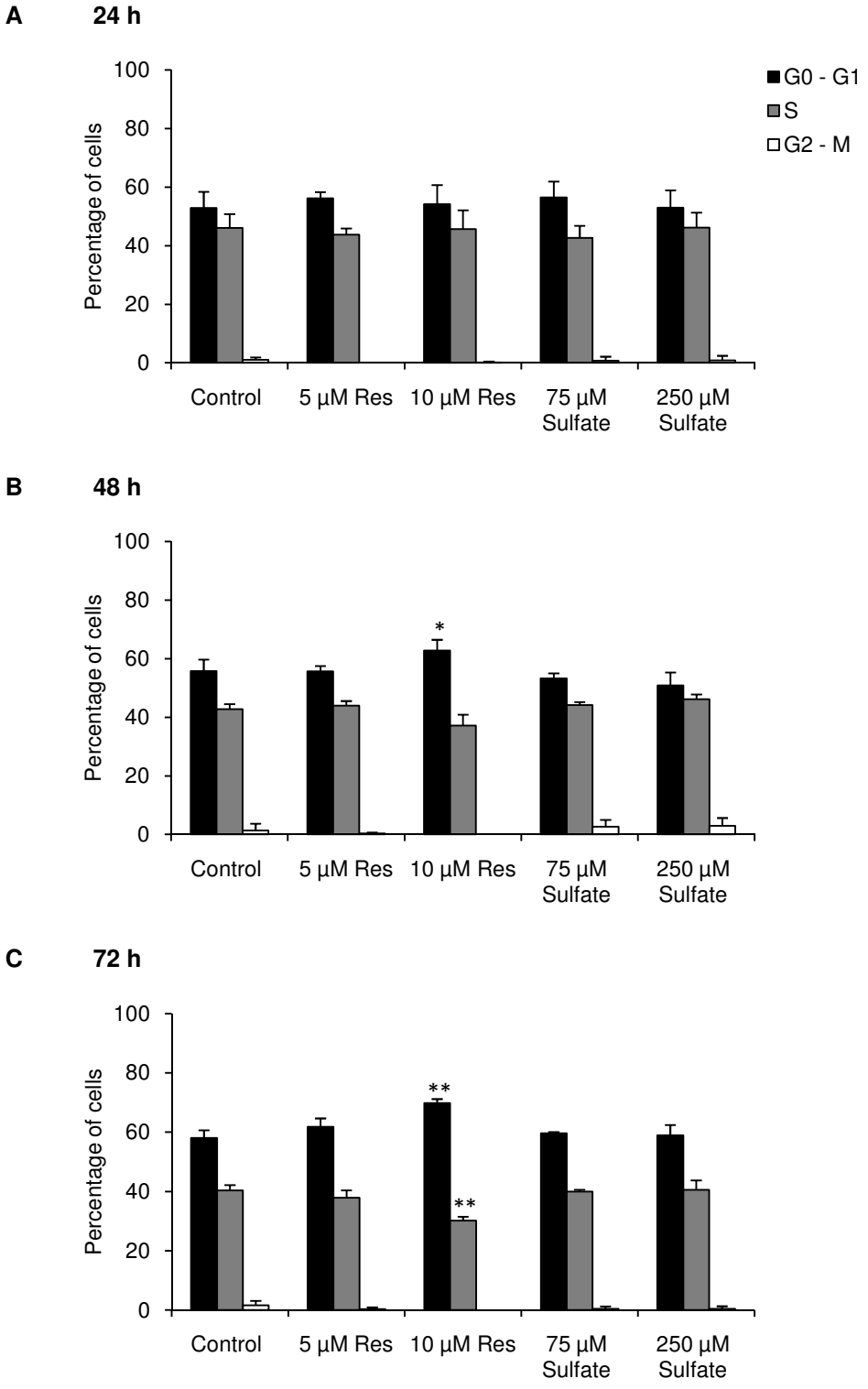

Figure 5.32 Distribution of HCEC cells in stages of the cell cycle following incubation with resveratrol and resveratrol monosulfates

Percentage of HCEC cells in each stage of the cell cycle at 24, 48 and 72 h post-treatment with 5 and 10 µM of resveratrol and 75 and 250 µM of resveratrol sulfates. Asterisks indicate level of significance following One-Way ANOVA analysis (*$P \leq 0.01$, **$P \leq 0.002$).

5.5.2 Apoptosis by Annexin V-FITC staining

Apoptosis analysis by flow cytometry quantifies the percentage of apoptotic, necrotic and live cells in a population. Apoptosis was measured in all three cell lines following treatment with 10 µM of resveratrol and 75 and 250 µM of sulfates at 24, 48 and 72 h post-treatment, using the Annexin V-FITC assay. Cell proliferation assays showed a large reduction in cell numbers treated with resveratrol and sulfates at these concentrations relative to control; this assay was employed to determine whether the reduction was related to cell death.

5.5.2.1 Analysis of apoptosis in HCA-7 cells

In all of the groups the majority of cells were alive, with lower numbers of apoptotic and even fewer necrotic cells. At 24 h (Figure 5.33) there appeared to be an increase in the amount of apoptosis in the cells following all of the treatments, with the most obvious increase after 10 µM of resveratrol. There was also a small reduction in the number of live cells in the treated groups compared to control, however, none of these changes were found to be significant. At 48 h there also was a small increase in the apoptosis in the treated groups above control, but this was also not found to be significant. At 72 h no changes in the profiles were evident between the control and treated cells.

5.5.2.2 Analysis of apoptosis in HT-29 cells

For all three cell lines investigated the most apparent differences following treatment were found in HT-29 cells (Figure 5.34). This cell line was also the most sensitive to the anti-proliferative effect described previously. The increase in the fraction of apoptotic cells although not significant at 24 h, reached significance at 72 h following exposure to 250 µM of resveratrol sulfates ($P \leq 0.05$; One-Way ANOVA). At 72 h the amount of apoptosis in the 250 µM sample was 6.0 ± 2.0% compared to 1.7 ± 0.5% in control cells. The percentage of live cells was also

significantly reduced with this treatment from 95.8 ± 0.8 to 89.5 ± 1.5% in control and treated cells respectively *(P ≤ 0.005*; One-Way ANOVA*)*. At this concentration of sulfates, the number of necrotic cells increased significantly relative to control at both 48 and 72 h (from 0.7 ± 0.3 to 1.4 ± 0.1% in the latter). The lower concentrations of resveratrol and sulfates also caused an increase in the percentage of apoptotic cells, although these changes were not found to be significant.

5.5.2.3 Analysis of apoptosis in HCEC cells

In the HCEC cells at 24 h (Figure 5.35) there was no difference in the number of live, apoptotic and necrotic cells between the control and treatment groups. At 48 and 72 h timepoints, there was a slight but non-significant increase in the number of apoptotic cells following incubation with resveratrol and a lesser effect in cells exposed to 75 µM of the sulfates. None of the alterations reached significance for any of the treatments and the sulfates did not appear to have any real dose-related effect on either apoptosis or necrosis.

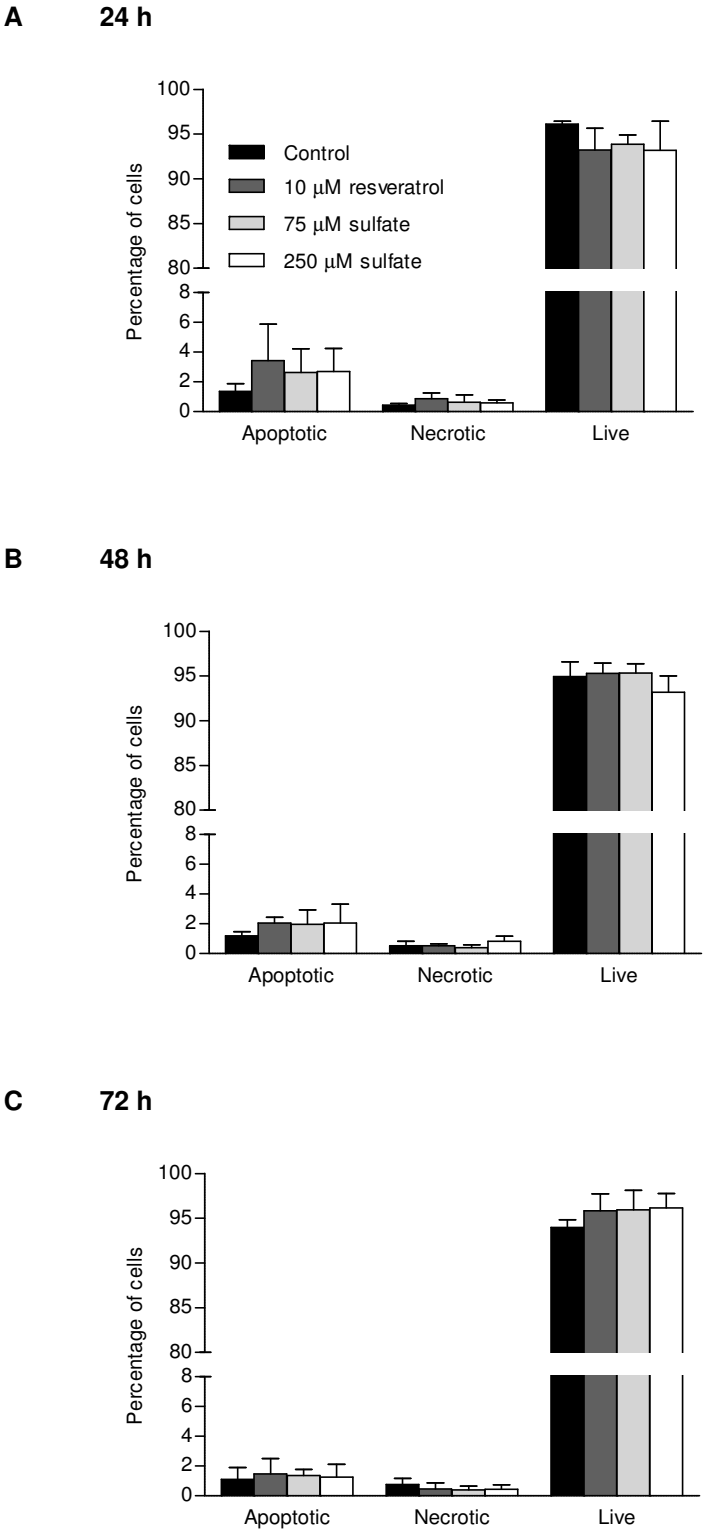

Figure 5.33 Percentage of apoptotic, necrotic and live HCA-7 cells following incubation with resveratrol and resveratrol monosulfates

Percentage of apoptotic, necrotic and live HCA-7 cells at 24, 48 and 72 h post-treatment with 10 µM of resveratrol and 75 and 250 µM of resveratrol sulfates. Note the break in the y-axis.

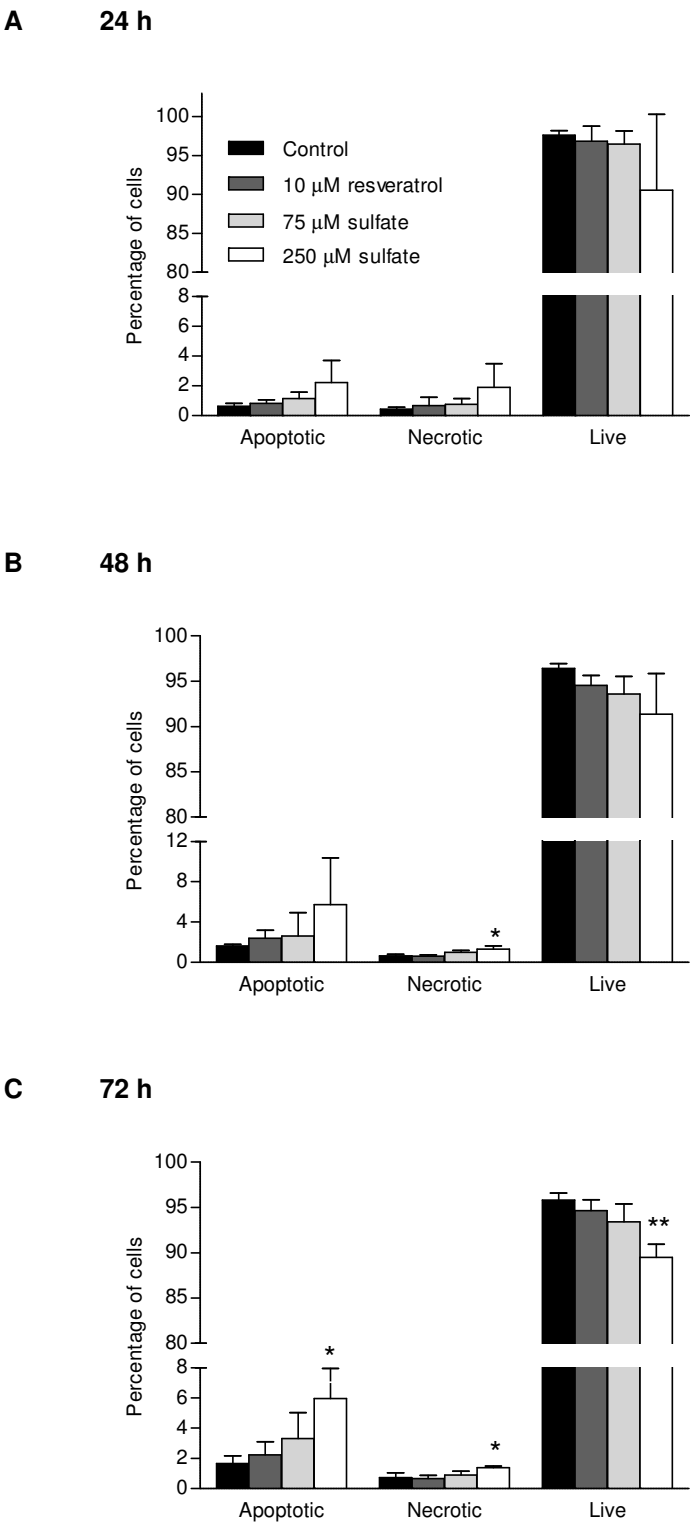

Figure 5.34 Percentage of apoptotic, necrotic and live HT-29 cells following incubation with resveratrol and resveratrol monosulfates

Percentage of apoptotic, necrotic and live HT-29 cells at 24, 48 and 72 h post-treatment with 10 µM of resveratrol and 75 and 250 µM of resveratrol sulfates. Asterisks indicate level of significance following One-Way ANOVA analysis (*$P \leq 0.05$, **$P \leq 0.005$). Note the break in the y-axis.

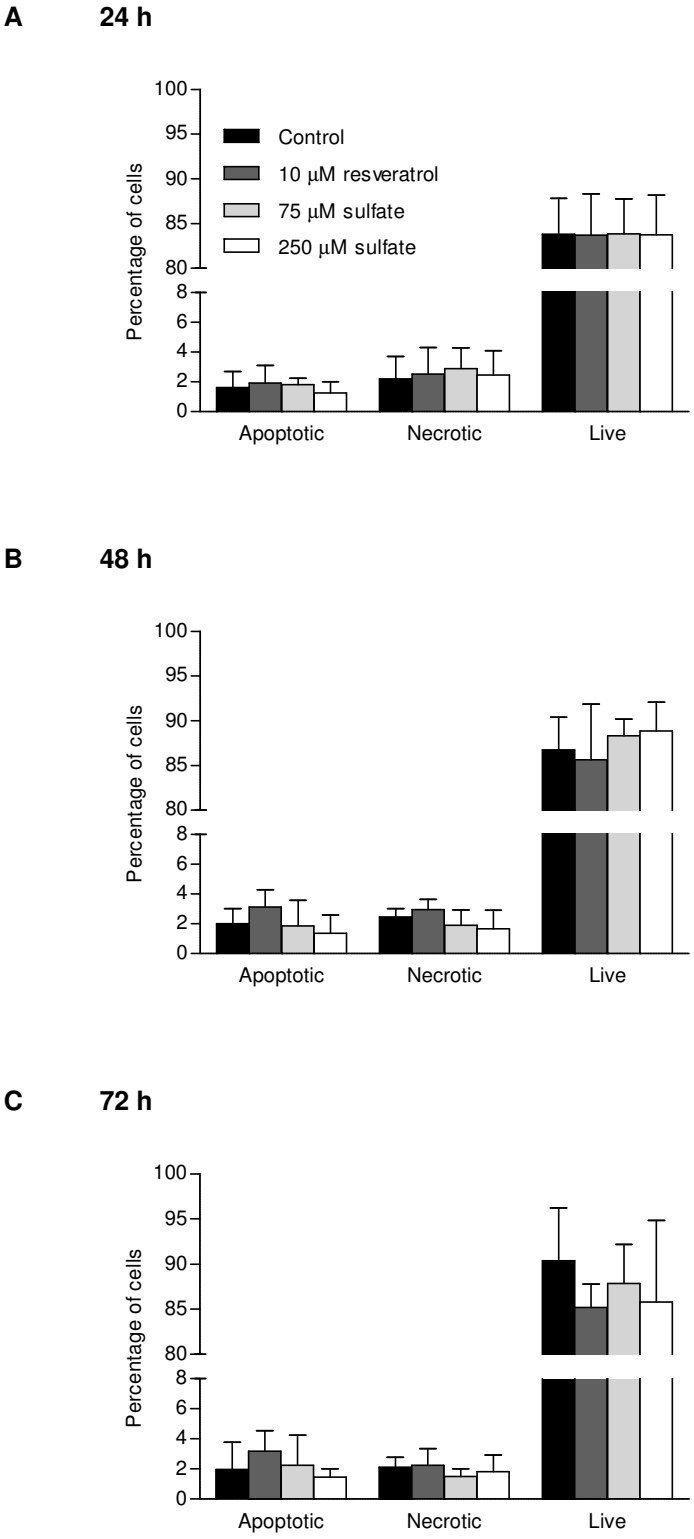

Figure 5.35 Percentage of apoptotic, necrotic and live HCEC cells following incubation with resveratrol and resveratrol monosulfates

Percentage of apoptotic, necrotic and live HCEC cells at 24, 48 and 72 h post-treatment with 10 µM of resveratrol and 75 and 250 µM of resveratrol sulfates. Note the break in the y-axis.

5.5.3 Apoptosis by cleavage of caspase-3

5.5.3.1 Analysis of caspase-3 in HT-29 cells

In order to corroborate findings obtained with the annexin V-FITC assay, a second assay was employed to determine the extent of apoptosis observed in HT-29 cells. The change in apoptosis was most prominent with HT-29 cells; however, this was only significant at the highest concentration of the sulfates. The method of analysis involves caspase-3 detection as a measure of cell death since this protein is activated in apoptotic cells and plays a direct role in the cleavage of many key cellular proteins [192].

The 48 and 72 h timepoints in HT-29 cells were selected for analysis of caspase-3, as significance was reached at these two timepoints with the annexin V-FITC assay. Cells were treated with resveratrol and the monosulfate mixture with the same concentrations as those used for the annexin V-FITC assay. Cells treated with etoposide were analysed in parallel as a positive control. Etoposide is a DNA-damaging agent that can induce subcellular structural changes associated with apoptosis. Etoposide was used as a positive control in human HCT-116 colon cells where it induced apoptosis [193].

The assay carried out here is described in Section 2.2.6.9 (Materials and Methods). Sample analysis was by flow cytometry. Representative dot plots illustrating the differential staining of cells in control samples and following treatment with the sulfates and etoposide are given in Figure 5.36. Experiments were performed in triplicate and the data combined for the 48 and 72 h timepoints to allow quantitative comparison between test and control incubations (Figure 5.37). Example dot plots of additional control samples are given in Figure 7.5 (Appendix).

At 48 and 72 h there was an increase in the caspase positive staining for all treatment groups relative to the solvent control. However, this elevation only reached significance for 250 µM sulfate and 100 nM etoposide (on both days). At the 250 µM concentration 11.4 ± 3.1% of cells were positively stained, compared to 10.5 ± 5.7% following 10 µM of resveratrol and 2.7 ± 1.5%

for the solvent control at 72 h. The reduction in caspase negative staining following sulfate treatments, although significant, did not reach levels of significance found in the etoposide-treated cells at 72 h.

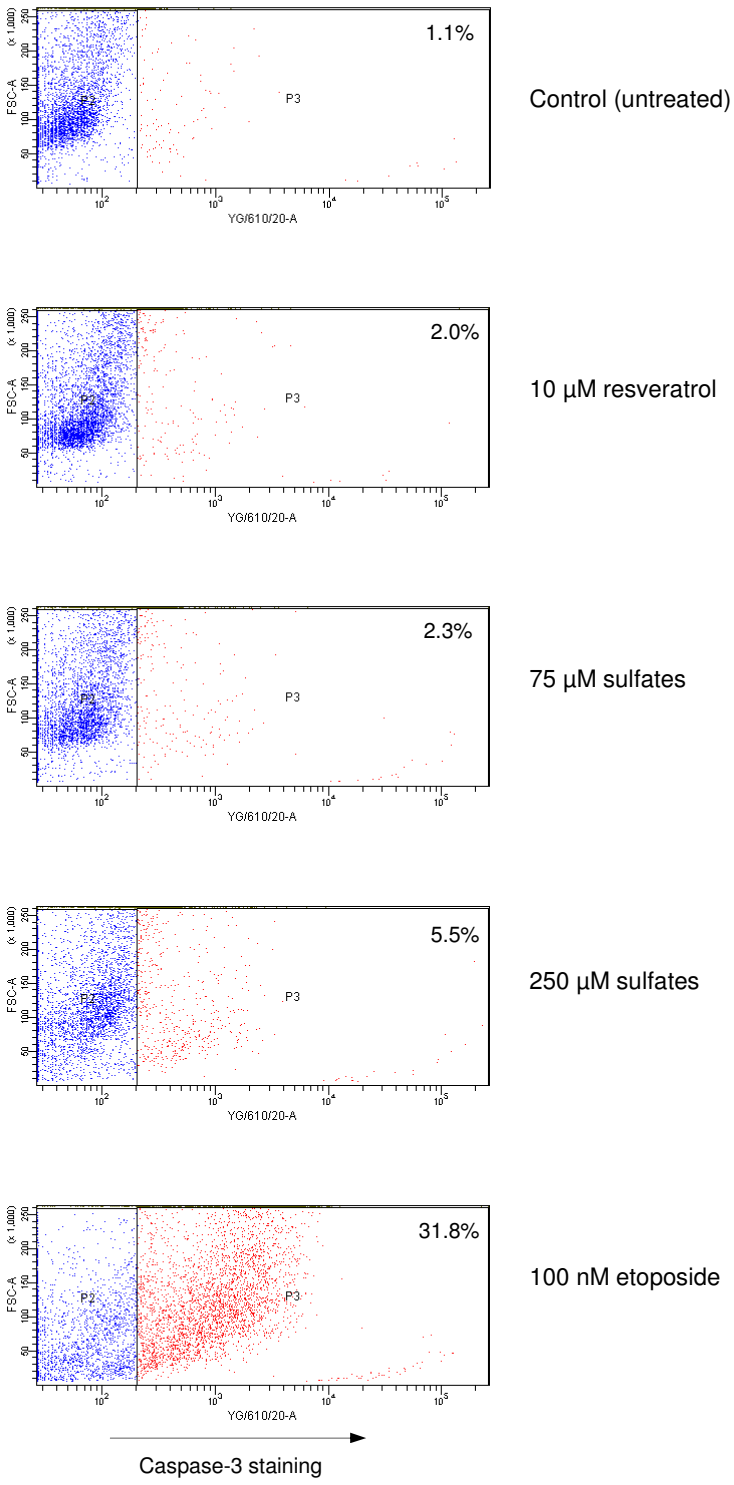

Figure 5.36 Representative dot plots for caspase-3 staining in HT-29 cells

Representative dot plots showing the differential staining for caspase-3 in HT-29 cells following treatment with 10 µM of resveratrol, 75 and 250 µM of resveratrol sulfates, 100 nM of etoposide (positive control) and control (untreated). Cells were treated for 72 h and analysed by flow cytometry. Staining was with cleaved-caspase-3 rabbit monoclonal primary antibody, and goat anti-rabbit secondary antibody. P2 and P3 indicate caspase-3 negative and caspase-3 positive staining respectively. Percentage values for positive staining are provided within each Figure.

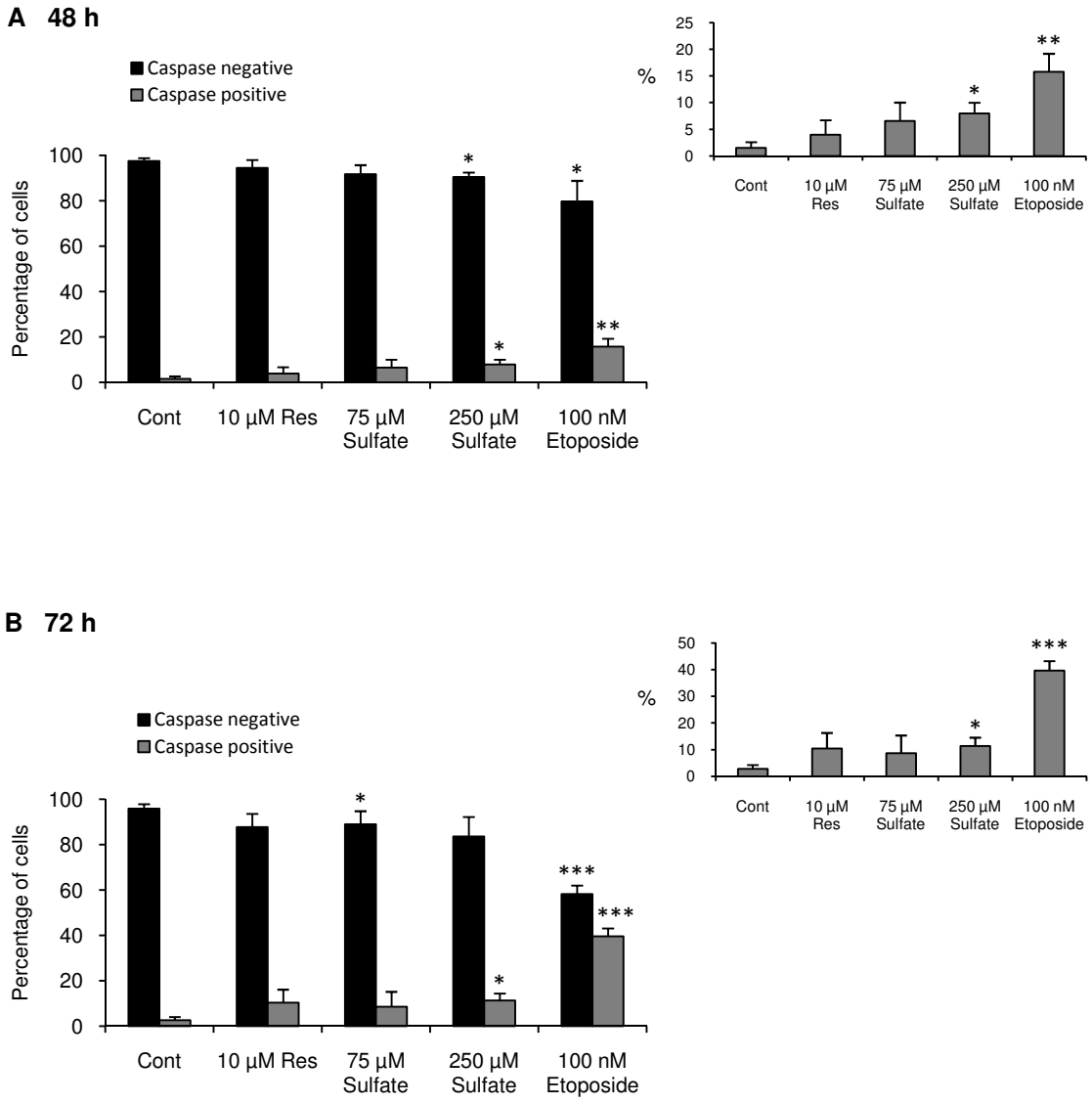

Figure 5.37 Caspase staining in HT-29 cells following resveratrol and monosulfate treatment

Percentage of caspase positive and caspase negative-staining in HT-29 cells at 48 h (**A**) and 72 h (**B**) post-treatment with 10 µM of resveratrol, 75 and 250 µM of resveratrol monosulfates and 100 nM of etoposide (positive control). Insets show the percentage of caspase positive staining more clearly. Asterisks indicate level of significance following Student's t-Test analysis (equal variance) (*$P \leq 0.01$, **$P \leq 0.005$, ***$P \leq 0.0001$).

5.6 Discussion

One of the alterations in physiology that is characteristic of cancer cells is their intrinsic or acquired ability to evade apoptosis and continue proliferating [59]. Many studies have investigated the anti-proliferative effects of resveratrol on cancer cell lines including human-derived breast, prostate and colon cancer [194], [195], [155]. Resveratrol has also undergone extensive mechanistic testing *in vitro*, in efforts to explain its various biological properties. In contrast, the predominant species *in vivo*, metabolites of resveratrol, have had limited investigations into their potential chemopreventive activity. It is possible that some of the effects attributed to resveratrol, may at least in part, be due to the major metabolites.

In this project, initial investigations examined potential effects of metabolites by measuring changes in proliferation over seven days at a range of clinically relevant concentrations. A series of growth curves were established for resveratrol monosulfates, resveratrol-4'-*O*-glucuronide and resveratrol-3-*O*-glucuronide, together with a single concentration of resveratrol for comparison. With resveratrol sulfates, there was a dose-dependent reduction in the number of HCA-7 and HT-29 cells relative to control on both day three and day seven post-treatment, although this was more pronounced in HT-29 cells. The effectiveness of the sulfates to reduce cell numbers varied in the HCA-7 and HT-29 cells, as reflected by IC_{50} values of 131 ± 10.2 and 67.8 ± 8.4 µM respectively on day seven. In the 'normal', non-malignant HCEC cell line the sulfate mixture had no significant effect at concentrations up to 250 µM, indicating these cells are considerably less sensitive than the malignant cells used. In all three cell lines, 10 µM of resveratrol caused a significant reduction in cell number, compared to the control group. On day three post-treatment in HCA-7 and HT-29 cells, 10 µM of resveratrol resulted in approximately 46 and 62% of cells remaining relative to the control, whereas to achieve a 50% reduction in cell number, higher sulfate concentrations were required. Although the IC_{50} values were not calculated for resveratrol here, they are likely to be lower than most values reported in the literature. One study found IC_{50} values of 26.2 and 19.9 µM for HCA-7 and HT-29 cells respectively [155]. Far higher IC_{50} values of 78.2 ± 4.7, 94.5 ± 3 and 152.1 ± 17.6 µM were

published for HT-29 cells following resveratrol dosing in three separate studies [83], [196], [197], indicating the large variability in results from laboratories using cells of the same type.

The changes in proliferation observed as a consequence of sulfate treatment of the colon cells are consistent with the metabolites having a reduced activity relative to parent resveratrol as found by Miksits *et al*. who measured cell proliferation following resveratrol sulfate treatment in human malignant and non-malignant breast cancer cell lines [134]. Resveratrol-3-*O*-sulfate and resveratrol-4'-*O*-sulfate were both responsible for a significant reduction in the number of cells 48 h after treatment; the results from their study are summarised in Table 5.3.

	IC_{50} (µM), mean ± SD			
	MCF-7	**ZR-75-1**	**MDA-MB-231**	**MCF-10A**
Resveratrol	68.3 ± 2.6	82.2 ± 4.8	67.6 ± 4.1	20 ± 2.9
Resveratrol-3-*O*-sulfate	258 ± 16.9	> 350	189 ± 22.5	228.3 ± 14.0
Resveratrol-4'-*O*-sulfate	> 350	> 350	> 350	202.4 ± 19.9
Resveratrol-3,4'-*O*-disulfate	> 350	> 350	> 350	202.9 ± 24.0

Table 5.3 Cytotoxicity of resveratrol and sulfate metabolites in breast cancer cells. *In vitro* cytotoxicity of resveratrol and its sulfate metabolites on human breast cancer cell lines. MCF-7, ZR-75-1 and MDA-MB-231 are malignant breast cancer lines. MCF-10A is a non-malignant breast cancer cell line. IC_{50} values were calculated 48 h post-treatment. Table adapted from Miksits *et al*. [134].

In each of the breast cell lines, resveratrol was shown to be far more potent than the sulfates. For resveratrol-3-*O*-sulfate, the IC_{50} was 3.8, > 4.3 and 2.8-fold higher than with resveratrol in MCF-7, ZR-75-1 and MDA-MB-231 respectively. Therefore, in the ZR-75-1 cells, the IC_{50} for this sulfate was more than 350 µM. Resveratrol reduced cell proliferation by 11.4-fold more than resveratrol-3-*O*-sulfate in the non-malignant MCF-10A cells.

Where measurable, resveratrol-4'-*O*-sulfate had a consistently higher IC_{50} value compared to both resveratrol and resveratrol-3-*O*-sulfate in the malignant breast cells. Concentrations exceeding 350 µM were required to reduce the cell number by 50% in all of the malignant cell lines [134]. Synthesised standards of resveratrol-3,4'-*O*-disulfate were also tested, and concentrations of 350 µM resulted in a reduction in cell number of only 10 - 16% suggesting the disubstituted metabolite is even less active than the monosulfates. In a separate study also on MCF-7 cells, the percentage survival of cells following treatment with resveratrol trisulfate, resveratrol-3,4'-*O*-disulfate, resveratrol-3,5'-*O*-disulfate, resveratrol-3-*O*-sulfate and resveratrol-4'-*O*-sulfate ranged between 1.3 and 2.8-fold higher compared to treatment with an identical concentration of resveratrol [198]. Similar differences between the parent resveratrol and sulfated conjugates were observed following treatment with these compounds in KB cells, which are derived from a human carcinoma of the nasopharynx.

These data on the breast cancer cells indicate that free phenolic groups and the positions of these groups may be important determinants of cell inhibition. In MCF-7 cells, disulfates were the least potent of the metabolites tested [134]. The trisulfate was found to be slightly less active than the two disulfates tested [133]. The structure-activity relationship of resveratrol and its derivatives has been investigated on cancer cell growth [167] and it is likely that by reducing the number of free hydroxy groups, the activity of resveratrol is reduced. Different resveratrol analogues were synthesised, and an increased number of hydroxyl groups on the ring-structure of hexahydroxystilbene (6 in total) displayed the lowest IC_{50} concentrations for colon tumour cell toxicity, and also had the most effective free radical scavenging ability [167]. Activity has been suggested to depend on a number of factors including the number and position of hydroxyl groups, intramolecular hydrogen bonding, sterioisomery and double bonds [199]. The free radical scavenging activities of resveratrol sulfate metabolites has been examined previously by measuring the ability to quench the diphenyl-p-picrylhydrazyl (DPPH) radical. Whereas the activity of resveratrol-3-*O*-sulfate was comparable to resveratrol, it was somewhat lower for resveratrol-4'-*O*-sulfate, with the disulfates being much less active and the trisulfate inactive in this system [133], consistent with the findings of Szekeres *et al*. above [167].

Both of the previously mentioned studies, which examined the effects of the sulfates in MCF-7 breast cancer cells, did so using synthesised standards of single isomers. In the present study a mixture of two sulfates was used, making it impossible to compare differences in activity between the two. However, levels of uptake for the two sulfates were measured by HPLC-UV in the three colon cell lines incubated with either the sulfate mixture or resveratrol. This could possibly provide an indication of whether there was a preferential uptake of one isomer over the other, which might help attribute the anti-proliferative effects to a particular metabolite or indeed the parent resveratrol. Monosulfates spiked into media alone were found to be relatively stable over the course of one week, whereas in the presence of HCA-7 and HT-29 cells there was a reduction in concentrations in the media, accompanied by the formation of additional resveratrol species (more pronounced in the latter cells). In addition to the presence of resveratrol-3-*O*-sulfate and resveratrol-4'-*O*-sulfate, other metabolites formed were the sulfate glucuronide, resveratrol disulfate, resveratrol-4'-*O*-glucuronide and resveratrol-3-*O*-glucuronide; the identities of these compounds were confirmed by LC-MS/MS and comparison of retention time with authentic standards where possible. The presence of the monoglucuronides in the media suggests that sulfate uptake was followed by deconjugation within the cell to parent resveratrol and reconjugation to form 'new' metabolites, which exited the cells into the media by passive and/or active processes. Deconjugation may also have preceded the formation of the disulfate and sulfate glucuronide, although it is not a prerequisite. Whereas the metabolite profiles in media were similar following incubation with HCA-7 and HT-29 cells, the profile in HCEC cells was largely unchanged with only a small amount of disulfates formed in the media, consistent with minimal uptake of the sulfates by these cells.

To our knowledge, cellular uptake of resveratrol metabolites following incubation has only been measured in one study, and not using the sulfate metabolites, or cell lines tested here and not as comprehensively [133]. The uptake of resveratrol and resveratrol-3,5-disulfate were determined following incubation with MCF-7 cells. Cells grown in the presence of the disulfate were found not to contain any detectable metabolites or resveratrol after 24 h. However, following resveratrol cell incubations, resveratrol and disulfate were both identified in cellular extracts, but not resveratrol-4'-*O*-sulfate [133]. The cell pellet analysis carried out here in

HCA-7 and HT-29 cells showed that the 3-*O*-sulfate and 4'-*O*-sulfate metabolites were most prevalent. Resveratrol derivatives detected intracellularly were the sulfate glucuronide, resveratrol-4'-*O*-glucuronide, resveratrol-3-*O*-glucuronide, resveratrol disulfate and resveratrol. Assuming an equal degree of entry into the cells, it might be reasonable to expect 1.5-fold higher concentrations of resveratrol-3-*O*-sulfate intracellulary, relative to resveratrol-4'-*O*-sulfate, based on the ratio of the sulfate mixture. However, when sulfate-spiked media was incubated with HCA-7 cells, the change in media concentration for resveratrol-4'-*O*-sulfate was not dissimilar to that in media without cells suggesting a minimal level of uptake. In line with this, the resveratrol-3-*O*-sulfate C_{max} concentration was 14.5 times greater than resveratrol-4'-*O*-sulfate in HCA-7 cells and eight times greater in HT-29 cells, where the resveratrol-4'-*O*-sulfate concentration in media did decrease noticeably. This suggests a preferential uptake of resveratrol-3-*O*-sulfate. Resveratrol concentrations generated within the cells were generally low, with C_{max} concentrations 64 and 92-fold lower than those of resveratrol-3-*O*-sulfate in HCA-7 and HT-29 cells respectively. With respect to intracellular resveratrol concentrations following sulfate dosing, we cannot say for certain whether concentrations are due to spontaneous deconjugation of the sulfates, or (more likely) enzymatic conversion by the action of sulfatases. However, extraction of sulfate standards spiked into cells and extracted for quantitation (in the same way as samples), did not indicate the presence of resveratrol, suggesting that observed levels are unlikely to be related to degradation of sulfates during the extraction procedure.

Transport kinetics and metabolism of resveratrol have been studied in human Caco-2 colon adenocarcinoma cell line monolayers [154]. A concentration-dependent biotransformation of resveratrol in the Caco-2 cells to resveratrol sulfates and resveratrol glucuronides was demonstrated. The extensive resveratrol metabolism resulted in the formation of resveratrol-4'-*O*-glucuronide, resveratrol-3-*O*-glucuronide and resveratrol-3-*O*-sulfate. Formation of resveratrol-4'-*O*-glucuronide was minor, with only 3.7% conversion during treatment with 10 µM resveratrol, compared to 12% for the 3-*O*-glucuronide isomer. This is in contrast to the metabolism in both HCA-7 and HT-29 cells where resveratrol-4'-*O*-glucuronide was the more prominent of the two glucuronides formed. Glucuronidation in the current study was favoured at position four of the molecule, and this may be related to individual cell-type differences.

However, sulfation of resveratrol was shown to be prevalent in the Caco-2 cells treated with 10 μM of resveratrol, in agreement with results in HCA-7 and HT-29 cells here following resveratrol incubation. The same concentration applied to HepG2 cells resulted in conjugated resveratrol reaching 50% at 4 h and almost 100% at 8 h. This, together with the strong binding affinity of resveratrol to media proteins is likely to account for the rapid disappearance of resveratrol in media in the presence of cells [89].

Passive transport mechanisms have been suggested to be largely responsible for transport of resveratrol across the monolayer [154]. In human hepatic cells, resveratrol uptake was shown to involve a combination of passive diffusion and carrier-mediated processes, although passive uptake would be reduced by resveratrol protein binding [200]. Metabolite concentrations measured in the media following incubation of ZR-75-1 cells with resveratrol were 17-fold greater than those in the cell cytoplasm indicating an active and rapid transport system out of the cells into the medium [138]. Metabolite formation in the cytoplasm was found to increase linearly with increasing resveratrol concentration demonstrating that resveratrol is taken up by these cells.

In the different colon cell lines used in this study, there was variability in levels of uptake, intracellular concentrations and consequently the degree of metabolism. Human intestinal and lung cell lines exposed to β-carotene have also shown a large variation in intracellular levels of the parent and metabolites, with lower levels in the colon compared to lung cell lines [201]. Each cell line also had a distinct metabolite profile. There may be a number of cell specific differences responsible for the variable levels of uptake in the three cell lines tested here, for example uptake may be related to the presence or absence of specific carriers in the cell membranes. Organic anion-transporting polypeptides (OATPs) are a family of drug uptake transporters which have been found to be capable of transporting a large array of structurally divergent drugs [202]. It has been hypothesised that these multispecific transporters are responsible for the active uptake process of resveratrol [200]. [^{3}H]-Resveratrol uptake was followed in HepG2 tumour cells, and resveratrol influx was found to be significantly lower at 4°C compared to 37°C, consistent with the carrier-mediated transport in addition to passive diffusion

[200]. In a separate investigation, the functional characteristics of human OATP-B were compared to OATP-C using uptake studies of radiolabelled oestrone-3-sulfate and oestradiol-17beta-glucuronide [203]. OATP-B accepted sulfate conjugates but not glucuronide conjugates, whereas OATP-C transported both. Therefore, these specific transporters or other OATPs may have a role in the uptake of resveratrol metabolites, and differences between intracellular sulfate metabolites observed in the cell lines in the current study may be related to a variable presence, or absence of OATPs.

Another determining factor in the concentration of sulfates found within the cells is the expression of SULTs which catalyse the sulfate conjugation of dietary polyphenols including resveratrol. SULT1A1 has been reported to catalyse the formation of two sulfated metabolites [139]. In MDA-MB-231 cells incubated with resveratrol, the cytoplasm and intracellular medium were firstly analysed and found to contain some resveratrol and higher levels of resveratrol-3-*O*-sulfate. Transfection of these cells with human SULT1A1 led to reduced intracellular concentration of resveratrol due to enhanced sulfation, compared to non-transfected cells. This alteration in metabolism correlated with a higher IC_{50} in the transfected cells compared to the non-transfected cell line [138]. The authors attributed the effects to sulfate conjugation.

In both HCA-7 and HT-29 cells, consistently higher intracellular resveratrol concentrations were achieved following incubation with 75 µM of sulfates compared to resveratrol (10 µM) (Figure 5.27). In HCA-7 cells resveratrol concentrations were 3.4-fold higher after treatment with the sulfates for 1 h. Similarly, in the HT-29 cells 2.9-fold higher resveratrol concentrations in sulfate-treated compared to resveratrol-treated cells were present at the same timepoint. Despite the lower intracellular levels of resveratrol detected, 10 µM of resveratrol was more potent in HCA-7 cells than 75 µM of sulfates at both 72 and 168 h after dosing. In HT-29 cells, there was a comparable inhibition of cell number at these concentrations at 72 h, whereas at 168 h the sulfates were almost twice as effective at reducing cell number compared to 10 µM of resveratrol. Extracellular resveratrol concentrations were higher with resveratrol incubation, and it is possible that resveratrol could have a binding affinity for the cell membrane, and this binding contributes to the anti-proliferative effects. When the uptake and distribution of

resveratrol was followed in prostate stromal and prostate epithelial cells using [^{3}H]-resveratrol, considerable binding of [^{3}H]-resveratrol to proteins in cell extracts was observed within ~2 minutes [204]. This suggests a rapid initial uptake/binding of resveratrol by the cells. The distribution of radioactivity varied in the prostate stromal and epithelial cells, although the highest levels in both were preferentially localised in the membrane/organelles (approximately 40%) [204]. The differences in distribution in various cell compartments, along with the rapid incorporation into cells suggest that there may be significant resveratrol levels attached to the membrane fractions of the colon cell lines in the present study. Furthermore, resveratrol levels may not have not been detected by the extraction method employed, which discards cell membranes and debris.

Effects of resveratrol have been examined on membrane properties of model systems consisting of unilameller liposomes of phosphatidylcholine [205]. In their study, location of resveratrol pointed to a membrane distribution, with the compound penetrating into the acyl membrane region with its polar hydroxyl group near the headgroup region of the membrane. Another study found that the highest level of specific [^{3}H]-resveratrol binding evaluated in rat brain subcellular fractions was detected in the plasma membrane fractions followed by the nuclear and large cellular components [206]. The [^{3}H]-resveratrol binding to the plasma membrane fraction was shown to be significantly reduced by trypsin digestion and boiling for 10 min (by approximately 80% for each), suggesting that the binding sites are of a proteinaceous nature [206]. In the current study trypsin was used to detach cells from flasks at the time of harvesting. The extraction method from pellets relied on freeze-thaw cycles in liquid nitrogen interspersed with rapid heating at 50°C. The protein debris was also discarded, and it is possible that all of these factors may have reduced resveratrol levels being detected. Han and colleagues used competition binding experiments to show that [^{3}H]-resveratrol binding was competed for by various natural and synthetic polyphenolic compounds with epigallocatechin gallate, epicatechin-3-gallate and resveratrol being the most potent. The authors suggested that these high affinity sites present at the level of the plasma membrane are functionally relevant and may serve as polyphenol 'receptors' initiating a cascade of events leading to their various biological effects [206].

Another possible explanation for the low intracellular resveratrol levels in the colon cell lines and relatively high level of activity compared to the sulfates could be related to resveratrol following a non-conventional dose response relationship. Therefore, at a low concentration of resveratrol there may be a greater effect on the cells compared to higher concentrations. Unusual dose-activity relationships have recently been reported for resveratrol in a number of human cell lines [207], [208]. For example, resveratrol has been shown to exhibit a biphasic effect in endothelial progenitor cells *in vitro*, where it increased nitric oxide synthase expression at 1 µM, but had an inhibitory effect at higher concentrations of 60 µM [209]. In the same study, these findings were confirmed in a murine model of aorta repair *in vivo*. Resveratrol at a dose of 10 mg/kg increased endothelial nitric oxide synthase expression and the number of endothelial progenitor cells in the circulation in injured arteries, whereas at a higher dose of 50 mg/kg these responses were not elicited. However, it is important to note that the majority of the work that has investigated these relationships is associated with cardiovascular changes. Another possibility could be that metabolites block, or have some opposing actions to resveratrol, so higher concentrations of metabolites in a cell may prevent resveratrol from activating signalling pathways.

The ability of resveratrol glucuronides to reduce cell number was also assessed in HCA-7 and HT-29 cell lines. The resveratrol glucuronides were synthesised separately enabling any potential reduction in cell number to be attributed to a specific glucuronide isomer. The reduction in proliferation was not as marked as that seen following treatment with the sulfates or resveratrol. In the HCA-7 cells the only significant reduction reached with resveratrol-3-*O*-glucuronide was at concentrations of 100, 125 and 250 µM (72 h post-treatment only). Resveratrol-4'-*O*-glucuronide had no significant effect at any of the concentrations tested in this cell line. HT-29 cells appeared to be the more sensitive cell line to both glucuronides, with significant reductions achieved at concentrations of 75 µM and above for the 3-*O*-glucuronide and 100 µM and above for the 4'-*O*-glucuronide (at 72 h). In both cell lines and with both glucuronides, any reduction in cell number was less pronounced on day seven, perhaps suggesting a reduction in the glucuronide stability over the week, or that the cells had overcome any initial anti-proliferative effects. The cell proliferation data indicate a greater anti-proliferative

activity of resveratrol-3-*O*-glucuronide above resveratrol-4'-*O*-glucuronide. This could be related to improved uptake, possibly due to a higher binding affinity/transport within the cellular membrane, or an increased cytotoxicity due to differences between the isomers. Uptake studies would be useful for the glucuronides to determine whether, like in HCEC cells, there is minimal uptake which might help to account for their limited activity. Investigations into the resveratrol glucuronide metabolites are less common than those on the sulfate metabolites. However, one published study investigated the cytotoxicity of the two glucuronide isomers on peripheral blood mononuclear cells (PBMCs) and found that neither metabolite was cytotoxic at concentrations of up to 300 µM, in contrast to resveratrol which was cytotoxic at concentrations of 30 µM, 90 µM and 270 µM. Their activity against HIV-1 infection was also measured (in synergy with didanosine) and neither isomer had any effect up to concentrations of 300 µM [152]. Based on the limited activity (and availability) of the glucuronides, experiments investigating uptake and metabolism were only carried out with the resveratrol sulfates in this project.

As described earlier, the sulfate metabolites caused a significant reduction in proliferation of colon cancer cells, particularly at the higher concentrations. To help determine whether the sulfate treatment was causing cells to arrest or inducing apoptosis, cell cycle analysis was performed using flow cytometry. Where significant differences in the profiles relative to the control cells were observed, they were only achieved at the higher concentrations of compounds (10 µM of resveratrol and 250 µM of the sulfate mixture). In HCA-7 cells there was a significant increase in the number of cells in S-phase following resveratrol and sulfate treatment at 24 h. This effect remained at 48 h for the sulfate, along with significant reductions in the G0 - G1 and G2 - M phases. In HT-29 cells significant differences relative to the control were found at 24, 48 and 72 h, but only for 250 µM of sulfate with an increase in S-phase alone. There appeared to be a reduction in the proportion of cells in G0 - G1 with increasing sulfate treatment, however these changes were not significant. Finally, in HCEC cells there was no significant difference between control groups and any of the sulfate-treated groups. The only significance was achieved following treatment with the positive control, 10 µM resveratrol, which

resulted in an increase in G0 - G1 (indicative of apoptosis or necrosis) at 48 and 72 h relative to the solvent control, as well as a reduction in S-phase at 72 h.

Literature supports the role of resveratrol as an agent that can alter the passage of cells through the cell cycle, whereas to our knowledge cell cycle analysis has been carried out on resveratrol metabolites in only one study [133]. The authors showed that in HL-60 human acute leukaemia cells, resveratrol was active, causing an accumulation of cells in the G1 phase. However, sulfate metabolites were inactive in this system. In HT-29 cells, published data suggests that resveratrol can cause a pronounced reduction in the percentage of cells in the G2 - M phase, which is compensated by an accumulation of cells in the G0 - G1 phase [196]. However, this particular study used concentrations more than 9-fold greater than in the experiments here, which might account for the differences. In a study which examined cell cycle changes in Caco-2 and HCT-116 colon cancer cell lines, following resveratrol treatment, there was a significant increase in the number of cells in S-phase for both cell lines at concentrations ranging from 12.5 - 200 µM [85], which is similar to the findings in the HCA-7 and HT-29 cells here. The majority of other studies have used concentrations much greater than the 5 and 10 µM of resveratrol used here; however, the general trends are similar.

The lack of effect of resveratrol sulfate on the cell cycle progression in HCEC cells is consistent with the absence of anti-proliferative activity and may be explained by the extremely low intracellular concentration detected as a result of this exposure. In accordance with the proliferation data, significant differences were only found with resveratrol-treated HCEC cells. The general lack of effect in HCA-7 and HT-29 cells on the cell cycle, despite the reduction in cell numbers, suggests that perhaps the compounds affected cells in a non-cell cycle stage specific fashion. In the study by Hoshino *et al.*, although none of the sulfate metabolites were found to affect the cell cycle, a different cell line was employed to those used here [133]. Apoptosis in the cell lines here may have accounted for the results generated from the cell cycle analysis and the reduction in cell proliferation.

Therefore, markers of apoptosis were measured using annexin V-FITC staining in all three cell lines, and analysed using flow cytometry. In HCA-7 cells there appeared to be a slight increase in apoptosis at 24 and 48 h, however the change was not significant. In HCEC cells, again there were no significant changes, as would be expected for the sulfates, but also none with resveratrol (although levels of apoptosis were slightly elevated above the other treatment groups at all times). Of the three cell lines, the HT-29 cells were most sensitive, with significant increases in apoptosis and necrosis occurring, but only following treatment with 250 µM of sulfates. At 48 and 72 h there were significant increases in necrosis. Also at these timepoints, there were increases in apoptosis in the treated cells; however, the increases were small, less than 5% above control. Significance was reached with the highest concentration of sulfates at 72 h, and the corresponding reduction in the number of live cells was also highly significant.

The effects of resveratrol treatments on apoptosis were determined in SW480 human colon cells [82]. In these cells, resveratrol underwent apoptosis in a dose- and time-dependent manner at concentrations ranging from 10 - 100 µM, measured at 48 and 72 h. In HT-29 cells incubated with 1, 10 and 100 µg/ml of resveratrol for 24 and 48 h high levels of apoptosis were induced at the higher two concentrations, but not at the lowest [210]. Various studies such as these have demonstrated a significant degree of apoptosis *in vitro*, but the concentrations used to observe an effect are typically much higher than the 10 µM used here, and often above achievable levels in humans. Neither the resveratrol nor the sulfate metabolites caused a large amount of apoptosis. The fact that there was no significance achieved in the level of apoptosis with 10 µM resveratrol in this study may be related to the concentration not being high enough. However, a reasonable reduction in cell proliferation was observed with 10 µM in the current study, which would therefore suggest either an increase in the cells becoming cytostatic or apoptotic/necrotic, or a combination of the processes. The HT-29 cell line was shown to have significant changes with respect to apoptosis, and therefore this cell line was selected for analysis of caspase-3. Caspase-3 is a frequently activated death protease, which catalyses the cleavage of many cellular proteins [192], and was therefore a useful additional measure of apoptosis. At 48 and 72 h following treatment of 250 µM sulfates and 100 nm etoposide, there was a significant increase in the caspase-3 positive staining compared to control levels. There

was a corresponding reduction in the caspase negative cells, which reached statistical significance following both treatments. Resveratrol (10 µM) and sulfates (75 µM) appeared to increase the positive staining compared to control at 48 and 72 h, however, the changes were not found to be significant. These findings are in agreement with results from the annexin V-FITC assay in this study, where significant increases in apoptotic and live cells were only observed at the highest concentration of resveratrol sulfates after 72 h of treatment. The most obvious change was achieved with the chemotherapy drug etoposide, at both timepoints. Following etoposide treatment for 48 and 72 h there was more than a doubling of positive staining in cells, compared with only a slight increase in positive staining for all other treatment groups.

In a separate study, effects of resveratrol on caspase-3-like activity were determined over time after incubation with 150 and 250 µM of resveratrol. At the lower concentration, caspase-3-like activity increased significantly by 250%, 300% and 340% above control values [83]. The increase in caspase activity was first evident at 12 h, with an increase of 275% above control cells. When lower concentrations of resveratrol (10 - 100 µM) were used for 24 h incubations, a significant increase above control was only achieved at concentrations equal to, or exceeding, 100 µM. These results support a time- and dose-dependent increase in caspase-3 activity, with the highest activation (7-fold above control cells) induced by 250 µM of resveratrol [83]. Significant increases in caspase-3 activity have also been described in Caco-2 cells, 24 h after dosing [85]. Similarly, resveratrol induced apoptosis through one or several caspase-dependent pathways in SW480, SW620 and HCT-116 human colon carcinoma cell lines [82].

One of the health properties for which resveratrol is known is its ability to affect lifespan and age-related markers. This was examined in the short-lived fish *Nothobranchius furzeri* [211] where a 59% increase in lifespan was observed over the course of the study and resveratrol was also found to delay motor and cognitive age-related decline. Increases in longevity have also been demonstrated in other species including *Caenorhabditis elegens* [212], *Drosophila melanogaster* [213] and *Saccharomyces cerevisiae* [213,214]. Age-related diseases are associated at the cellular level with senescence. When 10 µM of resveratrol was used to

chronically treat endothelial cells, it induced elevated levels of reactive oxygen species (ROS), associated with an increase in the number of cells in S-phase [65]. Furthermore, cell accumulation in S-phase was shown to result in increased senescence. Two nicotinamide adenine dinucleotide phosphate-oxidase (NADPH) oxidases were identified; Nox1 and Nox4, which are major targets of resveratrol and primary sources of ROS that act upstream of the observed S-phase accumulation. This might explain the observed increase of cells in S-phase following sulfate treatment, and also account for the limited amount of cell death (as detected by apoptosis and caspase assays), due to increased levels of senescence. Assays for the detection of senescence involve cytochemical staining of cells [215], and would not have been picked up by the annexin V-FITC and caspase assays used in this study. Resveratrol has also been shown to inhibit cell growth and induce senescence in osteosarcoma (U-2 OS) and lung adenocarcinoma (A549) cells by altering DNA metabolism [216]. Chronic administration of subapoptotic concentrations of resveratrol in HCT-116 cells also induced senescence-like growth arrest as determined by cell staining [217]. A common feature of both these studies was that resveratrol dosing was long-term.

In the present study, the increases in the S-phase were most prominent following dosing with 250 µM of the sulfates. Based on the intracellular concentration data presented earlier for HCA-7 and HT-29 cells, it is evident that following a single treatment of the cells with sulfates for one week, there is a continuous presence of resveratrol within the cells containing levels higher than those achieved with a single 10 µM resveratrol dose. Senescence induction might require this continuous presence, or regular pulses of resveratrol, as suggested by Heiss *et al.* [217]. Unlike the sulfate-treated cells, where increases in S-phase were consistent and significant, following 10 µM dosing with resveratrol, there was a significant increase of HCA-7 cells in S-phase at 24 h only. This may be due to the single treatment and loss of resveratrol over time from media, in addition to the relatively low concentration of resveratrol. The lack of effects seen with the cell cycle analysis, annexin V-FITC and caspase assays following treatment, is likely to be related to the low concentration. As part of a further investigation, it would be useful to assess whether there is any senescence occurring in the sulfate-treated HCA-7 and HT-29 cells, by following the change in expression of β-galactosidase - a biomarker that identifies

senescent human cells *in vitro*, and is expressed by senescent, but not presenescent cells [67]. At the same time, senescence could be measured following single and repeat resveratrol dosing.

A separate area of investigation would be to determine whether autophagy is induced by these compounds. Autophagy is a fundamental self-degradation process that is characterised by the formation of double-layered vesicles (autophagosomes) around intracellular cargo for delivery to lysosomes and proteolytic degradation [218]. Microtubule-associated protein 1 light chain 3 (LC3) is the only well-characterised protein that is specifically localised to autophagic structures throughout the process from phagophore to lysosomal degradation [219]. This protein has been shown to be up-regulated in a number of human cancer cell lines including colon [220] and breast [221]. In the investigation on breast cancer cells, autophagy was found to be induced by resveratrol as a caspase-independent cell death mechanism [221]. Initial investigation into the effect of resveratrol sulfates on induction of autophagy in the colon cell lines which has been undertaken as part of the current research, indicates that there is induction of autophagy by the sulfates. Furthermore, this appears to be cell-specific, with the greatest change occurring in HT-29 cells, with little or no effect in the HCEC cells, which is consistent with the cell proliferation data. Further work is required to verify these suggestions.

An important question that this set of data raises is whether the observed intracellular presence of resveratrol following sulfate dosing is responsible for the effects seen with sulfates on proliferation, cell cycle, apoptosis and caspase-3 staining. A useful experiment would be to measure the effect on cell proliferation with sulfates co-incubated with and without sulfatase inhibitors. Sulfatase inhibitors may reduce or prevent any enzymatic conversion to resveratrol and might help rule out any activity as a result of resveratrol generated *in vitro*. Following on from this, it would be interesting to determine whether the sulfates modulate some of the major targets in colon cell lines, for example COX activity, which resveratrol is known to affect *in vitro*. The effects of sulfates against some of the targets, such as inhibition of COX-1 and COX-2 activity, have already been tested with resveratrol-3-*O*-sulfate and resveratrol-4'-*O*-sulfate in human embryonic kidney HEK-293 cells [133] and the results are tabulated in Table 5.4.

	IC_{50} (µM), mean ± SD		
	Resveratrol	**Resveratrol-3-*O*-sulfate**	**Resveratrol-4'-*O*-sulfate**
COX-1	6.65 ± 2.5	3.6 ± 0.8	5.55 ± 1.73
COX-2	0.75 ± 0.52	7.53 ± 4.7	8.95 ± 1.2

Table 5.4 Effect of sulfate metabolites on COX-1 and COX-2 inhibition. *In vitro* inhibition of COX-1 and COX-2 in human embryonic kidney (HEK-293) cell lines by resveratrol and its sulfate metabolites. Data taken from [133].

These data show that the IC_{50} for inhibition of COX-1, by either sulfate, particularly resveratrol-3-*O*-sulfate, is lower than with resveratrol, although COX-2 inhibition is more than 10 times weaker. In a separate study which also analysed inhibition of COX-1 and COX-2, resveratrol-4'-*O*-sulfate had IC_{50} values of 5.1 ± 0.55 µM and 2.5 ± 0.35 µM respectively, consistent with the findings above [135]. However, for resveratrol-3-*O*-sulfate, IC_{50} values were 68 ± 2.8 µM and > 300 µM respectively. The values for resveratrol-3-*O*-glucuronide were also high (150 ± 5.8 µM and > 300 µM for COX-1 and COX-2 respectively). No indication of why there were differences was given by the authors. The COX enzymes are responsible for catalysing the first stage in the oxidation of arachidonic acid to prostaglandin H2, a common precursor for the prostaglandins (e.g. PGE_2), which can stimulate tumour cell growth. Therefore, inhibition of this enzyme may be an important function for a chemopreventive agent.

In addition, only resveratrol-4'-*O*-sulfate was shown to inhibit the induction of NF-κB to a similar degree as resveratrol, although the IC_{50} values were over 100-fold higher with the sulfate. NF-κB plays an important role in tumour formation and progression, therefore, inhibition of this transcription factor may be beneficial. Nitric oxide production and quinone reductase (QR1) expression were all reduced by resveratrol and the sulfate metabolites; however metabolite effects were consistently less marked than those achieved with resveratrol [133]. Excessive nitric oxide causes inflammatory diseases and cancer; therefore, reducing levels may be a mechanism of chemoprevention. Quinone reductase 1 (QR1) and QR2 enzymes are high affinity targets of resveratrol. The induction of QR1 is considered a biomarker for cancer prevention, since the function of QR1 is to inactivate harmful xenobiotic compounds. The

function of QR2 is less well-defined, although it behaves in a similar way to QR1. However, when the potential inhibitory effect on QR2 by sulfate metabolites was measured, there was no change, although there was in the presence of resveratrol [135].

In a different study investigating potential mechanisms of resveratrol metabolites another panel of enzymes were screened for activity [133]. Aromatase activity was inhibited by all of the metabolites with reductions similar to, or slightly lower than resveratrol. The greatest reductions were observed with resveratrol-3,5-disulfate and resveratrol-3,4'-disulfate (22.5 ± 0.64% and 20.5 ± 0.43%), compared to resveratrol inhibition (34.8 ± 1.21%) [133]. Aromatase inhibitors prevent the synthesis of oestrogen, which has been an important target for the prevention of breast cancer. The effect of resveratrol on the expression and enzyme activity of aromatase has been investigated in breast cancer cells, where resveratrol inhibited aromatase activity with an IC_{50} value of 25 µM in MCF-7 cells [222].

The reduced activity of the resveratrol metabolites compared to resveratrol that has been discussed in this chapter is perhaps not surprising in light of some of the literature which has also investigated the activity of metabolites of other xenobiotic substrates of conjugating enzymes. Metabolites of the chemopreventive agents quercetin and genistein have also been evaluated for activity [223], [224]. In the quercetin study, quercetin-3'-sulfate and quercetin-3-glucuronide were examined for their ability to affect endothelial cell proliferation and angiogenesis. Whilst quercetin and quercetin-3-glucuronide inhibited VEGF-induced endothelial cell functions and angiogenesis, quercetin-3'-sulfate had an opposing effect, indicating that the effects of circulating conjugates are different depending on the metabolite [223]. The antioxidant properties of genistein-4'-sulfate and genistein-4'-7-disulfate and their effects on platelet aggregation, monocyte and endothelial function were investigated. Antioxidant assays indicated that genistein is a relatively weak antioxidant and the sulfated metabolites were even less potent, which is consistent with data for resveratrol and its metabolites. Sulfation masks important hydroxyl groups, which could result in a decreased antioxidant potential, as well as a reduction of other functions. This data supports the idea that the conjugates have differing effects, which are dependent on their structure. Morphine-6-

glucuronide was tested for potential activity in a study where the metabolite was synthesised and administered to patients. The authors concluded that it is likely that the majority of the therapeutic benefit of morphine is mediated by morphine-6-glucuronide [225]. For resveratrol metabolites it is still a possibility that there are target(s) for which the metabolites are more effective, and this requires further investigation. Also as part of further investigations, additional experiments could use a mixture of metabolites, which more accurately reflect the *in vivo* situation, in order to determine whether there is an additive or synergistic effect of multiple metabolites.

With all of the metabolites, their *in vitro* effects may not necessarily reflect their *in vivo* function. As suggested by Wang and colleagues [152], metabolites may provide a source for regenerating resveratrol at various sites within the body by human sulfatases. As discussed in the previous chapter, the work with sulfate dosing in mice indicates that resveratrol can also be formed from the sulfate metabolites *in vivo*. Quercetin-7- and quercetin-3-glucuronide incubated with HepG2 cells were shown to undergo hydrolysis of the glucuronide by endogenous β-glucuronidase followed by sulfation to quercetin-3'-sulfate [226]. In certain disease states, such as cancer, it has been reported that β-glucuronidase activity was elevated compared to healthy individuals [227]. Therefore, glucuronidation (and sulfation) in the body may have a role in detoxification, disposition, and prolonging the effectiveness of resveratrol in humans.

The metabolite concentrations generated in the plasma of healthy volunteers and colon tissues of cancer patients discussed in Chapter 3, justify the concentrations used in the *in vitro* experiments here. The reduction in cellular proliferation with sulfates in the colon cells indicates that they can elicit effects at concentrations within the observed range. Based on existing data from recent studies, sulfate metabolites may possess useful properties, such as hitting molecular targets, for example COX enzymes, scavenging free radicals and increasing QR1 expression, at concentrations below those required to reduce cancer cell proliferation [133], [135]. It is possible that some of these effects may be related to regeneration of resveratrol *in vitro*.

CHAPTER 6: CONCLUDING DISCUSSION

Colorectal cancer is the third most common cancer diagnosed in the United States, and the second leading cause of death due to cancer [228]. Risk of developing this disease is related to lifestyle and diet. Chemoprevention through dietary agent(s) would be a useful strategy for reducing the cancer risk and possibly preventing its onset, whilst having a low potential for unwanted side effects. Resveratrol has been investigated as a chemopreventive agent in preclinical models, and has undergone PK evaluation studies in humans, which have recently been reviewed [229], [230]. The biological activity and bioavailability of resveratrol metabolites is important in understanding the potential beneficial effects of resveratrol.

In the dose escalation study performed in this project, healthy volunteers consumed daily doses of 0.5 - 5 g resveratrol for 29 days. Average C_{max} concentrations of resveratrol in plasma were consistently below those of its metabolites across all dose groups. Metabolite concentrations in this study, as well as several others have been reported as resveratrol equivalents, based on the extraction and UV absorption characteristics of resveratrol [107], [86], [159]. When three selected sets of volunteer samples (per dose group) were reanalysed and the C_{max} values recalculated using metabolite standards, concentrations were even higher. The average resveratrol-3-*O*-sulfate and resveratrol-3-*O*-glucuronide C_{max} concentrations in volunteer samples were 6.8 and 8.2 µM respectively based on resveratrol standard curves. The corresponding concentrations increased to 23.2 µM and 24.6 µM respectively, when metabolite standard curves were used to determine levels. Similarly, sulfate and glucuronide levels in human tissues were higher than those cited [159], with fold increases of 1.7 and 1.6 respectively. Therefore, based on calculations with the sulfate standards, an average of 21.5 ± 32.3 nmol/g (21.5 µM) of resveratrol-3-*O*-sulfate was detected in right-sided tumours following repeated 1.0 g doses of resveratrol in all patients examined. There was great variability between tissue samples and between patients; achievable concentrations were much higher than the group average levels, with resveratrol-3-*O*-sulfate reaching an average of 185.3 ± 272.7 nmol/g across tissues in one patient, and a maximum of 638 nmol/g in one tissue sample. These data highlight the possibility for metabolite accumulation in human colon and tumour

tissue, which are targets for chemoprevention. Metabolite concentrations have been determined in liver and kidney tissues following oral administration of resveratrol to Wistar rats [71]. However, to our knowledge this is the first time that they have been accurately quantified in humans.

To assess the potential of resveratrol metabolites to cause reductions in cellular proliferation, growth curves in human HCA-7, HT-29 and HCEC colorectal cell lines were established, using a range of concentrations, as determined from the levels generated in humans in the current studies. One of the limitations of the work on the sulfates here was that the treatment consisted of a mixture of resveratrol-3-*O*-sulfate and resveratrol-4'-*O*-sulfate at a ratio of 3: 2. Although resveratrol-3-*O*-sulfate was more prominent *in vivo*, and more abundant in the mixture, the ratio of the sulfates in the authentic mixture did not exactly reflect levels found in human samples. Resveratrol-4'-*O*-sulfate was a minor metabolite in both plasma and tissues. Taking plasma as an example, the average C_{max} resveratrol-4'-*O*-sulfate concentrations across the 5 g dose level were between 29 and 85-fold lower than the corresponding concentrations of resveratrol-3-*O*-sulfate. Since resveratrol sulfates are not commercially available, and chromatographic separation of the quantities required for this research would have been very difficult, both metabolites were tested together. Importantly, the synthesised mixture still allowed evaluation of several properties of these metabolites.

The resveratrol sulfates were shown to inhibit cell growth in the cell proliferation assays, with IC_{50} values of 67.8 ± 8.4 µM and 131 ± 10.2 µM in HT-29 and HCA-7 cells respectively, but no effect in the normal tissue-derived HCEC cell line. These differences in growth inhibition could be related to a number of factors including the presence, or absence of known metabolite transporters such as OATPs. These transporters are predominantly responsible for the uptake of oestone-3-sulfate in Caco-2 cells [231]. Differential expression of OATPs may result in altered extents of metabolite uptake. Another possibility could be polymorphisms of drug-metabolising enzymes exhibited by the different cells, which affect metabolism and may consequently alter cellular proliferation. Uptake studies of the sulfates and resveratrol were conducted as part of this research, as a possible means of explaining the differential activity.

Sulfate uptake, as measured by intracellular concentrations, was correlated with anti-proliferative effect. Intracellular levels were greatest in the HT-29 cells, which also had the highest cell growth inhibition following treatment. Transport of resveratrol-3-*O*-sulfate into cells was higher than resveratrol-4'-*O*-sulfate in both cell lines, perhaps indicating a greater role of resveratrol-3-*O*-sulfate in the cell growth inhibition. Some assumptions can be made based on the few published studies where resveratrol sulfates were synthesised and tested separately for their biological activity [134], [133], [135]. The two studies which investigated the anti-proliferative activity of these monosulfates demonstrated that resveratrol-3-*O*-sulfate was the more potent in MCF-7 breast cancer cells [134], [133]. This was also the case in KB cells, (derived from a human carcinoma of the nasopharynx) [133]. Despite the reduced anti-proliferative activity of resveratrol-4'-*O*-sulfate compared to the 3-*O*-isomer, the minor metabolite was shown to be more active in assays relating to NF-κB inhibition [133], and caused a similar or greater degree of COX-1 and COX-2 enzyme inhibition [135]. Therefore, it is possible that even with a limited uptake into cells resveratrol-4'-*O*-sulfate can elicit beneficial effects.

Resveratrol was formed intracellularly at low levels following monosulfate dosing in the malignant cell lines used here. Therefore, the possibility cannot be excluded that the effects in the cells are mediated by resveratrol. Conversion of metabolites to resveratrol *in vitro* (or *in vivo*) has not previously been shown. Intracellular resveratrol concentrations were also assessed by HPLC-UV, and surprisingly, resveratrol concentrations in the sulfate-treated cells were higher than those in the resveratrol-treated cells even though this was associated with a smaller antiproliferative effect. This could be due to the avid metabolism of resveratrol to its metabolites *in vitro*, as demonstrated when incubated with cells [154], [89]. One way of addressing which compound is responsible for the *in vitro* activity observed might be to use sulfatase inhibitors to prevent sulfate conversion to parent, during the course of cell incubations. If cell proliferation was still reduced in the presence of inhibitors, this would suggest that the sulfates were predominantly responsible for changes in cell proliferation.

Additional analyses were performed to investigate metabolite and resveratrol action in cells. Alterations in the cell cycle were determined, and cell death was measured using apoptosis

assays and identification of caspase-3 activation. Based on the reductions in cell proliferation, particularly at the highest sulfate concentrations, the small changes detected using these assays were not thought to be of sufficient magnitude to explain the proliferation data. Results from the *in vitro* studies suggested that the sulfate metabolites exert their effects largely through caspase-3 independent cell death. Resveratrol has been shown to induce senescence [216], [65], [217] and autophagy [232], [233], and these are both mechanisms through which sulfate metabolites might act to reduce cell numbers, and they require further investigation.

Pharmacokinetic studies in mice helped to provide valuable information regarding metabolite bioavailability and tissue distribution. The absolute bioavailabilities of resveratrol-3-*O*-sulfate and resveratrol-4'-*O*-sulfate were approximately 14% and 3% respectively. Although resveratrol bioavailability was not calculated here, in previous investigations, resveratrol was between 30% and 38% bioavailable [131], [130]. Both sulfate metabolites showed much poorer bioavailability, particularly resveratrol-4'-*O*-sulfate, which may be due to their hydrophilic nature, which facilitates rapid excretion from the body [234]. Also, being more polar, the metabolites may not be absorbed from the GI tract as efficiently as resveratrol. The monosulfates were present in all of the mouse tissues analysed, with the highest concentrations in the mucosa, followed by the liver, with measurable levels in lung and pancreas. Additional metabolites that were detected included resveratrol sulfate glucuronides, resveratrol disulfate and resveratrol-3-*O*-glucuronide, suggesting the occurrence of deconjugation and/or conjugation processes in the liver and GI tract. These metabolites have all been identified in humans following resveratrol dosing [107]. Another important objective of monosulfate dosing in mice was to determine whether the conversion of metabolites to parent resveratrol was possible *in vivo* as well as *in vitro*. Resveratrol was detected in plasma and all of the tissues analysed. The highest C_{max} concentration (14.9 nmol/g) was found in the mucosa, possibly due to the large presence of deconjugating enzymes in the GI tract. These data support the findings from the cellular uptake experiments, where sulfate conversion to resveratrol was also shown to occur. The formation of resveratrol from the metabolites would be catalysed by sulfatase enzymes occurring *in vitro* and *in vivo* and there could also be spontaneous hydrolysis in tissues and/or cells. Concentrations could be related to different degrees of activity and/or variable expression of enzymes in

different tissues of the mice, or in cells. Based on the findings in mice, it is possible that at least some of the resveratrol measured in the human colon is a result of local metabolite conversion, or via enterohepatic circulation following biliary excretion. A useful extension to the work in mice would be to examine potential efficacy of the sulfates, for example through feeding studies in a relevant mouse model, such as the *Apc*$^{min+}$ colorectal carcinogenesis model. The effectiveness of resveratrol administration in *Apc*$^{min+}$ mice has already been demonstrated, where it was shown to reduce adenoma load by 27% [80] and the formation of small intestinal tumours by 70% compared to the control groups [93].

Most of the work undertaken here focussed on the resveratrol monosulfates. The two monoglucuronides were also tested for their antiproliferative activity in the HCA-7 and HT-29 cell lines. Both glucuronides had a limited level of activity but cell proliferation after seven days was only significantly reduced after treatment with the highest metabolite concentrations of 250 µM. However, an improved activity was observed after three days of exposure, with significant reductions in proliferation at concentrations starting at 75 µM. It is possible that the glucuronides are not stable for the course of seven days and degrade under the standard cell culture conditions, resulting in a more pronounced effect at the early timepoint. In general, the relatively large molecular size of the glucuronides may also hinder their entry into cells, thereby reducing their ability to alter cellular proliferation. The lack of sulfate uptake and inability to alter cellular proliferation was demonstrated in HCEC cells. Consistent with these findings, when monosulfates, monoglucuronides and disulfate were incubated with neuroblastoma cells, there was a lack of cellular uptake (in contrast to resveratrol), and consequently resveratrol metabolites did not have any impact on the cell viability [235].

Cellular uptake, stability and the presence of cellular transporter proteins are all factors that could be investigated in future studies. A lack of activity for resveratrol glucuronides has previously been described in cell-based assays for measuring anti-HIV activity, and inhibition of COX enzymes [152], [135]. However, it is possible that they may have other useful properties, such as antioxidant capacity. Quercetin glucuronide metabolites have been shown to inhibit LDL oxidation, thereby contributing to the antioxidant pool in the blood [236]. Furthermore,

quercetin glucuronide, like the parent, inhibited vascular smooth muscle cell hypertrophy [237]. The metabolites of the green tea polyphenol, epigallocatechin-3-gallate (EGCG) dose-dependently inhibited the growth of colon cancer and intestinal cell lines and prevented arachidonic acid release and nitric oxide production [238]. These results suggest that metabolites of EGCG retain the growth inhibitory, anti-inflammatory, and pro-oxidant activities of EGCG *in vitro*, and may play a role in disease prevention *in vivo.*

The research described in this thesis focussed on resveratrol mono-conjugated metabolites, however, some of the other identified resveratrol metabolites may be worthy of investigation. Additional metabolites detected in patient plasma and colon tissue were resveratrol disulfate (although concentrations were low), resveratrol trisulfate and resveratrol diglucuronide. Resveratrol diglucuronide has only been detected in humans following piceid administration [108], whereas resveratrol trisulfate has only previously been reported in rats [71]. These are all metabolites that may play a role in the activity of resveratrol, although it is unlikely that they contribute greatly to cancer cell inhibition, as they are quantitatively minor metabolites. Also, an increased number of hydroxyl groups on the resveratrol ring-structure is associated with higher cytotoxicity [239], therefore di- and tri- metabolites are likely to show poorer activity. If one other metabolite were selected for investigation, resveratrol sulfate glucuronide would be a good candidate for a number of reasons. Here, it was shown to be present in human plasma, and interestingly, it was more prominent in plasma of patients that had received resveratrol, compared to healthy volunteers. Sulfate glucuronide was a major metabolite generated in human colon/tumour tissues, where it reached consistently high levels. It was also a prominent metabolite in plasma and tissues collected from mice after sulfate dosing, and in HT-29 cells and media supernatant after resveratrol treatment, highlighting its significance. The three multiple peaks, which were often not fully resolved from one another, are likely to be isomers of resveratrol sulfate glucuronide. Sulfate glucuronide isomers have previously been identified in a rodent study in which the bile and perfusate of Wistar rats was analysed following liver perfusion with 20 µM resveratrol [145]. Bile was treated with β-glucuronidase, resulting in large reductions of the sulfate glucuronide peaks and a concomitant increase in the sulfate and resveratrol peak (with increase in the latter peak likely to be related to enzymatic deconjugation

of resveratrol-3-*O*-glucuronide). Analogous treatment with sulfatase resulted in complete disappearance of the sulfate glucuronides and increases in resveratrol-3-*O*-glucuronide and resveratrol, with some formation of resveratrol-4'-*O*-glucuronide [145]. Until now, the study in rats was the only one which identified sulfate glucuronides. However, two resveratrol sulfate glucuronides have recently been identified in pigs [157], which are physiologically more closely related to humans than mice. It is possible that the different sulfate glucuronides may possess a variety of activities, and to our knowledge this metabolite(s) has not yet been tested. The position of functional groups has been found to be an important determinant of activity [199]. For example, quercetin glucuronides can retain some biological activity at expected plasma concentrations depending on conjugation position [240].

Interestingly, whereas all of the metabolites and resveratrol detected in the human colon had higher concentrations in tissues originating from right-sided tissues (probably due to increased absorption), this was not the case for sulfate glucuronides. Patients who received the 1.0 g resveratrol doses had mean sulfate glucuronide concentrations of 21.1 ± 9.3 and 23.9 ± 15.8 nmol/g across all left and right-sided tissue samples respectively. This is an important finding, as any effects that this metabolite might posses would be across the total GI tract. Or at least, it is possible that like resveratrol sulfates, the sulfoglucuronide conjugates could also serve as an inactive pool of resveratrol, resulting in resveratrol delivery to target tissue(s). Deconjugation to the intermediary sulfate(s) might also be beneficial, as indicated by the cell proliferation data. The high concentrations and generalised presence of sulfate glucuronide would make it an ideal source for resveratrol regeneration. Further investigation could examine the metabolite contribution, if any, to resveratrol formation *in vivo*. Similarly, the same could be done with the glucuronide metabolites. Sulfate conversion to resveratrol has been shown to occur in the current work, both *in vitro* and *in vivo*. Therefore, all of the metabolites might prolong the effects of resveratrol, with a continuous cycle of deconjugation and reconjugation. If this were the case, it is possible that the total contribution of resveratrol from metabolites, could reach efficacious concentrations in a number of target tissues.

Once the effects of individual metabolites were determined, a useful investigation would be to test the effects of a cocktail of these metabolites *in vitro*. It may be that the metabolites act synergistically or even antagonistically with one another, or that there is an additive effect with other metabolites and/or resveratrol. When a mixture of anthocyanins and colonic metabolites (at physiological concentrations) were evaluated for their effects on platelet aggregation and activation function, the mixture was active. However, when the individual components were tested separately at the same concentrations as in the mixture, they showed no activity, indicating synergism of the different components. The results indicate that these particular polyphenols as well as the metabolites of dietary polyphenols tested can act as potential cardiovascular health promoters [241]. A different angle of investigation would be to examine the effects of low concentrations of metabolites on proliferation. Unpublished studies from our research group have recently demonstrated the occurrence of unusual dose-response relationships for resveratrol. It would be helpful to determine whether a similar type of action occurs with its metabolites. An alternate dosing strategy could also be employed, for example, repeated metabolite dosing regimes to mimic the *in vivo* concentrations which might occur in humans following daily resveratrol dosing.

The limited investigations into resveratrol metabolites indicate that they possess some degree of activity, although this is normally far below that of the parent, and seems to be cell specific. Several mechanisms relating to cancer chemoprevention including QR1 induction, DPPH free radical scavenging and COX inhibitory activities have been shown to be altered by the conjugates. Based on the resveratrol-3-*O*-sulfate concentrations reaching the plasma and tissue compartments, these may be high enough to effect changes on at least some of these processes including cancer cell proliferation, free radical scavenging and COX inhibition. It has been recommended that resveratrol doses below 1.0 g per day should be tested [86], and tissue resveratrol-3-*O*-sulfate colon tissue levels generated after this dose (on the right-side) were of an order of magnitude sufficient to exert beneficial effects.

In summary, as part of this research, the metabolite profiles in healthy volunteers and colorectal cancer patients were determined. Novel metabolites, which have not previously been found in

humans after resveratrol dosing were reported, and included resveratrol trisulfate, resveratrol diglucuronide and resveratrol sulfate glucuronide. The synthesis of authentic monosulfate and monoglucuronide metabolites allowed accurate plasma and tissue concentrations to be determined. In addition, it allowed an assessment of various metabolite properties following *in vitro* and *in vivo* administration. The results demonstrate for the first time that resveratrol monosulfate metabolites have antiproliferative activity in colorectal cancer cell lines. These metabolites were also shown to be taken up by cancer cells, where they provided a source for resveratrol generation. Similarly, resveratrol generation from sulfate metabolites was also demonstrated to occur *in vivo*, a process which has been speculated upon, but not yet reported. The results presented in this thesis suggest a contributory role of resveratrol metabolites in the pharmacological activity of resveratrol. Future work should evaluate the potential chemopreventive properties of resveratrol metabolites more comprehensively and define the mechanisms through which they may exert their effects.

APPENDIX

Patient	Sex	Age	Tumour location	Medication	Reason for medication	Day 0	Day 2	Day 3 - 5	Day 8
C12	Female	80	Left	Insulin mixtard Simvastatin Movicol	Diabetic Cholesterol lowering Constipation	✓ ✓ ×	✓ ✓ ✓	✓ ✓ ✓	✓ ✓ ✓
C13	Female	76	Left	Diazepam Atenolol	Anxiety Hypertension	✓ ×	✓ ×	✓ ✓	✓ ✓
C14	Female	78	Right	None					
C110	Female	72	Left	None					
C114	Female	60	Left	Zolpidem Bisoprolol	Aid sleeping Palpitations	✓ ✓	✓ ✓	✓ ✓	✓ ✓
C117	Female	71	Right	None					
C119	Male	62	Left	Movicol Salbutamol Beclomethasone Flixonase	Constipation Asthma Asthma Allergic rhinitis	✓ ✓ ✓ ✓	✓ ✓ ✓ ✓	✓ ✓ ✓ ✓	✓ ✓ ✓ ✓
C120	Female	65	Left	Mebeverine Estraderm patch Perinodopril Bisoprolol	Irritable bowel syndrome Hormone replacement Hypertension Hypertension	✓ ✓ ✓ ✓	✓ ✓ ✓ ✓	✓ ✓ ✓ ✓	✓ ✓ ✓ ✓
C122	Female	60	Right	None					
C133	Male	80	Left	Doxazosin Furosemide Isosorbide mononitrate Atorvastatin	Hypertension Diuretic Ischaemic heart disease Cholesterol lowering	✓ ✓ ✓ ✓	✓ ✓ ✓ ✓	✓ ✓ ✓ ✓	✓ ✓ ✓ ✓

Table 7.1 Colorectal cancer patient characteristics and their medications during the course of 0.5 g resveratrol repeat dosing

The sex, age and location of tumours of colorectal cancer patients receiving 0.5 g resveratrol for eight days. Also included are the medications taken by patients during the course of the trial.

Patient	Sex	Age	Tumour location	Medication	Reason for medication	Day 0	Day 2	Day 3 - 5	Day 8
C223	Male	73	Right	Ramipril Lercanidipine Furosemide Atenolol Rosuvastatin Aspirin	Hypertension Hypertension Diuretic Hypertension Cholesterol lowering Thromboprophylaxis	✓ ✓ ✓ ✓ ✓ ✓	✓ ✓ ✓ ✓ ✓ ×	✓ ✓ ✓ ✓ ✓ ×	✓ ✓ ✓ ✓ ✓ ×
C224	Female	48	Right	Ferrous sulfate Thyroxine	Anaemia Hypothyroidism	✓ ✓	✓ ✓	✓ ✓	✓ ✓
C225	Male	64	Left	Prednisolone Lansoprazole Amlodipine	Idiopathic thrombocytopenic purpura Acid indigestion Hypertension	✓ ✓ ×	✓ ✓ ✓	✓ ✓ ✓	✓ ✓ ✓
C226	Male	81	Left	Lansoprazole	Acid indigestion	✓	✓	✓	✓
C227	Male	82	Left	Felodipine Atenolol Aspirin	Hypertension Hypertension Thromboprophylaxis	✓ ✓ ✓	✓ ✓ ×	✓ ✓ ×	✓ ✓ ×
C228	Male	76	Left	None					
C229	Female	67	Right	None					
C230	Male	83	Right	Bendrofluazide Ramipril Simvastatin	Hypertension Hypertension Cholesterol lowering	✓ ✓ ✓	✓ ✓ ✓	✓ ✓ ✓	✓ ✓ ✓
C231	Male	49	Left	None					
C232	Female	57	Right	Mebeverine	Irritable bowel syndrome	✓	✓	✓	✓

Table 7.2 Colorectal cancer patient characteristics and their medications during the course of 1.0 g resveratrol repeat dosing

The sex, age and location of tumours of colorectal cancer patients receiving 1.0 g resveratrol for eight days. Also included are the medications taken by patients during the course of the trial.

0.5 g resveratrol	Tissue Levels (nmol/g)					
	Proximal to Tumour		Tumour		Distal to Tumour	
	Left	Right	Left	Right	Left	Right
Resveratrol	0.67 ± 0.72 (0 - 3.0)	18.6 ± 17.4 (0 - 45.9)	0.63 ± 0.69 (0 - 1.80)	8.33 ± 6.06 (3.1 - 15.0)	0.48 ± 0.47 (0 - 1.04)	4.94 ± 4.82 (1.95 - 13.5)
Resveratrol-3-*O*-glucuronide	0	86.0 ± 125 (0 - 317)	0	0.73 ± 1.26 (0 - 2.18)	0	0.64 ± 0.46 (0 - 0.94)
Resveratrol-4'-*O*-glucuronide	0.17 ± 0.34 (0 - 0.93)	7.91 ± 11.2 (0 - 28.2)	0	0.29 ± 0.50 (0 - 0.87)	0.28 ± 0.43 (0 - 0.99)	0
Resveratrol sulfate glucuronide	17.1 ± 20.8 (0 - 61.1)	44.5 ± 47.9 (0 - 149)	12.8 ± 15.9 (0 - 34.6)	5.09 ± 7.86 (0 - 14.2)	20.0 ± 39.7 (0 - 121)	0
Resveratrol-3-*O*-sulfate	0.82 ± 0.77 (0 - 2.84)	34.0 ± 48.6 (0.67 - 128)	0.44 ± 0.70 (0 - 1.90)	3.09 ± 2.13 (0.68 - 4.75)	0.94 ± 1.17 (0 - 3.40)	2.37 ± 0.43 (1.86 - 2.93)
Resveratrol-4'-*O*-sulfate	0	1.21 ± 1.78 (0 - 4.52)	0.25 ± 0.43 (0 - 1.02)	0.26 ± 0.46 (0 - 0.79)	0	0.17 ± 0.38 (0 - 0.85)

Table 7.3 Average resveratrol and metabolite concentrations (as equivalents) in sections of human colon and tumour tissue after 0.5 g repeat resveratrol dosing. Concentration of resveratrol and its metabolites in normal tissue (proximal or distal to the tumour) and tumour tissue in colorectal cancer patients who received 0.5 g resveratrol for eight days (in nmol/g of tissue). Concentrations are separated for left-sided (splenic flexure, descending colon, sigmoid colon, and rectum) and right-sided (caecum, ascending colon and hepatic flexure) tumour and tissues. Metabolite concentrations in all patient samples are calculated as resveratrol equivalents, based on resveratrol standard curves. Values are the mean ± SD of seven samples from tissues on the left side and three from the right side, with one tumour sample and between one and three normal tissue samples per patient. The range is given in brackets.

1.0 g resveratrol	Tissue Levels (nmol/g)					
	Proximal to Tumour		Tumour		Distal to Tumour	
	Left	Right	Left	Right	Left	Right
Resveratrol	1.21 ± 1.33 (0 - 5.23)	674 ± 1303 (10.1 - 3774)	2.07 ±3 .27 (0.30 - 8.68)	94.1 ± 89.2 (12.7 - 195)	2.07 ± 3.25 (0.28 - 9.40)	62.5 ± 76.2 (10.7 - 272)
Resveratrol-3-*O*-glucuronide	0.19 ± 0.22 (0 - 0.61)	10.8 ± 17.2 (0 - 50.8)	lod**	0.75 ± 0.70 (0 - 1.85)	0.28 ± 0.29 (0 - 0.71)	0.83 ± 0.81 (0 - 3.24)
Resveratrol-4'-*O*-glucuronide	0.43 ± 0.41 (0 - 1.22)	1.71 ± 1.87 (0 - 5.31)	0.38 ± 0.47 (0 - 1.05)	0.53 ± 0.79 (0 - 1.78)	0.53 ± 0.48 (0 - 1.35)	0.83 ± 0.77 (0 - 2.37)
Resveratrol sulfate glucuronide	19.5 ± 4.82 (10.7 - 27.3)	27.1 ± 21.6 (10.4 - 94.6)	20.7 ± 5.04 (11.7 - 25.4)	29.1 ± 12.8 (16.4 - 50.6)	25.2 ± 17.2 (4.55 - 51.8)	18.4 ± 5.76 (9.6 - 29.4)
Resveratrol-3-*O*-sulfate	0.67 ± 0.56 (0 - 1.73)	67.2 ± 119 (3.87 - 366)	0.16 ± 0.39 (0 - 0.95)	10.4 ±1 3.6 (1.80 - 33.4)	1.10 ± 1.21 (0 - 3.57)	5.82 ± 3.02 (1.59 - 11.9)
Resveratrol-4'-*O*-sulfate	lod	3.43 ± 3.36 (0.32 - 12.6)	lod	3.09 ± 4.72 (0 - 11.33)	loq	0.90 ± 0.70 (0 - 2.18)

Table 7.4 Average resveratrol and metabolite concentrations (as equivalents) in sections of human colon and tumour tissue after 1.0 g repeat resveratrol dosing. Concentration of resveratrol and its metabolites in normal tissue (proximal or distal to the tumour) and tumour tissue in colorectal cancer patients who received 1.0 g resveratrol for eight days (in nmol/g of tissue). Concentrations are separated for left-sided (splenic flexure, descending colon, sigmoid colon, and rectum) and right-sided (caecum, ascending colon and hepatic flexure) tumour and tissues. Metabolite concentrations in all patient samples are calculated as resveratrol equivalents, based on resveratrol standard curves. Values are the mean ± SD of six samples from tissues on the left side and five from the right side, with one tumour sample and between one and three normal tissue samples per patient. The range is given in brackets.

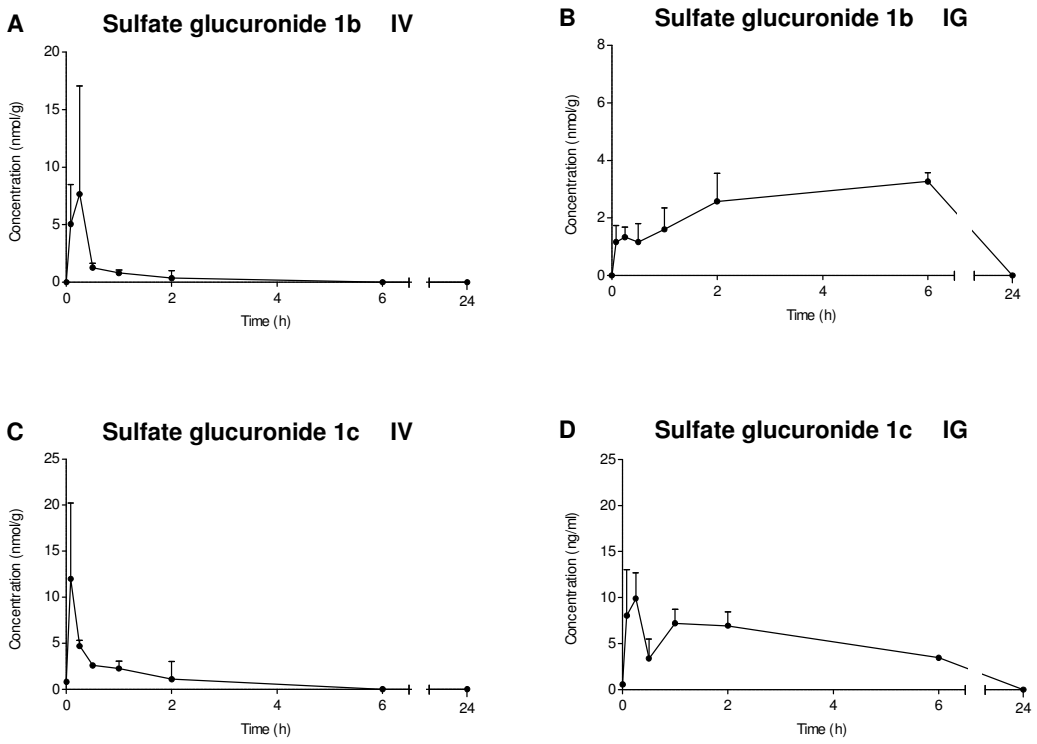

Figure 7.1 Concentrations of resveratrol sulfate glucuronide isomers in mouse liver following IV and IG monosulfate dosing

Concentrations of resveratrol sulfate glucuronide isomers (1b, and 1c) formed in mouse liver over 24 h following IV (**A** and **C**) and IG dosing (**B** and **D**) of 6 and 120 mg/kg resveratrol monosulfates respectively (calculated using a standard curve of resveratrol-3-*O*-sulfate). Values for each point are the mean + SD of three mice per group. Note the break in the x-axis between 6 and 24 h.

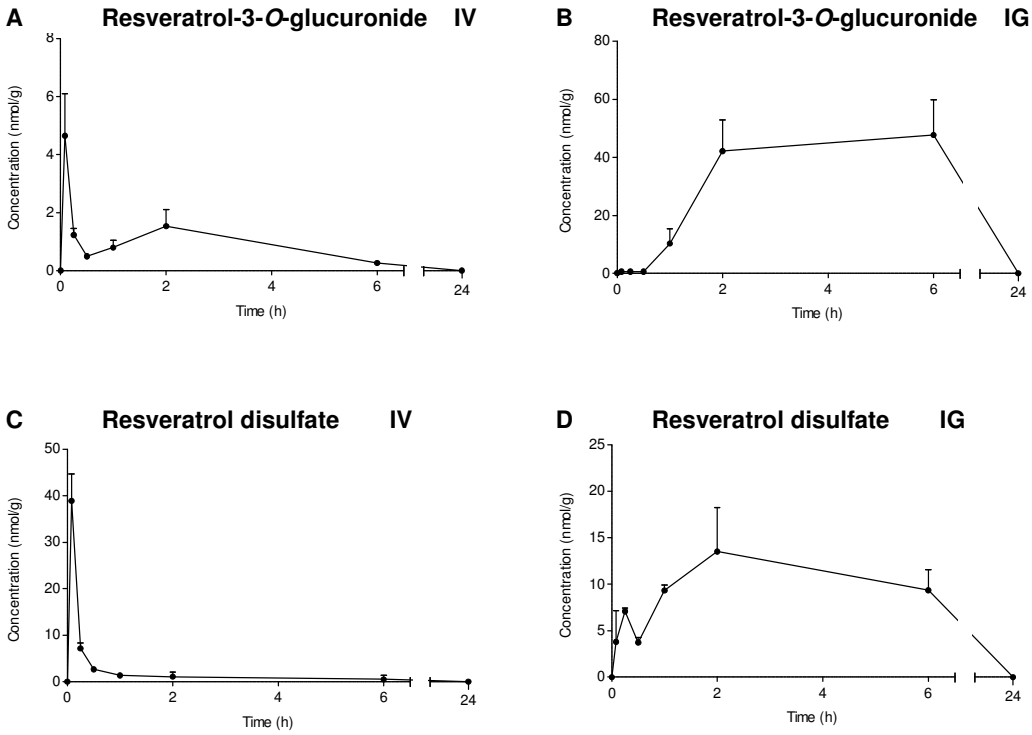

Figure 7.2 Concentrations of resveratrol-3-*O*-glucuronide and resveratrol disulfate in mouse liver following IV and IG monosulfate dosing

Concentrations of resveratrol-3-*O*-glucuronide formed in mouse liver over 24 h following IV (**A**) and IG dosing (**B**) of 6 and 120 mg/kg resveratrol monosulfates respectively. Resveratrol disulfate concentration profiles following the same two routes of administration are shown by (**C**) and (**D**) respectively. Values for each point are the mean + SD of three mice per group. Note the break in the x-axis between 6 and 24 h.

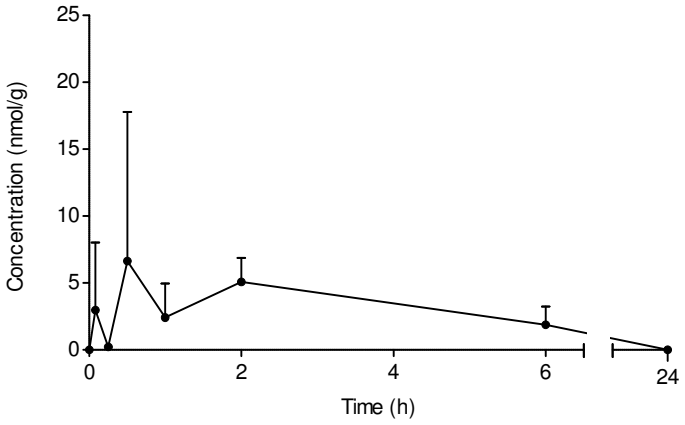

Figure 7.3 Concentrations of resveratrol-3-*O*-glucuronide in mouse lung following IG monosulfate dosing

Concentrations of resveratrol-3-*O*-glucuronide formed in mouse lung over 24 h following IG dosing of 120 mg/kg resveratrol monosulfates. Values for each point are the mean + SD of three mice per group. Note the break in the x-axis between 6 and 24 h.

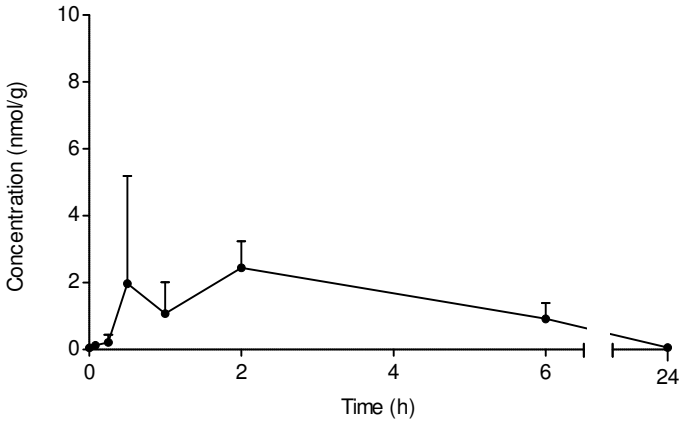

Figure 7.4 Concentrations of resveratrol-3-*O*-glucuronide in mouse pancreas following IG monosulfate dosing

Concentrations of resveratrol-3-*O*-glucuronide formed in mouse pancreas over 24 h following IG dosing of 120 mg/kg resveratrol monosulfates. Values for each point are the mean + SD of three mice per group. Note the break in the x-axis between 6 and 24 h.

A Control (untreated), unstained cells

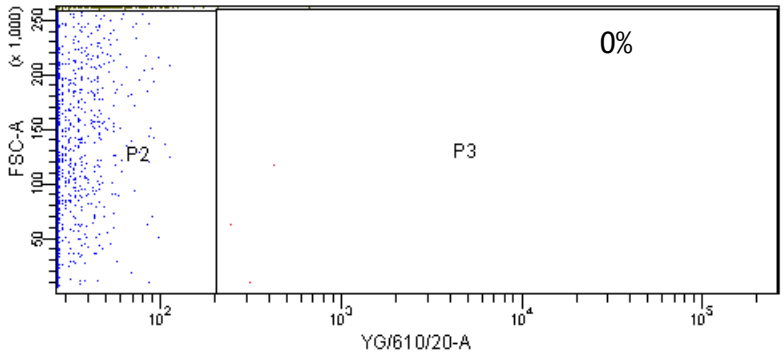

B Control (untreated), cells stained with secondary antibody only

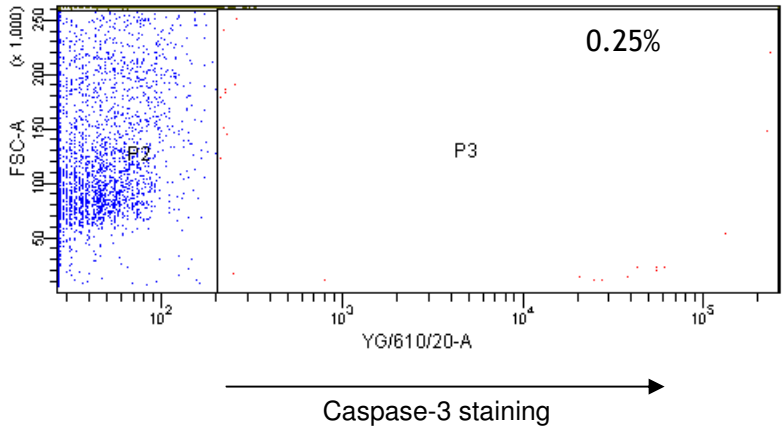

Figure 7.5 Representative dot plots showing differential cell staining for caspase-3
Staining is shown in control cells without antibody (**A**), and with secondary antibody only (**B**) following analysis by flow cytometry. P2 and P3 indicate caspase-3 negative and caspase-3 positive staining respectively. Percentage values for positive staining are provided within each figure.

Patel, K.R.; Brown, V.A. et al. 'Clinical Pharmacology of Resveratrol and Its Metabolites in Colorectal Cancer Patients' in Cancer Research, 2010, 70 (19), pp. 7392-7399.
DOI: 10.1158/0008-5472.CAN-10-2027

Brown, V.A.; Patel, K.R. et al. 'Repeat Dose Study of the Cancer Chemopreventive Agent Resveratrol in Healthy Volunteers: Safety, Pharmacokinetics, and Effect on the Insulin-like Growth Factor Axis' in Cancer Research, 2010, 70 (22), pp. 9003-9011.
DOI: 10.1158/0008-5472.CAN-10-2364

REFERENCES

1. Ruddon R. Cancer Biology. Oxford: Oxford University Press; 1995.
2. Parkin DM. Global cancer statistics in the year 2000. Lancet Oncol 2001;2(9):533-543.
3. Peto J. Cancer epidemiology in the last century and the next decade. Nature 2001;411(6835):390-395.
4. Barchana M, Liphshitz I, Rozen P. Trends in colorectal cancer incidence and mortality in the Israeli Jewish ethnic populations. Fam Cancer 2004;3(3-4):207-214.
5. Doll R, Peto R. The causes of cancer: quantitative estimates of avoidable risks of cancer in the United States today. J Natl Cancer Inst 1981;66(6):1191-1308.
6. Sandler RS, Lyles CM, Peipins LA, McAuliffe CA, Woosley JT, Kupper LL. Diet and risk of colorectal adenomas: macronutrients, cholesterol, and fiber. J Natl Cancer Inst 1993;85(11):884-891.
7. Boyle P. Cancer, cigarette smoking and premature death in Europe: a review including the Recommendations of European Cancer Experts Consensus Meeting, Helsinki, October 1996. Lung Cancer 1997;17(1):1-60.
8. Boffetta P, Hashibe M, La Vecchia C, Zatonski W, Rehm J. The burden of cancer attributable to alcohol drinking. Int J Cancer 2006;119(4):884-887.
9. Dragan YP, Sargent L, Xu YD, Xu YH, Pitot HC. THE INITIATION-PROMOTION-PROGRESSION MODEL OF RAT HEPATOCARCINOGENESIS. Proceedings of the Society for Experimental Biology and Medicine 1993;202(1):16-24.
10. Trosko JE. Commentary: is the concept of "tumor promotion" a useful paradigm? Mol Carcinog 2001;30(3):131-137.
11. Surh YJ. Cancer chemoprevention with dietary phytochemicals. Nat Rev Cancer 2003;3(10):768-780.
12. Preston-Martin S, Pike MC, Ross RK, Jones PA, Henderson BE. Increased cell division as a cause of human cancer. Cancer Res 1990;50(23):7415-7421.
13. Schulte-Hermann R, Timmermann-Trosiener I, Barthel G, Bursch W. DNA synthesis, apoptosis, and phenotypic expression as determinants of growth of altered foci in rat liver during phenobarbital promotion. Cancer Res 1990;50(16):5127-5135.
14. Yuspa SH, Hennings H, Saffiotti U. Cutaneous chemical carcinogenesis: past, present, and future. J Invest Dermatol. Volume 67; 1976. p 199-208.
15. Verma AK, Conrad EA, Boutwell RK. Differential effects of retinoic acid and 7,8-benzoflavone on the induction of mouse skin tumors by the complete carcinogenesis process and by the initiation-promotion regimen. Cancer Res 1982;42(9):3519-3525.
16. Fearon ER, Vogelstein B. A genetic model for colorectal tumorigenesis. Cell 1990;61(5):759-767.
17. Grady WM. Genetic testing for high-risk colon cancer patients. Gastroenterology 2003;124(6):1574-1594.

18. Jones LA, Chilton JA, Hajek RA, Iammarino NK, Laufman L. Between and within: international perspectives on cancer and health disparities. J Clin Oncol 2006;24(14):2204-2208.
19. Giovannucci E, Rimm EB, Stampfer MJ, Colditz GA, Ascherio A, Willett WC. Intake of fat, meat, and fiber in relation to risk of colon cancer in men. Cancer Res 1994;54(9):2390-2397.
20. Cho E, Smith-Warner SA, Ritz J et al. Alcohol intake and colorectal cancer: a pooled analysis of 8 cohort studies. Ann Intern Med 2004;140(8):603-613.
21. Otani T, Iwasaki M, Yamamoto S et al. Alcohol consumption, smoking, and subsequent risk of colorectal cancer in middle-aged and elderly Japanese men and women: Japan Public Health Center-based prospective study. Cancer Epidemiol Biomarkers Prev 2003;12(12):1492-1500.
22. Howard RA, Freedman DM, Park Y, Hollenbeck A, Schatzkin A, Leitzmann MF. Physical activity, sedentary behavior, and the risk of colon and rectal cancer in the NIH-AARP Diet and Health Study. Cancer Causes Control 2008;19(9):939-953.
23. Stoneham M, Goldacre M, Seagroatt V, Gill L. Olive oil, diet and colorectal cancer: an ecological study and a hypothesis. J Epidemiol Community Health 2000;54(10):756-760.
24. Rougier P, Mitry E. Epidemiology, treatment and chemoprevention in colorectal cancer. Ann Oncol 2003;14 Suppl 2:ii3-5.
25. Miyoshi Y, Ando H, Nagase H et al. Germ-line mutations of the APC gene in 53 familial adenomatous polyposis patients. Proc Natl Acad Sci U S A 1992;89(10):4452-4456.
26. Gupta RA, Dubois RN. Colorectal cancer prevention and treatment by inhibition of cyclooxygenase-2. Nat Rev Cancer 2001;1(1):11-21.
27. Half E, Bercovich D, Rozen P. Familial adenomatous polyposis. Orphanet J Rare Dis 2009;4:22.
28. Alkhouri N, Franciosi JP, Mamula P. Familial adenomatous polyposis in children and adolescents. J Pediatr Gastroenterol Nutr 2010;51(6):727-732.
29. Jullumstro E, Lydersen S, Moller B, Dahl O, Edna TH. Duration of symptoms, stage at diagnosis and relative survival in colon and rectal cancer. Eur J Cancer 2009;45(13):2383-2390.
30. Labianca R, Beretta GD, Kildani B et al. Colon cancer. Crit Rev Oncol Hematol 2010;74(2):106-133.
31. Dukes C. The classification of cancer of the rectum. Journal of Pathology and bacteriology 1932;35:323-332.
32. Mason P. Colorectal cancer - the disease and its management. Hospital Pharmacist 2004;11:175 - 177.
33. Macdonald JS. Adjuvant therapy of colon cancer. CA Cancer J Clin 1999;49(4):202-219.

34. Saad ED, Hoff PM. Chemotherapy of Metastatic Colorectal Cancer. Curr Treat Options Gastroenterol 2005;8(3):239-247.
35. Jordan K, Kellner O, Kegel T, Schmoll HJ, Grothey A. Phase II trial of capecitabine/irinotecan and capecitabine/oxaliplatin in advanced gastrointestinal cancers. Clin Colorectal Cancer 2004;4(1):46-50.
36. Hong WK, Sporn MB. Recent advances in chemoprevention of cancer. Science 1997;278(5340):1073-1077.
37. Greenhough A, Smartt HJ, Moore AE et al. The COX-2/PGE2 pathway: key roles in the hallmarks of cancer and adaptation to the tumour microenvironment. Carcinogenesis 2009;30(3):377-386.
38. Tomozawa S, Tsuno NH, Sunami E et al. Cyclooxygenase-2 overexpression correlates with tumour recurrence, especially haematogenous metastasis, of colorectal cancer. Br J Cancer 2000;83(3):324-328.
39. Oshima M, Dinchuk JE, Kargman SL et al. Suppression of intestinal polyposis in Apc delta716 knockout mice by inhibition of cyclooxygenase 2 (COX-2). Cell 1996;87(5):803-809.
40. Baron JA, Cole BF, Sandler RS et al. A randomized trial of aspirin to prevent colorectal adenomas. N Engl J Med 2003;348(10):891-899.
41. Giovannucci E, Rimm EB, Stampfer MJ, Colditz GA, Ascherio A, Willett WC. Aspirin use and the risk for colorectal cancer and adenoma in male health professionals. Ann Intern Med 1994;121(4):241-246.
42. Thun MJ, Namboodiri MM, Calle EE, Flanders WD, Heath CW, Jr. Aspirin use and risk of fatal cancer. Cancer Res 1993;53(6):1322-1327.
43. Wolfe MM, Lichtenstein DR, Singh G. Gastrointestinal toxicity of nonsteroidal antiinflammatory drugs. N Engl J Med 1999;340(24):1888-1899.
44. Steinbach G, Lynch PM, Phillips RK et al. The effect of celecoxib, a cyclooxygenase-2 inhibitor, in familial adenomatous polyposis. N Engl J Med 2000;342(26):1946-1952.
45. Phillips RK, Wallace MH, Lynch PM et al. A randomised, double blind, placebo controlled study of celecoxib, a selective cyclooxygenase 2 inhibitor, on duodenal polyposis in familial adenomatous polyposis. Gut 2002;50(6):857-860.
46. Solomon SD, Pfeffer MA, McMurray JJ et al. Effect of celecoxib on cardiovascular events and blood pressure in two trials for the prevention of colorectal adenomas. Circulation 2006;114(10):1028-1035.
47. Shureiqi I, Baron JA. Curcumin chemoprevention: the long road to clinical translation. Cancer Prev Res (Phila) 2011;4(3):296-298.
48. Rao CV, Rivenson A, Simi B, Reddy BS. Chemoprevention of colon carcinogenesis by dietary curcumin, a naturally occurring plant phenolic compound. Cancer Res 1995;55(2):259-266.

49. Perkins S, Verschoyle RD, Hill K et al. Chemopreventive efficacy and pharmacokinetics of curcumin in the min/+ mouse, a model of familial adenomatous polyposis. Cancer Epidemiol Biomarkers Prev 2002;11(6):535-540.
50. Lao CD, Ruffin MTt, Normolle D et al. Dose escalation of a curcuminoid formulation. BMC Complement Altern Med 2006;6:10.
51. Cheng AL, Hsu CH, Lin JK et al. Phase I clinical trial of curcumin, a chemopreventive agent, in patients with high-risk or pre-malignant lesions. Anticancer Res 2001;21(4B):2895-2900.
52. Sharma RA, McLelland HR, Hill KA et al. Pharmacodynamic and pharmacokinetic study of oral Curcuma extract in patients with colorectal cancer. Clin Cancer Res 2001;7(7):1894-1900.
53. Arber N, Levin B. Chemoprevention of colorectal cancer: ready for routine use? Curr Top Med Chem 2005;5(5):517-525.
54. King RJB. Cancer Biology: Prentice Hall; 2006.
55. Malumbres M, Barbacid M. To cycle or not to cycle: a critical decision in cancer. Nat Rev Cancer 2001;1(3):222-231.
56. Park MT, Lee SJ. Cell cycle and cancer. J Biochem Mol Biol 2003;36(1):60-65.
57. Arber N, Hibshoosh H, Moss SF et al. Increased expression of cyclin D1 is an early event in multistage colorectal carcinogenesis. Gastroenterology 1996;110(3):669-674.
58. Gescher A, Pastorino U, Plummer SM, Manson MM. Suppression of tumour development by substances derived from the diet--mechanisms and clinical implications. Br J Clin Pharmacol 1998;45(1):1-12.
59. Hanahan D, Weinberg RA. The hallmarks of cancer. Cell 2000;100(1):57-70.
60. Anto RJ, Mukhopadhyay A, Denning K, Aggarwal BB. Curcumin (diferuloylmethane) induces apoptosis through activation of caspase-8, BID cleavage and cytochrome c release: its suppression by ectopic expression of Bcl-2 and Bcl-xl. Carcinogenesis 2002;23(1):143-150.
61. Kern M, Pahlke G, Balavenkatraman KK, Bohmer FD, Marko D. Apple polyphenols affect protein kinase C activity and the onset of apoptosis in human colon carcinoma cells. J Agric Food Chem 2007;55(13):4999-5006.
62. Yoo HG, Jung SN, Hwang YS et al. Involvement of NF-kappaB and caspases in silibinin-induced apoptosis of endothelial cells. Int J Mol Med 2004;13(1):81-86.
63. Wu M, Kang MM, Schoene NW, Cheng WH. Selenium compounds activate early barriers of tumorigenesis. J Biol Chem 2010;285(16):12055-12062.
64. Ewald JA, Desotelle JA, Wilding G, Jarrard DF. Therapy-induced senescence in cancer. J Natl Cancer Inst 2010;102(20):1536-1546.
65. Schilder YD, Heiss EH, Schachner D et al. NADPH oxidases 1 and 4 mediate cellular senescence induced by resveratrol in human endothelial cells. Free Radic Biol Med 2009;46(12):1598-1606.

66. Collado M, Blasco MA, Serrano M. Cellular senescence in cancer and aging. Cell 2007;130(2):223-233.
67. Dimri GP, Lee X, Basile G et al. A biomarker that identifies senescent human cells in culture and in aging skin in vivo. Proc Natl Acad Sci U S A 1995;92(20):9363-9367.
68. Adrian M, Jeandet P, Veneau J, Weston LA, Bessis R. Biological activity of resveratrol, a stilbenic compound from grapevines, against Botrytis cinerea, the causal agent for gray mold. Journal of Chemical Ecology 1997;23(7):1689-1702.
69. Fabris S, Momo F, Ravagnan G, Stevanato R. Antioxidant properties of resveratrol and piceid on lipid peroxidation in micelles and monolamellar liposomes. Biophys Chem 2008;135(1-3):76-83.
70. Trela BC, Waterhouse AL. Resveratrol: Isomeric Molar Absorptivities and Stability. J Agric Food Chem 1996;44(5):1253-1257.
71. Wenzel E, Soldo T, Erbersdobler H, Somoza V. Bioactivity and metabolism of trans-resveratrol orally administered to Wistar rats. Mol Nutr Food Res 2005;49(5):482-494.
72. Jeandet P, Bessis R, Maume BF, Meunier P, Peyron D, Trollat P. Effect of Enological Practices on the Resveratrol Isomer Content of Wine. J Agric Food Chem 1995;43(2):316-319.
73. Goldberg DM, Yan J, Ng E et al. A Global Survey of Trans-Resveratrol Concentrations in Commercial Wines. Am J Enol Vitic 1995;46(2):159-165.
74. Sanders TH, McMichael RW, Jr., Hendrix KW. Occurrence of resveratrol in edible peanuts. J Agric Food Chem 2000;48(4):1243-1246.
75. Gusman J, Malonne H, Atassi G. A reappraisal of the potential chemopreventive and chemotherapeutic properties of resveratrol. Carcinogenesis 2001;22(8):1111-1117.
76. Burns J, Yokota T, Ashihara H, Lean ME, Crozier A. Plant foods and herbal sources of resveratrol. J Agric Food Chem 2002;50(11):3337-3340.
77. Jang M, Cai L, Udeani GO et al. Cancer chemopreventive activity of resveratrol, a natural product derived from grapes. Science 1997;275(5297):218-220.
78. Eichholzer M, Luthy J, Gutzwiller F, Stahelin HB. The role of folate, antioxidant vitamins and other constituents in fruit and vegetables in the prevention of cardiovascular disease: the epidemiological evidence. Int J Vitam Nutr Res 2001;71(1):5-17.
79. Gescher AJ, Steward WP. Relationship between mechanisms, bioavailibility, and preclinical chemopreventive efficacy of resveratrol: a conundrum. Cancer Epidemiol Biomarkers Prev 2003;12(10):953-957.
80. Sale S, Tunstall RG, Ruparelia KC, Potter GA, Steward WP, Gescher AJ. Comparison of the effects of the chemopreventive agent resveratrol and its synthetic analog trans 3,4,5,4'-tetramethoxystilbene (DMU-212) on adenoma development in the Apc(Min+) mouse and cyclooxygenase-2 in human-derived colon cancer cells. Int J Cancer 2005;115(2):194-201.
81. Mahyar-Roemer M, Kohler H, Roemer K. Role of Bax in resveratrol-induced apoptosis of colorectal carcinoma cells. BMC Cancer 2002;2:27.

82. Delmas D, Rebe C, Lacour S et al. Resveratrol-induced apoptosis is associated with Fas redistribution in the rafts and the formation of a death-inducing signaling complex in colon cancer cells. J Biol Chem 2003;278(42):41482-41490.
83. Juan ME, Wenzel U, Daniel H, Planas JM. Resveratrol induces apoptosis through ROS-dependent mitochondria pathway in HT-29 human colorectal carcinoma cells. J Agric Food Chem 2008;56(12):4813-4818.
84. Lee SC, Chan J, Clement MV, Pervaiz S. Functional proteomics of resveratrol-induced colon cancer cell apoptosis: caspase-6-mediated cleavage of lamin A is a major signaling loop. Proteomics 2006;6(8):2386-2394.
85. Wolter F, Akoglu B, Clausnitzer A, Stein J. Downregulation of the cyclin D1/Cdk4 complex occurs during resveratrol-induced cell cycle arrest in colon cancer cell lines. J Nutr 2001;131(8):2197-2203.
86. Chow HH, Garland LL, Hsu CH et al. Resveratrol modulates drug- and carcinogen-metabolizing enzymes in a healthy volunteer study. Cancer Prev Res (Phila Pa) 2010;3(9):1168-1175.
87. Yu C, Shin YG, Kosmeder JW, Pezzuto JM, van Breemen RB. Liquid chromatography/tandem mass spectrometric determination of inhibition of human cytochrome P450 isozymes by resveratrol and resveratrol-3-sulfate. Rapid Commun Mass Spectrom 2003;17(4):307-313.
88. Gerhauser C, Klimo K, Heiss E et al. Mechanism-based in vitro screening of potential cancer chemopreventive agents. Mutat Res 2003;523-524:163-172.
89. Lancon A, Hanet N, Jannin B et al. Resveratrol in human hepatoma HepG2 cells: metabolism and inducibility of detoxifying enzymes. Drug Metab Dispos 2007;35(5):699-703.
90. Dong Z. Molecular mechanism of the chemopreventive effect of resveratrol. Mutat Res 2003;523-524:145-150.
91. Huang C, Ma WY, Goranson A, Dong Z. Resveratrol suppresses cell transformation and induces apoptosis through a p53-dependent pathway. Carcinogenesis 1999;20(2):237-242.
92. Sengottuvelan M, Viswanathan P, Nalini N. Chemopreventive effect of trans-resveratrol--a phytoalexin against colonic aberrant crypt foci and cell proliferation in 1,2-dimethylhydrazine induced colon carcinogenesis. Carcinogenesis 2006;27(5):1038-1046.
93. Schneider Y, Duranton B, Gosse F, Schleiffer R, Seiler N, Raul F. Resveratrol inhibits intestinal tumorigenesis and modulates host-defense-related gene expression in an animal model of human familial adenomatous polyposis. Nutr Cancer 2001;39(1):102-107.
94. Tessitore L, Davit A, Sarotto I, Caderni G. Resveratrol depresses the growth of colorectal aberrant crypt foci by affecting bax and p21(CIP) expression. Carcinogenesis 2000;21(8):1619-1622.

95. Subbaramaiah K, Dannenberg AJ. Cyclooxygenase 2: a molecular target for cancer prevention and treatment. Trends Pharmacol Sci 2003;24(2):96-102.
96. Evans AE, Ruidavets JB, McCrum EE et al. Autres pays, autres coeurs? Dietary patterns, risk factors and ischaemic heart disease in Belfast and Toulouse. Qjm 1995;88(7):469-477.
97. Masia R, Pena A, Marrugat J et al. High prevalence of cardiovascular risk factors in Gerona, Spain, a province with low myocardial infarction incidence. REGICOR Investigators. J Epidemiol Community Health 1998;52(11):707-715.
98. Wang Z, Huang Y, Zou J, Cao K, Xu Y, Wu JM. Effects of red wine and wine polyphenol resveratrol on platelet aggregation in vivo and in vitro. Int J Mol Med 2002;9(1):77-79.
99. Bradamante S, Barenghi L, Piccinini F et al. Resveratrol provides late-phase cardioprotection by means of a nitric oxide- and adenosine-mediated mechanism. Eur J Pharmacol 2003;465(1-2):115-123.
100. Avellone G, Di Garbo V, Campisi D et al. Effects of moderate Sicilian red wine consumption on inflammatory biomarkers of atherosclerosis. Eur J Clin Nutr 2006;60(1):41-47.
101. Pezzuto JM. Resveratrol as an Inhibitor of Carcinogenesis. Pharmaceutical Biology 2008;46(7-8):443-573.
102. Goldberg DM, Yan J, Soleas GJ. Absorption of three wine-related polyphenols in three different matrices by healthy subjects. Clin Biochem 2003;36(1):79-87.
103. Meng X, Maliakal P, Lu H, Lee MJ, Yang CS. Urinary and plasma levels of resveratrol and quercetin in humans, mice, and rats after ingestion of pure compounds and grape juice. J Agric Food Chem 2004;52(4):935-942.
104. Walle T, Hsieh F, DeLegge MH, Oatis JE, Jr., Walle UK. High absorption but very low bioavailability of oral resveratrol in humans. Drug Metab Dispos 2004;32(12):1377-1382.
105. Urpi-Sarda M, Jauregui O, Lamuela-Raventos RM et al. Uptake of diet resveratrol into the human low-density lipoprotein. Identification and quantification of resveratrol metabolites by liquid chromatography coupled with tandem mass spectrometry. Anal Chem 2005;77(10):3149-3155.
106. Vitaglione P, Sforza S, Galaverna G et al. Bioavailability of trans-resveratrol from red wine in humans. Mol Nutr Food Res 2005;49(5):495-504.
107. Boocock DJ, Faust GE, Patel KR et al. Phase I dose escalation pharmacokinetic study in healthy volunteers of resveratrol, a potential cancer chemopreventive agent. Cancer Epidemiol Biomarkers Prev 2007;16(6):1246-1252.
108. Burkon A, Somoza V. Quantification of free and protein-bound trans-resveratrol metabolites and identification of trans-resveratrol-C/O-conjugated diglucuronides - two novel resveratrol metabolites in human plasma. Mol Nutr Food Res 2008;52(5):549-557.

109. Ortuño J, Covas M-I, Farre M et al. Matrix effects on the bioavailability of resveratrol in humans. Food Chemistry 2010;120(4):1123-1130.
110. Nunes T, Almeida L, Rocha JF et al. Pharmacokinetics of trans-resveratrol following repeated administration in healthy elderly and young subjects. J Clin Pharmacol 2009;49(12):1477-1482.
111. Kennedy DO, Wightman EL, Reay JL et al. Effects of resveratrol on cerebral blood flow variables and cognitive performance in humans: a double-blind, placebo-controlled, crossover investigation. Am J Clin Nutr 2010;91(6):1590-1597.
112. Almeida L, Vaz-da-Silva M, Falcao A et al. Pharmacokinetic and safety profile of trans-resveratrol in a rising multiple-dose study in healthy volunteers. Mol Nutr Food Res 2009;53 Suppl 1:S7-15.
113. la Porte C, Voduc N, Zhang G et al. Steady-State pharmacokinetics and tolerability of trans-resveratrol 2000 mg twice daily with food, quercetin and alcohol (ethanol) in healthy human subjects. Clin Pharmacokinet 2010;49(7):449-454.
114. Patel KR, Brown VA, Jones D, R B. Clinical Pharmacology of Resveratrol and its Metabolites in Colorectal Cancer Patients. Cancer Research 2010;70(19).
115. Zamora-Ros R, Urpi-Sarda M, Lamuela-Raventos RM et al. Diagnostic performance of urinary resveratrol metabolites as a biomarker of moderate wine consumption. Clin Chem 2006;52(7):1373-1380.
116. Vitrac X, Desmouliere A, Brouillaud B et al. Distribution of [14C]-trans-resveratrol, a cancer chemopreventive polyphenol, in mouse tissues after oral administration. Life Sci 2003;72(20):2219-2233.
117. Williams LD, Burdock GA, Edwards JA, Beck M, Bausch J. Safety studies conducted on high-purity trans-resveratrol in experimental animals. Food Chem Toxicol 2009;47(9):2170-2182.
118. Juan ME, Vinardell MP, Planas JM. The daily oral administration of high doses of trans-resveratrol to rats for 28 days is not harmful. J Nutr 2002;132(2):257-260.
119. Crowell JA, Korytko PJ, Morrissey RL, Booth TD, Levine BS. Resveratrol-associated renal toxicity. Toxicol Sci 2004;82(2):614-619.
120. Brown VA, Patel KR, Viskaduraki M et al. Repeat dose study of the cancer chemopreventive agent resveratrol in healthy volunteers: safety, pharmacokinetics, and effect on the insulin-like growth factor axis. Cancer Res 2010;70(22):9003-9011.
121. Einspahr JG, Alberts DS, Gapstur SM, Bostick RM, Emerson SS, Gerner EW. Surrogate end-point biomarkers as measures of colon cancer risk and their use in cancer chemoprevention trials. Cancer Epidemiol Biomarkers Prev 1997;6(1):37-48.
122. Ibrahim YH, Yee D. Insulin-like growth factor-I and cancer risk. Growth Horm IGF Res 2004;14(4):261-269.
123. Ma J, Pollak MN, Giovannucci E et al. Prospective study of colorectal cancer risk in men and plasma levels of insulin-like growth factor (IGF)-I and IGF-binding protein-3. J Natl Cancer Inst 1999;91(7):620-625.

124. Rinaldi S, Cleveland R, Norat T et al. Serum levels of IGF-I, IGFBP-3 and colorectal cancer risk: results from the EPIC cohort, plus a meta-analysis of prospective studies. Int J Cancer 2010;126(7):1702-1715.
125. Shankar S, Singh G, Srivastava RK. Chemoprevention by resveratrol: molecular mechanisms and therapeutic potential. Front Biosci 2007;12:4839-4854.
126. Wang D, Hang T, Wu C, Liu W. Identification of the major metabolites of resveratrol in rat urine by HPLC-MS/MS. J Chromatogr B Analyt Technol Biomed Life Sci 2005;829(1-2):97-106.
127. Potter GA, Patterson LH, Wanogho E et al. The cancer preventative agent resveratrol is converted to the anticancer agent piceatannol by the cytochrome P450 enzyme CYP1B1. Br J Cancer 2002;86(5):774-778.
128. De Santi C, Pietrabissa A, Spisni R, Mosca F, Pacifici GM. Sulphation of resveratrol, a natural compound present in wine, and its inhibition by natural flavonoids. Xenobiotica 2000;30(9):857-866.
129. de Santi C, Pietrabissa A, Mosca F, Pacifici GM. Glucuronidation of resveratrol, a natural product present in grape and wine, in the human liver. Xenobiotica 2000;30(11):1047-1054.
130. Marier JF, Vachon P, Gritsas A, Zhang J, Moreau JP, Ducharme MP. Metabolism and disposition of resveratrol in rats: extent of absorption, glucuronidation, and enterohepatic recirculation evidenced by a linked-rat model. J Pharmacol Exp Ther 2002;302(1):369-373.
131. Kapetanovic IM, Muzzio M, Huang Z, Thompson TN, McCormick DL. Pharmacokinetics, oral bioavailability, and metabolic profile of resveratrol and its dimethylether analog, pterostilbene, in rats. Cancer Chemother Pharmacol 2010.
132. Juan ME, Maijo M, Planas JM. Quantification of trans-resveratrol and its metabolites in rat plasma and tissues by HPLC. J Pharm Biomed Anal 2010;51(2):391-398.
133. Hoshino J, Park EJ, Kondratyuk TP et al. Selective synthesis and biological evaluation of sulfate-conjugated resveratrol metabolites. J Med Chem 2010;53(13):5033-5043.
134. Miksits M, Wlcek K, Svoboda M et al. Antitumor activity of resveratrol and its sulfated metabolites against human breast cancer cells. Planta Med 2009;75(11):1227-1230.
135. Calamini B, Ratia K, Malkowski MG et al. Pleiotropic mechanisms facilitated by resveratrol and its metabolites. Biochem J 2010;429(2):273-282.
136. Kaldas MI, Walle UK, Walle T. Resveratrol transport and metabolism by human intestinal Caco-2 cells. J Pharm Pharmacol 2003;55(3):307-312.
137. Yu C, Shin YG, Chow A et al. Human, rat, and mouse metabolism of resveratrol. Pharm Res 2002;19(12):1907-1914.
138. Murias M, Miksits M, Aust S et al. Metabolism of resveratrol in breast cancer cell lines: impact of sulfotransferase 1A1 expression on cell growth inhibition. Cancer Lett 2008;261(2):172-182.

139. Miksits M, Maier-Salamon A, Aust S et al. Sulfation of resveratrol in human liver: evidence of a major role for the sulfotransferases SULT1A1 and SULT1E1. Xenobiotica 2005;35(12):1101-1119.
140. Olas B, Wachowicz B, Saluk-Juszczak J, Zielinski T, Kaca W, Buczynski A. Antioxidant activity of resveratrol in endotoxin-stimulated blood platelets. Cell Biol Toxicol 2001;17(2):117-125.
141. Manna SK, Mukhopadhyay A, Aggarwal BB. Resveratrol suppresses TNF-induced activation of nuclear transcription factors NF-kappa B, activator protein-1, and apoptosis: potential role of reactive oxygen intermediates and lipid peroxidation. J Immunol 2000;164(12):6509-6519.
142. Aggarwal BB, Shishodia S. Molecular targets of dietary agents for prevention and therapy of cancer. Biochem Pharmacol 2006;71(10):1397-1421.
143. Kojima M, Morisaki T, Sasaki N et al. Increased nuclear factor-kB activation in human colorectal carcinoma and its correlation with tumor progression. Anticancer Res 2004;24(2B):675-681.
144. Cuendet M, Oteham CP, Moon RC, Pezzuto JM. Quinone reductase induction as a biomarker for cancer chemoprevention. J Nat Prod 2006;69(3):460-463.
145. Maier-Salamon A, Hagenauer B, Reznicek G, Szekeres T, Thalhammer T, Jager W. Metabolism and disposition of resveratrol in the isolated perfused rat liver: role of Mrp2 in the biliary excretion of glucuronides. J Pharm Sci 2008;97(4):1615-1628.
146. Alfaras I, Juan ME, Planas JM. trans-Resveratrol reduces precancerous colonic lesions in dimethylhydrazine-treated rats. J Agric Food Chem 2010;58(13):8104-8110.
147. Jung CM, Heinze TM, Schnackenberg LK et al. Interaction of dietary resveratrol with animal-associated bacteria. FEMS Microbiol Lett 2009;297(2):266-273.
148. Iwuchukwu OF, Nagar S. Resveratrol (trans-resveratrol, 3,5,4'-trihydroxy-trans-stilbene) glucuronidation exhibits atypical enzyme kinetics in various protein sources. Drug Metab Dispos 2008;36(2):322-330.
149. Aumont V, Krisa S, Battaglia E et al. Regioselective and stereospecific glucuronidation of trans- and cis-resveratrol in human. Arch Biochem Biophys 2001;393(2):281-289.
150. Sabolovic N, Humbert AC, Radominska-Pandya A, Magdalou J. Resveratrol is efficiently glucuronidated by UDP-glucuronosyltransferases in the human gastrointestinal tract and in Caco-2 cells. Biopharm Drug Dispos 2006;27(4):181-189.
151. Kuhnle G, Spencer JP, Chowrimootoo G et al. Resveratrol is absorbed in the small intestine as resveratrol glucuronide. Biochem Biophys Res Commun 2000;272(1):212-217.
152. Wang LX, Heredia A, Song H et al. Resveratrol glucuronides as the metabolites of resveratrol in humans: characterization, synthesis, and anti-HIV activity. J Pharm Sci 2004;93(10):2448-2457.

153. Boocock DJ, Patel KR, Faust GE et al. Quantitation of trans-resveratrol and detection of its metabolites in human plasma and urine by high performance liquid chromatography. J Chromatogr B Analyt Technol Biomed Life Sci 2007;848(2):182-187.
154. Maier-Salamon A, Hagenauer B, Wirth M, Gabor F, Szekeres T, Jager W. Increased transport of resveratrol across monolayers of the human intestinal Caco-2 cells is mediated by inhibition and saturation of metabolites. Pharm Res 2006;23(9):2107-2115.
155. Sale S, Verschoyle RD, Boocock D et al. Pharmacokinetics in mice and growth-inhibitory properties of the putative cancer chemopreventive agent resveratrol and the synthetic analogue trans 3,4,5,4'-tetramethoxystilbene. Br J Cancer 2004;90(3):736-744.
156. Asensi M, Medina I, Ortega A et al. Inhibition of cancer growth by resveratrol is related to its low bioavailability. Free Radic Biol Med 2002;33(3):387-398.
157. Azorin-Ortuno M, Yanez-Gascon MJ, Pallares FJ et al. Pharmacokinetic Study of trans-Resveratrol in Adult Pigs. J Agric Food Chem 2010.
158. Crowell J, McCormick D, Cwik M, Kapetanovic I. Toxicokinetics of resveratrol in dogs. Toxicology Letters 2007;172(Supplement 1):S102-S102.
159. Patel KR, Brown VA, Jones DJ et al. Clinical pharmacology of resveratrol and its metabolites in colorectal cancer patients. Cancer Res 2010;70(19):7392-7399.
160. Lin JH, Chiba M, Baillie TA. Is the role of the small intestine in first-pass metabolism overemphasized? Pharmacol Rev 1999;51(2):135-158.
161. Scalbert A, Williamson G. Dietary intake and bioavailability of polyphenols. J Nutr 2000;130(8S Suppl):2073S-2085S.
162. Lu LJ, Anderson KE. Sex and long-term soy diets affect the metabolism and excretion of soy isoflavones in humans. Am J Clin Nutr 1998;68(6 Suppl):1500S-1504S.
163. Tanaka E. Gender-related differences in pharmacokinetics and their clinical significance. J Clin Pharm Ther 1999;24(5):339-346.
164. Juan ME, Alfaras I, Planas JM. Determination of dihydroresveratrol in rat plasma by HPLC. J Agric Food Chem 2010;58(12):7472-7475.
165. Kahn ME, Senderowicz A, Sausville EA, Barrett KE. Possible mechanisms of diarrheal side effects associated with the use of a novel chemotherapeutic agent, flavopiridol. Clin Cancer Res 2001;7(2):343-349.
166. Blumenstein I, Keseru B, Wolter F, Stein J. The chemopreventive agent resveratrol stimulates cyclic AMP-dependent chloride secretion in vitro. Clin Cancer Res 2005;11(15):5651-5656.
167. Szekeres T, Fritzer-Szekeres M, Saiko P, Jager W. Resveratrol and resveratrol analogues--structure-activity relationship. Pharm Res 2010;27(6):1042-1048.
168. Biasutto L, Marotta E, Bradaschia A et al. Soluble polyphenols: synthesis and bioavailability of 3,4',5-tri(alpha-D-glucose-3-O-succinyl) resveratrol. Bioorg Med Chem Lett 2009;19(23):6721-6724.

169. Mukherjee S, Ray D, Lekli I, Bak I, Tosaki A, Das DK. Effects of Longevinex (modified resveratrol) on cardioprotection and its mechanisms of action. Can J Physiol Pharmacol 2010;88(11):1017-1025.
170. Juan ME, Gonzalez-Pons E, Planas JM. Multidrug resistance proteins restrain the intestinal absorption of trans-resveratrol in rats. J Nutr 2010;140(3):489-495.
171. MacLean C, Moenning U, Reichel A, Fricker G. Closing the gaps: a full scan of the intestinal expression of p-glycoprotein, breast cancer resistance protein, and multidrug resistance-associated protein 2 in male and female rats. Drug Metab Dispos 2008;36(7):1249-1254.
172. Hebden JM, Gilchrist PJ, Perkins AC, Wilson CG, Spiller RC. Stool water content and colonic drug absorption: contrasting effects of lactulose and codeine. Pharm Res 1999;16(8):1254-1259.
173. Garcea G, Berry DP, Jones DJ et al. Consumption of the putative chemopreventive agent curcumin by cancer patients: assessment of curcumin levels in the colorectum and their pharmacodynamic consequences. Cancer Epidemiol Biomarkers Prev 2005;14(1):120-125.
174. Scott E, Khan M, Hemingway D et al. Comparison of [14C]-resveratrol pharmacokinetics and target tissue distribution in humans following a pharmacological and dietary dose using accelerator mass spectrometry (AMS). National Cancer Research Institute Annual Meeting 2010.
175. Nguyen AV, Martinez M, Stamos MJ et al. Results of a phase I pilot clinical trial examining the effect of plant-derived resveratrol and grape powder on Wnt pathway target gene expression in colonic mucosa and colon cancer. Cancer Manag Res 2009;1:25-37.
176. Juan ME. Plasmatic levels of trans-resveratrol in rats. Food Research International 2002;35:195-199.
177. Abd El-Mohsen M, Bayele H, Kuhnle G et al. Distribution of [3H]trans-resveratrol in rat tissues following oral administration. Br J Nutr 2006;96(1):62-70.
178. Maier-Salamon A, Bohmdorfer M, Reznicek G, Thalhammer T, Szekeres T, Jaeger W. Hepatic Glucuronidation of Resveratrol: Interspecies Comparison of Enzyme Kinetic Profiles in Human, Mouse, Rat and Dog. Drug Metab Pharmacokinet 2011.
179. Andlauer W, Kolb J, Siebert K, Furst P. Assessment of resveratrol bioavailability in the perfused small intestine of the rat. Drugs Exp Clin Res 2000;26(2):47-55.
180. Alfaras I, Perez M, Juan ME et al. Involvement of breast cancer resistance protein (BCRP1/ABCG2) in the bioavailability and tissue distribution of trans-resveratrol in knockout mice. J Agric Food Chem 2010;58(7):4523-4528.
181. van de Wetering K, Feddema W, Helms JB, Brouwers JF, Borst P. Targeted metabolomics identifies glucuronides of dietary phytoestrogens as a major class of MRP3 substrates in vivo. Gastroenterology 2009;137(5):1725-1735.

182. Kitamura Y, Kusuhara H, Sugiyama Y. Functional characterization of multidrug resistance-associated protein 3 (mrp3/abcc3) in the basolateral efflux of glucuronide conjugates in the mouse small intestine. J Pharmacol Exp Ther 2010;332(2):659-666.
183. Enokizono J, Kusuhara H, Sugiyama Y. Regional expression and activity of breast cancer resistance protein (Bcrp/Abcg2) in mouse intestine: overlapping distribution with sulfotransferases. Drug Metab Dispos 2007;35(6):922-928.
184. Santner SJ, Feil PD, Santen RJ. In situ estrogen production via the estrone sulfatase pathway in breast tumors: relative importance versus the aromatase pathway. J Clin Endocrinol Metab 1984;59(1):29-33.
185. Gamage N, Barnett A, Hempel N et al. Human sulfotransferases and their role in chemical metabolism. Toxicol Sci 2006;90(1):5-22.
186. Crozier A, Jaganath IB, Clifford MN. Dietary phenolics: chemistry, bioavailability and effects on health. Nat Prod Rep 2009;26(8):1001-1043.
187. Luo Z, Saha AK, Xiang X, Ruderman NB. AMPK, the metabolic syndrome and cancer. Trends Pharmacol Sci 2005;26(2):69-76.
188. Wang D, Xu Y, Liu W. Tissue distribution and excretion of resveratrol in rat after oral administration of Polygonum cuspidatum extract (PCE). Phytomedicine 2008;15(10):859-866.
189. Wang D, Zhang Z, Ju J, Wang X, Qiu W. Investigation of piceid metabolites in rat by liquid chromatography tandem mass spectrometry. J Chromatogr B Analyt Technol Biomed Life Sci 2010;879(1):69-74.
190. Bakhtiarova A, Taslimi P, Elliman SJ et al. Resveratrol inhibits firefly luciferase. Biochem Biophys Res Commun 2006;351(2):481-484.
191. Jannin B, Menzel M, Berlot JP, Delmas D, Lancon A, Latruffe N. Transport of resveratrol, a cancer chemopreventive agent, to cellular targets: plasmatic protein binding and cell uptake. Biochem Pharmacol 2004;68(6):1113-1118.
192. Porter AG, Janicke RU. Emerging roles of caspase-3 in apoptosis. Cell Death Differ 1999;6(2):99-104.
193. Kim MY, Trudel LJ, Wogan GN. Apoptosis induced by capsaicin and resveratrol in colon carcinoma cells requires nitric oxide production and caspase activation. Anticancer Res 2009;29(10):3733-3740.
194. Lanzilli G, Fuggetta MP, Tricarico M et al. Resveratrol down-regulates the growth and telomerase activity of breast cancer cells in vitro. Int J Oncol 2006;28(3):641-648.
195. Kampa M, Hatzoglou A, Notas G et al. Wine antioxidant polyphenols inhibit the proliferation of human prostate cancer cell lines. Nutr Cancer 2000;37(2):223-233.
196. Sgambato A, Ardito R, Faraglia B, Boninsegna A, Wolf FI, Cittadini A. Resveratrol, a natural phenolic compound, inhibits cell proliferation and prevents oxidative DNA damage. Mutat Res 2001;496(1-2):171-180.

197. Li H, Wu WK, Zheng Z et al. 3,3',4,5,5'-Pentahydroxy-trans-stilbene, a resveratrol derivative, induces apoptosis in colorectal carcinoma cells via oxidative stress. Eur J Pharmacol 2010;637(1-3):55-61.
198. Hoshino J, Park EJ, Kondratyuk TP et al. Selective synthesis and biological evaluation of sulfate-conjugated resveratrol metabolites. J Med Chem;53(13):5033-5043.
199. Ovesna Z, Horvathova-Kozics K. Structure-activity relationship of trans-resveratrol and its analogues. Neoplasma 2005;52(6):450-455.
200. Lancon A, Delmas D, Osman H, Thenot JP, Jannin B, Latruffe N. Human hepatic cell uptake of resveratrol: involvement of both passive diffusion and carrier-mediated process. Biochem Biophys Res Commun 2004;316(4):1132-1137.
201. Franssen-van Hal NL, Bunschoten JE, Venema DP, Hollman PC, Riss G, Keijer J. Human intestinal and lung cell lines exposed to beta-carotene show a large variation in intracellular levels of beta-carotene and its metabolites. Arch Biochem Biophys 2005;439(1):32-41.
202. Kim RB. Organic anion-transporting polypeptide (OATP) transporter family and drug disposition. Eur J Clin Invest 2003;33 Suppl 2:1-5.
203. Tamai I, Nozawa T, Koshida M, Nezu J, Sai Y, Tsuji A. Functional characterization of human organic anion transporting polypeptide B (OATP-B) in comparison with liver-specific OATP-C. Pharm Res 2001;18(9):1262-1269.
204. Hsieh TC. Uptake of resveratrol and role of resveratrol-targeting protein, quinone reductase 2, in normally cultured human prostate cells. Asian J Androl 2009;11(6):653-661.
205. Brittes J, Lucio M, Nunes C, Lima JL, Reis S. Effects of resveratrol on membrane biophysical properties: relevance for its pharmacological effects. Chem Phys Lipids 2010;163(8):747-754.
206. Han YS, Bastianetto S, Dumont Y, Quirion R. Specific plasma membrane binding sites for polyphenols, including resveratrol, in the rat brain. J Pharmacol Exp Ther 2006;318(1):238-245.
207. Calabrese EJ, Mattson MP, Calabrese V. Dose response biology: the case of resveratrol. Hum Exp Toxicol 2010;29(12):1034-1037.
208. Scott EN, Gescher AJ, Steward WP, Brown K. Development of dietary phytochemical chemopreventive agents: biomarkers and choice of dose for early clinical trials. Cancer Prev Res (Phila) 2009;2(6):525-530.
209. J G, Cq W, Hh F et al. Effects of resveratrol on endothelial progenitor cells and their contributions to reendothelialization in intima-injured rats. J Cardiovasc Pharmacol 2006;47(5):711-721.
210. Szende B, Tyihak E, Kiraly-Veghely Z. Dose-dependent effect of resveratrol on proliferation and apoptosis in endothelial and tumor cell cultures. Exp Mol Med 2000;32(2):88-92.

211. Valenzano DR, Terzibasi E, Genade T, Cattaneo A, Domenici L, Cellerino A. Resveratrol prolongs lifespan and retards the onset of age-related markers in a short-lived vertebrate. Curr Biol 2006;16(3):296-300.
212. Wood JG, Rogina B, Lavu S et al. Sirtuin activators mimic caloric restriction and delay ageing in metazoans. Nature 2004;430(7000):686-689.
213. Bauer JH, Goupil S, Garber GB, Helfand SL. An accelerated assay for the identification of lifespan-extending interventions in Drosophila melanogaster. Proc Natl Acad Sci U S A 2004;101(35):12980-12985.
214. Howitz KT, Bitterman KJ, Cohen HY et al. Small molecule activators of sirtuins extend Saccharomyces cerevisiae lifespan. Nature 2003;425(6954):191-196.
215. Gary RK, Kindell SM. Quantitative assay of senescence-associated beta-galactosidase activity in mammalian cell extracts. Anal Biochem 2005;343(2):329-334.
216. Rusin M, Zajkowicz A, Butkiewicz D. Resveratrol induces senescence-like growth inhibition of U-2 OS cells associated with the instability of telomeric DNA and upregulation of BRCA1. Mech Ageing Dev 2009;130(8):528-537.
217. Heiss EH, Schilder YD, Dirsch VM. Chronic treatment with resveratrol induces redox stress- and ataxia telangiectasia-mutated (ATM)-dependent senescence in p53-positive cancer cells. J Biol Chem 2007;282(37):26759-26766.
218. Barth S, Glick D, Macleod KF. Autophagy: assays and artifacts. J Pathol 2010;221(2):117-124.
219. Nakatogawa H, Suzuki K, Kamada Y, Ohsumi Y. Dynamics and diversity in autophagy mechanisms: lessons from yeast. Nat Rev Mol Cell Biol 2009;10(7):458-467.
220. Trincheri NF, Follo C, Nicotra G, Peracchio C, Castino R, Isidoro C. Resveratrol-induced apoptosis depends on the lipid kinase activity of Vps34 and on the formation of autophagolysosomes. Carcinogenesis 2008;29(2):381-389.
221. Scarlatti F, Maffei R, Beau I, Codogno P, Ghidoni R. Role of non-canonical Beclin 1-independent autophagy in cell death induced by resveratrol in human breast cancer cells. Cell Death Differ 2008;15(8):1318-1329.
222. Wang Y, Lee KW, Chan FL, Chen SA, Leung LK. The red wine polyphenol resveratrol displays bilevel inhibition on aromatase in breast cancer cells. Toxicological Sciences 2006;92(1):71-77.
223. Donnini S, Finetti F, Lusini L et al. Divergent effects of quercetin conjugates on angiogenesis. Br J Nutr 2006;95(5):1016-1023.
224. Rimbach G, Weinberg PD, de Pascual-Teresa S et al. Sulfation of genistein alters its antioxidant properties and its effect on platelet aggregation and monocyte and endothelial function. Biochim Biophys Acta 2004;1670(3):229-237.
225. Osborne R, Thompson P, Joel S, Trew D, Patel N, Slevin M. The analgesic activity of morphine-6-glucuronide. Br J Clin Pharmacol 1992;34(2):130-138.
226. O'Leary KA, Day AJ, Needs PW, Mellon FA, O'Brien NM, Williamson G. Metabolism of quercetin-7- and quercetin-3-glucuronides by an in vitro hepatic model: the role of

human beta-glucuronidase, sulfotransferase, catechol-O-methyltransferase and multi-resistant protein 2 (MRP2) in flavonoid metabolism. Biochem Pharmacol 2003;65(3):479-491.

227. Boyer MJ, Tannock IF. Lysosomes, lysosomal enzymes, and cancer. Adv Cancer Res 1993;60:269-291.
228. Labianca R, Merelli B. Screening and diagnosis for colorectal cancer: present and future. Tumori 2010;96(6):889-901.
229. Patel KR, Scott E, Brown VA, Gescher AJ, Steward WP, Brown K. Clinical trials of resveratrol. Ann N Y Acad Sci 2011;1215(1):161-169.
230. Cottart CH, Nivet-Antoine V, Laguillier-Morizot C, Beaudeux JL. Resveratrol bioavailability and toxicity in humans. Mol Nutr Food Res 2010;54(1):7-16.
231. Sai Y, Kaneko Y, Ito S et al. Predominant contribution of organic anion transporting polypeptide OATP-B (OATP2B1) to apical uptake of estrone-3-sulfate by human intestinal Caco-2 cells. Drug Metab Dispos 2006;34(8):1423-1431.
232. Puissant A, Robert G, Fenouille N et al. Resveratrol promotes autophagic cell death in chronic myelogenous leukemia cells via JNK-mediated p62/SQSTM1 expression and AMPK activation. Cancer Res 2010;70(3):1042-1052.
233. Singletary K, Milner J. Diet, autophagy, and cancer: a review. Cancer Epidemiol Biomarkers Prev 2008;17(7):1596-1610.
234. Signorelli P, Ghidoni R. Resveratrol as an anticancer nutrient: molecular basis, open questions and promises. J Nutr Biochem 2005;16(8):449-466.
235. Kenealey JD, Subramanian L, van Ginkel P et al. Resveratrol Metabolites Do Not Elicit Early Pro-apoptotic Mechanisms in Neuroblastoma Cells. J Agric Food Chem 2011.
236. Morand C, Crespy V, Manach C, Besson C, Demigne C, Remesy C. Plasma metabolites of quercetin and their antioxidant properties. Am J Physiol 1998;275(1 Pt 2):R212-219.
237. Yoshizumi M, Tsuchiya K, Suzaki Y et al. Quercetin glucuronide prevents VSMC hypertrophy by angiotensin II via the inhibition of JNK and AP-1 signaling pathway. Biochem Biophys Res Commun 2002;293(5):1458-1465.
238. Lambert JD, Sang S, Hong J, Yang CS. Anticancer and anti-inflammatory effects of cysteine metabolites of the green tea polyphenol, (-)-epigallocatechin-3-gallate. J Agric Food Chem 2010;58(18):10016-10019.
239. Murias M, Handler N, Erker T et al. Resveratrol analogues as selective cyclooxygenase-2 inhibitors: synthesis and structure-activity relationship. Bioorg Med Chem 2004;12(21):5571-5578.
240. Day AJ, Bao Y, Morgan MR, Williamson G. Conjugation position of quercetin glucuronides and effect on biological activity. Free Radic Biol Med 2000;29(12):1234-1243.
241. Rechner AR, Kroner C. Anthocyanins and colonic metabolites of dietary polyphenols inhibit platelet function. Thromb Res 2005;116(4):327-334.